SEMI-VOLATILE ORGANIC COMPOUNDS IN UNDERGROUND COAL GASIFICATION EFFLUENTS: FROM SAMPLE PREPARATION TO DATA ANALYSIS

IOANNIS SAMPSONIDIS

SUBMITTED IN FULFILMENT OF THE REQUIREMENTS FOR THE DEGREE OF
Doctor of Philosophy

SCHOOL OF ENGINEERING

COLLEGE OF SCIENCE AND ENGINEERING

UNIVERSITY OF GLASGOW

APRIL 2019

Abstract

Effluents produced from the coal conversion industry, particularly from coal gasification, are complex mixtures, rich in semi-volatile organic compounds (SVOCs). In the case of underground coal gasification (UCG), the production of syngas is accompanied by significant amounts of wastewater and tar, the detailed characterisation of which is required for risk assessment and disposal purposes but also for identification of components of high economic value. This characterisation is challenging as these effluents are unique, both in their physico-chemical nature and their SVOC content.

Here, a close-to-exhaustive SVOC characterisation of UCG wastewater was performed, with the development of a novel micro-extraction method, which utilises three physico-chemical effects: ultrasonication, emulsification and salting-out. The delivery of ultrasound in the samples was performed using a novel system that transmits ultrasound into a vessel's contents through its wall, and was named high-intensity vessel-wall sonication (HIVS). The developed ultrasound-assisted surfactant-enhanced salting-out emulsification micro-extraction (UASESOEME) method proved to be successful in the extraction of SVOCs from UCG wastewater, overcoming limitations of previous methods. The HIVS technique was also applied in the development of a fast and precise ultrasound-assisted extraction (UAE) method for coal tar and in the development of an ultrasound-assisted derivatisation (UAD) method for derivatising extracts from both wastewater and coal tar, significantly enhancing their gas chromatographic analysis. Analytical methods for gas chromatography coupled to mass spectrometry (GC-MS) and comprehensive gas chromatography coupled to time-of-flight mass spectrometry (GCxGC-TOFMS) were also developed to analyse the extracts.

The above methods were applied in the extraction of SVOCs from three time-series of samples (two from simulated *ex-situ* UCG experiments and another from an *in-situ* field-scale UCG trial) and in the extraction of a series of leachates from tar leaching experiments performed with tars of increasing weathering/processing. Analyses yielded comprehensive datasets that were processed using a custom data processing approach and analysed using exploratory and multivariate statistical analysis techniques for sample classification and marker discovery. Time-series analysis indicated several SVOCs as markers, mostly oxygen and nitrogen containing compounds, most of which are not commonly considered in gasification studies; the differences between the two matrices was also highlighted, indicating coal tar as the most representative of the two. Analysis of leachates showed that they can be classified based on their SVOC signature according to the parent tar type; also, tars were shown to continue leaching SVOCs after weathering/processing and that their solubility is dependent on the ionic strength of the leaching medium.

Acknowledgements

First and foremost, I would like to thank my supervisors, Dr. Caroline Gauchotte-Lindsay, Dr Ian Watson and the late Prof. Paul Younger for all their support, motivation and guidance throughout my PhD research. A big thank you to my family for all their emotional and financial support during my academic career, especially to my wife, Anastasia, for always being there for me and without whom I wouldn't have reached so far. I would also like to thank all my Glasgow friends, office mates, past and present members of the water and environment research group, especially Ignatios, Sotiris, Sotiria, Athina, Eri, Nikos, Andrea, Kevin, Alex, Pradeep, Ili, Fabien, Kate, Felipe, Jeanine and Melissa for making my PhD an enjoyable experience. Another thank you goes to members of staff from the School of Engineering especially the lab technicians Julie Russell, Anne McGarrity and Timothy Montgomery and also Elaine McNamara from the School's office for all the support they provided.

I would also like to acknowledge the following: Dr Krzysztof Kapusta from the Polish Central Mining Institute (GIG) for providing the gasification waste-water and UCG coal tar samples; Ms Mara Knapp, from the Department of Civil Engineering at the University of Strathclyde for providing the pitch sample and technical assistance; the Technical Services Department of the School of Engineering at the University of Glasgow for providing aid with adapter manufacturing and Mr Colin Towers from Crawford Scientific for the useful discussions on the subject of Gas Chromatography.

This project has received funding through a scholarship from the School of Engineering at the University of Glasgow and from the European Union's Seventh Framework Programme for research, technological development and demonstration under grant agreement no [608517] - "Technology Options for Coupled Underground Coal Gasification and CO2 Capture and Storage".

Portions of information contained in this thesis are produced from the Chromatof® GCxGC analysis software provided by LECO

Declaration

I declare that, except where explicit reference is made to contribution of others, this thesis is the result of my own work and has not been submitted for any other degree at University of Glasgow or any other institution.

Ioannis Sampsonidis

Στους προπαππούδες μου, Αναστάση και Ανέστη, για όλα όσα υπέφεραν

Contents

List of Tables

List of Figures

Nomenclature

5,5-DMH	5,5-dimethylhydantoin
AMDIS	Automated Mass Spectral Deconvolution Identification System
BBBT	bis(p-butoxybenzylidene) a,a'-bi-p-toluidine
BHT	Butylated hydroxytoluene
BSA	bis(trimethylsilyl)acetamide
BSTFA	N,O-Bis(trimethylsilyl)trifluoroacetamide
BTEX	Benzene, Toluene, Ethylbenzene and Xylene isomers
CCC	Circumscribed Central Composite
CMC	Critical micelle concentration
COD	Chemical oxygen demand
CPME	Cyclopentyl methylether
CRIP	Controlled retractable injection point
CSIC	Consejo Superior de Investigaciones Científicas (Spanish National Research Council)
CTAB	Cetyltrimethylammonium bromide
DCM	Dichloromethane
DLLME	Dispersive liquid-liquid- extraction
DNAPL	Dense non-aqueous phases liquid
DOE	Design of Experiments
DoE	Department of Energy (US)

ELW	Extended linked well
ESFDB	Experiment-specific feature database
EU	European Union
FFAP	Free fatty acid phase
FMGP	Former manufacturer gas plant
FP7	Seventh Framework Programme
GC	Gas chromatography
GC-FID	Gas chromatography coupled to flame ionisation detector
GC-MS	Gas chromatography coupled to mass spectrometry
GCxGC	Comprehensive two-dimensional gas chromatography
GCxGC-TOFMS	Comprehensive two-dimensional gas chromatography coupled to time-of-flight mass spectrometry
GIG	Główny Instytut Górnictwa (Polish Central mining institute)
HIVS	High-intensive vesse-wall sonication
HPLC	High performance liquid chromatography
HPLC-DAD	High performance liquid chromatography coupled to diode array detector
INCAR	Instituto Nacional del Carbón (Spanish National Coal Institute)
LLE	Liquid-liquid extraction
LLNL	Lawrence Livermore National Laboratory (US)
LNAPL	Light non-aqueous phase liquid
LVW	Linked Vertical Wall
NAPL	Non-aqueous phase liquid
NTIS	National Technical Information Service (US)
oPLS-DA	ortho Parial Least Squares Discriminant Analysis
OSTI	Office of Scientific and Technical Information (US)

PAHs	Polycyclic aromatic hydrocarbons
PCA	Principal Component Analysis
PLE	Pressurised liquid extraction
PLS-DA	Partial Least Squares Discriminant Analysis
RSM	Response surface methodology
SPE	Solid phase extraction
sPLS-DA	sparce Partial Least Squares Discriminant Analysis
SVOC	Semi-volatile organic compound
Syngas	Synthesis gas
THCM	Thermo-Hydro-Chemical-Mechanical
TMCS	Trimethylchlorosilane
TOC	Total organic carbon
TOPS	Technology Options for Coupled Underground Coal Gasification and CO2 Capture and Storage
UAD	Ultrasonication-assisted derivatisation
UAE	Ultrasound-assisted extraction
UASEME	Ultrasound-assisted surfactant-enhanced emulsification micro-extraction
UASESOEME	Ultrasound-assisted surfactant-enhanced salting-out emulsification micro-extraction
UCG	Underground coal gasification
US	Ultrasound
USAEME	Ultrasound-assisted emulsification microextraction
USALLE	Ultrasound-assisted liquid-liquid extraction
USEPA	United States environmental protection agency
WFMGP tar	Weathered former manufacturer gas plant tar
WRI	Western Research Institute (US)

Chapter 1

Introduction

1.1 Background

Estimations for the exhaustion of oil and gas have shown that these resources will be depleted during the middle and late 21th century respectively[1]. Taking this into account, along with the ever-increasing energy demand and the fact that renewable sources cannot be considered fully sustainable yet, the energy industry is considering the use of underground coal gasification (UCG) that can, potentially, give access to trillions of tonnes of coal that is considered un-minable using conventional coal extraction techniques.

This PhD project started as part of the FP7 TOPS (Technology Options for Coupled Underground Coal Gasification and CO_2 Capture and Storage) project[2] which was funded by the European Commission and its main objective was to investigate the feasibility of UCG, both in the European Union (EU) and worldwide, while addressing various issues that govern the application of UCG, like site selection, environmental impact and coupling with on site CO_2 storage.

Within this project, the team at the University of Glasgow, was involved in the environmental impact assessment of the UCG process, which included potential environmental risks from subsidence and ground-water pollution. Ground-water pollution was to be assessed by analysing samples from the main experimental part of the project which was the conduction of several *ex-situ* coal gasification experiments using a custom-made, high pressure coal-block gasification reactor which was located at Poland's Central Mining Institute (Glowny Instytut Gornictwa - GIG) and more specifically at the laboratory of experimental installations located at Barbara mine in Mikolow, near the city of Katowice. The primary purpose of these experiments was to obtain information regarding the composition of synthesis gas (syngas) under various gasification conditions and using different gasification agents.

Participation in this project gave access to valuable samples from both the project detailed

above and from other UCG experiments performed in the GIG. These samples include waste-water from two *ex-situ* reactor experiments and coal tar from a real scale UCG trial. Samples were taken in time intervals during each experiment which allows their study as a time-series. Analysis of the semi-volatile organic compound (SVOC) content of the samples may prove invaluable for the environmental monitoring of the process, but also to identify potentially retrievable components of high economic value and to provide information that may aid in the better understanding of UCG.

The strategy employed for sample preparation is based on ultrasound-assisted small volume liquid-liquid extraction for aqueous samples and ultrasound-assisted extraction extraction for tar samples. Sample analysis is based mainly on gas chromatography coupled to mass spectrometry (GC-MS), gas chromatography coupled to flame ionisation detector (GC-FID) and comprehensive two dimensional gas chromatography couple to time-of-flight mass spectrometry (GCxGC-TOFMS). Data from un-targeted analyses are processed using a custom data processing pipeline and further analysed using a selection of multivariate statistical methods (e.g. principal component analysis (PCA) and partial least squares discriminant analysis (PLS-DA)).

1.2 Research aim and Objectives

The aim of the research presented in this thesis is the investigation of the SVOC content of UCG produced waste-water and tar in order to gain new knowledge on the composition of these effluents; this may assist the community to the better understanding of the complex phenomena that take place inside a UCG reactor and the possible environmental implications that these may have. To achieve the aims the following objectives were set:

- Develop a fast and precise method, based on ultrasound-assisted liquid-liquid extraction, for the analysis of UCG produced waste-water without the need of fractionation; optimise gas chromatography (GC) set-ups for the analysis of these samples using GC-MS and GCxGC-TOFMS.
- Develop a method for the fast and precise analysis of UCG produced tars, based on ultrasound-assisted extraction, without the need of fractionation and the use of multiple techniques; optimise GC set-ups for the analysis of these samples using GC-MS and GCxGC-TOFMS.
- Develop a miniaturised method, based on ultrasonication, for the derivatisation of the sample extracts from the previously developed methods in order to further enhance their GC-MS and GCxGC-TOFMS analysis

- Apply data analysis approaches that can unravel the complex chemical data produced from the methods, determine chemical differences between samples and suggest SVOCs as markers/global indicators during UCG
- Test the behaviour of UCG produced tars when in contact with water with a series of leaching experiments

1.3 Thesis outline

The thesis includes 8 chapters and details the development of a complete approach from sample preparation to data analysis for the processing of effluents from UCG.

Chapter 2 provides the reader with information that are necessary to better understand the origin of the samples; this includes information regarding the nature of the coal but also the processes that produce SVOCs from coal. This is done in the form of a brief literature review. More specifically, the chapter provides information on coal formation, classification and composition; it includes details about reactions of coal that are relevant with SVOC production like oxidation, pyrolysis and gasification and, finally, these processes are presented within the concept of UCG, detailing related theoretical aspects.

Chapter 3 includes a brief review on the already existent methods for the analysis of waste-water; it also details the development of a sample preparation and analysis scheme for the exhaustive characterisation of SVOCs in UCG waste-water. It includes the use of a novel ultrasonication system and the suggestion of a new comprehensive two-dimensional gas chromatography (GCxGC) set-up.

Chapter 4 details the literature on tar analysis and presents the development of a method for the analysis of tars using a novel ultrasonication system and a reverse phase GCxGC set-up.

Chapter 5 provides a brief review of UCG trials related to the thesis and presents the development of a pipeline for the exploratory data analysis of effluents from four UCG trials. It includes the analysis of literature data, a series of waste-water samples from two *ex-situ* UCG trial performed using a large scale reactor and the analysis of a series of tar samples from a field-scale UCG trial. The analysis indicates marker compounds that are produced during the trials including their corresponding patterns.

Chapter 6 presents the development of a derivatisation method aimed to derivatise extracts from UCG effluents like waste-water and coal tar. It employs a novel ultrasonication system and includes details on the enhancements that the derivatisation process offers. A brief review of existing sonication assisted derivatisation methods is provided at the beginning.

Chapter 7 details the results of a leaching experiment in water from three types of tars: UCG tar, weathered tar from a former manufactured gas plant (FMGP) site and pitch; it also details

a leaching experiment aimed to investigate the leaching behaviour of UCG tar in water of different salinities. The methods developed in previous chapters are applied here in order to characterise the content of the leachates and to compare them using data analysis tools.

Chapter 8 presents the conclusions of the thesis including future work suggestions by the author.

Chapter 2

The nature of coal and SVOC related processes

2.1 Introduction

Since this thesis deals with the analysis of SVOCs in effluents that are being produced during UCG, the author considers the provision of a condensed version of the basics of coal formation and conversion essential, so that the reader develops an understanding of the nature and origin of the samples that are analysed in the thesis; however, the amount of information provided is limited to the context of the thesis.

This chapter provides a brief literature review on coal, discussing some of its general aspects like formation and oxidation, but also coal conversion processes such as pyrolysis and gasification, which are the processes that produced the samples that are analysed later in the thesis. A detailed description UCG is given, along with process phenomena relevant to the production of SVOCs. As mentioned in Section 1.3, p.3, brief literature reviews that deal with the context of each chapter are provided in their corresponding introductions in a modular fashion.

2.2 Regarding coal

A large amount of information contained in the following sections is given from works the are considered classic in coal science and coal chemistry such as the "The Chemistry of Coal" by Berkowitz[3], the first supplementary volume of "Chemistry of Coal Utilization" edited by ell[4] and the second supplementary volume edited by low[5]; the rest of the bibliography is limited to individual articles. Although coal research has declined in recent years, it is still undertaken in several institutes around the world such as the Energy Institute at the College

of Earth and Mineral Sciences in Pennsylvania State University, the Spanish National Coal Institute (Instituto Nacional del Carbón (INCAR)) of the Spanish National Research Council (Consejo Superior de Investigaciones Científicas (CSIC), Royal School of Mines at Imperial College in London, Max Planck Institute for Coal Research in Mulheim, Indian Institute of Technology and China University of Mining and Technology[6].

2.2.1 Coal formation

Coal is formed through two main processes: diagenesis (or peatification) and metamorphic development (also referred to a coalification)[3,7,8]. Diagenesis involves the exposure of dead plant matter to the atmosphere, where both abiotic oxidation and fungal/bacterial decomposition take place. During this stage several transformations happen regarding the chemical content of the dead plant matter, some of which are listed in Table 2.1. These processes result in a what is described as a "structurally undifferentiated humus"[3], into which additional matter is ingrained such as resins, pollen or inorganic material[3,7].

Table 2.1: Transformations in the chemical content of dead plant matter during diagenesis, detailing precursor substances and corresponding products. Compiled from Berkowitz[3]

Precursors	Products
fats,waxes,resins	various polymers (oxygen promoted)
pigments (e.g chlorophyl)	molecular rearrangement (e.g. porphyrins)
Cellulose matter	simple sugars
lignin	humic acids and benzenoid acids
glucosides	sugars, aglycons
proteins	slimes, amino acids

The extend of the decay depends on the availability of oxygen which can be significantly different depending on the environment and the dominant process that takes place during diagenesis (Table 2.2)[3]. Once diagenesis terminates, the metamorphic development process begins, however, the extent of diagenesis depends on a lot of factors, such as period of exposure, temperature (higher temperatures result to faster decay), alkalinity (higher alkalinity - more intensive decay) and the local ground water regime. Decaying processes can take place simultaneously or successively and the heterogeneity of the final coal depends on the variety of precursors/processes[3].

Metamorphic development or coalification is an abiotic process that takes place once diagenesis reaches its end. During coalification, coal loses its moisture and the internal structure changes significantly. As time passes by and pressure and temperature increase, the coal is compacted (Figure 2.1) and a number of chemical reactions take place that result in an increase in the carbon content of the coal and a decrease in its oxygen and hydrogen content[3,7,8]. Coalification advances through a series of reactions, starting with dehydration, de-

Table 2.2: Transformations in the chemical content of dead plant matter during diagenesis. Compiled from Berkowitz [3]

Environment	Dominant process	Result
Dry, full exposed	abiotic oxidation	humic acids
Swampy, shallow	fungal/anaerobic bacterial oxidation	gels, slimes
Stagnant	putrification	sapropel

carboxylation, dehydroxylation and condensation which occur below 150°C and continues with reactions such as cyclization and dehydrogenation which require higher temperatures that are provided mainly through teutonic events. Higher rank coals, such as anthracite, may require temperatures up to 450°C to form. Interestingly, aliphatic and hydroaromatic components trapped in the structure of the coal may survive all but the final coalification steps [3].

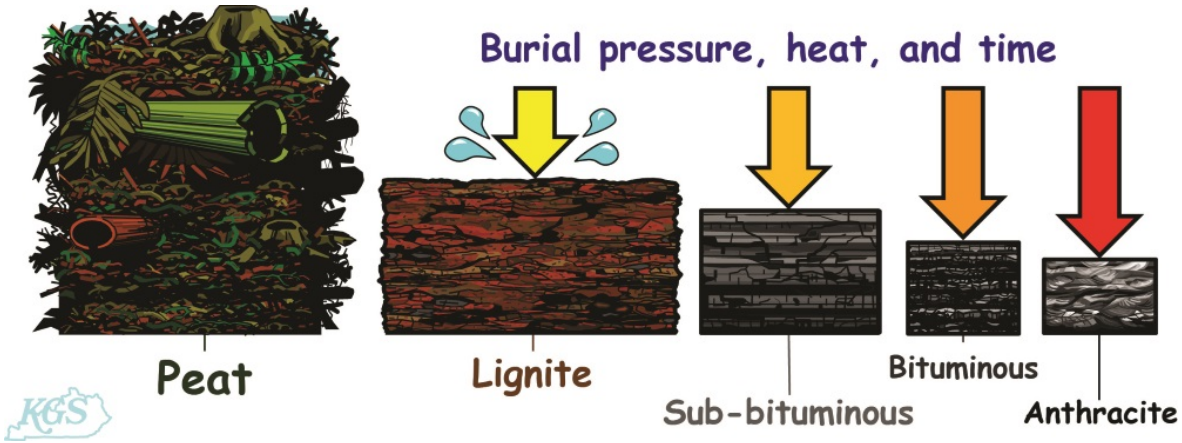

Figure 2.1: Coalification process. Coal starts from peat and it slowly increases in rank as time passes by and temperature and burial pressure increase. Credit: Greb and Kentucky Geological Survey [9]

2.2.2 Coal classification and petrography

There are several coal classification systems, ranging from graphical that were used earlier during the 20th century (Figure 2.2) to tabular that were established after the 1950s. Berkowitz [3] suggests that most of the classification systems are designed for humic coals that were aerobically altered, at least during a period of their evolution, while sapropelic coals are generally not included in the ranking systems as they are far less abundant. O'Keefe *et al.* [10] in a recent review article on the issue of coal classification, indicate that the overall consensus suggests classifying coal using two separate terms: coal type and coal rank. Coal type classifies coals into two major groups, humic and sapropelic (banded and non-banded respectively) and further subcategories based on petrographic composition [10]. Coal rank refers to

changes caused by the coal's thermal maturity during metamorphic development and reflects changes in the moisture content, percentage of carbon, percentage of hydrogen, percentage of volatile matter and calorific value[11].

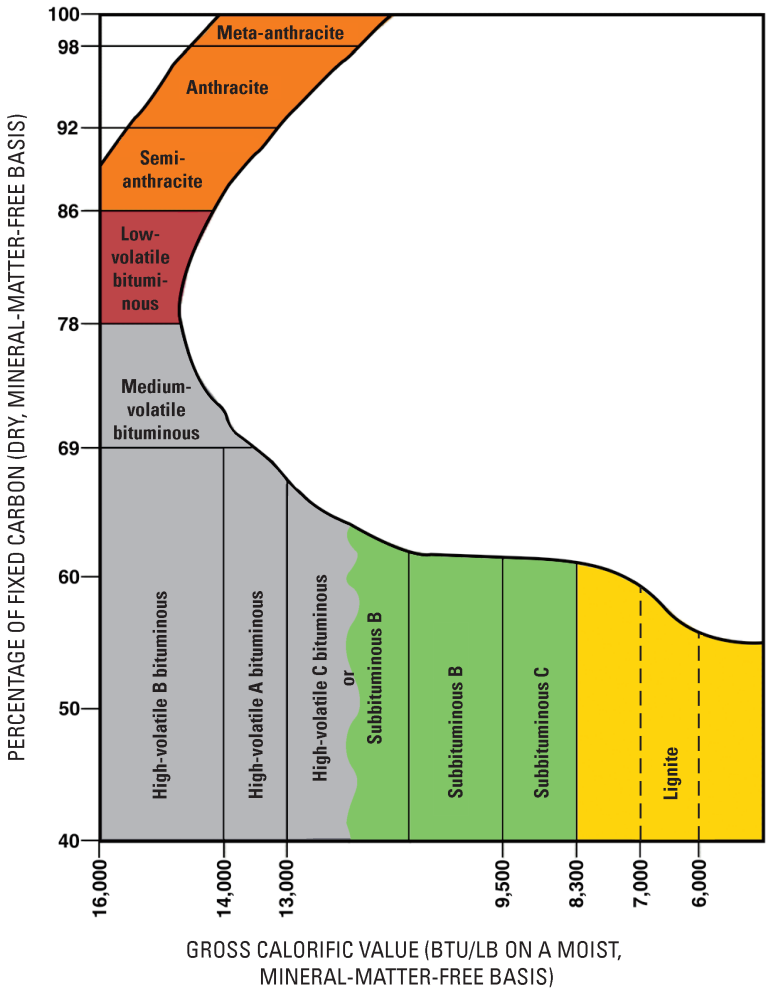

Figure 2.2: Coal ranking according to percentage of fixed carbon and gross calorific value. Reproduced from Schweinfurth[12] - product of US federal government

Berkowitz[3] comments that, although coal rank increases with depth, this is true mostly for undisturbed strata and a single seam, while in the case of comparison between multiple seams it can only account for the degree of maturation of the coal and not to indicate structural similarities adding that, in most cases, coal is "a uniquely constituted organic conglomerate".

Macroscopically coal is formed from four microlithotypes: vitrain, clarain, durain and fusain, with each one varying in appearance (Table 2.3)[3,8]. Each one of the lithotypes is a complex mixture of microlithotypes that are also referred to as macerals. These belong in three large groups: vitrinite, exinite and intertinite. Each maceral is comprised from different botanical components and cross-maceral differentiation can be performed both optically by direct observation using a microscope or by measuring other properties such as colour and

reflectance[3].

Table 2.3: Coal microlithotypes and their appearance along with maceral groups and their botanical origin. Composed from[3,8]

Microlithotype	Appearance
Vitrain	bright, black, narrow, glossy or vitreous, cracks, breaks into cubes
Clarain	semi-bright, Black, silky, straight layers or lenticular masses
Durain	Grey black, dull, rough surface, layers or lenticular masses
Fusain	charcoal like, small lenses, soft and friable, charcoal like
Maceral group	**Botanical origin**
Vitrinite	humic gels, wood, bark, cortical tissues
Exinite	algal remains, leaves, resins, waxes, fungal spores
Inertinite	carbonized woody tissues, detrital matter, fungal spores, mycelia

Precise ranking in recent years is performed based on reflectance analysis, however, as carbon content is increasing it becomes more difficult to differentiate between lithotypes[3,7]. In equally ranked coals, microlithotypes differ mostly in their hydrogen content rather than in their carbon content, however as the carbon content increases, hydrogen differences become smaller and almost indistinguishable when the carbon content is above 94%[3,13].

2.2.3 Mineral composition and functional groups

Mineral matter is not a part of the coal forming process, but it can enter the coal during different stages of the process. It can be found dissolved in the water, as particles or combined with the organic matter[7]. During diagenesis, wind or water may carry inorganic matter and bring it into contact with the decaying plant matter. During metamorphosis, mineral matter is deposited into the coal while being carried from surrounding waters[3]. Mineral matter, including trace elements, is mostly studied out of environmental interest however, there are cases where minerals have a catalytic action to certain reactions[3].

Aside from the differences in the carbon and hydrogen composition of coal, the existence of functional groups in coal may provide useful information regarding its composition end especially in the forms that oxygen, hydrogen and sulphur exist in the coal. Oxygen is abundant in low rank coals (<75% C) where carbocylic groups represent approximately 25% of the oxygen and hydroxyl groups up to 50% of the oxygen[3]. The content of hydroxyl groups in the coal has been shown to correlate negatively with carbon percentage, indicating a reverse relationship with rank[14]. During metamorphic development most of the -OCH_3 and -COOH groups are eliminated and in coals of more than 82% C the oxygen is in the -OH and -C=O groups[3,15] (Figure 2.3). Most of the organic nitrogen in coal is heterocyclic while amines, nitrates and cyano compounds are relatively limited[3]. Sulphur is less abundant that nitrogen an it exists in three forms: pyritic, sulphate and organic[14].

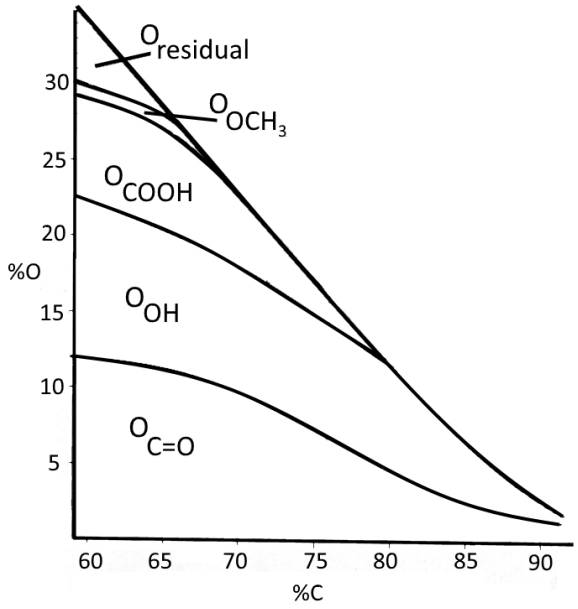

Figure 2.3: Distribution of oxygen species in the vitrains from different coal rank. Horizontal axis depicts carbon content (C%) and vertical axis oxygen content (O%). Adapted /redrawn from Blom [15]

2.3 Related coal processes

Since this thesis deals with the effluents that are being produced during gasification, the review will be limited to the processes and phenomena that involved the production and reactions of these liquids.

2.3.1 Oxidation by air/oxygen

Coals (except anthracites) are very sensitive to oxygen with even small amounts impacting their properties [3,14]. Once coal is exposed, oxygen is chemically absorbed onto its surface and several functional groups are developed that have acidic properties such as -OH, -COOH and =CO [3]. The primary degradation products of oxidation include humic acids, low weight organic acids (e.g. formic), CO, CO_2 and H_20. The development of functional groups may be in the following order: phenols $->$ quinones & acid anhydrides $->$ carboxylic acids [3,16] (Figure 2.4).

The primarily formed humic acids are degraded to sub-humic acids with initial products including hymatomelanic (yellow, light brown) / fulvic acids (white to yellow) and then benzenoid and polycarboxylic acids. All of these substances are complex and difficult to characterise mixtures [3]. Regarding their composition, sub-humic acids are mixtures of other components and their reactions give smaller molecules that are commonly found in other coal related products like coal tar [3,17] (Figure 2.5).

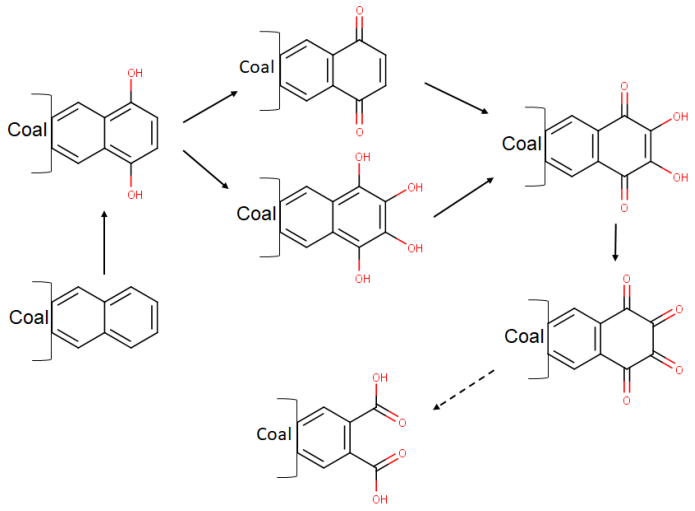

Figure 2.4: Reaction steps in the oxidation of coal (composed/adapted from Berkowitz[3])

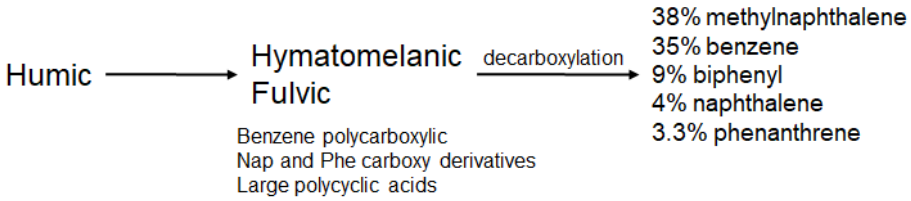

Figure 2.5: Degradation products of humic acids that derived from coal[3,17]

Temperature plays an important part during air oxidation with products differing significantly. Oxidation at temperatures below 70°C will produce little humic acid while at temperatures above 70°C humic acid production become significant. At temperatures exceeding 150°C breakdown products of humic acid begin to be formed and prolonged exposure may result in a complete conversion of the coal to humic acids and breakdown products[3].

2.3.2 Pyrolysis

The word pyrolysis comes from the Greek words πύρ (meaning fire) and λύσις (meaning here separation/breakdown/dismantlement) and refers to the thermal decomposition of materials. Pyrolysis is performed in an inert atmosphere but can also be performed in reactive atmospheres, e.g. when performed under hydrogen it is referred to as hydropyrolysis.

Regarding coal conversion, pyrolysis was mainly used for the production of coke but also to produce gases (e.g. ethylene), the production of chemicals (e.g. from petroleum), or even to produce synthetic fuels from coal. During pyrolysis, coal may lose up to 70% of its weight[18]. Pyrolysis has been used extensively in coal science in order to study various properties of coal and is also referred to as devolatilisation, or as carbonisation in commercial settings.

Pyrolysis of coal according to Berkowitz[3] takes place in three stages: limited thermal alter-

ation, active decomposition and secondary degasification. Limited thermal alteration takes place at temperatures below the temperature of active decomposition[3,19] (T_d) which has been set at 350-400°C[3,20], where the volatile content of the coal starts being devolatilised until secondary degasification (which begins at approximately 550°C), after which most of what is left is coal residue with few non-aromatic configurations[3]. According to Howard[20] decomposition continues until 950°C. There are several phenomena that take place during each decomposition stage, but the main effects are moisture loss for pyrolysis temperature $T_p < T_d$, loss of volatile content for $T_p < 550$°C and pyrolysis gases production for $T_p > 550$°C[3] (Table 2.4).

Table 2.4: Temperature dependent stages of coal decomposition during pyrolysis[3]

limited thermal alteration ($<T_d$) *moisture loss*	**active decomposition** (T_d-550°C) *loss of volatile content*	**secondary degasification** (>550°C) *emission of gases*
molecular rearrangement	molecular fragmentation	CO, CO_2: thermal breakdown
loss of CO, CO_2, H_2S	free radicals in residues	H_2: condensation of aromatics
partial dehydroxylation	dehydrogenation	CH_4: autohydrogenation
partial decarbohylation	scission of CH_2 bridges	H_2O:
metamorphic development effects	ring ruptures	

During pyrolysis, apart from the gases that are being produced during secondary degasification, the residues that are considered products of pyrolysis are light oils & tars (mostly counted together), aqueous liquor (liquid products) and coke which is the solid residue that is left after the coal has lost all its moisture and volatile content (Figure 2.6). The liquids products that are produced depend on several factors and parameters but the main are coal rank, petrographic composition (which determine the H/C and O/C ratios), pyrolysis type and maximum pyrolysis temperature which the liquids have been exposed to[3]. Regarding oils and tars, these are being classified by the industry as low temperature tar and high temperature tar, mostly referring to the maximum temperature of the carbonization[3–5].

Low temperature tars are considered those that have been produced at 500-600°C; they are generally heterogenous and have a high number of alkylbenzenes and other groups such as phenols and diols, methyl-pyridines, n-paraffins and olefins, all of which are in low percentages. Low temperature tars from lignite also have high percentages of alkanes (10%)[3,19,20].

High temperature tars are being produced at temperatures above 600 °C up to approximately 800-100°C. They are more homogenous and aromatised than low temperature tars, they have a high amount of benzene, toluene, ethylbenzene and xylene (BTEX) as the low boiling components, high percentages of naphthalene (10%), high boiling phenols and tar bases. The high boiling components are mostly 3-4 ring polycyclic aromatic hydrocarbons (PAHs) like anthracene, phenanthrene and acenaphthene but also high boiling heterocycles. Also, pitch in high temperature tar, accounts for a large percentage of the tar (50%), most of which is comprised by a large number of unidentified heavy aromatic compounds (>4rings)[3,19,20].

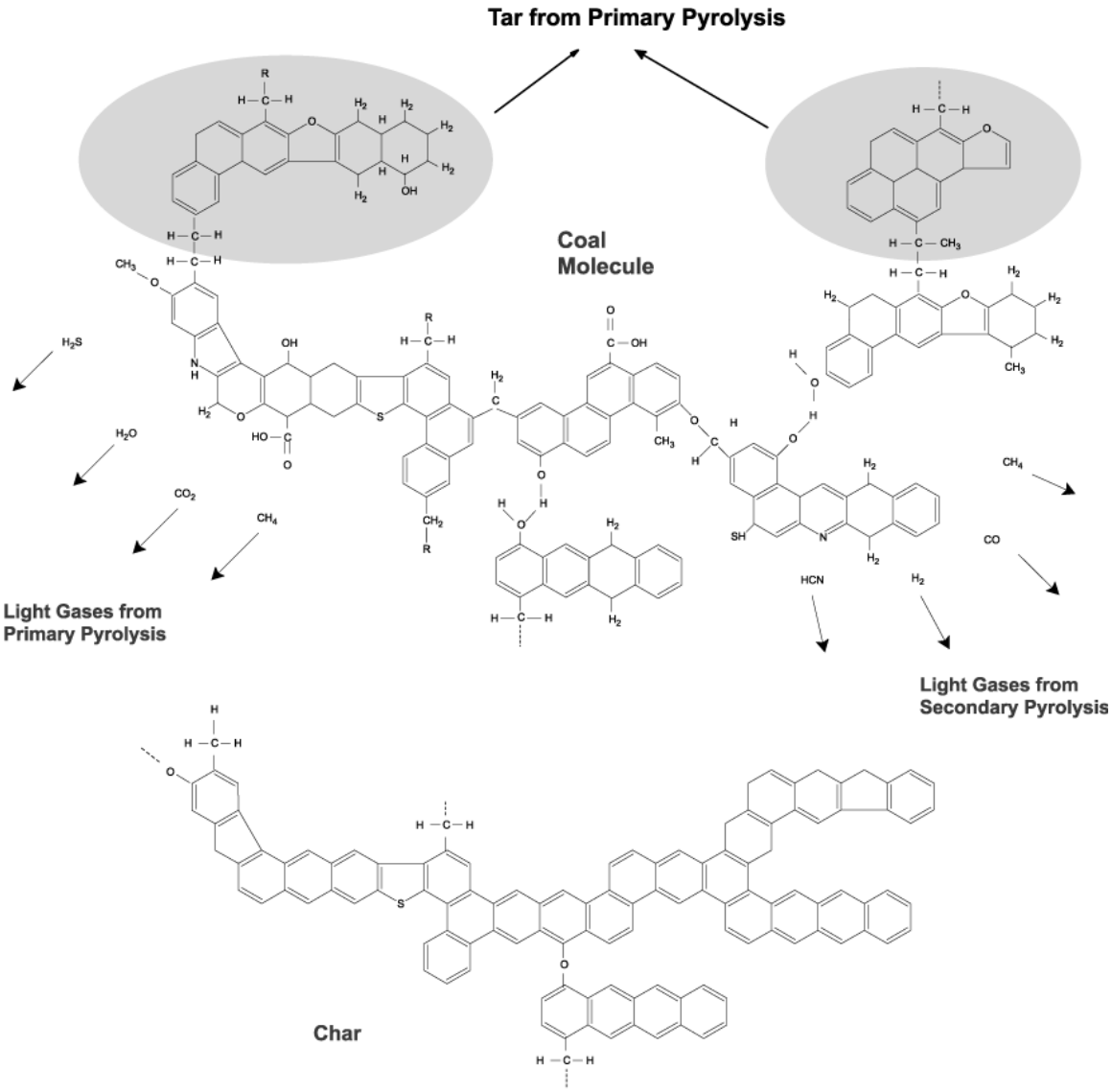

Figure 2.6: Coal molecule during the stages of pyrolysis, indicating the parts that are expected to form tar and char during the process. Copied from Veras *et al.* [21]

Tars that have been retained into pyrolysis systems, e.g. trapped within coke particles, may undergo secondary reactions like thermal cracking, where light hydrocarbons may react and form larger aromatic moieties[22,23]. Especially in the case of pyrolysis where the atmosphere is not reactive, thermal cracking may result in many radicals leading to condensation of aromatics[23].

2.3.3 Gasification

The aim of the process of gasification is to convert all the organic carbon of the coal into a gaseous combustible form that can be used for other purposes. To accomplish this, gasification is performed with around one fifth to one third of the oxygen needed for the complete

combustion of the coal. The gas that is produced during gasification is also referred to as syngas (from synthesis gas) and its combustible components are H_2, CO and low levels of CH_4. It also contains significant amounts of CO_2, and small amounts of other gases such as H_2S and acetylene[18,24]. Gasification can be performed both at the surface and underground (*in-situ*). When gasification is performed underground it is referred to as underground coal gasification (UCG) and it is discussed thoroughly in the next section. Surface gasifiers are not discussed as they are outside the context of the thesis.

Gasification of coal essentially includes two major processes: pyrolysis and gasification. During pyrolysis the coal is heated to produce char, liquids and gases. Devolatilisation temperatures are coal rank dependant and begin at around 320 °C[25]; after 400 °C the pyrolysis reactions take place[18]. Pyrolysis is responsible for around 70% of the weight loss of the coal during coal conversion. As the temperature rises above 700 °C, the process of gasification begins where char reacts with the gasifying agent (oxygen, steam) to produce ash and gases[18]. The main gasification reactions that produce the heat that is required for the gasification to take place is combustion (1) and partial combustion (2) (oxidation reactions).

$$C + O_2 \rightleftharpoons CO_2 \quad \Delta H = -405.9kj/mol \quad (1)$$

$$C + \tfrac{1}{2} O_2 \rightleftharpoons CO \quad \Delta H = -123.1kj/mol \quad (2)$$

The produced heat drives the Boudouard (3) and the water gas reaction (4) to produce carbon monoxide and hydrogen. Hydrogasification (5) (which is significantly pressure dependant) also takes place (reduction reactions).

$$C + CO_2 \rightleftharpoons 2\,CO \quad \Delta H = 159.7kj/mol \quad (3)$$

$$C + H_2O \rightleftharpoons CO + H_2 \quad \Delta H = 118.9kj/mol \quad (4)$$

$$C + 2\,H_2 \rightleftharpoons CH_4 \quad \Delta H = -87.4kj/mol \quad (5)$$

Finally, the composition of the final gas is affected by the water-gas shift reaction (6) and methanation (7).

$$CO + H_2O \rightleftharpoons H_2 + CO_2 \quad \Delta H = 159.7kj/mol \quad (6)$$

$$CO + 3\,H_2 \rightleftharpoons CH_4 + H_2O \quad \Delta H = 118.9kj/mol \quad (7)$$

Coal volatiles undergo secondary reactions which, unlike pyrolysis, happen in a reactive atmosphere due to the existence of H_2, CO_2 and H_2O. Due to the high temperatures during gasification, reactions happen in the gas phase. Tar (and thus SVOCs) decomposition may speed up when CO_2 and H_2O are present[23] since they react with free radicals (studies show the existence of steam favours cracking[26]). The gaseous environment of gasification also includes H_2 with which radicals may react faster, thus, SVOC decomposition may be suppressed since the reaction of the radicals with H_2 may cause the molecules to be reformed[23]. However, this effect appears to be temperature dependant[27].

2.4 Underground Coal Gasification

Underground coal gasification is the process of *in-situ* conversion (partial combustion) of coal deposits into combustible gaseous products (H_2, CO, CH_4) cumulatively referred to, as mentioned above, as syngas. UCG is performed as an alternative to coal mining in coal seams that cannot be accessed or are too expensive to mine using conventional techniques. Instead of mining the coal and gasifying it on the surface in a gas manufacturer plant, UCG takes place underground inside the actual coal seam by introducing gasifying agents using boreholes. The injection well is used to inject the gasifying agent and ignite the seam (which can be air, oxygen, steam or their mixtures) and the production well is used to transfer the produced syngas to the surface for further processing (Figure 2.7). UCG is similar to surface gasification regarding the chemical reactions involved[1,28–30].

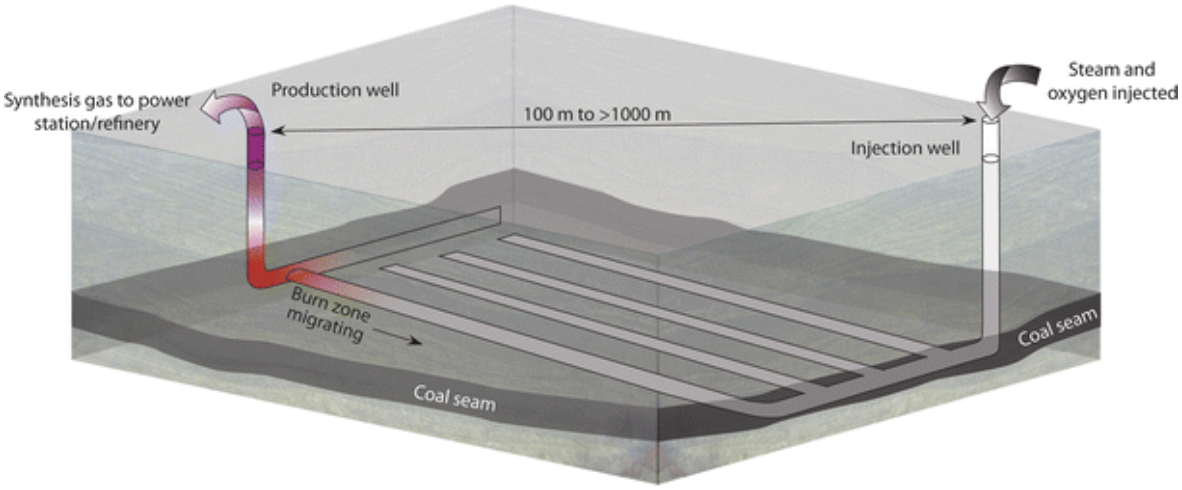

Figure 2.7: Typical installation layout during an underground coal gasification (UCG) operation. Injection and production wells are visible along with multiple channels inside the coal seam where the gasification takes place. Reproduced from Younger[30] with permission.

After ignition of the coal seam and initiation of the gasification process, coal starts to lose its moisture content and undergoes pyrolysis above approximately 400°C. Accompanying the release of hydrogen-rich matter during gasification are coal tars, hydrocarbon gases and aqueous liquor. The residual tar that is trapped in the seam is also gasified at higher temperatures releasing gases, tar vapours and solid residues[28]. According to Younger *et al.*[29], the produced syngas contains approximately 80% of the initial calorific value of the gasified coal. Measurements taken from UCG operations have shown that syngas composition varies as follows: hydrogen (11-35%), carbon monoxide (2-16%), methane (1-8%), carbon dioxide (12-28%) while also including other minor components[29].

UCG was conceived as an idea during the late 19th century but was not applied in a large scale until the early 20th century in the Soviet Union. Although several UCG research projects existed both in Europe and the United States throughout the century, the technol-

ogy was not commercialised. UCG operations in Russia ceased in 1996 but there is still an active commercial UCG plant in Uzbekistan[31]. Most of the application of UCG in the Soviet Union was performed without extensive environmental investigations and theoretical model development on UCG, both of which were introduced during the 1970s when the major UCG projects took place in the United States (US)[32]. Several projects were performed in the US over a course of nearly 15 years and several public and private organisations were involved in these projects including the Lawrence Livermore National Laboratory (LLNL) and the Western Research Institute (WRI), while the Department of Energy (DoE) was also involved[33]. Work performed during these projects was published in the form of technical reports, conference proceedings (in total 14 underground coal gasification symposiums organised annually) and journal papers (mostly in the "In situ" journal). Readers are referred to databases such as the LLNL on-line library, the Office of Scientific and Technical Information (OSTI) and the National Technical Information Service (NTIS) for further access to related material.

There are four general methods for performing UCG: linked vertical well (LVW) by a) hydrofracking and/or reverse combustion, b) by an in-seam borehole, c) using a controlled retractable injection point (CRIP) and d) UCG in steeply dipping seams[28] (detailed explanation of each method goes further than the purpose of this review). From a process engineering perspective, the principal mechanisms that govern the UCG process are: mass transport, combustion, cavity growth and spalling. In order to simulate the process, the implementation of a Thermo-Hydro-Chemical-Mechanical (THCM) approach is required[2].

Like conventional pyrolysis and gasification, UCG produces significant amounts of SVOCs; however, it cannot be viewed simply as pyrolysis or gasification but as a mix of both processes. In order to better understand the production of SVOCs, one must rely on theoretical models that explain the various temperature regions and phenomena that take place within the UCG cavity. Theory on temperatures zones and the regions within a UCG reactor can be traced back to Gibb and Partners[34] who made suggestions for gas composition and temperature profiles along the length of the cavity. After a number of UCG trials in the United States, Gunn and Krantz[32] developed two models to describe UCG, a packed bed model for UCG operations with no permeability enhancement, and the open channel gasification model (Figure 2.8), which describes the type of gasification that takes place in UCG within an introduced high permeable path (such as in the majority of modern UCG operations). The model divides the gasification cavity into three major zones: the combustion zone, closest to the injection well, the gasification zone and the devolatilization zone, furthest from the injection well. Syngas is mainly produced in the gasification zone where the major gasification reactions take place. The devolatilisaton zone is leading the UCG front (which moves towards the production well) and this is where coal is dried and stripped from its volatile content and, eventually, takes the form of coke which is the form of carbon that reacts with the oxidants into syngas.

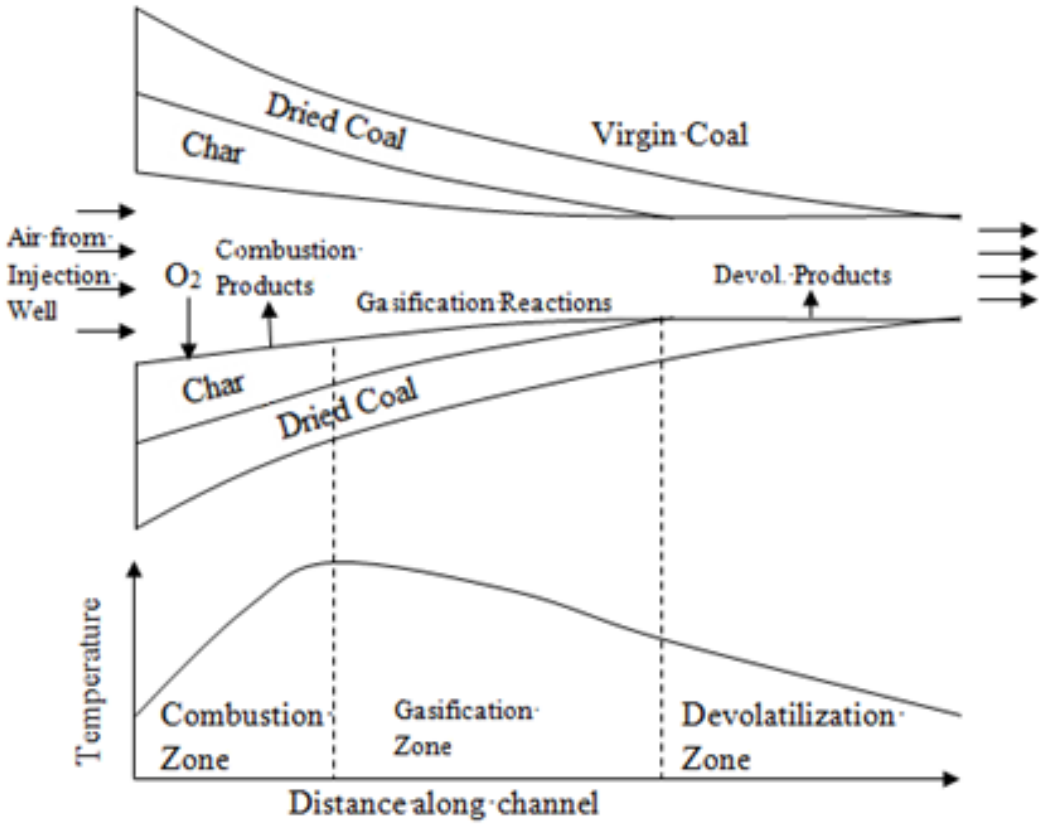

Figure 2.8: Open channel gasification model as suggested by Gunn and Krantz[32]. Reproduced from Khan *et al.*[35]. Three distinct zones are visible: combustion, gasification and devolatilization

More recent models have re-evaluated/enhanced some of the concepts from Gunn and Krantz[32] suggesting that gasification takes place in both the high and mid-temperature zones and devolatilisation also takes place throughout the UCG cavity[28,36] (Figure 2.9A); there are also models that are focusing on the cavity walls in order to describe several additional transport phenomena that take place[25,37–41] (Figure 2.9B).

Regarding the production of SVOCs an attempt is made here to qualitatively hypothesise the different phenomena that take place inside the UCG cavity and affect the production of SVOCs (Figure 2.10). Considering that the reactor is in a steady state and assuming that there are three temperature zones (taking into account the maximum temperature), volatile matter will get pyrolised at the walls of the cavity (as long as there is enough temperature to move into active decomposition) and provided there is a flux inwards/towards the cavity, volatiles are carried into the open cavity in a gaseous form. There, depending on the region of the reactor the following may happen: *upstream:* volatile matter may get combusted/gasified upstream depending on temperature and oxygen availability *midstream:* volatile matter released midstream may undergo a series of secondary reactions in a reactive environment as the products of gasification from the upstream region travel downstream; gasification may

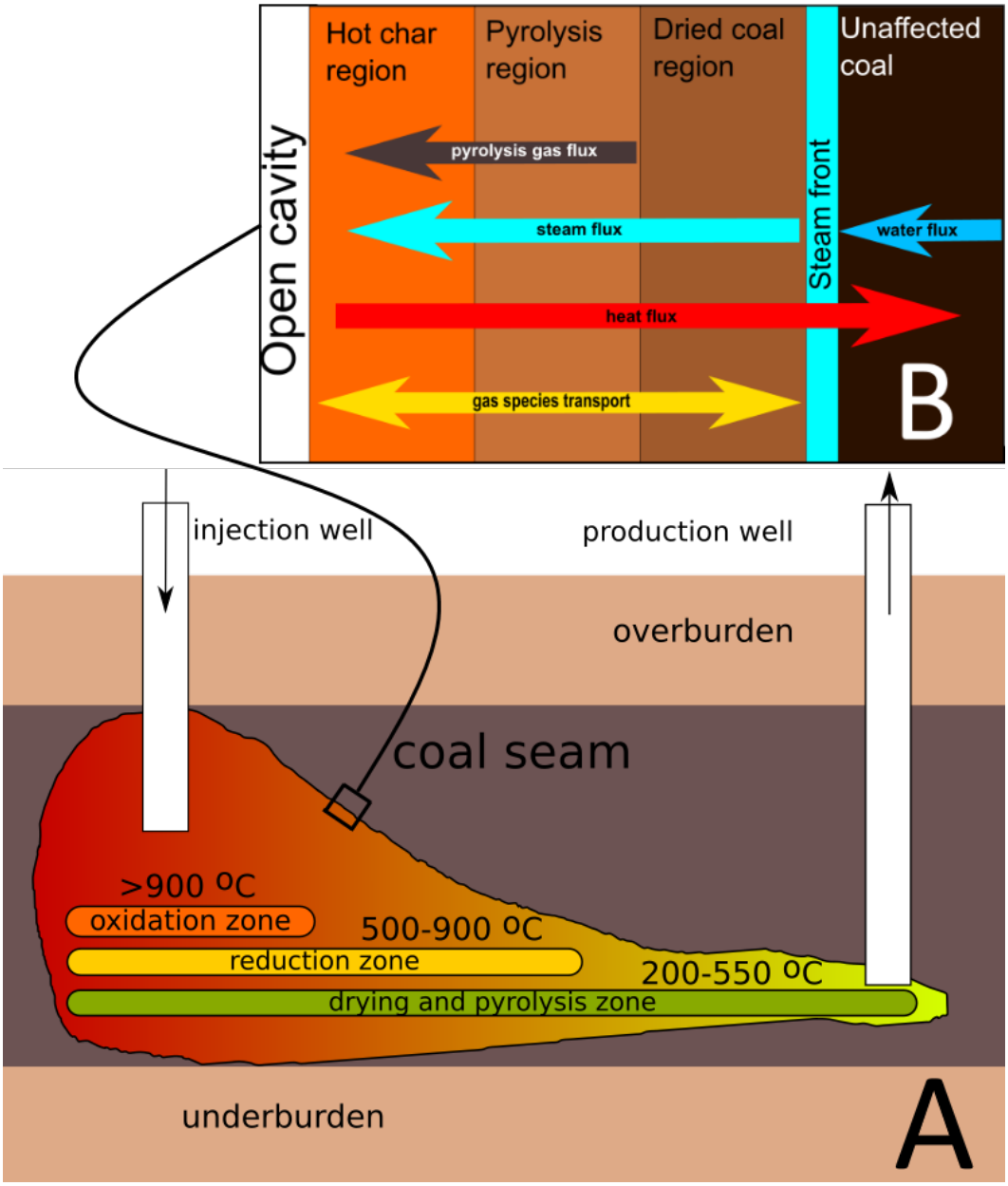

Figure 2.9: A: Schematic of the processes involved in a UCG cavity along with corresponding temperatures at each zone. The oxidation zone is confined close to the injection well, the reduction zones expands further and finally the drying and pyrolysis zone expands throughout the cavity but is more dominant at the lower temperature zone (based on Couch [28], Camp and White [36]) **B:** Cross section of the cavity wall showing the oxidation and reduction zones along with flux phenomena that take place (Adapted from Glaser and Owen [37])

also happen depending on temperature and O_2 availability *downstream:* what will happen downstream depends mostly on temperature and ranges from devolatilisation/pyrolysis in a reactive environment to just limited thermal alteration and moisture loss.

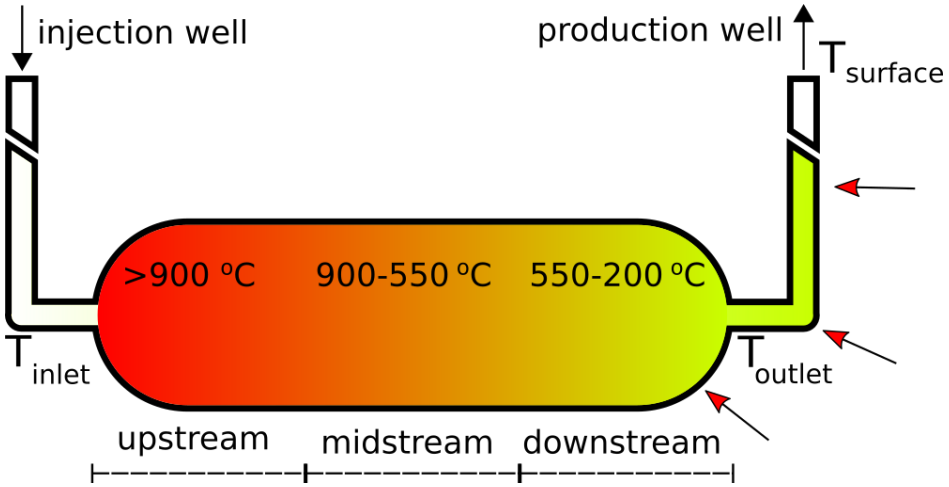

Figure 2.10: Schematic of a hypothetical UCG reactor depicting three regions that are determined by their maximum temperatures: upstream, midstream and downstream. The red arrows close to the outlet and the production well indicate areas where tar condensation/fractionation may take place

Depending on downstream cavity temperatures and the temperature difference between $T_{surface}$ and T_{outlet}, heavy compounds may condense downstream at the cooler parts of the cavity/infrastructure and tars may fractionate as they move along the production well. This distillation/fractionation phenomenon was first suggested by King *et al.*[42] and confirmed later by simulated distillations[43,44]. It appears that adequate temperatures at the cavity outlet are essential in order for SVOCs to evacuate the cavity[45] and this was confirmed more recently in a field trial conducted at the GIG[46] where approximately 60% of the tars were calculated to remain underground.

The major organic species that are associated with UCG groundwater pollution are phenolic compounds followed by BTEX, PAHs and nitrogen containing heterocyclic compounds. Inorganic species of concern include ammonia, sulphate, cyanides and heavy metals[47,48].

However, as shown above, coal is a complex material and its conversion processes are also complex (Section 2.3.2 & 2.3.3 - Figure 2.6). The break-down of coal may result in hundreds or even thousands of different organic compounds; a significant number of these compounds are expected to be found in the effluents of the aforementioned conversion processes[3,20,49]. This is also true in the case of underground coal gasification[48,50]. From an environmental risk assessment point of view, only a small amount of organic compounds are monitored in UCG condensates[47,51], however the complexity of the UCG effluents and their potential variability calls for more comprehensive analysis; this is especially true regarding semi-volatile organic compounds which are expected to be the primary organic constituents[52]. Detailed analysis

of their content may provide invaluable information on unravelling the complex physico-chemical phenomena that take place during UCG. An investigation of the organic nature of these effluents is provided in the following chapters.

Chapter 3

Analysis of SVOCs in coal gasification waste-water

3.1 Introduction

The process of underground coal gasification, and coal gasification in general, produces by-products such as tars and aqueous condensates that end up in the production stream along with syngas. These are separated from syngas at a condenser or a gas scrubber located along the production pipeline (Figure3.1). Water in the aqueous condensates, that are also referred to as waste-water or aqueous liquor, is formed from condensed water vapour that was originally either coal moisture, pyrogenic water from hydrogen combustion or, in the case of UCG, water ingress from the surroundings of the coal seam[40,53,54].

Analysis of gasification waste-waters is important as they are a by-product of the UCG industry and operators are responsible for its proper management, treatment and disposal. Therefore, a complete risk assessment for UCG trials must take under consideration the chemistry of the effluents as research has shown they are associated with high levels of acute toxicity[54]. Waste-water composition is also desirable for determining any retrievable components of high economic value and for deciding on waste-water treatment strategies. UCG waste-waters are very complex matrices which are rich in both inorganic and organic compounds, and regardless of treatment options operators may also be required to investigate for the retrieval of components of economic value e.g. phenol[55]. Research has shown that the levels and occurrence of various compounds in these condensates may be influenced by several factors such as coal rank[54] and gasification conditions[56]. One can conclude that high risk factors along with process economics and the possibility of gaining new process understanding makes the analysis of UCG waste-water both necessary and desirable. Overall, there is a consensus that, at least in the freshly produced aqueous condensates, the main semi-volatile

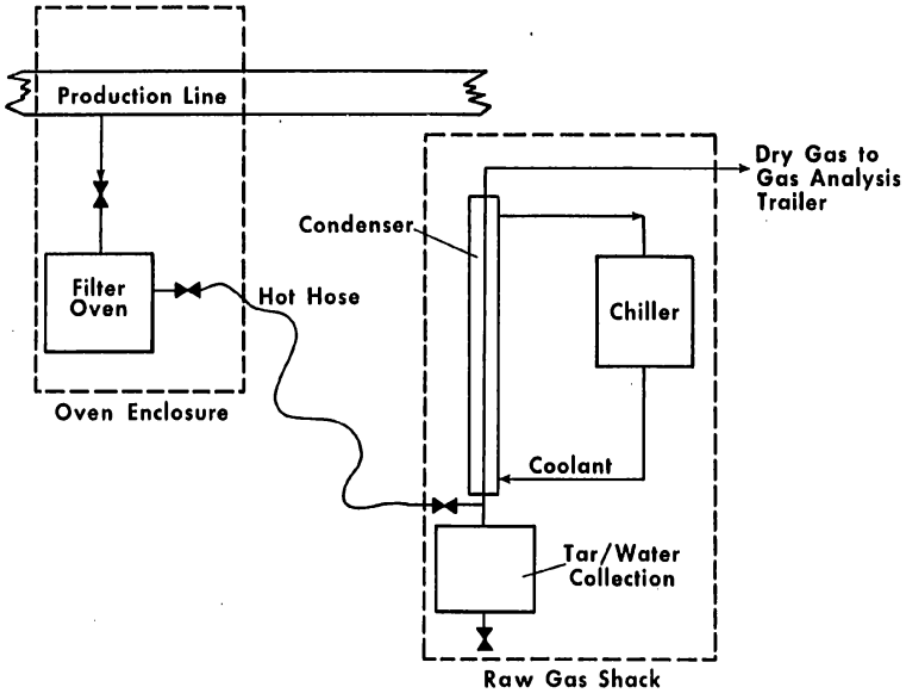

Figure 3.1: Online system for the collection of tar and waste-water during the Rocky Mountain I UCG trial. Copied from Barbour *et al.*[44] credit: U.S. Department of Energy, Western Research Institute

organic compounds (SVOCs) are phenolics, while other organic components include benzene, toluene, ethylbenzene and xylene isomers (BTEX), polycyclic aromatic hydrocarbons (PAHs), pyridines, anilines, quinolines, organic acids and more polar compounds such as hydantoins[54,57–61]. Their complex nature along with very large differences between the concentration levels of the various components makes the characterisation of coal gasification waste-water a challenging task[57].

Reports of coal gasification waste-water analysis date back to the 1970s where Schmidt *et al.*[52] applied a "salting-out" enhanced, dichloromethame (DCM) based liquid-liquid extraction (LLE) method to extract SVOCs from waste-water produced from a coal gasification of 6 coals that were gasified using the the "Synthane" process. The method required around 2L of sample and significant amounts of DCM; basic and acidic fractions were analysed separately using GC-MS. The extracted water showed about 60-80% phenolic content and 20 compounds were found to be present in all 6 waste-waters. Pellizzari[62] performed a semi-targeted approach to analyse coal gasification waste-water and tar. The approach includes purging a volume of the sample with helium in a special apparatus to remove volatiles and semi-volatiles and trapping them on a Tenax cartridge from where they were later removed thermally. SVOCs that remained in waste-water and tar samples were extracted with Freon-TF® and then analysed with gas chromatography[50,62]. Although the method appears to be

exhaustive it included the use of multiple steps, specialised equipment, multiple GC set-ups and the use of chlorofluorocarbons that are not environmentally friendly[63]. Stuermer *et al.*[48] applied a multi-step LLE scheme for the extraction of coal gasification water using DCM into acidic, neutral and basic fractions. Although the method was exhaustive, it required large amount of sample (1800mL), large amounts of solvent (1600mL) and a significant number of extraction steps (26) that make the method very labour intensive and expensive, and the analysis of multiple samples would require large amount of time and solvent. Tobben *et al.*[64] suggested a similar extraction method to process laboratory produced coal waste-water first by separating the dissolved compounds in organophilics and hydrophylics following additional fractionation into organophilic acids bases and neutrals. The method was exhaustive and provided a good fractionation approach but it is also labour intensive. On a more direct approach, Humenick and Mattox[60] analysed UCG waste-water by direct aqueous GC injections for phenols on a free fatty acid phase (FFAP) column. Phenols were analysed using the same set-up for UCG produced tar/oils after dissolution 2% in hexane. Non-phenolics were analysed by solvent extraction following back-extraction of phenolics and pre-concentration before injection on a poly(dimethylsiloxane) SP2100 column. A BBBT (bis(p-butoxybenzylidene) a,a'-bi-p-toluidine) column was used for the separation of PAHs. Although the method provided quantitative results for many compounds, it required multiple GC set-ups and the direct injection of aqueous solutions are not recommended due to the large volume expansion of H_2O and possible column deterioration. The complexity of coal gasification waste-water became even more obvious when Wang and Zhao[57] applied a multiple fractionation, multiple technique set-up to fully characterise gasification waste-water. This was performed by multiple LLE extractions, fractionation and resin absorption with chemical oxygen demand analysis (COD) between steps to access the organic content after each extraction. The extracts were analysed using both liquid and gas chromatography with the application of derivatisation in some steps. Although this approach appears appealing in terms of how exhaustive it is, it is labour intensive and expensive and certainly not very useful when the analysis of multiple fractions is required with the aim of performing cross-sample comparisons.

From a sample preparation point of view, it would be highly desirable to move the above methods in to a micro-scale so that they better fit the modern analytical lab. Dispersive liquid-liquid micro-extraction (DLLME) was initially considered an attractive option for transferring the waste-water extraction methods into a micro-scale. It includes extraction of analytes from aqueous samples by injecting an organic solvent (like dichloromethane or toluene) together with a polar solvent, (methanol, acetonitrile) called the disperser, into an aqueous sample. The polar solvent helps the less-polar solvent to disperse into the sample and form an emulsion[65]. Although DLLME was originally developed for the extraction of PAHs[65] and initially may appeared as a good choice for the extraction of coal gasification

waste-water, it was not considered further. This is because the addition of a polar disperser solvent alters the aqueous sample by making it more organophilic, thus, for the more polar compounds, like phenols, this will have an effect on the partition coefficients between the sample and the extraction solvent. Evidence to support this appear in the literature where the developed methods focus mostly on alkyl phenols, for example Bernardo *et al.* [66] reports recoveries for cresols as low as 45.2% (with recoveries increasing with increasing alkylation) while Zgola-Grzeskowiak [67] reports a recovery for octylphenol at 66%. Consecutively, the search for a more suitable micro-extraction technology was focused on ultrasound enhanced methods.

According to Suslick [68] "ultrasound causes high energy chemistry" and does so through the formation and collapse of bubbles in a liquid phase, a phenomenon referred to as acoustic cavitation. Cavity collapse is accompanied by enormous local temperatures and pressure [68,69] also referred to as "hot spots". Some of the phenomena that incur in sonochemistry (the application of ultrasound in chemistry) through cavitation are bond breakage (sonolysis), emission of light (sonoluminescence), and reaction catalysis (sonocatalysis) [68,70]. Until recently the use of ultrasound (US) for sample preparation was not at all common with the previous decade being a set-point for its application in the field of analytical chemistry [71]. US assisted liquid sample preparation methods include a wide range of reactions such as derivatisation, oxidation and hydrolysis and ultrasound assisted LLE, emulsification and homogenization. US application is not limited to liquid samples and includes solid-liquid extractions [72]. Two types of ultrasonic generators can exist in a laboratory: ultrasonic baths and ultrasonic probes. Ultrasonic baths are primarily designed for degassing and cleaning glassware and only allow for time to be optimised while featuring a typical decline in power with time and a non-uniform ultrasound transmission, both of which can result in poor reproducibility [71,72]. Especially the non-uniformity of sonication baths was demonstrated by Kotowska *et al.* [73] where placing the tube on different location in the bath showed different extraction efficiencies. In addition, sonication frequency cannot be changed in ultrasonic baths and the fact that not all baths use the same frequency may lead to replication/reproducibility issues. Low energy transmittance is also an issue with sonication baths where high amounts of energy are needed, for example when digesting organic matter for chemical oxygen demand determinations [71,74]. These limitations do not apply in the case of ultrasonic probes which can significantly improve emulsification and mass transfer between two immiscible liquid phases. It has been shown that the emulsification rates during ultrasonic induced emulsification with a sonication probe is significantly higher than with a sonication bath [75]. Operational parameters of ultrasonic probes that can be optimised are power, pulse duration and amplitude and can be optimised using multivariate designs [71,72].

Ultrasonic emulsification between two immiscible phases takes place when ultrasound induced cavities are both produced and collapse; the phenomenon requires the presence of a

gas (e.g. air in atmospheric pressure) and cannot take place *in vacuo*[76]. Cavitation causes fragmentation of one phase into the other resulting in a sub-micron emulsion that hugely increases contact surface between phases[77,78]. Generally, it can be said that ultrasonic emulsification is results of multiple phenomena with complex relationships[76,78–80]. The potential of ultrasound assisted emulsification in analytical chemistry was first demonstrated by Pérez-Serradilla *et al.*[81] who simultaneously extracted polar and non-polar compounds from grape seeds, acorn and alperujo. The extraction was performed by placing the sample and immersing a sonication probe in a beaker containing a 80:20 solution of n-hexane and methanol-water mixture. The application of sonication here had a double effect - extracting the compounds from the sample and emulsifying the mixture into which the extracted compounds solubilised and into which mass transfer took place, transferring polar compounds to the methanol-water phase and non-polar compounds to hexane. The emulsion was removed and disrupted by centrifugation and each phase, water-methanol and n-hexane, were analysed using high performance liquid chromatography coupled to diode array detector (HPLC-DAD) and gas chromatography coupled to mass spectrometry (GC-MS) respectively (extraction time between 9-20min).

Ultrasound assisted emulsification is also used in liquid-liquid extraction (USALLE), when extracting components from an aqueous phase into an organic phase. Relative to the scope of this chapter are the extraction of PAHs, phenolics, and other compounds of similar nature from coal gasification wastewaters. Regarding PAHs, Saleh *et al.*[82] demonstrated the use of ultrasound-assisted emulsification micro-extraction (USAEME) in the extraction of PAHs from water samples using low-density solvents. Here a small volume of toluene (14μL) is injected into a water sample in home-made glass centrifuge tube and sonicated for 30s. The emulsion is broken by centrifuging and 4μL of solvent are collected through a narrow capillary-like opening at the top of the tube and injected in a GC-FID. The method reports relative low extraction recoveries with naphthalene having the lowest (59.2%) but higher PAHs are extracted more efficiently (pyrene 77.6%, chrysene 90.5%). Although the method is promising, the use of a complex home-made tube and the relative low recoveries are not very desirable. Ozcan *et al.*[83] developed a similar ultrasound-assisted emulsification-microextraction (USAEME) method for extracting PAHs from water this time by injecting 100μL of chloroform instead of a low-density solvent and sonicating for 15min in a ultrasonic bath. The emulsion is broken with centrifugation and the organic phase is sedimented and recovered with a syringe. They compared the method's performance with traditional LLE and solid phase extraction (SPE) reporting higher recoveries in spiked/fortified tap water for the USAEME method (for naphthalene: USAEME $95 \pm 5\%$, LLE: $81 \pm 4\%$ and SPE: $68 \pm 7\%$). However, since chlorinated solvents are hazardous and not environmentally friendly their use should be generally avoided. Thus, Cheng *et al.*[84] developed a method based on low-density USAEME but by adding a surfactant in order to further enhance the

ultrasonic emulsification process (a concept firstly introduced by Wu *et al.* [85] for carbamate pesticides analysis - ultrasound-assisted surfactant-enhanced emulsification microextraction (UASEME) is considered a variant of dispersive liquid-liquid microextraction DLLME). This method includes the addition of 20μL of cyclohexane along with 10μL of TWEEN® 80 surfactant into a glass tube containing 5mL of sample with 6% NaCl (which aids the extraction by salting-out during phase separation) and sonicating for 1min. The tube is fitted with a rubber plug, inverted and recovering the organic phase by puncturing the rubber plug with a syringe. Only relative recoveries are reported, and specifically for naphthalene the relative recovery values are 108% for tap water, 80% and 119% for waste-water.

Regarding phenolic compounds, Pizarro *et al.* [86] reported the optimisation of a USAEME method for the analysis of haloanisoles and volatiles phenols in wine using GC-MS/MS. The method includes the injection of 200μL of carbon disulphide into 5 mL of sample with 3% NaCl and sonicating at 40°C for 7min. Emulsions were broken by centrifuging and analysed using GC-MS/MS. Recovery values for validation are reported only for haloanisoles but from the method development section it can be seen that the highest recoveries for volatile phenols with carbon disulphide as the solvent are approximately 90% for ethylguaiacol, 35% for ethylphenol and 22% for vinylphenol. Kotowska *et al.* [73] developed a USAEME method to determine phenols and pharmaceuticals in municipal waste-waters. The method includes injecting 40μL along with 300μL of acetic anhydride (derivatisation reagent) into a glass tube containing 5mL of sample and 0.4g of sodium hydrogen phosphate. The tube is placed into an ultrasonic bath and sonicated for 5min. The emulsion is disrupted by centrifugation, the organic phase recovered and injected to a GC-MS for analysis. Reported recovery values for phenols are between 94-108%. Reboredo-Rodríguez *et al.* [87] applied USAEME in determining phenols in a non-aqueous matrix, olive oil. The method included the injection of a MeOH:H2O 80:20 mixture into a mixture of 3g of oil and 6mL of hexane in a polypropylene tube. The mixture was shaken in a vortex and placed in the ultrasonic bath for 15min. The emulsion was broken by centrifugation, the sedimented phase was removed, the process was repeated a second time and the sedimented phases were combined and injected in a HPLC-DAD for analysis. Recoveries ranged from 115% to 91%. Although the addition of a surfactant would first seem at it may trap the phenolic compounds into micelles, performing UASEME with a surfactant concentration far below the critical micelle concentration (CMC) and just enough to in aid the dispersion would prevent this.

After reviewing the available methods in the literature for analysing coal gasification waste-water it became obvious that the development of an exhaustive microextraction method will greatly benefit the field since most of the available methods for the exhaustive extraction of SVOCs from coal gasification waste-water are time and labour intensive, use a lot of extraction steps, large quantities of solvent and require large amounts of sample. On the other hand, to the author's knowledge, no microextraction methods are available for the exhaustive,

untargeted extraction of SVOCs from waste-water since the available methods are focused on specific compound groups such as PAHs and phenols. Therefore, a fast microextraction method for the exhaustive extraction of SVOCs will not only be more appealing than traditional methods to laboratories that characterise gasification waste streams (due to the minimal amount of time and effort required to process a sample and comprehensive results to operators faster), but it would also benefit the analytical chemistry community that deals with untargeted analysis such as foodomics and environomics. Here, the use of USAEME is demonstrated in the development a fast and precise, close-to-exhaustive extraction method for SVOCs from coal gasification waste-water. The method employs a unique vessel-wall sonication system that can direct focused energy directly inside the contents of a glass vessel without coming into contact with the sample. The probe is commercially available but significant enhancements are introduced by the author for the use of glass vessels. Since the effect of salting-out plays a significant part in the extraction, a new method term is suggested: ultrasound-assisted surfactant enhanced salting-out emulsification microextraction - UASESOEME.

3.2 Materials and methods

3.2.1 Chemicals

Cyclopentylmethyl ether (CPME) stabilised with 50ppm butylated hydroxytoluene (BHT), 2-picoline, o-cresol, benzoic acid, 5,5-dimethylhydantoin (5,5-DMH), phenanthrene, cetyltrimethylammonium bromide (CMC - 0.92 to 1.0 mM) (CTAB) and 4-fluorophenol were obtained from ACROS Organics. Toluene, cyclohexane, phenol, naphthalene, indole, 1-fluoronaphthalene and 5-fluoroindole were obtained from Sigma Aldrich. Benzonitrile, 4-fluoro-2-methylpyridine and 4-bromo-2,6-dimethylpyridine were obtained from Alfa Aesar.Phenol-d6 and naphthalene-d8 were obtained from Supelco, o-xylene and 1-methylnapthalene from Fluka and lastly, HCl, KOH, NaOH, NaCl and Na_2SO_4 were obtained from Fisher. All reagents were of analytical grade or better. Type-1 water was milli-Q from Millipore. The coal gasification waste-water sample was obtained from an *ex-situ* coal gasification experiment performed in the Laboratory of Experimental Installations of the Central Mining Institute (GIG) located in Katowice, Poland. Coal tar partitioning water was prepared using weathered tar from a former manufactured gas plant (WFMGP) by adding 1.02g of weathered tar (DNAPL008[88] (dense non-aqueous phase liquid (DNAPL)) into a 500mL glass bottle, topping up with water containing 0.01N $CaCl_2$ (0.555g of $CaCl_2$ in 1000mL H_2O) and placing on an orbital shaker for 18h then equilibrating in the dark for at least 3 days[89].

Model compound selection In order to accurately assess and optimise the effects and parameters of the extraction process for optimal analyte recovery, a study on model compounds was performed. The study involved the use of ten model compounds covering a broad spectrum of partition coefficients, solubilities and polarities. These compounds were selected to be as representative as possible of the compounds present in UCG waste-water and selection was based on compiling data from the literature while taking into account the compounds' physicochemical properties, such as the octanol-water partition coefficient (logP or K_{OW}) (the ratio of a compound's concentration in octanol to its concentration in the aqueous phase in a two-phase octanol/water system) which is a measure of a compound's hydrophobicity. A list of the selected compounds (along with some of their physical properties) can be seen in Table 3.1 and their chemical structures in Figure 3.2.

Table 3.1: Selected model compounds with some of their properties

Compound	logP	S[1][mg/mL]	[D][1]	Hpc[2][atm m3/mol]
5,5-dimethylhydantoin	-0.45	67.2	2.032	2.77E-09
o-picoline	0.89	47.1	1.278	9.96E-06
benzoic acid	1.63	4.31	3.428	3.81E-08
phenol	1.67	120	2.087	3.33E-07
benzonitrile	1.83	2.60	2.171	5.21E-05
indole	2.07	0.647	0.443	5.28E-07
o-cresol	2.18	6.67	2.096	1.20E-06
naphthalene	2.96	0.0738	0.00	4.40E-04
o-xylene	3.00	0.466	0.159	5.18E-03
phenanthrene	3.95	0.00119	0.031	4.23E-05

Where S: intrinsic solubility; D: dipole moment; Hpc: Henry's pressure constant

[1]Chemicalize was used for to predict this property, 2017, https://chemicalize.com/ developed by ChemAxon (http://www.chemaxon.com)

[2]US EPA. [2018]. Estimation Programs Interface Suite™ for Microsoft® Windows, v 4.11. United States Environmental Protection Agency, Washington, DC, USA.

From the compounds listed in Table 3.1, o-xylene, 2-picoline, phenol, o-cresol, napththelene, phenantherene, benzonitrile, benzoic acid and indole, all appear in UCG related literature[48,51,90]. The compound 5,5-dimethylhydantoin, is formed in the condensate during gasification by the Bucherer-Bergs reactions and it is normally analysed by high performance liquid chromatography (HPLC)[59], mainly due to its very high polarity (log K_{OW}) and hydrophilicity . This compound was included in the list because its extraction by the method, even in a small percentage, tests the potential of the method to extract and analyse high polarity compounds from coal gasification waste-water, while its existence in the condensate will indicate similarities of the *ex-situ* UCG process with the surface Lurgi gasifier.

Stock solutions of each model compound were prepared in ethanol. The compounds were split into three groups according to their water solubility. Group A stock solutions, consisted

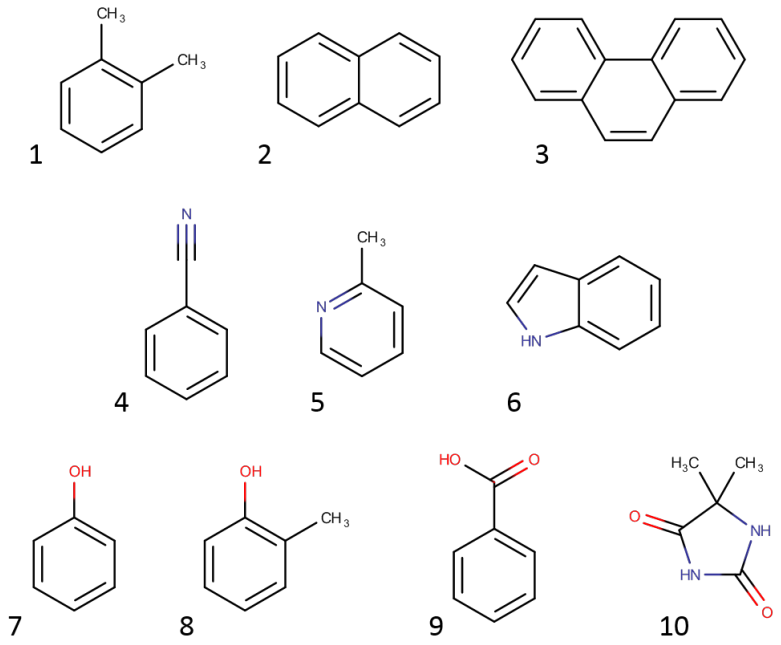

Figure 3.2: Chemical structure of the model compounds used for the development of the UASEME method. 1: o-xylene, 2: naphthalene, 3: phenanthrene, 4: benzonitrile, 5: 2-picoline, 6: indole, 7: phenol, 8: o-cresol, 9: benzoic acid, 10: 5,5-dimethylhydantoin. Marvin was used for drawing and displaying the chemical structures, Marvin 18.22.0, 2018, ChemAxon (http://www.chemaxon.com)

of phenol, o-cresol, benzonitrile, benzoic acid, indole, 2-picoline and 5,5-dimethylhydantoin were prepared at 20000 mg/L; group B, o-xylene and napthalene, were prepared at 10000 mg/L and group C, phenanthrene, was prepared at 1000 mg/L. The samples were stored at -20°C. From this initial stock solutions a series of standards were prepared for use in method development. The following internal standards were used according to each study 1-methylnapthalene 1000mg/L, phenol-d6 1000mg/L and naphthalene-d8 1000mg/L. Standard solution for calibration curves are described separately in each section.

3.2.2 GC analysis

Three GC systems were used for sample analysis, a GC coupled to flame ionisation detector (GC-FID), a GC couple to a mass spectrometer (GC-MS) and a comprehensive two-dimensional gas chromatography coupled to time-of-flight mass spectrometry system (GCxGC-TOFMS).

GC-FID Each analysis was performed on an Agilent 7890B GC system using a Restek Rtx-PCB capillary column (0.25mm i.d. x 60m length, 0.25um film thickness). Two temperature programming methods were used. The first method was developed for the solvent

comparison experiments and the second for recovery calculation experiments. Regarding the solvent comparison experiments, oven programming had to be optimised so it could be use with all 3 solvents without any coelutions with solvents components and the analytes. System parameters for the first method are as follows: inlet temperature 300°C, injection volume 1μLwith a split ratio of 1:10, initial oven temperature 70°C, held for 7 min, then to 190°C at a rate of 10°C/min, then to 320°C at a rate of 60°C/min and held for 2min, helium flow rate was set at 2mL/min. For the second method: inlet temperature 300°C, injection volume 1μLwith a split ratio of 1:10, initial oven temperature 80°C, then to 190°C at a rate of 10°C/min, then to 320°C at a rate of 60°C/min and held for 3min, helium flow rate was set at 2mL/min. Detector temperature was 340°C in both cases.

GC-MS Each analysis was performed on an Agilent 5975C series GC-MS system using an Agilent (50%-Phenyl)-methylpolysiloxane phase (DB-17MS) capillary column (0.25mm i.d. x 60m length, 0.25um film thickness). Two methods were developed, one for surrogate recovery analysis and one for untargeted sample analysis. For surrogate recovery analysis the following parameters were used: inlet temperature 300°C, injection volume 1μLwith a split ratio of 1:200, initial oven temperature 70°C, held for 0.2 min, then to 220°C at a rate of 10°C/min and then to 320°C at a rate of 60°C/min held for 3min, helium flow rate was 1.4mL/min. For the untargeted analysis the following parameters were used: inlet temperature 300°C, injection volume 1μLwith a split ratio of 1:20, initial oven temperature 70°C, held for 0.2 min, then to 320°C at a rate of 3.5°C/min and held for 5min, helium flow rate was 1.4mL/min.

For the analysis of the surrogates in the extracts a targeted, quantitative selected ion monitoring (SIM) method was developed using the GC/MS; SIM methods generally provide The following concentration levels used for all compounds: 10, 50, 100, 150, 300, 450, 600 and 900 mg/L. Internal standards, retention times and ions used to quantify each compound are shown in Table 3.2.

Table 3.2: SIM method parameters for surrogate analysis

Compound	Internal standard	Retention time	Quantifying ion
4-fluoro-2-methylpyridine	phenol-d6	4.90	111
4-fluorophenol	phenol-d6	7.80	112
1-fluoronaphthalene	phenol-d6	10.80	146
5-fluoroindole	phenol-d6	13.80	135
4-bromo-2,6-dimethylphenol	phenol-d6	14.40	200

GCxGC-TOFMS Each analysis was performed on a Leco Pegasus® 4D equipped with a 4-stage Zoex® liquid nitrogen cooled modulator. A polar normal phase column set-up was

used with an Agilent (50%-Phenyl)-methylpolysiloxane phase DB-17MS column on the first dimension (0.25mm i.d. x 60m length, 0.25um film thickness) and a Restek Stabilwax™ (crossbond polyethylene glycol) column on the second dimension. Second dimension length was changed for each analysis: for total sample analysis 0.1m in the modulator, 0.15m in the secondary oven and 0.2m in the transfer line; for back-extracted sample analysis 0.1m in the modulator, 0.30m in the secondary oven and 0.2m in the transfer line. GC conditions: for the total sample, inlet temperature was set at 300°C, injection volume was 1μLwith a split ratio of 1:40, modulation time was 6s, initial oven temperature was 40°C, held for 0.2 min, then to 235°C at a rate of 3.5°C/min and held for 14min, helium flow rate was 1.4mL/min. For the back-extracted sample conditions were the same as in the total, except for the split ratio which was set to 1:20 and the modulation time which as set at 5s.

Chromatogram processing GC-MS chromatograms from the untargeted analysis were processed with AMDIS[91] (Automated Mass Spectral Deconvolution & Identification System) which offers a classic deconvolution algorithm for GC-MS. The following settings were used: peak width 32, two peak subtractions, high resolution, high sensitivity and high shape requirements. Signal to noise filter was set at 10 and a minimum of three models were needed for peak picking. The GCxGC-TOFMS chromatograms were treated with Chromatof® with the baseline offset set to 1, smoothing to 13, peak width 18-24 1st dimension & 0.15-0.6 2nd dimension. The integration approach was traditional and the signal to noise was set at 100.

3.2.3 The HIVS system

A novel technique using a novel ultrasound system is suggested by the author, in order to sonicate samples without the disadvantages of ultrasound baths and probes. The technique uses a newly developed, commercially available ultrasound system that offers the possibility to focus ultrasound directly in the contents of a closed vessel by transferring the ultrasound through the vessel's walls. The technique was named HIVS after **h**igh-**i**ntensity **v**essel-wall **s**onication. The system is employed throughout the method development chapters of the thesis. The operating principle is given in Figure 3.3. The technique employs a UP200St™ ultrasonic processor connected to specially designed sonotrode - VialTweeter™ (S26d10x10VialT™) attached to a vial press (UP200xt™). The system is manufactured by Hielscher Ultrasonics GmbH, Teltow, Germany (more information can be found on the manufacturer's website[92]).

In this chapter the HIVS system is used in order to enhance the emulsification phenomenon and increase the performance of the LLE process. The system directs ultrasound in the contents of the vessel uniformly and without losses associated with ultrasonic baths and the probe does not come into contact with the sample as in the case of probes. Firstly, the

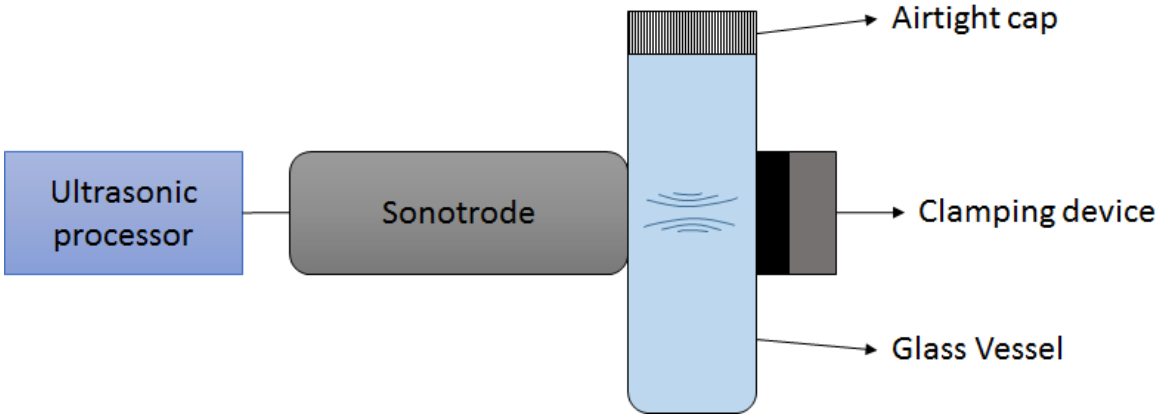

Figure 3.3: Operating principle of the HIVS technique. The techniques uses a special probe that transfers ultrasound directly into the contents of a vessel through the vessel's walls. Image ©*Ioannis Sampsonidis*

system had to be adapted for use with 15mL glass centrifuge tubes. For this purpose, in-house adapters were designed by the author (Figure Appendix A.1.1) in order to prevent the sonotrode from coming into direct contact with the glass vial, therefore increasing the chance of vial deterioration and breakage and sonotrode surface wear. The adapters were devised and designed by the author and manufactured with help from the Technical Services Department of the School of Engineering at the University of Glasgow. Once the tubes were fitted onto the sonication probe, the parameters of the sonication probe were tested using trial and error in order to determine the system's operating range. More specifically, the parameters that can be changed by the user are: mode of operation (power control or amplitude control), sonication time and pulsed or continuous operation (with pulses set in a percentage range). For LLE the sonotrode was operated in power mode. The maximum operating power for this application was determined to be 50-60W above which operating the system appeared unstable, with frequent vial breakages. Therefore, a safer operating intensity limit of 40W was used.

3.2.4 Solvent comparison

The compatibility of the green solvent CPME with analytical LLE was investigated by comparing its performance with two other low-density solvents that are commonly used in analytical LLE: toluene and cyclohexane. In comparison to these solvents, CPME has several advantages, some of which are its environmental compatibility ("CPME meets eight definitions out of the 12 Principles of Green Chemistry"[93]) and higher polarity[94]. Its higher polarity may allow the extraction of polar compounds that would otherwise be extracted only partially with the less polar solvents. Toluene is a commonly used solvent for LLE while cyclohexane, although less commonly used than toluene, has been used in the DLLME of

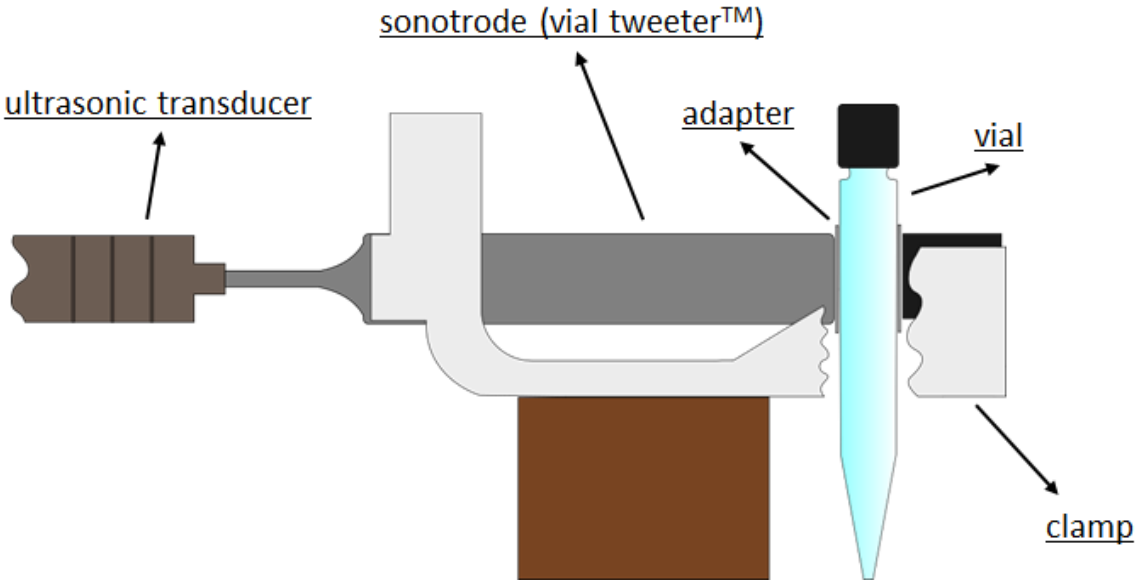

Figure 3.4: Fitting of the glass vials onto the sonotrode vial-tweeter to perform HIVS. For accurate images the reader is referred to Hielscher Ultrasonics website[92]. Image ©*Ioannis Sampsonidis*

organophosphorous pesticides[95] and the ultrasound-assisted extraction (UAE) extraction of PAHs in combination with acetone[96].

For this study 300mL of milli-Q water was spiked with the 10 model compounds in the following resulting concentrations: 10mg/L for 5,5-dimethylhydantoin, benzoic acid, phenol, indole, o-cresol, 2-picoline, and benzonitrile; 5mg/L for o-xylene and naphthalene and 0.5 mg/L for phenanthrene. The spiked solution was then split in two portions and the pH of the first portion was adjusted to below 2 (sol A) using HCl (8M) and of the second to above 12 (sol B) using KOH (12M). UASEME was performed on the HIVS system by transferring 9 mL of spiked water to a glass centrifuge tube, adding CTAB to a resulting concentration of 0.002mmol/L, rapidly injecting the 450μLof solvent and sonicating for 30s. UASEME conditions were selected using trial and error. Emulsion was broken by centrifuging at 2500rpm for 7mins and then collecting the organic phase. Each extraction was performed in triplicate for each solvent. Regarding analysis, 95μLof the organic phase were transferred to a 200μLglass insert and 5 μLof the 1-methylnapthalene internal standard was added. The mixture was then injected in the GC-FID with a method described in a following section. All analyses were performed in triplicate. For each analysis each analyte's response was divided with the response of the internal standard (Equation 3.1).

$$R_f = \frac{R_a}{R_{is}} \tag{3.1}$$

where: R_f=response factor; R_a=peak area ratio; R_{is}=internal standard area ratio

Since CPME is more soluble in water than the rest of the solvents, a portion of it is expected to be dissolved in the water, thus providing a slight pre-concentration effect that will make the responses slightly higher. In order to balance this effect each Rf is multiplied with a solubility factor which is the ratio of the maximum recovered solvent volume to the volume added for the extraction. Comparisons between solvents are tested for statistical significance using one-way analysis of variance (ANOVA) and if there is a statistical significance difference only the percentage increase is reported which is calculated using Equation 3.2.

$$\frac{R_{f2} - R_{f1}}{R_{f1}} * 100 \text{ where } R_{f2} > R_{f1} \tag{3.2}$$

where: R_{f1}=response factor one; R_{f2}=response factor two

3.2.5 UASEME optimisation

As mentioned above the sonication system was tested and operation limits for some of the parameters were determined. Since this type of application has not been performed in the past, a design of experiments (DOE) approach was employed in order to better understand the extraction process and attempt to model it so that optimised conditions are determined. The first step was to set up an initial screening design with the aim to narrow down factor values and roughly model the process in order to determine where optimised conditions are expected to be found. A full factorial design was prepared with 4 factors (2^4 design): time (in seconds), intensity (in Watt), pulse (percentage) and CTAB concentration [M]. The first 3 factors were set as numeric and CTAB concentration was set as categorical. The study was replicated 4 times (4 blocks), with each replicate having 16 runs with 4 centre points per replicate, resulting in a total of 20 runs per replicate, with each run representing a defined set of conditions as seen in Table 3.3. In total, 80 extractions were performed with each extraction injected twice in the GC-FID. The compounds modelled for sonication optimisation were phenol, o-cresol, benzonitrile, indole, napthalene and phenanthrene. In order to avoid performing each extraction for both acidic and basic pH (thus doubling the number of extractions) 2-picoline and benzoic acid were not included in the optimisation study as un-ionised compounds. The compound o-xylene was also excluded from the study as due to its very volatility it did not remain stable in the spiked solution throughout the course of the experiment.

A spiked solution was prepared at the beginning of each block (except in the case of block 1 and 2 where the same spike water solution was used). Spiking conditions were the same as in the solvent comparison experiment but without splitting the water in portions. Analyte areas were divided to the area of the internal standard and the response factor (Rf) was used for

Table 3.3: Initial design used for UASEME factor screening. Each run represents a unique combination of factor levels

RunOrder	Time[s]	Intensity[w]	Pulse[%]	CTAB
1	10	10	100	0.002
2	10	10	50	0.002
3	10	40	100	0.020
4	35	20	70	0.020
5	10	40	100	0.002
6	35	20	70	0.002
7	10	10	100	0.020
8	10	40	50	0.002
9	60	10	50	0.002
10	60	40	50	0.020
11	10	10	50	0.020
12	35	20	70	0.002
13	60	40	50	0.002
14	60	10	100	0.020
15	60	10	100	0.002
16	35	20	70	0.020
17	60	10	50	0.020
18	10	40	50	0.020
19	60	40	100	0.002
20	60	40	100	0.020

model fitting. Replicate Rfs for each condition were checked for outliers using Dixon's Q ratio with a significance level of 0.05%. The factorial design was analysed using the Minitab's DOE functionality and analysis included all higher order terms and blocks and each equation was averaged over the 4 blocks. Results from the screening study provided an initial understanding of process behaviour and indicated the experimental conditions for creating a more detailed modelling study in a reduced experimental space using the response surface methodology (RSM) approach. For the RSM study, sonication intensity and pulse were kept stable at 40W and 50% respectively and only the effect of time and CTAB concentration was investigated. The applied design, as seen in Table 3.4 was a full factorial, face-centered, central composite design, featuring 14 runs. This design was performed in two replicates with each replicate extraction injected twice in the GC-FID.

3.2.6 Salting out optimisation

For this study a quantitative method was developed so that the recovery values could be used instead of the response factors. This is because the addition of salts is expected to change the solubility of CPME in water, thus affecting the recovery values so the use of the response factor is no longer adequate. Model compounds were divided in three groups according

Table 3.4: Response surface design for modelling time and CTAB concentration for UASEME extraction

RunOrder	Time[s]	CTAB[M]
1	40	0.0000
2	20	0.0016
3	00	0.0000
4	00	0.0032
5	40	0.0032
6	20	0.0016
7	20	0.0016
8	20	0.0000
9	20	0.0032
10	20	0.0016
11	40	0.0016
12	20	0.0016
13	20	0.0016
14	00	0.0016

to their water solubility with different calibration curves for each group (Table 3.5). Each sample was spiked separately and directly in the sample tube in order to avoid the hydrocarbon evaporation effect that was observed in the previous studies. Recovery was calculated using the Equation 3.3, where C_r and C_s are the recovered and spiked concentrations of a compound respectively.

$$Recovery[\%] = \frac{C_r}{C_s} * 100\% \tag{3.3}$$

where: C_r=recovered concentration; C_s=spiked concentration

Several salts were considered in order to utilise the salting-out effect. The first extraction scheme used for the study is presented in Figure 3.5. An initial evaluation of the salting-out effect was performed in three conditions: no salt, 10% Na_2SO_4 and 10% NaCl. Every extraction was performed in three replicates and every replicate was injected three times in the GC-FID. Following this evaluation, 4 levels of Na_2SO_4 were also tested in order to define the optimal salt level: 0% 5% 10% and 15%. Every extraction was performed in three replicates and three injections were made on the GC-FID. Since Na_2SO_4 reported water solubility at 20°C is 13.9g/100mL and the extraction was performed at approx. 25°C, 15% w/v was assessed as the maximum salt concentration for the experiment.

3.2.7 Back-extraction

Since phenols are acidic, their stripping is performed through back-extracting the extracted sample in a blank water sample that contains a basic component such as NaOH. The back-

Table 3.5: Calibration groups along with calibration levels for the selected model compounds

Calibration level	Group A [mg/L]	Group B [mg/L]	Group C [mg/L]
7	300	150	15
6	225	112.5	11.25
5	150	75	7.5
4	75	37.5	3.75
3	30	15	1.5
2	15	7.5	0.75
1	3	1.5	

Internal standard	Group A compounds	Group B compounds	Group C compounds
1-methylnapthalene 50mg/L	5,5-dimethylhydantoin benzoic acid phenol indole o-cresol 2-picoline benzonitrile	naphthalene o-xylene	phenanthrene

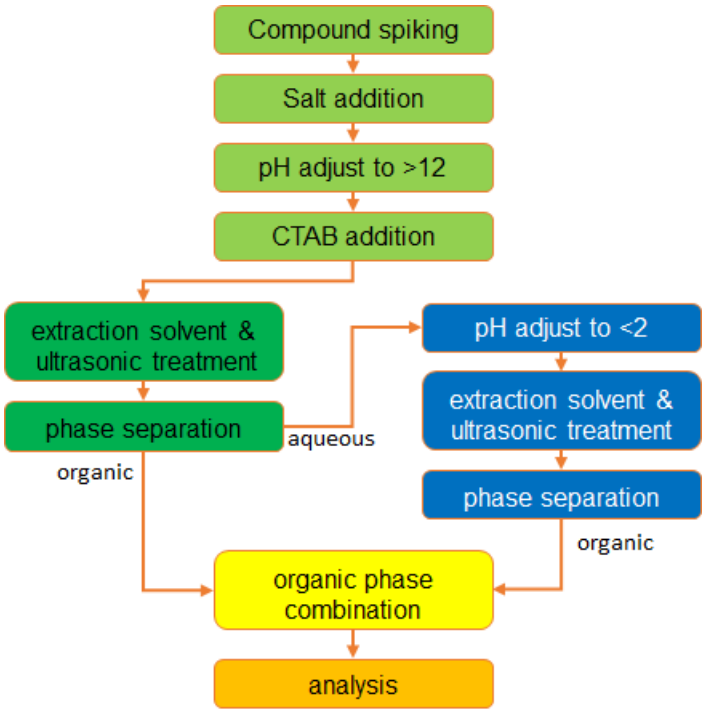

Figure 3.5: Extraction protocol used for the salting-out study

extraction step is not expected to completely remove the acidic components but rather strip them down to a certain level. For this particular step, the back-extraction solution is an aqueous solution containing 0.0022mmol CTAB (the same as the one of the sample in the normal extraction process), 5% NaOH and a small amount of salt (0.25% Na_2SO_4) to aid in phase separation. Back-extraction is performed by injecting 300μLof the total extracted sample in 9mL of the back-extraction solution in a 15mL glass tube and sonicating using the optimised UASEME conditions mentioned above. The phases are separated by centrifuging and the organic phase is collected and analysed using GC-MS.

3.2.8 Method validation

Once all the extraction conditions were optimised and the finalised extraction protocol was selected (Figure 3.6) the method was validated for precision and matrix effects. Method precision was studied by performing 6 replicate extractions within a day and 3 replicate extractions per day for the next two days. Each extraction was injected three times in the GC-FID and concentrations were determined using the calibration curve in Table 3.5.

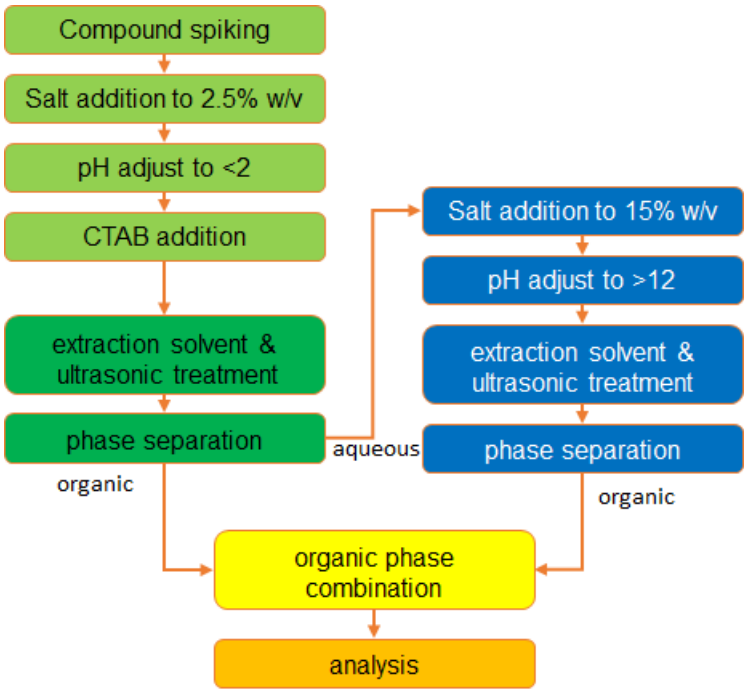

Figure 3.6: Final protocol for the extraction of SVOCs from coal gasification water

For the assessment of matrix effects and to measure extraction recovery in unknown waste-water samples, 5 halogen-labelled representative compounds were selected as surrogates (Table 3.6). Regarding matrix effects, 3 different matrices were used: milli-Q water, weathered tar water and gasification waste-water. Weathered tar is expected to be poor in oxygenated compounds such as phenols and richer in PAHs. Unlike the weathered tar water, fresh coal

gasification water is expected to be highly rich in phenols and naturally have a higher organic carbon content than weathered tar water.

Table 3.6: Selected surrogates along with some of their properties

Compound	logP	S[1][mg/mL]	[D][1]
4-fluoro-2-methylpyridine	1.03	26.5	0.688
4-fluorophenol	1.81	6.73	1.36
1-fluoronaphthalene	3.11	0.0405	1.94
5-fluoroindole	2.21	0.357	1.56
4-bromo-2,6-dimethylphenol	3.47	0.392	1.44

Where S: intrinsic solubility; D: dipole moment;

[1]Chemicalize was used for to predict this property, 2017, https://chemicalize.com/ developed by ChemAxon (http://www.chemaxon.com)

The effect of the volume of the organic solvent on surrogate recovery was also tested for two levels: 450μLper step (900μLtotal, enrichment ratio 1:10), 170μLand 60μLfor 1st and 2nd step respectively (230μLtotal, enrichment ratio 1:39). Each extraction was performed in 4 replicates and each replicate was injected 3 times.

3.3 Results and discussion

3.3.1 Solvent comparison for UASEME

Acidic extraction The aim of this section is the comparison of CPME with two other common extraction solvents (toluene and cyclohexane) in order to assess its efficiency and compound compatibility as an extraction solvent. For neutral hydrocarbons like o-xylene, naphthalene and phenanthrenene, all the solvents appeared to have the same extraction performance; no statistical differences were found with a one-way ANOVA for all three solvents (Figure 3.7). This is due to their low polarity. For the rest of the compounds the performance of cyclohexane is so poor that it is not considered and only statistical comparisons between CPME and toluene are made. For benzonitrile there is no statistically significant difference in the extraction between CPME and toluene, while for indole CPME extracts 29.2% more than toluene. Currently, this cannot be explained just by comparing the polarity properties of these compounds since benzonitrile is more polar than indole a better extraction would be expected with CPME. The differences in extraction performance are even more stressed when it comes to acidic compounds, which are naturally more polar than the other neutral compounds of the study (the pH here was $\leq$2).

CPME extracts 766.1% more phenol and 203.8% more o-cresol than toluene. This difference can be attributed to the fact that o-cresol is methylated in comparison to phenol and,

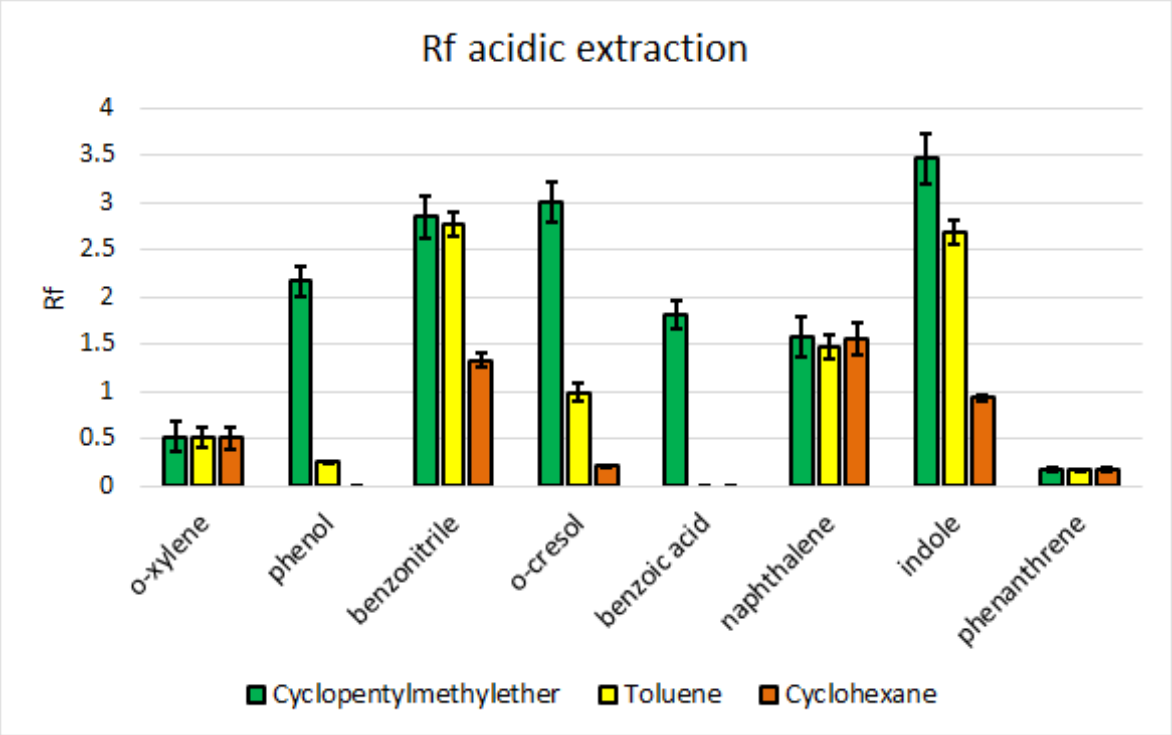

Figure 3.7: Rf (Equation 3.1) for the model compounds during the acidic extraction step

naturally exhibits more organophilic properties (Figure 3.2). Benzoic acid is detected only when CPME is used as an extraction solvent indicating the superiority of CPME in the extraction of acidic compounds. The compound 5,5-dimethylhydantoin although expected to be extracted during the acidic extraction wasn't detected with the applied GC-FID method.

Basic extraction Performance of the extraction solvents in basic pH can be seen in Figure 3.8. Neutral compounds are extracted in a very similar way as in the acidic extraction, with no statistical differences between solvents, further indicating that there is no significant effect of the pH in the emulsification and phase separation. Acidic compounds are hardly extracted since they are in their ionised forms in the solution however o-cresol exhibits some extraction with CPME, something that can be attributed to its relatively higher lipophilicity than phenol (Table 3.1). However, the basic compound 2-picoline appears to be extracted a bit better with toluene than with CPME, which although statistically significant it's not a considerable percentage increase (33.5%), and certainly not enough to overshadow the superior performance of CPME for the other compounds. Hence, as shown by the large differences in extraction efficiencies, it can be concluded that CPME is superior than both toluene and cyclohexane in the extraction of neutral and polar compounds associated with UCG.

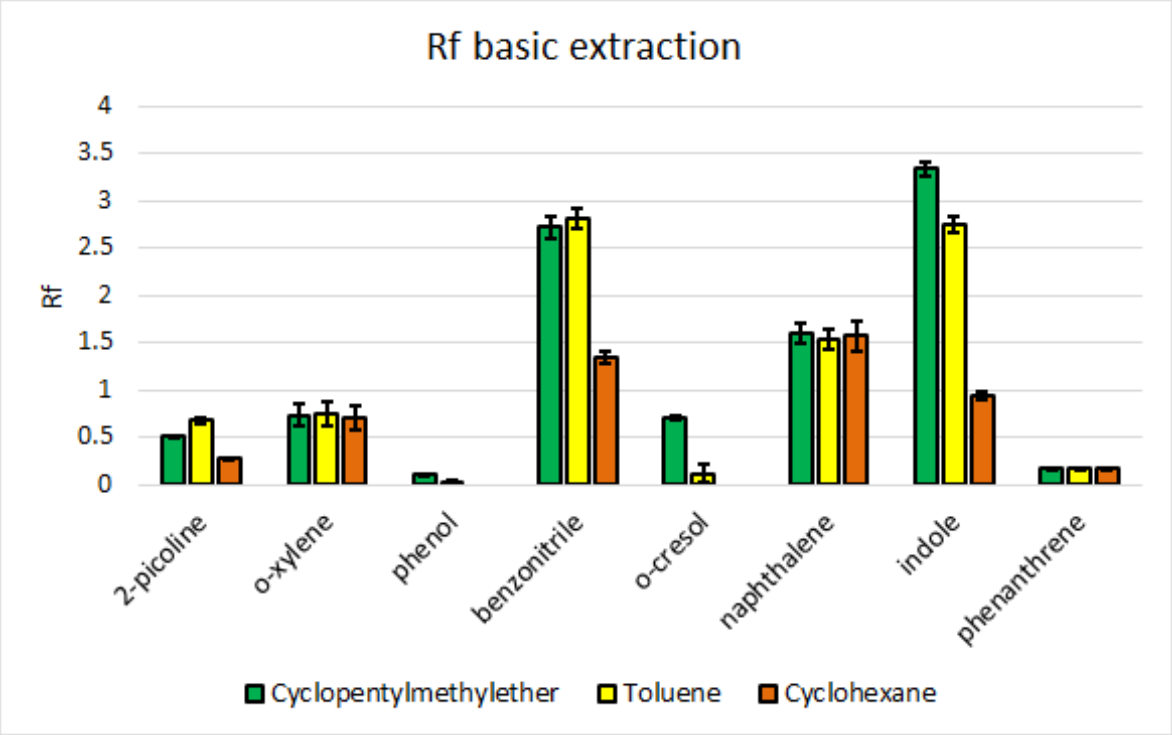

Figure 3.8: Response factors for the model compounds during the basic extraction step

3.3.2 UASEME optimisation

After the selection of CPME as a solvent, the extraction parameters had to be optimised for optimal compound recovery. This was achieved with the application of a DOE screening experiment and an RSM optimisation experiment. The factorial regression model (Table 3.3) was fitted with the response factors of the compounds that were included in the screening study. Performance of the models can be seen in Table 3.7. Once the models were fitted, Minitab's response optimiser function (which works by "identifying the combination of variable settings that jointly optimise a single response or a set of responses"[97]) was used and all the compounds' responses were jointly optimised in order to indicate the most desirable conditions were all of the R_f values are as high as possible. All the compounds were given the same weight for calculations (meaning their importance is considered identical). The optimisation plot along with the optimal values and the composite desirability values for each compound can be seen in Figure Appendix A.1.4. The optimal values provided from the response optimiser were time: 10s, intensity: 40W, pulse: 50% and CTAB 0.002M. However, these values are optimal values produced from linear models and they do not model curvature, but nevertheless they are a good indication of where the optimal conditions lie.

An RSM model was build next in a more confined experimental area for more accurate optimisation. Intensity was kept stable at 40W (above which tube breakage was frequent - although this was not systematically tested) and pulse at 50% (which was the lowest pulse

Table 3.7: Performance of the factorial regression models for the screening study. The values indicate how the models fit the data showing that the predictability of the models (R^2(pred)) is relatively poor however this is explained by poorly chosen maximum values especially for CTAB concentration. The overall fit to the data (R^2, R^2(adj)) is strong enought to indicate the direction/trend where the optimal conditions are found

	phenol	o-cresol	benzonitrile	indole	napthalene	phenanthrene
R^2 [%]	66.71	55.18	43.58	50.81	43.25	68.00
R^2(adj) [%]	55.80	40.99	25.42	35.23	25.27	57.70
R^2(pred) [%]	41.44	20.85	0.11	13.04	0.00	40.41

value of the screening study) and only time and CTAB concentration were modelled between 0s and 40s and and 0.000 and 0.0032M respectively. The maximum CTAB concentration was chosen after trial and error above which phase separation appeared less ideal. The design was face-centred (which restricts factor values to those provided to the model by the user) so that R_fs for zero factor values can be obtained, since negative values have no physical meaning in this case. Zero values also provide the opportunity to demonstrate the enhancing effect of both the addition of surfactant and of the sonication. A full quadratic model was fitted on the response factors for each compound in the RSM design and the performance of the models appear in Table 3.8. The r^2 values are much higher that the screening study indicating that the model is able to explain most of the variance in the data (average increase in r^2 of 57.5% and maximum increase 109.6% for benzonitrile). Feeding each model in Minitab's response optimiser function gives a visual impression of the response surface for each factor and each compound along with the optimal values for time and CTAB concentration (Figure 3.9). The models provide evidence that both the use of CTAB and the ultrasonication are beneficial in the extraction of SVOCs from water. The optimal values for the CTAB and sonication set for the final, optimised method were: time 28s, CTAB concentration 0.0022M, intensity 40W and pulse 50%. These conditions indicate that extraction takes place rapidly in less than 30s.

Table 3.8: Performance of the factorial regression models for response surface study. Quadratic models show good predictability for most compounds (R^2(pred)) and the models are a good fit to the data (R^2, R^2(adj))

	phenol	o-cresol	benzonitrile	indole	napthalene	phenanthrene
R^2	92.49	89.82	91.35	83.54	73.55	67.81
R^2(adj)	90.34	86.92	88.88	78.84	66.00	58.61
R^2(pred)	82.59	77.16	80.76	63.81	42.55	31.18

3.3.3 Salting-out optimisation

Once the optimum conditions for the UASEME were established the method development process focused on evaluating the salting-out effect on extraction recovery. The salting-out

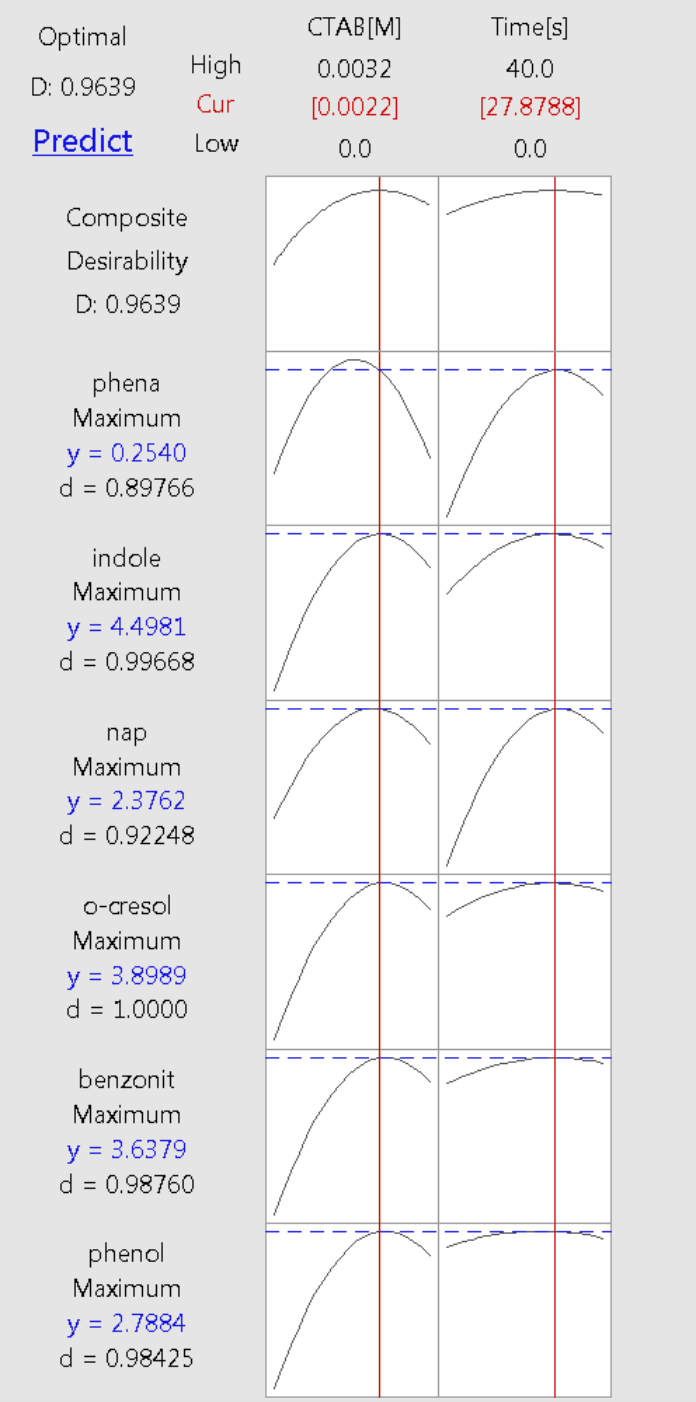

Figure 3.9: Optimisation plot for the response surface study produced from Matlab's response optimiser function. The red line indicates optimal values of composite desirability

effect was investigated as it has been shown that it has a beneficial effect in the extraction of organic compounds from water by reducing solubility[98]. Sodium salts like NaCl and Na_2SO_4, and magnesium salts like $MgSO_4$ and $MgCl_2$ have been studied in the past for salting-out effect[99]. However, magnesium salts cannot be used in this study due to the restriction of Mg(OH) formation in basic pH, preventing Mg^{2+} to exist in its ionic form in the basic solution, so only sodium salts were tested for the salting-out effect. Calibration curves for the model compounds for the the GC-FID analysis are give in Figure Appendix A.1.5. No salt, 10% Na_2SO_4 and 10% NaCl were compared (Figure3.10). Extraction of 2-picoline is significantly better with Na_2SO_4 (143.5% higher), with phenol and benzoic acid also showing some benefit from the salting-out process with Na_2SO_4 (19.5% for phenol and 11.1% for benozic acid). However, hydrocarbons like o-xylene, napthhalene and phenanthrene show less extraction. The addition of salt increases the evaporation of the more volatile compounds through the various sample preparation stages[100] as the addition of salt has an effect in the solubility of the compounds, so losses are expected when transferring sample volumes. This is more obvious with the most volatile compounds such as o-xylene that has the highest Henry's law constant (Table 3.1). Comparing between the two salts it appears that the salting-out effect of Na_2SO_4 on 2-picoline, phenol and benzoic acid is higher than that of NaCl. For this reason, Na_2SO_4 was selected as the salting-out agent for the study. Another observation is that phase separation appears better when adding a salt in the water sample before extraction, something which has been previously mentioned in the literature[84,101].

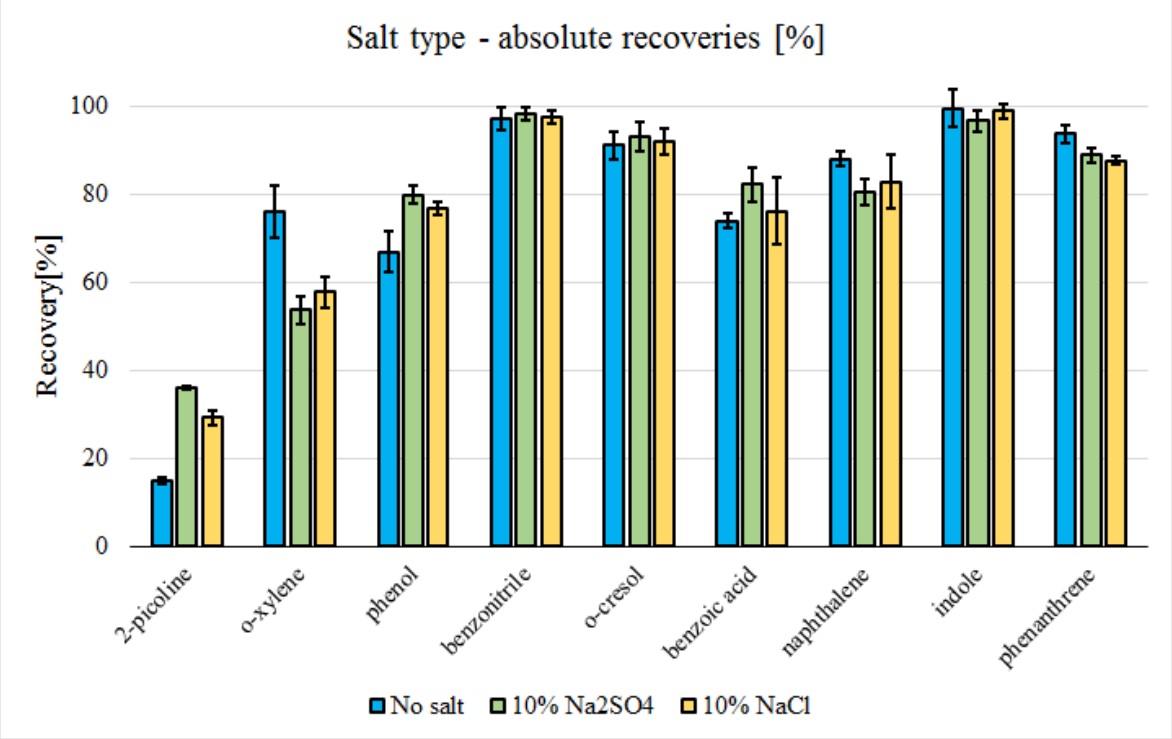

Figure 3.10: Effect of salt type on model compound recoveries. For each compound from left to right: no salt, 10% Na_2SO_4 and 10% NaCl

Extractions recoveries with increasing Na_2SO_4 appear on Figure 3.11. Increasing salt addition increases the extraction of 2-picoline. For phenol it appears that the salting-out effect is not as strong as in the case of 2-picoline and it also appears to stabilise after 10% salt, whereas in the case of benzoic acid it appears to be decreasing. Regarding the more volatile and less polar compounds such as o-xylene, increasing salt concentration is significantly increasing the evaporation of the compound through stripping during the sample preparation process, thus reducing its recovery. The same effect but in a smaller scale is observed for both naphthalene and phenanthrene. This contradicting effect make selection of an optimal salt concentration difficult, however since the extraction is taking place in two steps, it is possible to use the advantages of the salting-out effect without affecting significantly the recovery of the more volatile compounds. The extraction is performed in two steps: extraction of the acidic components first, while adding a small amount of salt (2.5%) in order to benefit both from salting-out effect and better phase separation without over-affecting the extraction of the more volatile components. Phenols are also extracted first to avoid possible dimerisation in acidic pH[64]. Addition of the rest of the salt (12.5%) is performed in the second step in the extraction of basic compounds. Neutrals (some of which are negatively affected by salt addition) are extracted mostly in the first step; the rest of the salt is added for the basic extraction step since bases like 2-picoline appear to benefit more from the salting-out process. After optimisation of the salt addition the extraction method had been completely optimised. The finalised protocol appears in Figure 3.6, and method validation is presented in the following section.

3.3.4 Back-extraction

As mentioned in the introduction, one of the properties that make coal gasification wastewater analysis so challenging is the fact that the concentration of different components in the sample can differ several orders of magnitude. This can be a problem particularly during the analysis step as the concentration of the primary components of the sample maybe overloading the column and saturating the detector, thus requiring split injections in higher split ratios. This can hinder the analysis of the micro-components of the sample as injecting the sample in split mode and in higher split ratios may not be enough to detect some of the sample's components, especially the higher molecular weight, low polarity SVOCs such as PAHs, the concentration of which is expected to be very low due to their low water solubility. To counter this issue a back-extraction step is introduced, which reduces the amount of the primary components in the sample, which in the case of coal gasification waste-water is primarily phenols. Back-extraction was tested while analysing an actual sample with the results presented in Section 3.3.6.

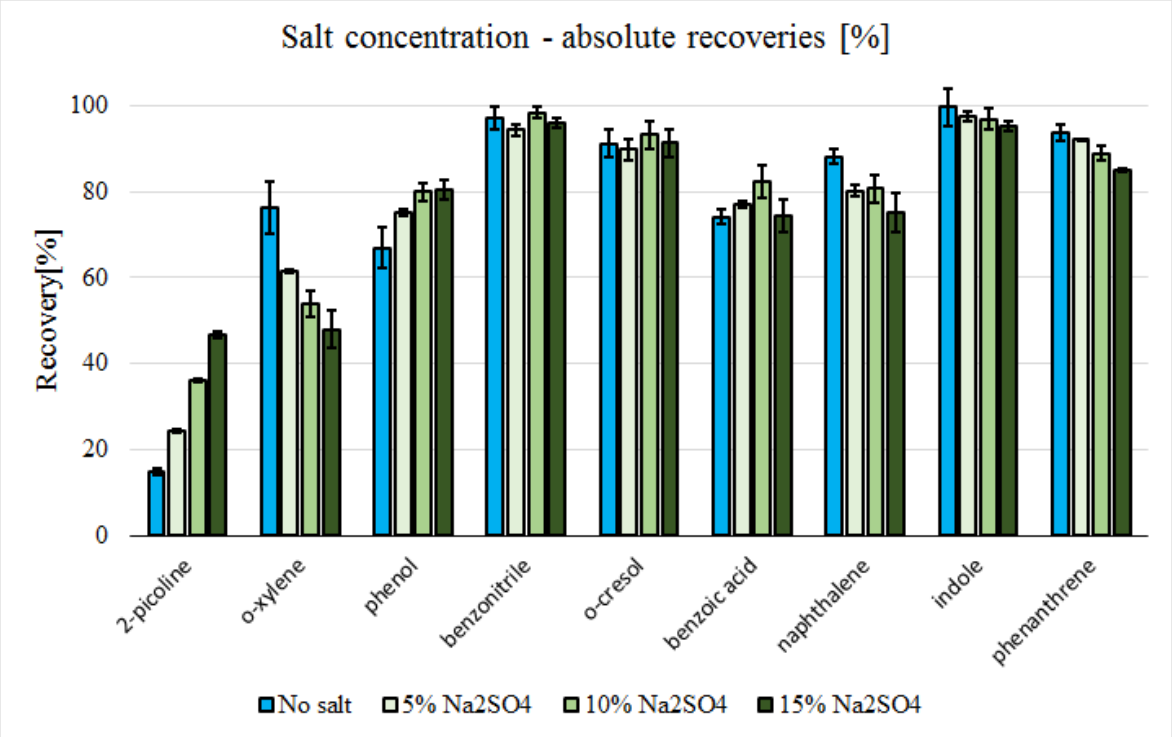

Figure 3.11: Effect of salt concentration on model compound recoveries. For each compound from left to right: no salt, 5% Na_2SO_4, 10% Na_2SO_4 and 15% Na_2SO_4

3.3.5 Method validation

The finalised conditions for the total extraction process are as follows: Sonication time: 28s, CTAB concentration in sample: 0.0022M, sonication power: 40W, pulse: 50%, Na_2SO_4 addition: 2.5% on the acidic step and 12.5% on the basic step. The method was validated for precision in three consecutive days (6 replicates the first day and 3 replicates the other two). The relative standard deviation for recoveries was calculated at 2.26% ranging from 1.62% for benzonitrile to 4.40% for benzoic acid. Generally, the method shows very good precision and acceptable recovery for most of the compounds (70%-130%) (Figure 3.12). Since the method is intended for cross sample comparisons and for un-targeted analysis, the low recovery values for some of the compounds are not concerning. As the evidence showed, recoveries can be optimised, by changing factors such as salt addition, as needed when developing a targeted method. In the present thesis where the aim is un-targeted cross sample comparison, precision is much more crucial that recovery.

A study of the effects that the matrix may have on compound recovery is essential as the extraction method is to be used on coal gasification waste-water samples which may have different properties. The performance of the calibration curve that was used for sample quantification appears in Figure Appendix A.1.6 where the regression coefficients are given. The matrices examined for this study were milli-Q water, weathered tar water and coal gasification waste-water. Differences in the extraction of 4-fluoro-2-methlypyridine are not sta-

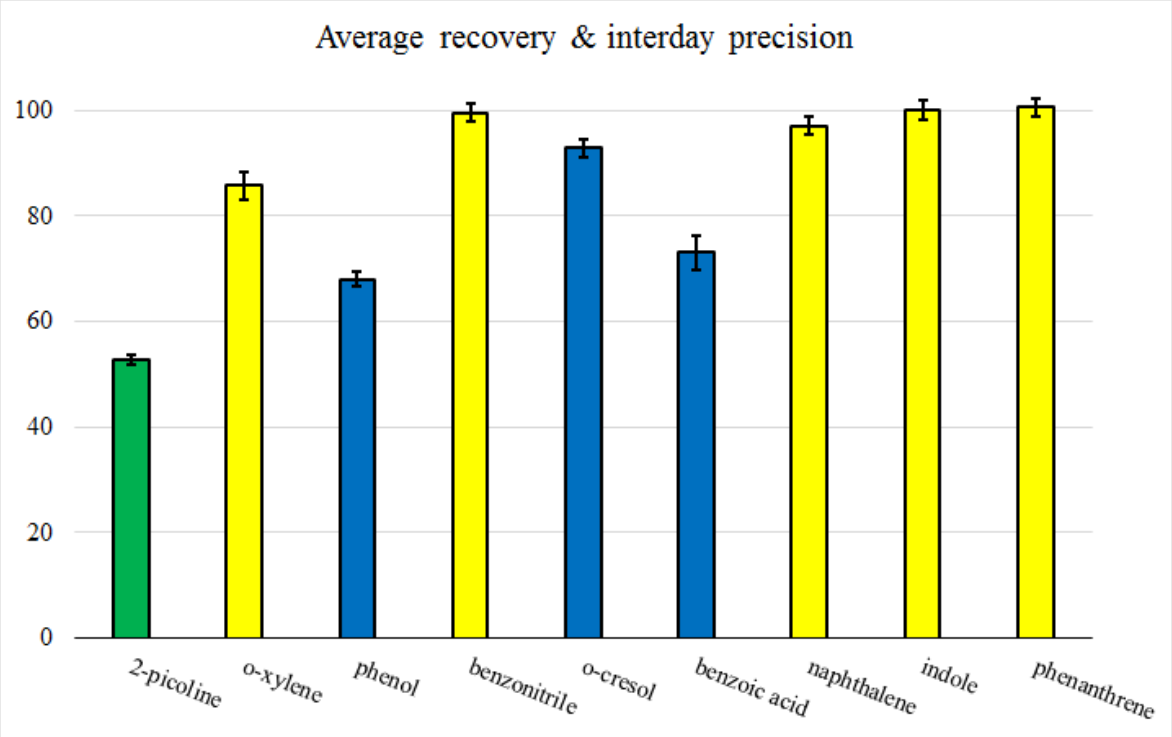

Figure 3.12: Interday precision of the extraction method. Yellow bars are for neutrals, blue for acids and green for bases. Compounds are presented by elution order. Recovery is represented by the y-axis and precision by the error bars located at the top of each bar

tistically significant (Figure 3.13). For 4-fluorophenol, 1-fluoronaphthalene, 5-fluoroindole and 4-bromo-2,6-dimethylphenol the differences are statistically significant between UCG and the other two types. With the differences (Equation 3.2) (highest to lowest) being: 1-fluoronaphthalene +9.3%, 4-fluorophenol +4%, 4-bromo-2,6-dimethylphenol +3.8% and 5-fluoroindole +2.4%. The differences for the latter 3 are practically small (since for 4-fluoro-2-methlypyridine the value was 1.4% which was deemed statistically insignificant) however, the same cannot be said for 1-fluoronaphthalene. These results indicate the need to monitor recovery in every sample extraction in order to account for variations in compound levels that may be introduced by the extraction process. For all recovery calculations, phenol-d6 was chosen as the internal standard. A smaller extraction solvent volume produces lower recoveries, especially for the lighter compounds (Figure Appendix A.1.7). However, it is expected that the higher enrichment ratio will make up for the lower recovery by providing higher sample pre-concentration.

3.3.6 Sample analysis

To illustrate the use of the method, two analyses of a UCG waste-water sample (sample 3 TOPS1 experiment - see Section Appendix A.1.1, p.174) are presented in this section, one using GC-MS (Figure 3.14) and one using GCxGC-TOFMS (Figure 3.15). The chro-

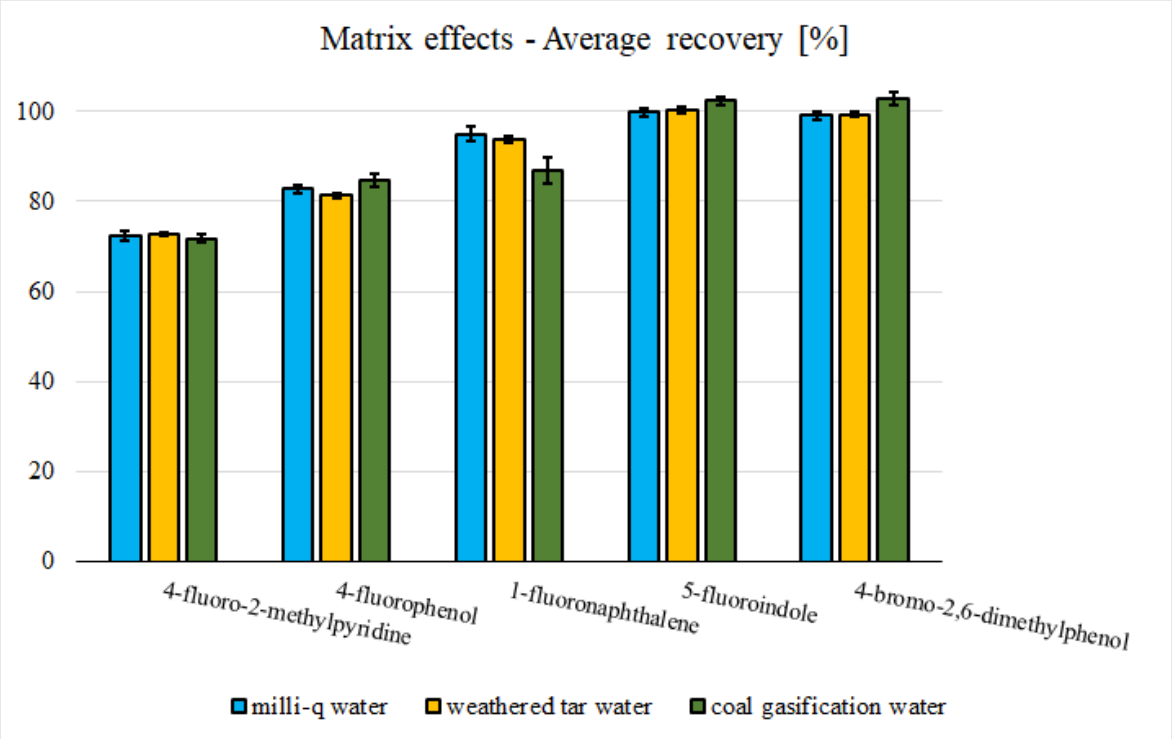

Figure 3.13: Effect of the matrix on the recovery of the 5 selected surrogates

matogram is focused on the micro-components of the sample and an overview in full scale can be seen at the upper right corner of the figure (Figure 3.14 A). An initial compositional assessment of the sample by chromatogram processing, as described in the materials and methods section, showed the sample is particularly rich in SVOCs including phenols (the primary components), PAHs, pyridines and heterocycles.

The application of the back-extraction process on the same sample in order to remove the bulk of the acidic components yielded the chromatogram seen in Figure 3.14 B. The back-extraction process removes approximately 93% of 4-fluorophenol and 84% of 4-bromo-2,6-dimethylphenol. Removal ratios for structurally similar compounds are expected to be close to the removal ratios of the surrogates. The scale of the chromatogram is set to focus on the micro-components of the sample, however, the overview on the upper right corner shows an overlay of the back-extracted sample to the total sample. The back extracted sample can be analysed further using a more sensitive method, such as a splitless injection, providing the ability to detect micro-components that would otherwise be undetectable using the current GC-MS set-up.

Analysis of the total sample using the GCxGC-TOFMS technique gives the chromatogram depicted in Figure 3.15 A (modulation time 6s). The used column set-up appears to be promising for the analysis of the samples. Analysis of the back-extracted sample gave the chromatogram depicted in Figure 3.15, B. The back-extraction effect removed some of the more polar components that had the highest 2nd dimension retention, thus allowing the use

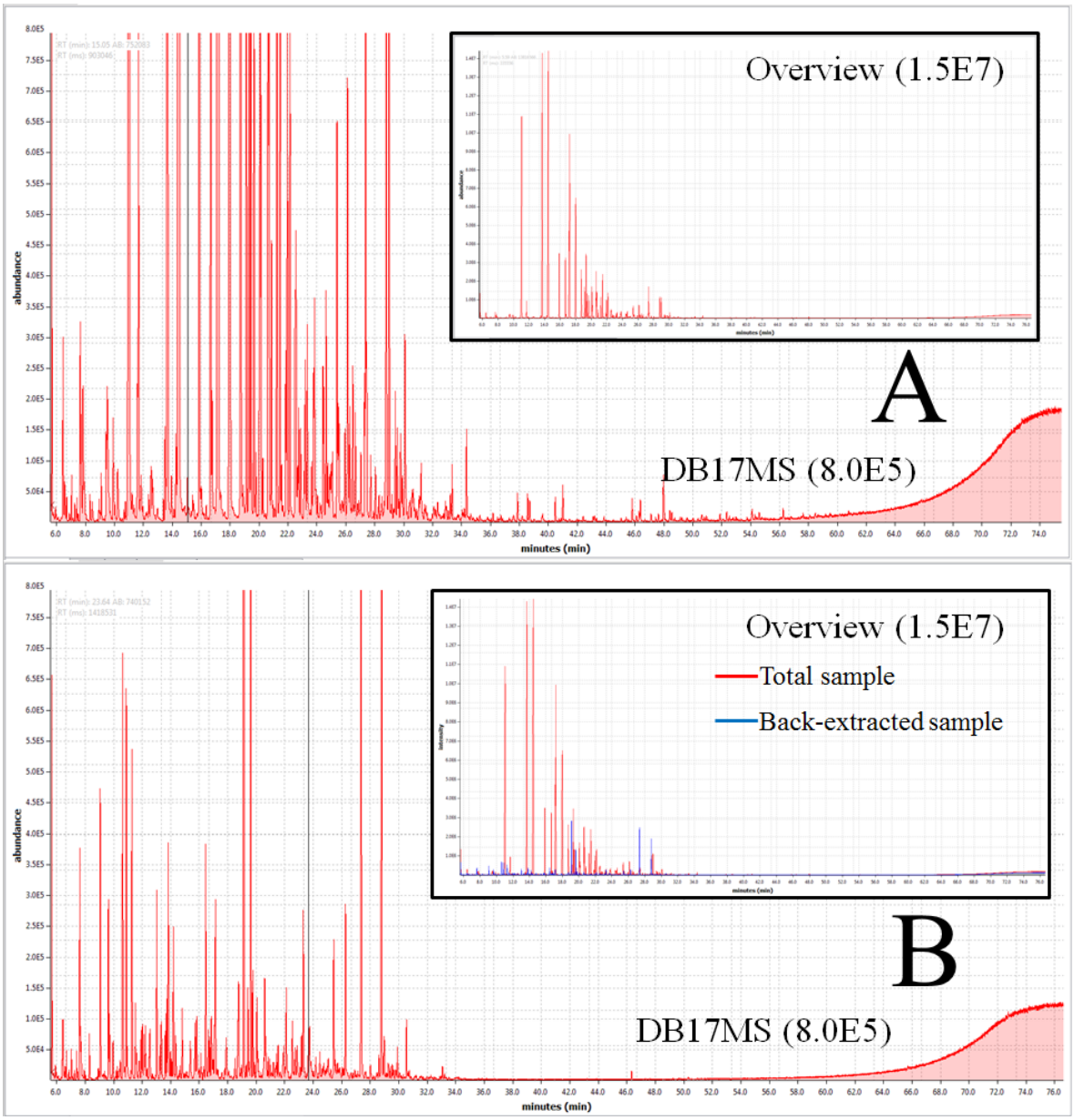

Figure 3.14: GC-MS chromatogram of an *ex-situ* coal gasification waste-water sample. Although the chromatogram is focused on the micro-components of the sample, an overview of the chromatogram in full scale can be seen in the upper right corner. A chromatogram of the total sample is on top (A) and that of the back-extracted sample on the bottom of the figure (B)

of a smaller modulation time (5s) and an additional loop in the secondary column (+0.15cm) to increase resolution on the second dimension. Also, it was possible to inject the back-extracted sample with a lower split ratio, which may increase identification of low concentration components.

Analysing all four chromatograms using the software and setting stated in the materials and methods section gave the results in Table 3.9. The chosen deconvolution and peak picking conditions were relatively strict, nevertheless, false positives are expected in both GC-MS

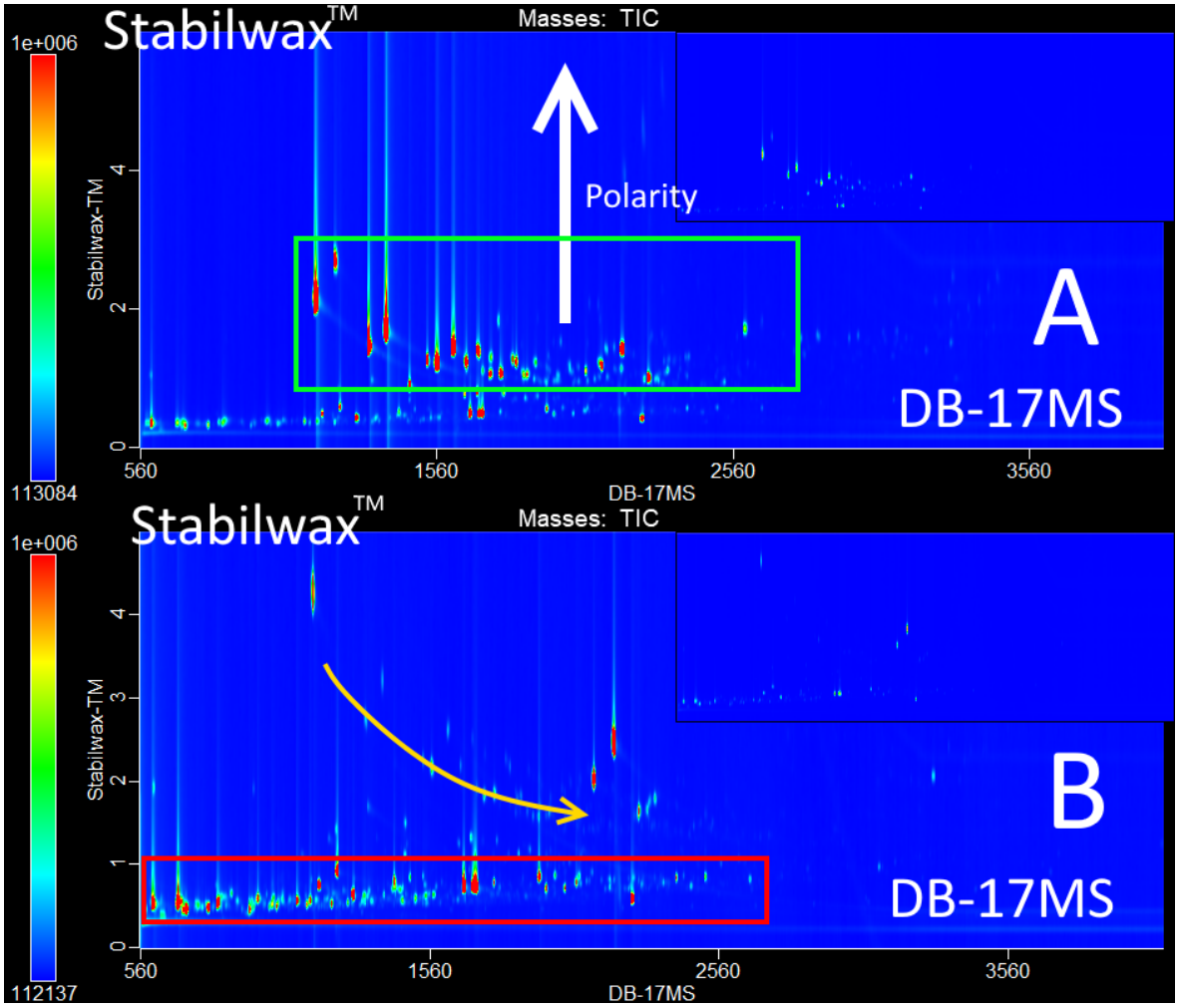

Figure 3.15: GCxGC-TOFMS chromatogram of an *ex-situ* coal gasification waste-water sample. Top:total sample. THe green square indicates the elution area of the majority of the phenolic compounds. Bottom: back-extracted sample. The yellow arrow indicates the order of elution pattern of phenols with increasing carbon number. The red square shows the area where the low polarity compounds elute. Increased separation and intensity in comparison with the total sample is evident for these compounds

and GCxGC-TOFMS analyses. However, this is an initial assessment with more detailed sample composition studies appearing in Chapter 5. Regarding the total sample it can be seen that almost twice the peaks are detected in GCxGC-TOFMS. This could be attributed to better separation and/or a more sensitive detector in the case of GCxGC-TOFMS; however, it can be also be partly attributed to software, since the deconvolution algorithms between Chromatof® and AMDIS are very different. Regarding the back-extracted sample, in the case of GC-MS almost half the peaks are detected in comparison with the total sample. However, in the case of GCxGC-TOFMS more than double the peaks are detected. Taking into account both the GC-MS result and the fact that the back-extraction process removes some of the more acidic compounds, this result was unexpected. However, this can be attributed to the additional loop in the second dimension oven in combination with a lower modulation

time and, possibly, to the smaller split ratio used. Additionally, removal of the larger components gave a much cleaner chromatogram, thus better performance is expected from the deconvolution algorithm. These results show that comprehensive chromatography significantly enhances the analysis of coal gasification waste-water. This is better understood by looking at the chromatograms in Figure 3.15, especially at the red square where the bulk of the phenols is eluted. This separation is not possible with either the normal nor the reverse phase GCxGC set-ups. The mechanism driving the separation is the high affinity of the phenols and the other polar compounds in the samples with the wax phase on the second dimension. This separation is achieved with only 0.15m of wax phase in the secondary oven and the author's knowledge this is the first instance where this set-up is used. Additionally, the back-extraction process enhances the separation of the less polar compounds (Figure 3.15, green square) due to the smaller modulation time and the larger amount of wax phase in the secondary oven. The elution patterns indicated by the yellow arrow that belongs to phenolic isomers substituted with increasing carbon chains shows that this set-up can assist with identification using the logical order of elution in these areas.

Table 3.9: Detected peaks/components and library matches in all four chromatograms. The peak yield is significantly higher for GCxGC-TOFMS chromatograms. The back extracted sample shows more peaks in the GCxGC-TOFMS analysis

	Total GC-MS	Total GCxGC-TOFMS	Back-ext GC-MS	Back-ext GCxGC-TOFMS
peak/components	634	883	394	1135

3.4 Conclusions

The novel UASESOME method that was developed for a close-to-exhaustive extraction of SVOCs from gasification waste-water presents several novel features. To the author's knowledge this is the first attempt to use CPME in analytical LLE. CPME proved to be an excellent extraction solvent for SVOCs from water, especially for the most polar ones. It is expected that the applications of CPME are not limited to gasification waste-water and possible uses for the extraction or organic compounds from other type of aqueous matrices are certainly worth investigating. The developed method also includes, for the first time, the use of HIVS which is a system that was developed as part of this thesis. To the author's knowledge, the HIVS technique has not been used in the past for analytical applications and further development and uses of the technique in the field of analytical chemistry are expected. This may include possible adaptations for other types of samples and further development of the used sonotrodes to allow for more robust use.

The suggested GCxGC set-up that was introduced here and is referred to from now on as "polar normal phase" shows that it is possible to separate mixtures of very polar compounds that would otherwise be very hard to separate. Further development of exhaustive microextraction techniques like the one presented in this chapter may change the way LLE is performed, introducing more green methods, that use less sample, less solvent and are much faster than traditional methods.

As demonstrated above, this chapter includes the development of a time efficient and precise method for the analysis of coal gasification waste-water. As previously developed methods are more time-consuming and labour intensive, the method presented above can be a useful tool in the hands of coal gasification operators. With a sample preparation and analysis time of less than two hours, the method can be used in UCG trials for the analysis of samples coming directly from the production stream of a UCG cavity of even from a surface gasifier. Considering that UCG run is performed in the course of several days/weeks the method may provide operators with a near real-time picture of the SVOCs present in the process stream. This may aid not only for environmental monitoring of the process, but also to identify retrievable components of economic value and increase the understanding of a very complex process such as UCG.

Chapter 4

Analysis of SVOCs in coal tar from gasification

4.1 Introduction

Coal tar is a viscous dark liquid that is a by-product of coal devolatilisation and gasification[4], including underground coal gasification. During a UCG trial, tars are usually collected in a large separator located at the surface (see Figure 5.3, p.77) but sampling can also take place by redirecting a small percentage of the production line in a more controlled sampling environment located in a laboratory (Figure 3.1, p.22). In lab-scale pilot trials, more elaborate sampling systems are used, for example the effluent sampling system that was employed in the Mellon Institute Riser reactor system[102], which has multiple temperature-controlled traps (Figure 4.1).

As for their environmental impact, coal tar is released to the environment as a non-aqueous phase liquid (NAPL), which can be either less dense than water (light non-aqueous phase liquid (LNAPL)) or denser than water (dense non-aqueous phase liquid (DNAPL)) (Figure 4.2); tars contain a vast and complex range of organic compounds, with a large range of polarity and aqueous solubility. Coal tar has multiple uses in the industry such as fuel, wood impregnating agent, in roofing and paving materials and in the making of dyes; it also has medical uses[103]. However, its adverse health effects are well known as it is classified as a category 1 carcinogen from the International Agency for Research on Cancer (IARC)[104].

The chemical characterisation of coal tar that derived from surface coal gasification peaked during the 1960s, where researchers had already formed a good idea of the organic compounds that exist in coal tar[105–107]. Usually, coal tar characterisation methods rely on fractionation and the use of multiple protocols[108]; however, recent advances in analytical instrumentation, such as the commercialisation of comprehensive two-dimensional gas chro-

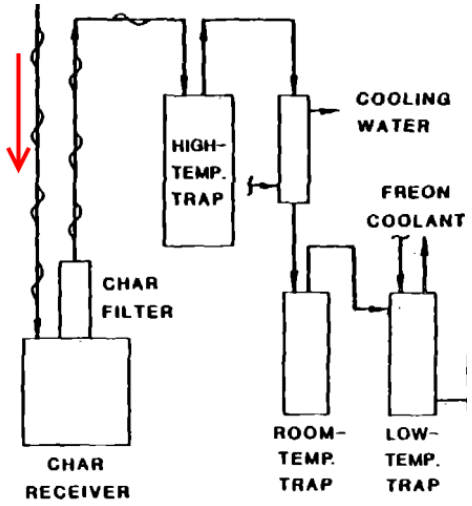

Figure 4.1: Sampling system of the riser reactor at the Mellon Institute. It comprises of four units, a char receiver, a high temperature trap with no temperature control, a room temperature trap before which the effluents are cooled down to room temperature and a low temperature trap operated with a freon coolant. Red arrow indicates effluent flow. Copied from Fillo *et al.* [102], credit: U.S. Department of Energy, Mellon Research Institute

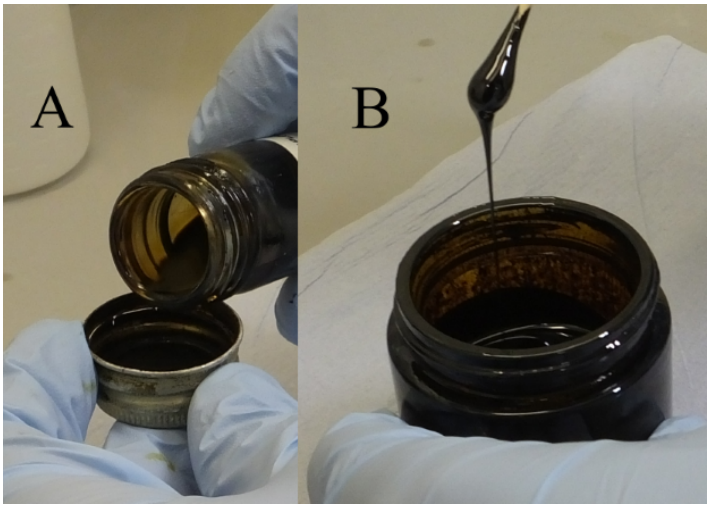

Figure 4.2: Typical NAPLS. On the left a less-dense than water NAPL and on the right a more dense than water NAPL (pitch)

matography, have allowed the development of fast, one-step methods; applications during the last decade include coal tar analysis from FMGP sites [109–111] and creosote [112–115]. However, when a greater degree of detail is required, both fractionation and comprehensive gas chromatography are cumulatively applied, allowing new insights into the complexity of coal tar [49], with the expected trade-off in sample preparation time, additional equipment required for fractionation, multiple analysis and multiple set-ups needed to analyse each fraction.

Regarding UCG derived coal tar, several characterisation studies took place during the UCG trials of the 1970-80s performed in the United States. The trials were relatively limited in detail, focusing mostly on the physico-chemical properties of tars and on large compound

groups deriving from fractionation of the tars[42,44,116–118]. Recently published research on the characterisation of coal tars produced during UCG trails in Poland[46,119] provide additional information on these types of tars. However, these studies, although more thorough than older studies, are still focused on the determination of classic physico-chemical properties, with little focus on individual organic compounds, further indicating the need for detailed mass spectrometric determinations of these type of tars.

Coal tar is being constantly produced within the course of a UCG trial and advanced knowledge of its composition as a by-product is important for multiple reasons, including its potential use as a petrochemical feedstock, possible link of its composition with reaction and process conditions but also due to the adverse environmental effects of its components[42]. Several methods exist in the literature for the analysis of coal tar. The United States environmental protection agency (USEPA) suggests Method 3580[120] for analysis of DNAPLs, which includes dissolution of the tar into methylene chloride (1 gram of tar in 10 mL of solvent), spiking with a surrogate, addition of sodium sulphate, shaking and sample clean-up using a Pasteur pipette loosely packed with glass wool. Afterwards, the sample can be further cleaned-up, analysed or fractionated[108]. The method is fast and it is used under the assumption that the tar is completely dissolved with manual shaking. The amount of solvent used is relatively large while the use of glass wool, if untreated, may be a source of adsorption for active compounds. McGregor *et al.*[109] developed a tar analysis method that requires no fractionation where each tar sample is extracted in one step using pressurised liquid extraction (PLE) and subsequently analysed by GCxGC-TOF MS[109]. This study demonstrated the feasibility of one-step tar analysis while further application of this approach led to insights such as the forensic classification of FMGPs based on GCxGC-TOFMS fingerprinting and the application of statistical techniques[110]. The method requires no fractionation, but it involves several steps. For the tar sample to be compatible with PLE it has to be transformed in a pseudo-solid matrix by grinding the tar along with diatomaceous earth and Na_2SO_4 with a mortar and pestle, making the method labour intensive. Grinding also introduces mechanical stresses which may influence volatiles and increasing sample preparation time. Also, the PLE tar extract must be pre-concentrated by evaporation adding into the sample preparation time where there is also a risk of influencing the recovery of volatiles. However, recovery values for surrogates (with the lightest being d8-naphthalene) were reported to be above 76%. Gallacher *et al.*[112] reported a variant of this method but with removing the manual grinding step and placing the coal tar directly in the cell along with diatomaceous earth and Na_2SO_4 and reported similar recoveries.

The tar extraction method that is developed in this chapter is partially based on USEPA method 3580[120] while retaining the advantages of comprehensive two-dimensional gas chromatography. The aim of the method is the precise extraction and analysis of tar, with as less sample preparation as possible, in order to provide the minimum sampling-to-results time.

This way UCG operators can have information of tar composition in the process stream in a relatively short time. This is the second method that is developed in the thesis and together with the waste-water extraction method, they are suggested as a full sample preparation and analysis pipeline for effluents that are produced from UCG. Since tar is also produced from the surface gasification of coal but also from other processes, like biomass gasification, the method has a wide range of possible usage. Here, the HIVS system is utilised in aiding the extraction process, while the potential of replacing DCM (which is the primary solvent in USEPA Method 3580[120]) with CPME is also explored. Overall, the method is expected to be fast, simple, with minimal invasiveness to the tar samples, thus, achieving greater sample representativeness in the analysis.

4.2 Materials and methods

4.2.1 Chemicals

CPME (stabilised with 50ppm BHT) and 4-fluorophenol were obtained from ACROS Organics. Cyclohexane, 1-fluoronaphthalene, 5-fluoroindole, 1-fluorododecane, fluorene-d10, chrysene-d12 and 1-bromo-2-naphthol were obtained from Sigma Aldrich. Reagents 4-fluoro-2-methylpyridine and 4-bromo-2,6-dimethylpyridine were obtained from Alfa Aesar. Phenol-d6 and naphthalene-d8 were obtained from Supelco and lastly, DCM and Na_2SO_4 were obtained from Fisher. Phenanthrene-d10 was obtained from Isotec. All of the reagents were of analytical grade or better.

While BHT makes a good injection standard because it is stable and already added in CPME by the manufacturer. Having a constant concentration, sample to sample, human error and variation introduced by dilutions is removed. An additional solution of 100mg/L of cyclohexane in CPME was prepared for use as an injection standard in the first part of the screening study where solvent ratios are not stable. The internal standard used for method validation was a 1000mg/L mixture of three compounds: phenol-d6, naphthalene-d8 and phenathrene-d10.

The method was developed using coal tar pitch provided by Koppers Carbon Materials & Chemicals Pty Ltd (Figure 4.2, left). It is expected that coal tar will be more easily extracted than coal tar pitch (since pitch is a heavier version of coal tar) so a method developed for coal tar pitch should be easily applied to the extraction of coal tar without expecting any losses in extraction efficiency.

4.2.2 GC analysis

Three GC systems were used for sample analysis, a GC coupled to flame ionisation detector (GC-FID), a GC couple to a mass spectrometer (GC-MS) and a comprehensive two-dimensional gas chromatography coupled to time-of-flight mass spectrometry system (GC-xGC-TOFMS).

GC-FID Each analysis was performed on an Agilent 7890B GC system using an Agilent phenyl arylene polymer DB-5 capillary column (0.25mm i.d. x 30m length, 0.25um film thickness). System parameters for the method are as follows: inlet temperature 300°C, injection volume 1μLwith a split ratio of 1:20, initial oven temperature 100°C, hold for 0.2 min, then to 325°C at a rate of 10°C/min and hold for 10min, helium flow rate was set at 2mL/min. Detector temperature was set at 345°C.

GC-MS Each analysis was performed on an Agilent 5975C series GC/MSD system using an Agilent (50%-Phenyl)-methylpolysiloxane phase DB-17MS capillary column (0.25mm i.d. x 60m length, 0.25um film thickness). Three methods were developed, one for surrogate recovery analysis and two for untargeted sample analysis.

For surrogate recovery analysis the following parameters were used: inlet temperature 300°C, injection volume 1μLwith a split ratio of 1:200, initial oven temperature 70°C, hold for 0.2 min, then to 220°C at a rate of 10°C/min and then to 320°C at a rate of 60°C/min hold for 14min, helium flow rate was 1.4mL/min.

Regarding surrogate analysis, a quantitative method was developed for the analysis of the surrogates with 6 concentration levels used for all compounds: 1.125, 2.25, 4.5, 9, 22.5 and 45 mg/L. Details of the calibration curve include internal standards for each surrogate, retention times and ions used to quantify each compound are shown in Table 4.1.

Table 4.1: SIM method parameters for surrogate analysis

Compound	Internal standard	Retention time	Quantifying ion
4-fluoro-2-methylpyridine	phenol-d6	4.85	111
4-fluorophenol	phenol-d6	7.71	112
1-fluorododecane	napthalene-d8	9.87	57
1-fluoronaphthalene	napthalene-d8	10.78	146
5-fluoroindole	napthalene-d8	13.80	135
4-bromo-2,6-dimethylphenol	napthalene-d8	14.39	200
fluorene-d10	phenanthrene-d10	16.46	176
1-bromo-2-naphthol	phenanthrene-d10	17.07	222
chrysene-d12	phenanthrene-d10	22.25	240

For untargeted analysis the following parameters were used: inlet temperature 300°C, injection volume 1μLwith a split ratio of 1:20 for the first method and 1:50 for the second method, initial oven temperature 70°C, hold for 0.2 min, then to 320°C at a rate of 3.5°C/min and hold for 20min, helium flow rate was 1.4mL/min. In untargeted analysis for less diluted samples (such as the 1:2 diluted samples) and heavier tars (such as tars from FMGPs or coal tar pitch) the inlet temperature was lowered to 250°C so that entrance of heavy-boiling/non-ionisable components in the sample path is discouraged.

In all methods the transfer-line temperature was set to 280°C, source temperature was set to 230°C and quadropole temperature to 150°C. The source temperature was kept at 230°C as it is preferable for high-boiling, non/ low-ionisable components to condense in the source which is easier to clean rather than in the more delicate parts of the mass spectrometer (such as the mass analyser).

GCxGC-TOFMS Each analysis was performed on a Leco Pegasus 4D equipped with a Zoex liquid nitrogen cooled modulator. A reverse phase column set-up was used with an Agilent (50%-Phenyl)-methylpolysiloxane phase DB-17MS column on the first dimension (0.25mm i.d. x 60m length, 0.25um film thickness) and a Restek 1,4-bis-(dimethylsiloxy)-phenylene dimethyl polysiloxane phase Rxi-5Sil MS™ column on the second dimension (0.25mm i.d. x 1.50m length (0.1m in the modulator, 1.20m in the secondary oven and 0.2m in the transfer line), 0.25um film thickness). Inlet temperature was set at 300°C, injection volume 1μL with a split ratio of 1:50, modulation time was 4s, initial oven temperature 70°C, held for 0.2min, then to 320°C at a rate of 3.5°C/min and held for 20min, helium flow rate was 1.4mL/min. Other conditions of analysis of tar samples are reported in the corresponding materials and methods sections for each chapter.

Chromatogram processing Once the method was developed, chromatograms of pitch that were analysed with 1:10 and 1:2 dilution ratios were compared for peak picking performance. This was done using two set-ups for AMDIS: one for major components with the following settings: peak width 32, two peak subtractions, medium resolution, medium sensitivity, high shape requirements signal to noise filter-10 and minimum models-5; one for minor components with the following settings: peak width 32, two peak subtractions, high resolution, high sensitivity, high shape requirements signal to noise filter-10 and minimum models-3. For Chromatof® baseline offset was set to 1, peak width 16 (1st dimension) and 0.12-0.14 (second dimension), traditional integration approach and signal-to-noise filter was set at 100.

4.2.3 Indicative sample analysis

Indicative sample analysis is provided for visualisation of the results of the developed method and for comparing the performance of the two dilution ratios. An underground coal gasification tar sample (sample 1, Barbara II trial, Table5.1, p.76) was analysed using the GC-FID and GC-MS with the two dilution ratios. A brief evaluation of the peak picking performance between the two dilution ratios was performed using the two AMDIS deconvolution approaches given above. Additionally, the UCG tar sample was analysed using the GCxGC-TOFMS and compared with a pitch sample that was analysed using the same method. A brief description of the results is given along with differences between the chromatograms that demonstrate the use of the developed method for different tar samples.

4.2.4 The HIVS system

The HIVS system had to be adapted for use with 9mL glass crimp-top vials. The same adapters were used as in the waste-water extraction method which were designed to make vial mounting easier and prevent the sonotrode from coming into direct contact with the glass vial, effectively decreasing the chance of vial deterioration and breakage and sonotrode surface wear. Once the vials were fitted onto the sonication probe, the parameters of the sonication probe were tested using trial and error in order to determine the system's operating range. Since the crimp-top vials are more robust than the 15mL centrifuge vials used in the UASESOME method, the maximum operational power was set to 50W.

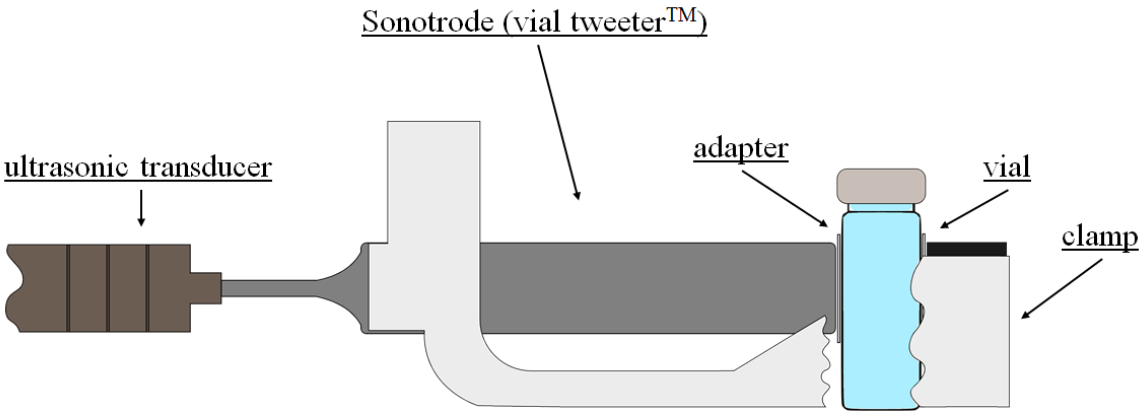

Figure 4.3: Fitting of the 9mL glass vials onto the sonotrode vial-tweeter to perform HIVS. Image ©*Ioannis Sampsonidis*

4.2.5 Screening design for UAE

The application of the HIVS system in the extraction of tar is tested by applying a DOE design and screening three factors: time, intensity and solvent (Table 4.2). Although DCM is

the solvent of choice for USEPA waste dilution method 3580A [120], the performance of CPME was also studied as it proved to be a superior solvent in the extraction of polar compounds from wastewater and is also compatible with less polar compounds such as PAHs that are the primary constituents of coal tar. For this study approximately 0.3gr (with an accuracy of 0.1gr) of tar were weighted into a 9mL crimp top vial, the mass of the tar was recorded and approximately twice the amount of Na_2SO_4 was added in the vial along with the tar. For the extraction-dissolution of tar, 3 mL of solvent were added into the vial (following the 1:10 dilution ratio of method 3580A) using a syringe, the atmosphere in the vial was replaced with N_2 by fitting a three way valve into each vial (fitted with a luer syringe needle) and alternating three times between vacuum (using a vacuum pump) and N_2 (at 10psi); this is done to remove air and prevent sample oxidation during the intensive sonication process. The vial was then mounted on the sonotrode and sonicated at the indicated intensity and for the indicated amount of time. The vial was then centrifuged at 2000rpm for 5min for solids separation, the crimp seal was removed and approximately 2mL of the extract were transferred to the top of a Pasteur pipette that was loosely packed with cotton wool so that any remaining large particles are filtered out. The filtrate was then stored at -20°C until analysis. Before analysis, 10μLof each sample was transferred into a 200μL glass vial insert containing 70μL of CPME and 20μLof the injection standard solution and the sample was injected in the GC-FID. CPME was used as the dilution solvent in order to minimise contamination of the FID detector from HCl forming from DCM [121], minimise the use of DCM, and because it is more stable on the autosampler in room temperature in comparison to the very volatile DCM. The response used for data analysis was the total chromatogram area excluding solvent peaks, deducting the blank area and dividing by the area of the injection standard (in this case cyclohexane). For the screening study the samples were also analysed complimentary on a UV double beam spectrophotometer. For this analysis, 60μL of each extract were diluted 1:50 in acetonitrile and the sample was scanned from 200 to 400nm. The reference blanks were a 1:50 mixture of each solvent in acetonitrile.

Once the factor levels trends were understood, the effect of the extraction time was also screened. Samples were prepared as above except for weighting the tar sample with 0.001gr accuracy. Also, DCM was used as the extraction solvent and sonication was performed with a fixed intensity of 50W. In total, six time points were studied, 5, 25, 45, 75, 105 and 145sec. Before injection of the extract on the GC-FID, each sample was diluted 1:10 in CPME. As above, the response used for data analysis was the total chromatogram area excluding solvent peaks and deducting the blank area and dividing by the area of the injection standard which in this case was BHT for the reasons mentioned above.

Table 4.2: Screening DOE design used for UAE factor screening. Each run represents a unique combination of factor levels

Run order	time	intensity	solvent
1	5	10	CPME
2	5	50	DCM
3	25	30	CPME
4	5	10	DCM
5	45	50	CPME
6	25	30	DCM
7	5	50	CPME
8	45	10	CPME
9	45	50	DCM
10	45	10	DCM
11	25	30	DCM
12	25	30	CPME

4.2.6 Method validation

After the selection of extraction conditions, the extraction protocol was validated for precision and matrix effects. For this purpose, 9 surrogates were selected that represent major compound classes found in coal tar: 4-fluoro-2-methylpyridine, 4-fluorophenol, 1-fluorododecane, 1-fluoronaphthalene, 5-fluoroindole, 4-bromo-2,6-dimethylphenol, fluorene-d10, 1-bromo-2-naphthol, chrysene-d12. A stock standard of the surrogate solution was prepared in 1:3 DCM:CPME at an initial concentration of 7500mg/L. Coal tar pitch was extracted by weighting 0.3g of coal tar pitch (with an accuracy of 0.001gr) in a 9mL crimp-top vial and adding approximately 0.6g of Na_2SO_4. Then vial was sealed and 3mL of DCM were added along with 40μLof the surrogate solution to a final concentration of 100mg/L. The atmosphere inside the vial was replaced with N_2 and the vial was then mounted onto the sonotrode and sonicated for 45s at 50W and with a pulse of 75%. Following sonication, the vial was removed from the sonotrode and placed into the centrifuge where it was centrifuged at 2000rpm for 5min. The vial was then decapped and 2mL of the supernatant where transfer into a glass pasteur pipette loosely filled with cotton. The filtrate was collected at the bottom of the pasteur pippete in a 4mL vial and stored at -20°C for analysis. In total, three method blank samples (identical process - no coal tar) and 6 coal tar pitch samples were extracted. Tar extracts were analysed in the GC-FID for precision evaluation using the total chromatogram area (as in the extraction time screening study) and both blanks and tar extracts were analysed on the GC-MS for precision evaluation, matrix effects and recovery assessment. For each injection 10μLof each filtrate were mixed with 5μLof the internal standard solution and 85μLof CPME. Each sample was injected three times.

4.3 Results and discussion

4.3.1 Screening design for UAE

For interpretation of the results of the factor screening DOE design, total chromatogram area response factors and UV absorption values were used as responses and loaded to Minitab to build three factorial regression models. For the first model the response was the total chromatogram area that corresponds to the bulk/aggregate values of SVOCs in coal tar. For the second model the UV absorption values for 254nm were used that correspond to the PAH index[122] (used for estimating the global PAH concentration in specific matrices). The response used for the third factorial regression model was the ratio A_{254nm}/A_{288nm} which is related to the proportion of light to heavy PAHs in the measured sample[122]. Performance of all three of the factorial regression models can be seen in Table 4.3

Table 4.3: Performance of the factorial regression models for the screening study

	Total area	A_{254nm}	A_{254nm}/A_{288nm}
R-sq [%]	99.96	99.77	98.14
R-sq(adj) [%]	99.84	99.16	93.20
R-sq(pred) [%]	94.67	90.92	7.02

The main effects plot from the total area factorial regression model can be seen in Figure 4.4. Both time and sonication intensity appear to have a positive effect on the extraction of SVOCs from coal tar. Regarding solvents, DCM performance on SVOC extraction is significantly better than the performance of CPME. The same trends can be observed when looking at the main effects plot of the factorial regression model for A_{254nm} in Figure Appendix A.2.1. At this point is must be noted that the absorption at 254nm refers to all UV absorbing compounds at this wavelength[123], which may include components that are not volatile enough to be analysed by gas chromatography.

As noted above, the ratio A_{254nm}/A_{288nm} is relative to the proportion of light to heavy PAHs in the sample. Monitoring this ratio is interesting as it may give additional information regarding the composition of the measured samples, but it can also provide a crude measure of extraction efficiency relative to PAH molecular weight. Looking at the main effects of the factorial regression model fitted on the A_{254nm}/A_{288nm} data (Figure 4.5A), it is seen that the ratio A_{254nm}/A_{288nm} decreases with sonication time while there is a small increase associated with intensity. The use of DCM instead of CPME gives a significant decrease in the ratio which indicates that DCM is better in extracting the heavier PAHs. By having a closer look at factor-to-factor interactions in Figure 4.5B, it appears that extraction time is more important when CPME is the extraction solvent. However, the effect of time and intensity appears to be cumulative in lowering the A_{254nm}/A_{288nm} ratio.

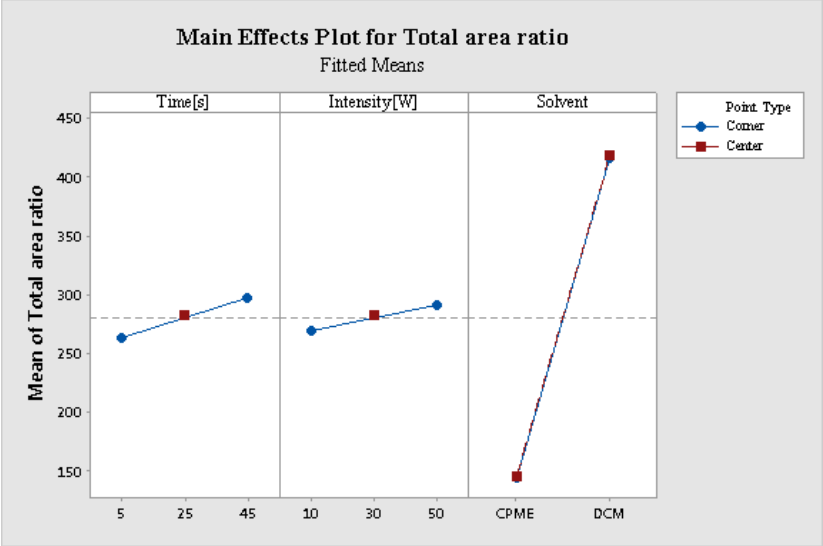

Figure 4.4: Main effects plot for the total chromatogram area regression model. The main effects shows how the response changes when altering the corresponding factor. Corner points are the maximum and minimum factor levels of the model while center points are values that lie in the middle of the two corner points

Following indication from the factorial regression models, the solvent chosen to be included in the extraction method was DCM. Sonication intensity was kept stable at 50W and the effect of sonication time on the extraction of SVOCs was further tested for different time intervals. Results from the study can be seen in Table 4.4. The time point where the total area ratio is higher is at 45s. Although the area increase from 5s to 45s is less than 10%, the trade-off for extra sample preparation time is not significant. An unexpected area increase at 145s can be explained by the high temperature increase observed at this time point (the vial getting too hot to the touch). Although the system was operated in pulse mode, an increase in temperature is expected, with the effect appearing cumulative as time passes. The temperature increase may cause solvent evaporation and also breakdown of structures that are polymerised in the sample[124] into smaller soluble molecules. Operating the sonotrode at these conditions is dangerous since the pressure increase in the vial by the devolatalising solvent and components can lead to explosion, septum failure and vial breakages, releasing the contents of the vial into the surrounding area. For the reasons noted above, 45s were chosen as the sonication time for validating the method.

4.3.2 Method validation

The precision of the extraction method was studied by preparing 6 extraction replicates using two methods: surrogate recovery precision using the GC-MS setup and total SVOC chromatogram area precision using the GC-FID. One of the replicates was removed from precision calculations as a loss of solvent during storage was suspected. Surrogate recover-

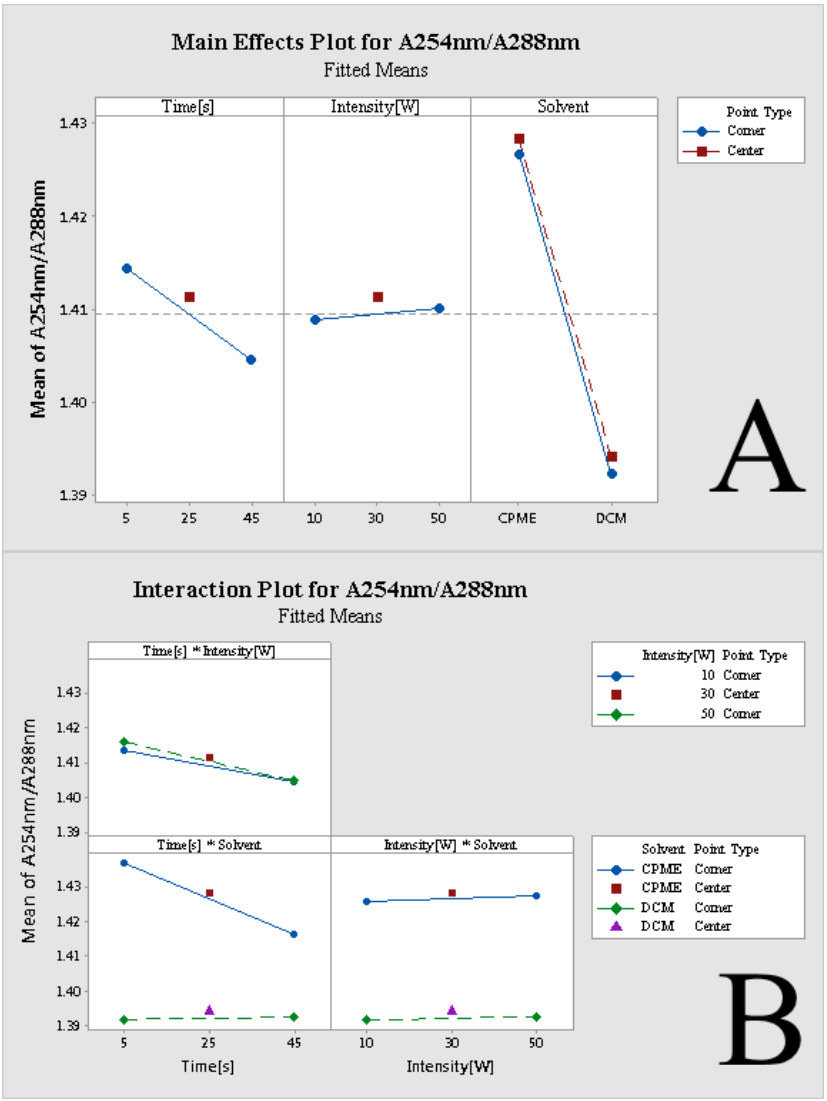

Figure 4.5: Main effects and interaction plot for the A_{254nm}/A_{288nm} factorial regression model. The main effects shows how the response changes when altering the corresponding factor. Corner points are the maximum and minimum factor levels of the model while centre points are values that lie in the middle of the two corner points. The interaction plot shows if there is any interaction between factors. Here it appears that extraction time has a stronger effect on the response when CPME is used as the extraction solvent

ies and extraction precision can be seen in Figure 4.6; the corresponding calibration curves are provided in Figure Appendix A.2.2. Regarding extraction precision, the average relative standard deviation for the surrogates was 1.29% with the minimum being 0.78% for 4-fluorophenol and the maximum 1.79% for 4-fluoro-2-methylpyridine. For the total area ratio, the relative standard deviation was calculated at 1.34%. The average recovery for the surrogates (non-blanks) was calculated at 99.38% ranging from 89.89% for 4-fluorophenol to 104.70% for 1-bromo-2-napthol, well within the 70-130% accepted range as stated in U.S. EPA SW-846 Method 8000D[125].

Figure 4.6 provides a visual indication of the matrix effects and recovery precision, based on

Table 4.4: Total area response for the time point study. Response factor is ratio of the total chromatogram area to the area of BHT. The reported standard deviation is from replicate GC-FID injections

Time [s]	Tota area response factor	Sd (inj, n=3)
5	153.6	1.1
25	159.6	0.9
45	167.9	1.2
75	157.5	0.4
105	146.4	0.4
145	160.5	1.8

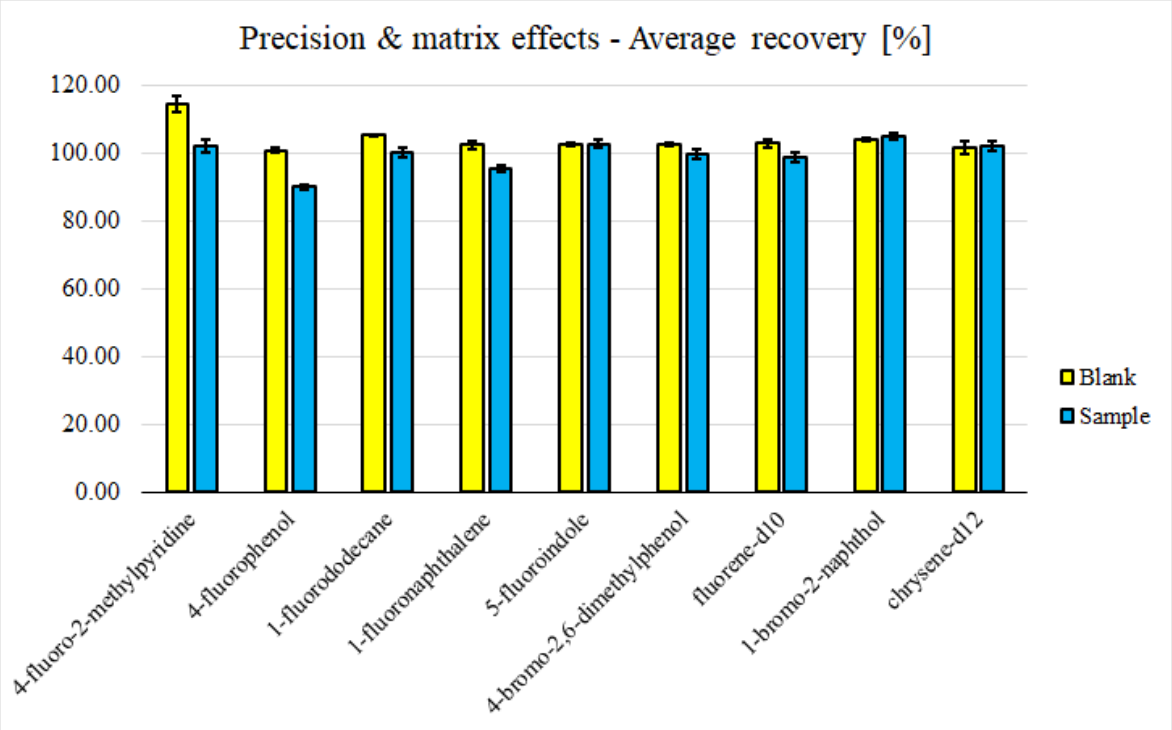

Figure 4.6: Surrogate precision and matrix effects of the tar extraction method. The average RSD is 1.29%. Surrogates appear by elution order

the surrogates. Statistical measures of differences between the blank and real sample extractions for each sample can be seen in Table 4.5. Statistical significance was measured using both parametric (t-test) and non-parametric (Mann-Whitney) tests since sample population is too small to make any rigid assumptions regarding normality. Matrix effects for 4-fluoro-2-methylpyridine and 4-fluorophenol appear to be the largest (difference of $+11.55\%$ and -11.29) with 1-fluoronaphthalene and 1-fluorododecane following (%Difference of 7.04 and 5.10 respectively). Effects for 5-fluoroindole, 1-bromo-2-naphthol and chrysene-d12 appear to be statistically insignificant.

Table 4.5: P-values for parametric and non-parametric statistical significance tests between blank and tar sample extractions along with percentage differences between the values. All the values correspond to a significance level of 95%.

	t-test	Mann-Whitney	%Difference
4-fluoro-2-methylpyridine	0.005	0.037	11.6
4-fluorophenol	0.000	0.037	11.3
1-fluorododecane	0.001	0.037	5.1
1-fluoronaphthalene	0.001	0.037	7.0
5-fluoroindole	0.885	1.000	0.1
4-bromo-2,6-dimethylphenol	0.013	0.037	2.8
fluorence-d10	0.015	0.037	4.0
1-bromo-2-naphthol	0.131	0.233	0.9
chrysene-d12	0.618	0.551	0.7

4.3.3 Indicative sample analysis

The GC-FID trace of an *in-situ* UCG tar sample (sample 1 from the Barbara II trial - see Section Appendix A.1.1, p.174) can be seen in Figure4.7. Analysis of the *in-situ* UCG tar sample using the GC-MS methods can be seen in Figure 4.8. The chromatogram is focused on the micro-components of the sample and an overview in full scale can be seen at the upper right corner of the figure.

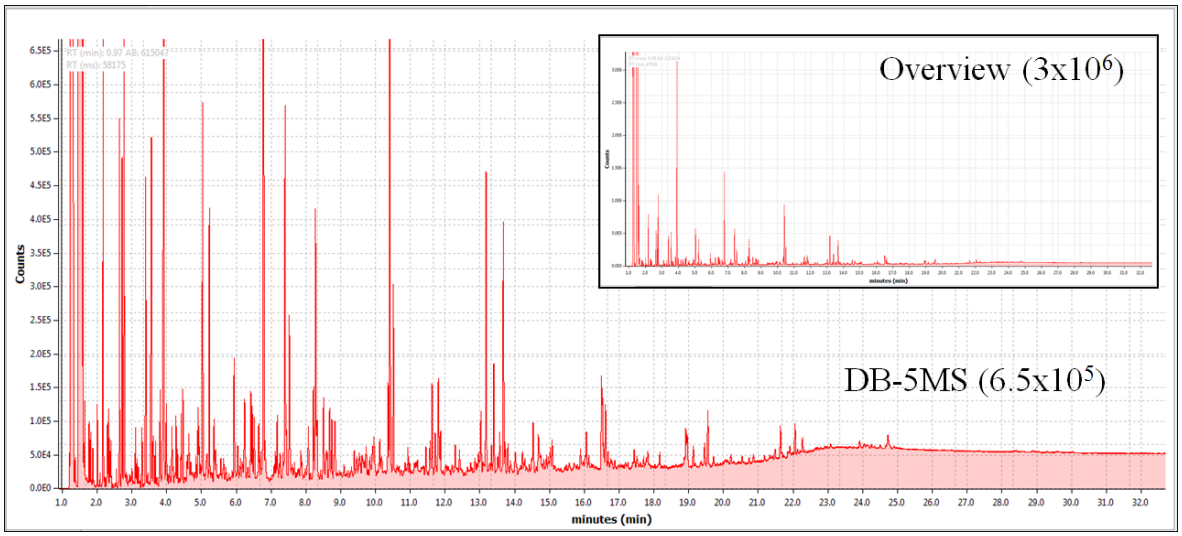

Figure 4.7: FID trace of an *in-situ* UCG tar sample. The chromatogram is focused on the micro-components of the sample with an overview in full scale given in the upper right corner

Analysis of the GC-MS chromatograms with AMDIS yielded the results presented in Table 4.6. Injecting the sample using the 1:2 dilution ratio gives an increase of 55.9% in detected components using the major components method and 28.8% using the minor components method. Both differences are significant from an identification point of view, providing the opportunity to identify more components. However, injecting the samples with the dilution

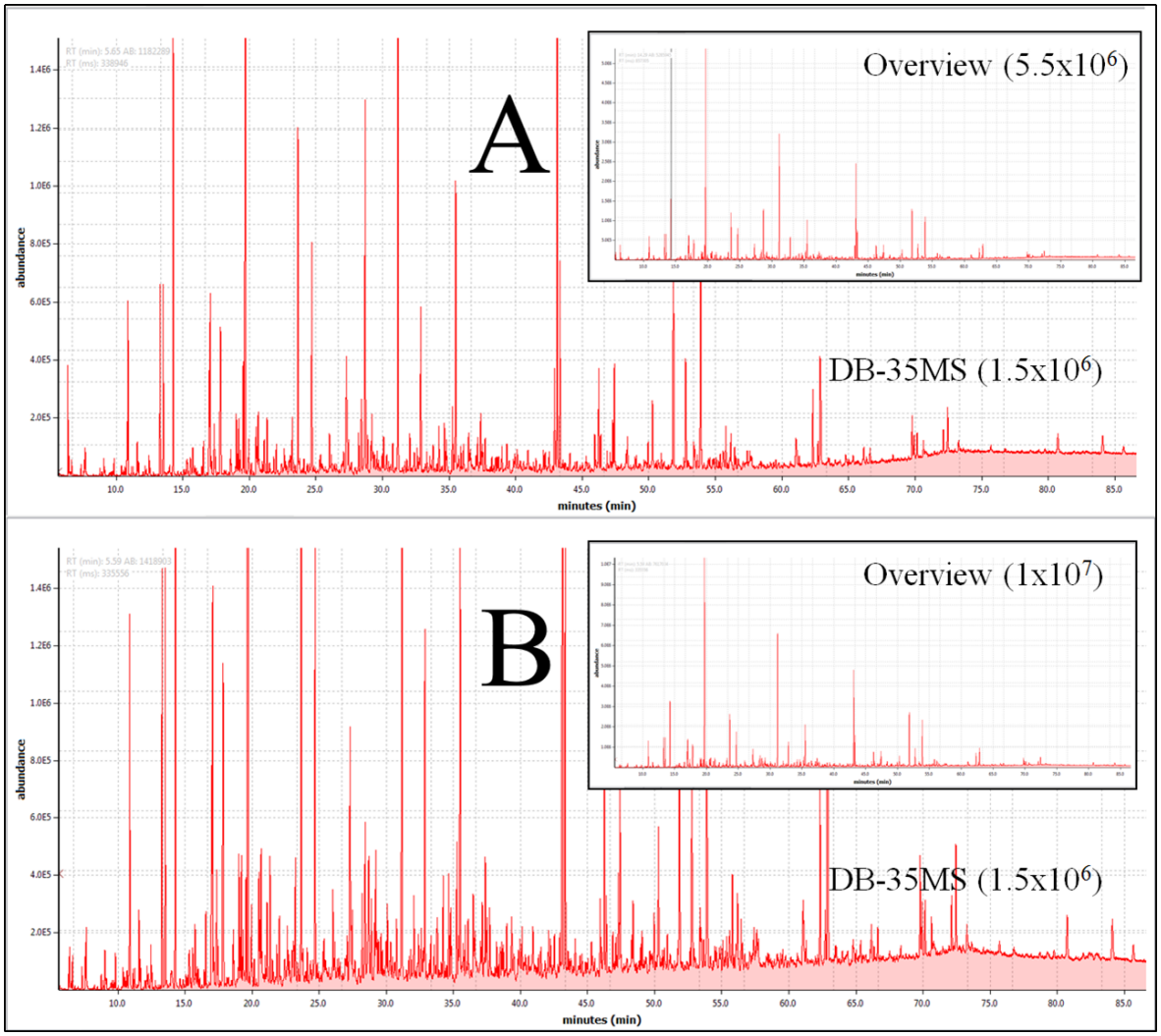

Figure 4.8: GC-MS chromatograms of an *in-situ* UCG tar sample. The chromatogram is focused on the micro-components of the sample with an overview in full scale given in the upper right corner. A chromatogram of the 1:10 diluted sample in on the top (A) and that of the 1:2 diluted sample on the bottom of the figure (B)

of 1:2 ratio is expected to foul the inlet liner, analytical column and ion source much sooner, possibly creating issues during the analysis of a series of samples. Therefore, the 1:10 dilution ratio was used for analysis of sample series for statistical analysis purposes where more injections are required and the 1:2 ratio is suggested for identification purposes. An initial compositional assessment of the sample by chromatogram processing, as described in the materials and methods section, showed the sample is particularly rich in SVOCs including, PAHs as the primary components, phenols, heterocycles and alkanes.

Analysis of the tar extracts from pitch and UCG using GCxGC-TOFMS appear in Figure 4.9. The differences between pitch and UCG tar can be seen just by looking at the chromatogram. Specifically, pitch is composed mainly of aromatics, with some aromatics being in a much higher percentage in the sample. Also, as indicated in Chapter 2, pitch resembles high tem-

Table 4.6: Detected components in the two GC-MS chromatograms. The peak yield is significantly higher for the 1:2 dilution sample

	Dilution 1:10 - GC-MS	Dilution 1:2 - GC-MS
components/method 1	179	279
components/method 2	1010	1301

perature tar, and this can be see by looking at the intensity of the late eluting compounds. On the other hand, UCG tar is much more complex, it contains a lot more different species of aromatics and also a significant number of alkanes and alkylbenzenes.

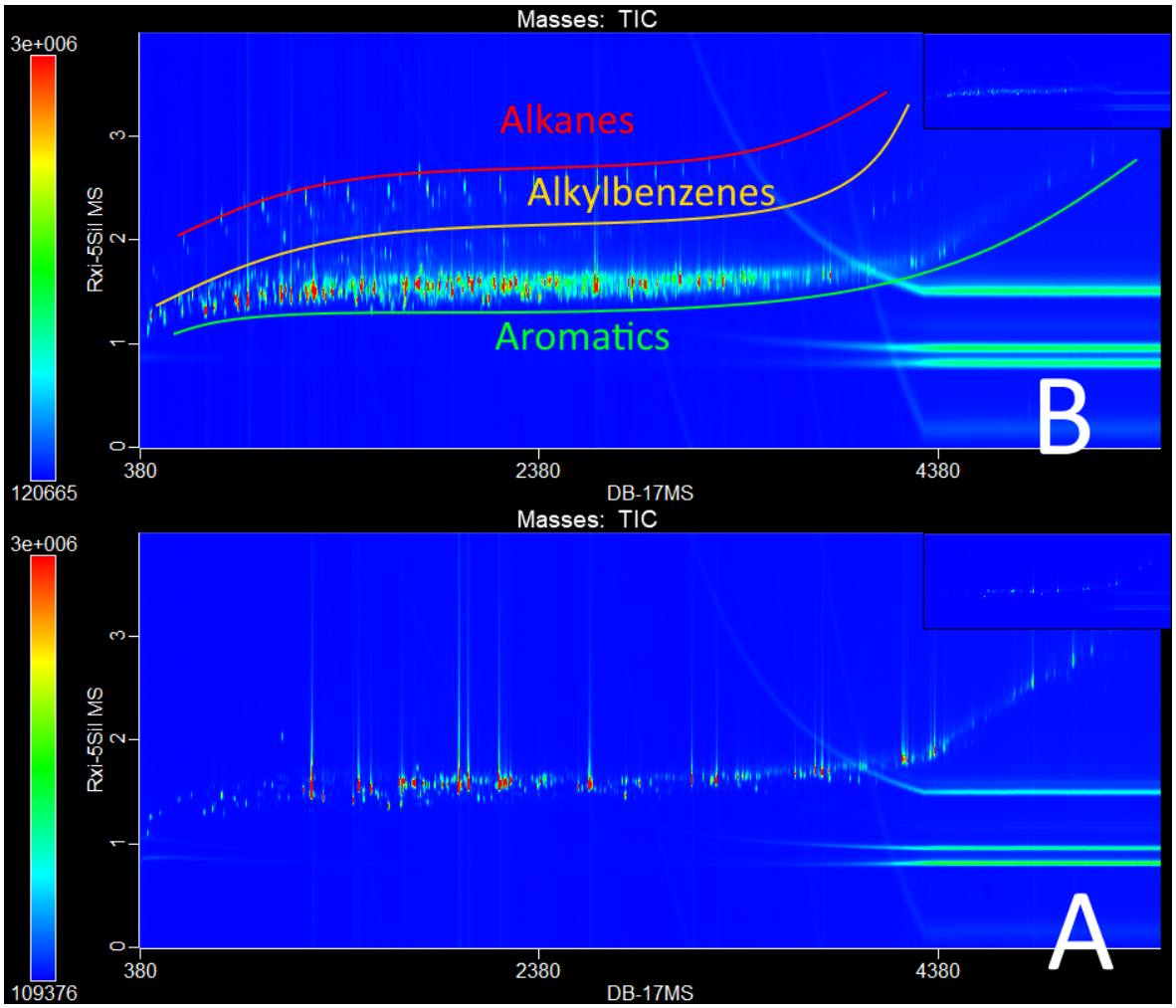

Figure 4.9: A: Pitch sample as analysed with the GCxGC-TOFMS method **B:** UCG sample as analysed with the GCxGC-TOFMS method. The elution patterns of n-alkanes, n-alkylbenzenes and aromatics are shown in the figure. Pitch sample is rich only in aromatics while the tar sample from UCG shows a number of alkanes and methylated benzenes. The differentiation between the samples is clear only by looking at the chromatogram.

4.4 Conclusions

The method described above is a significant improvement of the USEPA method 3580 specifically applied in the analysis of tar. It provides the analyst with a repeatable, hassle-free way to extract tar with minimal solvent usage and with a sample-to-results time of less than an hour (depending on the applied GC method). Sample preparation itself requires 15-20min in total (Figure 4.10). Very little manual labour is required, no sample preconcentration/evaporation is needed, and the number of consumables is kept as low as possible (9mL vial with septum, a glass Pasteur pipette with cotton wool and sample insert and vial). The method is high-throughput providing the analyst with the possibility to process several samples per day. Although the method was developed to process one sample at a time, the sonotrode provides the option of processing up to 5 samples simultaneously. This may require further research/method development since for more vials more power would probably be needed from the transducer in order to achieve the same result.

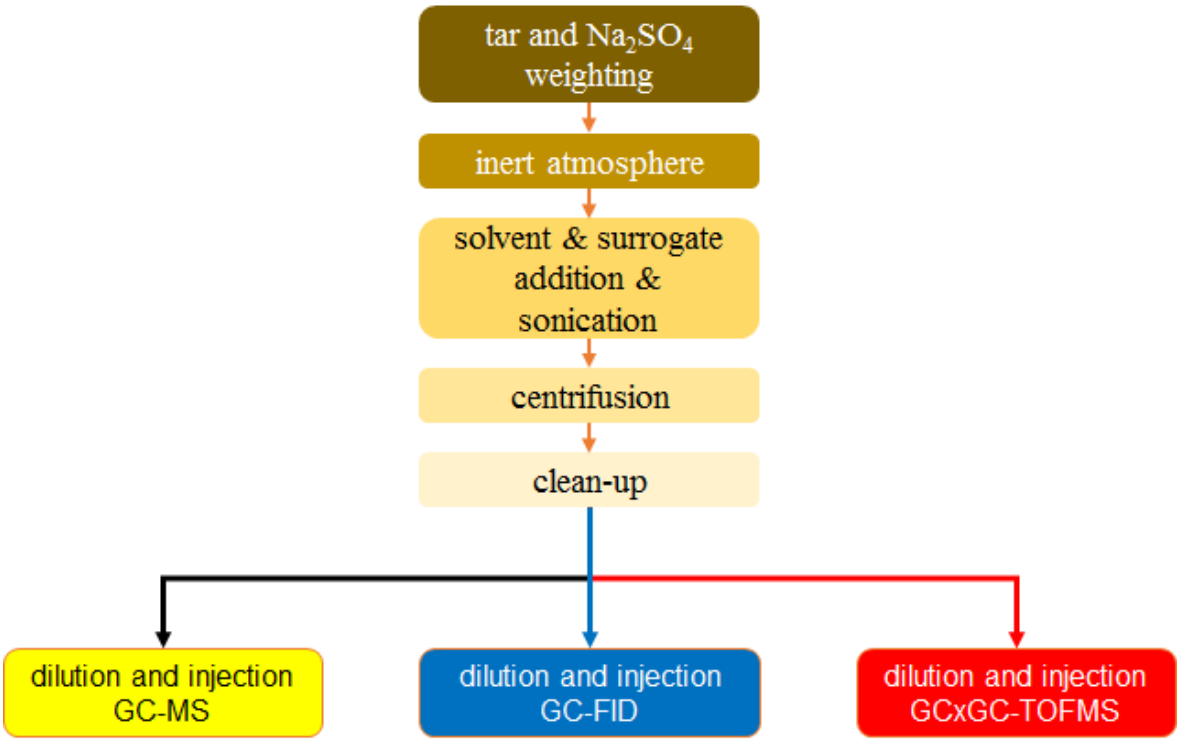

Figure 4.10: Graphical illustration of the UAE method

The method is expected to be useful to UCG and surface gasification operators that need a fast and effective way to analyse the SVOC composition of their production line condensates but also in environmental forensic applications as a fast alternative to lengthy fractionation methods. The method has great potential for application in contaminated soil extraction since it does not have the disadvantages of traditional sonication probes and maybe even be able to compete with pressurised solvent extraction. The most important advantages of

the developed method are: the time required to process the sample is very small (just a few minutes), apart from the sonotrode no extra equipment is needed and the sample is expected to be more representative since only a particulate filtering is performed with cotton wool. Future work would include using the same system to develop more miniaturised approaches where only a few drops of solvent would be needed to extract samples.

Chapter 5

Statistical exploratory analysis of the SVOC content in UCG waste-water and tar

5.1 Introduction

Field-scale underground coal gasification trials are large-scale trials which can normally take several days/weeks to complete and may involve several multidisciplinary teams including engineers, geologists and chemists. As mentioned in Chapter 2, the primary aim of UCG is the production of syngas, the composition of which is important in defining its heating value and constitutes a parameter that has been studied extensively. However, secondary effluents have not been studied as comprehensively as syngas, but they are also important from an environmental risk assessment point of view, economical retrieval of components, and to provide information for the better understanding of UCG.

For this reason, literature on several major UCG trials performed in the US were studied for usable SVOC data. One of the most well-known UCG gasification trials that was sponsored by public interest organisations is *Rocky Mountain I*, which was performed in November 1987 to February 1988 in Wyoming, USA (Figure5.1A)[33,126]. Although the aim of this experiment was focused on both technology verification for the extended linked well (ELW) and controlled retractable injection point (CRIP) techniques (Figure5.1B) and to address UCG environmental issues, to the author's knowledge, the publicly available chemical analysis studies are limited to monitoring cumulative chemical properties, inorganic parameters and some SVOCs such as BTEX, a few phenols and some heterocycles and PAHs[44,127]. More comprehensive SVOC data from UCG trials comes from older UCG trials and specifically from two previously published studies that involve semi-targeted and untargeted analysis of

UCG effluents: Pellizzari *et al.*[50] analysed samples from the Hanna II trial performed in 1976 and Humenick and Mattox[60] analysed samples from the Hanna IVB trial performed in 1979 (location of both trials can be seen in Figure 5.1A). In all cases the results from the literature indicate that during a UCG experiment there are several compositional changes both regarding generic chemical parameters and SVOCs.

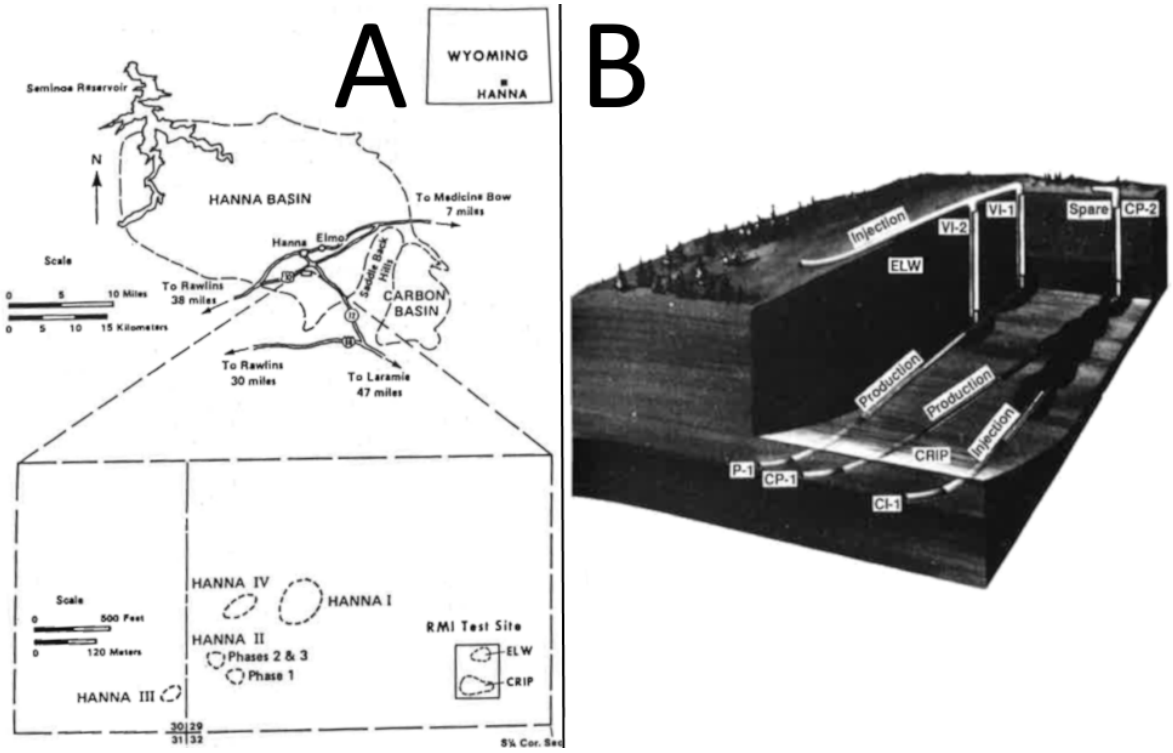

Figure 5.1: A: Location of the *Rocky Mountain 1* trial in the Hanna Basin, Wyoming, USA. Older UCG trials conducted in the area are also visible (image copied from Moody *et al.*[128]). **B:**: Cross-section showing the location of the wells for ELW and CRIP process (image copied from Cena *et al.*[129])

Pellizzari *et al.*[50] attempts to follow a purely untargeted approach to the analysis of both UCG waste-water and tar. For volatiles and some semi-volatiles waste-water was purged with helium which was subsequently passed through a condenser and the volatiles were trapped in a Tenax GC cartridge from which they were thermally recovered later. Semi-volatiles in tar and those that were not recovered in waste-water by the previous step were recovered by extracting the liquid samples with Freon-TF®. Although the analysis appears exhaustive, the amount and type of compounds varies between samples and no effort was made to monitor as many of the same compounds as possible between samples in order to make the data comprehensive enough to be useful for exploratory data analysis; also the quantitative information provided is largely incomplete. This makes following the desirable sample comparison approach somewhat problematic although this is expected since data analysis tools for mass spectrometry data were not yet developed when the study was conducted.

UCG waste-water and tar/oil was analysed by Humenick and Mattox[60] using multiple approaches. Phenolics were analysed by direct aqueous injections in a GC-MS equipped with a free fatty acid phase (FFAP) column. For the analysis of non-phenolics the samples were extracted using continuous solvent extraction with DCM, following back-extraction with a basic aqueous solution for the removal of phenolics. An evaporator was used to pre-concentrate the extracts which were then injected in a GC-MS fitted with a poly(dimethylsiloxane) SP2100 column. PAHs were analysed by GC-MS on a BBBT (bis(p-butoxybenzylidene) a,a'-bi-p-toluidine) column. Tar/oil samples were diluted 2% in hexane and then analysed same as waste-water. The data provided in this study are quantitative and organised into specific compounds the are accounted for in all samples, therefore, they can be used for exploratory statistical analysis.

As shown above, there is a lack of publicly available studies, therefore a knowledge gap, in the production of SVOCs during UCG. Among others, this can also be attributed to the fact that samples produced from UCG are very complex and hard to analyse holistically. Instrumental limitations that existed in the past are surpassed with the introduction of comprehensive chromatography (GCxGC) and high-performance mass spectrometric detectors (MSD and TOFMS), both of which are used in this chapter. New chemometric data analysis techniques have also been developed in recent years for the analysis of complex chemical data[130–132] (e.g. for biomarker discovery[133–135]) and can be possibly applied in the analysis of UCG samples.

Underground coal gasification secondary effluent samples that are to be analysed within this chapter belong to two types of categories: *ex-situ* produced waste-water and *in-situ* produced tar. Waste-water samples derived from two *ex-situ* gasification trials (TOPS1 and TOPS8) performed in the Laboratory of Experimental Installations of the Polish Central Mining Institute (GIG, Katowice, Poland). As mentioned earlier, these trials were part of a European Commission funded project that included the use of a high-pressure reactor to mimic UCG (Figure 5.2C).

All of the gasification trials that are mentioned in the present thesis were performed only once. Specifically, for *in-situ* trials, these are difficult to replicate mainly due to the morphological characteristics of the coal and the parameters that govern *in-situ* gasification such as cavity growth and water ingress. Regarding *ex-situ* gasification trials, although these would be easier to replicate than *in-situ* trials, however, most of the trials are performed either as a proof of concept or to monitor the effect of specific input parameters in either the heating value or composition of the syngas. Trials with replication are expected to be performed once the technology moves closer to commercialisation. Although the *ex-situ* gasification trials were performed inside a laboratory, the experiments are better described as large lab-scale, mainly due to the size of the reactor and the cost of running each experiment. Small, bench-scale experiments have been used in the early UCG studies to perform simulated gasification

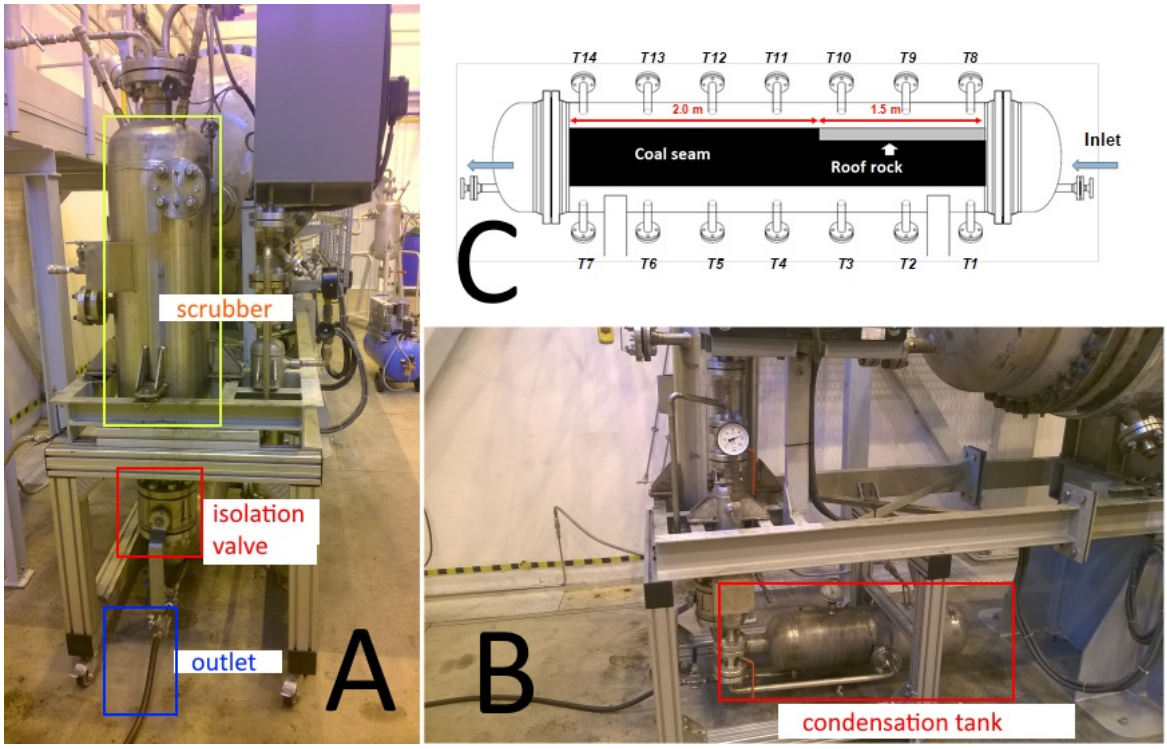

Figure 5.2: A: Outlet side of the reactor illustrating the position of the gas scrubber, the condensation tank isolation valve and the condensation tank outlet; **B:** Position and orientation of the condensation tank; **C:** Overview of the reactor and the methodology used to pack the reactor with coal

experiments[136] but their use is limited. Generally, high pressure coal block gasification experiments have been performed in the past by other Institutions apart from GIG[137–142], but those that mimic UCG haven't been attempted at this scale/pressure, so data that is produced by these experiments can be considered valuable and are expected to benefit the UCG and coal gasification community.

The aim of this chapter is to produce and analyse data from the samples described above in order to yield new knowledge and contribute to the better understanding of SVOC production during UCG, but also to assess the application of the novel analytical methodologies developed in Chapters 3 & 4 (Figures 3.6 & 4.10), including the application of data analysis strategies from other fields that haven't been used in the past in this context. By unravelling the complicated data that accompany the analysis of such complex mixtures as the secondary effluents of UCG, new insights into the chemical aspect of underground coal gasification are anticipated. Since the experiments were not replicated, the study of SVOCs in the effluents is aimed mostly at studying and identifying patterns and trends in the production of individual compounds or compound classes. The present study may create a realistic picture of the production of SVOCs in UCG providing insight that can be used for the better understanding of the process, for retrieval of components of economic value or to assist in the process of UCG study design and risk assessment. Although the number of samples analysed for the

needs of the thesis may be considered large enough to provide some initial understanding of SVOC production during UCG, the possibility of including literature data that can be analysed along with experimental data for comparison would reinforce the results, so data from Humenick and Mattox [60] were also included in the study.

5.2 Materials and methods

5.2.1 Chemicals

CPME (stabilised with 50ppm BHT) and 4-fluorophenol were obtained from ACROS Organics; Cyclohexane, 1-fluoronaphthalene, 5-fluoroindole, 1-fluorododecane, fluorene-d10, chrysene-d12 and 1-bromo-2-naphthol from Sigma Aldrich. Reagents 4-fluoro-2-methylpyridine and 4-bromo-2,6-dimethylpyridine were obtained from Alfa Aesar. Phenol-d6 and naphthalene-d8 were obtained from Supelco and DCM and Na_2SO_4 were obtained from Fisher Scientific. Phenanthrene-d10 was obtained from Isotec. All reagents were of analytical grade or better.

For waste-water analysis a surrogate spike solution was prepared of 1-fluoronaphthalene, 4-fluorophenol, 4-bromo-2,6-dimethylphenol, 5-fluoroindole, 4-fluoro-2-methylpyridine at a concentration of 9000 mg/L in ethanol (solution A). For tar analysis a surrogate spike solution was prepared of 1-fluoronaphthalene, 4-fluorophenol, 4-bromo-2,6-dimethylphenol, 5-fluoroindole, 4-fluoro-2-methylpyridine, fluorene-d10, chrysene-d12, 1-bromo-2-naphthol, fluoro-dodecane at a concentration of 7500mg/L in CPME (solution B). For waste-water analysis an internal standard solution of phenol-d6 and naphthalene-d8 was prepared and for tar analysis an internal standard solution of phenol-d6 and naphthalene-d8 and phenanthrene-d10 was prepared. Both internal standard solutions had a concentration of 1000mg/L in CPME.

As mentioned above, UCG secondary effluent samples are either *ex-situ* produced waste-water and *in-situ* produced tar and were sampled according to Table 5.1. All the samples mentioned above were provided from GIG directly to the University of Glasgow. Waste-water samples were stored at 4°C upon arrival and tar samples at -20°C.

5.2.2 Sample preparation

5.2.2.1 Sample origin

During sampling, the condensation tank is being filled with effluents for a specific time period (between 2 and 58hrs - Table 5.1) during the gasification run and is briefly isolated from the reactor and the rest of the system and then discharged through the outlet into large

vessels (Figure 5.2A). Waste-water samples from the condensation tank were taken with every discharge procedure. The sampling schedule for both trials can be seen in Table 5.1.

Table 5.1: Sampling schedule and time points for the gasification trials performed at GIG. For TOPS1 and TOPS8 samples correspond to sampling periods of accumulating effluents within the condensation tank while for Barbara II samples correspond to a specific time point

TOPS1		TOPS8		Barbara II	
Period [hrs]	Duration [hrs]	Period [hrs]	Duration [hrs]	Sample	Time [hrs]
0-24	24	0-2	2	1	Outset
24-48	24	2-60	58	2	24
48-72	24	60-69	33	3	48
72-96	24	69-102	33	4	72
96-120	24	102-116	14	5	96
120-148	28	116-146	30	6	120
		146-157	11	7	144
		157-190	33	8	168
		190-204	14		

The tar samples derived from a UCG experiment performed by the GIG at the "Barbara" mine located in Katowice, Poland[143]. Tar was sampled according to the schedule in Table 5.1. Samples were taken from the gaseous products collection system located at the surface above the mine and specifically from the tar drain located at the bottom of the tar separator as seen in Figure 5.3. As this was the second UCG experiment performed from the GIG at the Barbara mine (at least to the best of the author's knowledge) it is referred-to in the thesis as the *Barbara II* trial. Although it is unclear if the samples from the Barbara II trial refer to sampling periods (in regard to accumulation in the tar separator) or points in time, they represent incremental points in the gasification period and will be referred to from now on as single points in time.

The study from Humenick and Mattox[60] includes data from both tar/oil and waste-water, however, only tar data is used here. It is also expected that some of the compounds will have been quantitated following a semi-quantitation approach. In any case, a dataset was created from the appendix of the study and is, therefore, analysed in the chapter along with the experimental datasets. The sampling schedule for the Hanna IVB trial is given in Table 5.2. Two samples had to be dropped from further data analysis: one sample that corresponded to an earlier gasification period and a sample that was a composite from a different sampling system[60].

5.2.2.2 UCG waste-water samples

Samples were processed with the method developed for waste-water as described in Chapter 3 (Figure 3.6, p.38). The samples were removed from storage and for each sample a volume

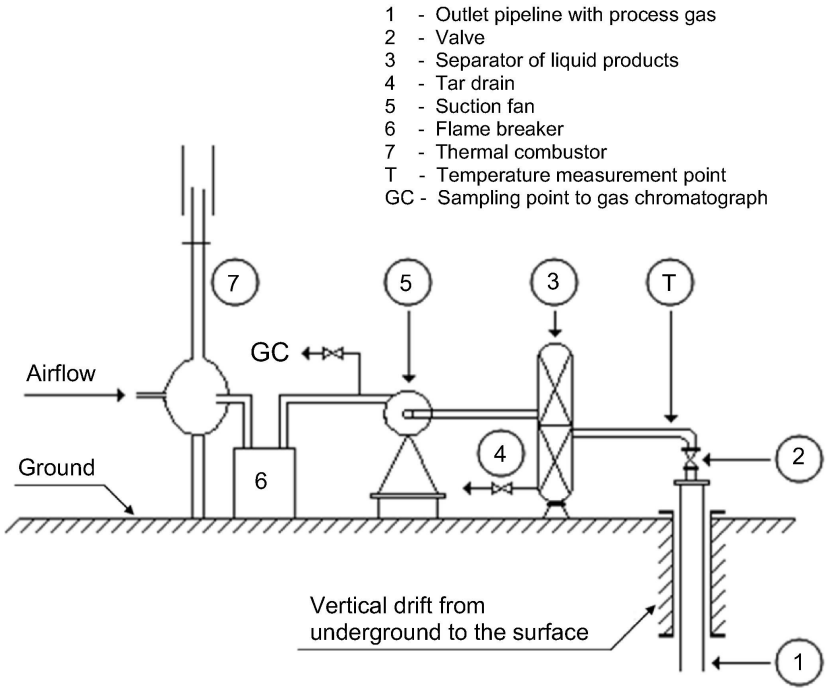

Figure 5.3: The gaseous product collection system located at the surface that was used for the Barbara II trial. Tar samples were collected at the tar drain (4) located at the bottom of the separator of liquid products (3). Reproduced from[143] with permission.

Table 5.2: Sampling schedule of the Hanna IVB experiment. Sampling duration vary between samples but still represent incremental points in time during the gasification experiment

Sample	Period	Duration [days]
28	3/9-12/9/79	9
30	12/9-15/9/79	3
32	15/9-16/9/79	1
34	16/9-19/9/79	4

of approximately 40mL was filtered through a 25mm CF/F glass filter (mounted on a 15mL glass microanalysis filter holder with a fritted glass filter support (Merck-Millipore, Merck KGaA, Darmstadt, Germany)). After filtering, exactly 9mL of each sample were poured into a 15mL deactivated glass centrifuge tube (Kimble Chase, Vineland, US). The samples were spiked with 10uL of solution A and 0.225g of Na_2SO_4 were added into each tube following vortex until the complete dissolution of the salt. Following salt addition, the pH of was adjusted to <2 using HCl and 9uL of the 2.2mmol CTAB solution were added to a final concentration of 0.0022mmol. Consequently, 450uL of CPME were rapidly injected into the sample using a 500uL glass syringe and the tube was quickly placed on the sonotrode and irradiated at 40W - 50%pulse for 28s. The solution was centrifuged for 7min at 2500rpm and the resulting phases were separated. The lower phase (aqueous) was transferred to a clean 15mL glass tube, 1.125g of Na_2SO_4 were added and vortexed until all the salt was

dissolved. The pH was adjusted to >12 using KOH and 450uL of CPME were injected rapidly into the sample which was mounted on the sonotrode and irradiated for 28s at 40W with a 50% pulse. The tube was then centrifuged as above, the lower aqueous phase was removed, and the organic phases were combined and stored at -20°C until analysis. Back-extraction (Section 3.2.7) is performed by injecting 300uL of the total extracted sample in 9mL of the back-extraction solution in a 15mL glass tube and sonicating using the optimised conditions mentioned above, centrifuging and recovering the organic phase as above.

5.2.2.3 UCG tar samples

Tar samples were extracted with the tar extraction method described in Chapter 4 (Figure 4.10). Approximately 0.3gr of tar were weighted in a 9mL deactivated crimp top vial (Chromacol, Thermo Fisher) with their weight recorded to an accuracy of 0.001gr. Twice the amount of Na_2SO_4 was added in the vial and the vial was sealed. Next, 3mL of DCM were added in the vial along with 40uL of solution B. The atmosphere in the vial was made inert by alternating three times between vacuum and 10psi of pure N_2 using a three-way PTFE valve that was fitted into the vial with a luer needle tip passing through a 0.45um filter. The vial was then mounted on the sonotrode and sonicated for 45s at a 50W intensity with a 70% pulse. Following sonication, each vial was centrifuged at 2000rpm for 7min, the crimp seal was removed and approximately 2mL of the supernatant was poured inside a glass Pasteur pipette that was loosely packed with lab-grade cotton wool. Filtrates were collected at the bottom in a 4mL vial and stored at -24°C until analysis.

5.2.3 Targeted GC-MS analysis

5.2.3.1 Targeted GC-MS for waste-water extracts

A targeted SIM method was used for the determination of surrogate concentration in the extract and subsequent recovery calculations. Details on the calibration curve and the development of the GC-MS methods are described in Section 3.2.8. The surrogates used here are: SR1: 4-fluoro-2-methylpyridine, SR2: 4-fluorophenol, SR3: 1-fluoronaphthalene, SR4: 5-fluoroindole, SR5: 4-bromo-2,6-dimethylphenol. For the creation of the calibration curve, 3 replicates of each calibration level were analysed in the following concentration: 10, 50, 100, 150, 300, 450, 600 and 900 mg/L. For each sample before analysis, 95uL of each sample was transferred to a 200uL vial insert and 5uL of the waste-water internal standard solution were added. Each analysis was carried out using an Agilent 5975C series GC/MSD system with an Agilent DB-17MS capillary column (0.25mm i.d. x 60m length, 0.25um film thickness). The analysis parameters were: inlet temperature 300°C, injection volume 1uL, split

ratio of 1:200, initial oven temperature 70°C, hold for 0.2 min, then to 220°C at a rate of 10°C/min and then to 320°C at a rate of 60°C/min hold for 3min. The inlet was operated at a constant flow rate of 1.4mL/min. Each extract was injected in duplicate and the averaged concentration was used to calculate the recovery

5.2.3.2 Targeted GC-MS for tar extracts

Each sample was prepared for analysis by transferring 95uL of each extract into a 200uL insert and adding 5uL of the tar internal standard solution. The insert was placed in a 1.5mL autosampler vial, capped and stored at -24°C until analysis. Surrogate calibration curve and GC-MS analysis method is described in detail in Chapter 4, Section 4.2.6, p.61. Surrogates used here are: SR1: 4-fluoro-2-methylpyridine, SR2: 4-fluorophenol, SR3: 1-fluorododecane, SR4: 1-fluoronaphthalene, SR5: 5-fluoroindole, SR6: 4-bromo-2,6-dimethylphenol, SR7: fluorene-d10, SR8: 1-bromo-2-naphthol, SR9: chrysene-d12. For the calibration curve, 6 concentration levels were used for all compounds: 1.125, 2.25, 4.5, 9, 22.5 and 45 mg/L. Parameters used for the analysis are as follows: inlet temperature 300°C, injection volume 1uL with a split ratio of 1:200, initial oven temperature 70°C, hold for 0.2 min, then to 220°C at a rate of 10°C/min and then to 320°C at a rate of 60°C/min hold for 14min, helium flow rate was 1.4mL/min.

5.2.4 Untargeted GC analysis

5.2.4.1 Untargeted GC-MS for waste-water extracts

Each of the samples prepared for targeted analysis were also subjected to GC-MS untargeted analysis. The following GC-MS parameters were used: inlet temperature 300°C, injection volume 1uL with a split ratio of 1:20, initial oven temperature 70°C, hold for 0.2 min, then to 320°C at a rate of 3.5°C/min and hold for 5min, helium flow rate was 1.4mL/min. Transfer line was held at 280°C, source temperature was set at 230°C and quadropole temperature at 150°C, detector scan range 50-550u.

5.2.4.2 Untargeted GC-MS for tar extracts

Prepared samples were analysed in using the following parameters: inlet temperature 250°C, injection volume 1uL with a split ratio of 1:75, initial oven temperature 70°C, hold for 0.2 min, then to 320°C at a rate of 3.5°C/min and hold for 20min; helium flow rate was 1.4mL/min. Transfer line was held at 260°C, source temperature was set at 230°C and quadropole temperature at 150°C, detector scan range was 50-550u.

5.2.4.3 Untargeted GCxGC-TOFMS for waste-water extracts

Comprehensive gas chromatographic analysis was performed on a LECO Pegasus 4D equipped with a two stage cryogenic modulator and coupled to a time-of-flight mass spectrometer. Column setup was an Agilent DB-17MS capillary column (0.25mm i.d. x 60m length, 0.25um film thickness) on the 1st dimension and a Stabilwax on the second dimension. (0.25mm i.d. x 0.45m length (modulator 0.1m, secondary oven 0.15m and transferline 0.2m) x 0.25um film thickness). Samples were injected as they were in the GC-MS analysis. Inlet temperature was held at 300°C, injection volume was 1uL with a split ratio of 1:40. Initial oven temperature was 40°C, hold for 0.2min then to 230°C at a rate of 3.5°C/min and hold for 14min. Secondary oven temperature was held at +15°C from the primary oven and modulator temperature at +15°C from the secondary oven temperature. Modulation period was set to 6s with a hot pulse of 1.8s. Transfer line temperature was set at 245°C and ion source temperature at 230°C. Mass spectrometer was scanning from 45u to 500u at an acquisition rate of 200Hz with an acquisition voltage of 1650V.

5.2.4.4 Untargeted GCxGC-TOFMS for tar samples

Each analysis was performed on a Leco Pegasus 4D equipped with a liquid nitrogen cooled modulator. A reverse phase setup column setup was used with an Agilent DB-17MS column on the first dimension (0.25mm i.d. x 60m length, 0.25um film thickness) and a Restek Rxi-5Sil MS™ column on the second dimension (0.25mm i.d. x 1.50m length (0.1m in the modulator, 1.20m in the secondary oven and 0.2m in the transfer line), 0.25um film thickness). Inlet temperature was set at 300°C, injection volume 1uL with a split ratio of 1:75, modulation time was 6s, initial oven temperature 70°C, hold for 0.2 min, then to 320°C at a rate of 3.5°C/min and hold for 20min, helium flow rate was 1.4mL/min. Transfer line temperature was set at 280°C and ion source temperature at 230°C. Mass spectrometer was scanning from 45u to 500u at an acquisition rate of 200Hz with an acquisition voltage of 1650V.

5.2.4.5 Data preparation and analysis

Although there are several available automatised tools/pipelines for preparing complex chemical data for data analysis[144–149], a sample-specific data processing methodology was developed for waste-water and tar samples. Chromatograms were first converted into the CDF file format. They are then loaded into R[150], aligned using the XCMS package[144] and then rebuild into CDF format and loaded to Openchrom®[151] where chromatograms are compared and those with the most peaks are selected. These chromatograms are then loaded into AMDIS[91] for deconvolution and feature extraction and to build the experiment specific feature database

(ESFDB). Once the database is complete it is then loaded to Openchrom where duplicate entries are removed along with possible false-positives. The finished database is then loaded into R and using the SIMAT[152] package the 3 most intense ions are chosen for each feature and a list is created. The list is then loaded to Matlab along with the CDF files and the Gavin package[153] is used to validate feature peaks, choose the appropriate integration parameters and rule-out potential duplicates/false positives or to correct integration/verification ions. Once the integration parameters are finalised, they are extracted and saved. Then Gavin integrates all the samples and returns a data table with the integrals of each feature for each sample. Each feature is given a unique index number to identify from the rest of the features. No index number is duplicated.

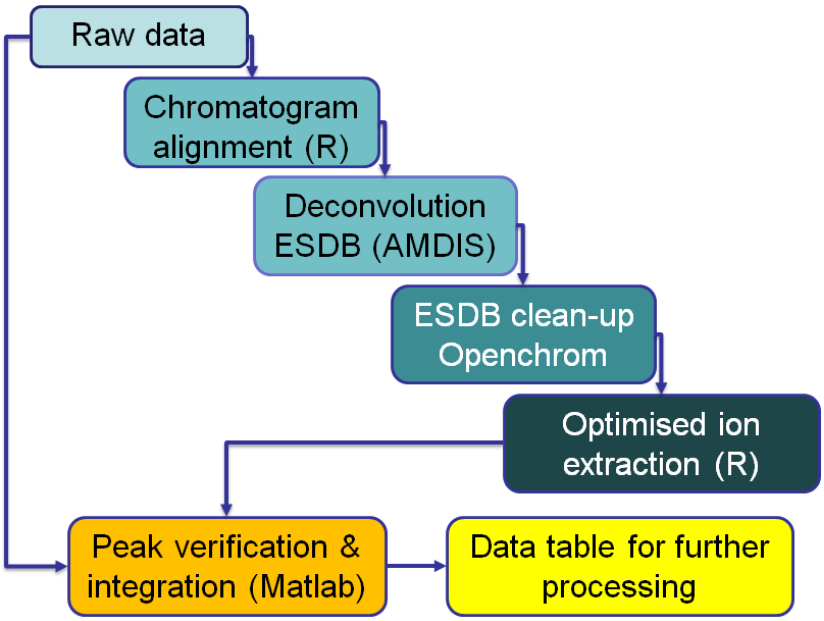

Figure 5.4: Pipeline that was used for the data analysis. The pipeline includes alignment of the chromatograms, deconvolution using AMDIS and extraction of the experiment specific database, clean-up of the database using Openchrom, extraction of the optimised ions list, import of the ion lists and raw data to Matlab in order to verify and integrate peaks and extraction of the data table

After extraction of the data table, the metaboanalyst package[154,155] and its front-end[156] were selected for exploratory data analysis. Metaboanalyst is a popular data analysis software package used by more than 60000 researchers in the field performing approximately 150000 analysis jobs per month[157]. Since the package requires a minimum of 3 injections per class, a third simulated injection is created using the mean values of each integrals for all available features. Where only one value is available then additional values are created close to the expected standard deviation range. The type of analysis used depends heavily on experiment parameters and the final goal of the analysis. In this chapter the aim is to perform exploratory data analysis, through ordination techniques, in order to identify trends and suggest compounds that can be used to better describe and understand the UCG process.

Targeted methods for these compounds may be developed in the future.

There are several data normalisation and transformation approaches available for the treatment of data from untargeted experiments that are applied in similar fields such as metabolomics[158]. These include: centering, that focuses on differences but not on similarities; normalisation to an internal standard, that removes variation introduced from injections; UV normalisation (autoscaling) that makes all features equally important; pareto normalisation that retains some of the quantitative information; vast normalisation which focuses on small fluctuations, level normalisation which focuses on relative response and log and power transformation which correct for heteroscedasticity and make skewed distributions more symmetric (normally distributed). In this study the data were normalised to an internal standard to remove variation from injections and transformed using the glog, which is a variant of the log transformation that is suitable with negative and zero values[159]. Glog transformation makes the distribution symmetrical while retaining the quantitative information and, as will be shown below, it provides very good grouping or the surrogates and internal standards when performing multivariate statistics.

Before data analysis, each dataset (apart from Hanna IVB) is first normalised to naphthalene-d8 and then glog transformed feature-wise. Initially, data analysis is performed using hierarchical clustering and visualised using a dendrogram in order to assess any meaningful clustering of the samples. A heatmap is also produced with samples reorganised with increasing time points (the data here are autoscaled). Features in the heatmap are grouped according to their time-wise behaviour during the gasification process. Since the data is high dimensional and to consider the strength of the relationships, Pearson's r is used as the distance measure in both cases.

Another type of analysis used is correlation analysis. This is performed to identify patterns in the dataset with gasification time. In particular, the correlation between time and feature values is explored in order to look for features that correlate positively or negatively with time points. This may be used to provide insight to the behaviour of compounds and compound classes during the duration of the experiment. Features that increase (or decrease) linearly with gasification time may be used to describe/monitor the UCG process.

The dataset is then analysed using the supervised multivariate statistical technique Partial Least Squares Discriminant Analysis (PLS-DA), where each time period (or time point) is considered a class, and it is utilised in an exploratory data analysis capacity. PLS-DA is used not only because it takes into account class order (since classes are presented by points in time during gasification - unlike PCA) but mainly because it provides a ranking system for significant features (variables) that may give insight into the sources of variation and discrimination between classes; it is, therefore, not used as a tool to classify samples[160]. Top ranked features by the PLS-DA model that drive the separation between classes are extracted

for pattern analysis. These features may be used as representative compounds; even more if the selection can be supported theoretically. Cross validation of each PLS-DA model is done automatically by metaboanalyst, which provides the statistics R^2 (the percentage of variance that the model accounts for the training set - fit to the data) and Q^2 (the percentage of variance that the model accounts for the test set - predictive capability); the closer Q^2 is to R^2 and to 1, the better the model[161]. Model over-fitting is checked while running 2000 permutations by randomly assigning class labels and building a new classifier each time. If the original label is significantly different that the distribution of the 2000 random permutations, then the model is not over-fitted. The loadings plot of the model is also checked to see if the surrogates/internal standards cluster around the 0,0 point. This will indicate that the source of variation in the model comes from variation in the chemical content of the samples and not from the sample preparation process.

Regarding, GCxGC-TOFMS data analysis, processing parameters were as in Section 3.2 for waste-water and Section 4.2 for tar. Further processing was performed by defining classification regions on the two-dimensional chromatograms using ChromaTOF®. The software then assigns each peak to a group according to the 1st and 2nd dimension retention time. The initial separation of aromatics and aliphatics is done with two major regions that are clearly defined in the two-dimensional chromatogram (Figure 5.5A) while the more detailed classification is performed by defining borders more meticulously, as can be seen in Figure 5.5B. Regardless, some degree of overlap is expected particularly in the aromatics region. Especially in the case of n-alkanes and n-alkylbenzenes, these have to be double checked in the peak table produced by the software as there is a chance of false positives. The peak tables are exported from ChromaTOF® to Microsoft Excel®(version 1811) where total peak areas are calculated.

The GCxGC-TOFMS data processing above also provides bubble plots. This type of visualisation gives an overview of the SVOC content with each peak being depicted as a bubble. The size of each bubble is proportionate to the peak area of each peak. On the top right corner of each plot a pie plot is attached (e.g. Figure 5.25). This plot provides the percentage of the area of the mid-hi polarity and low polarity peaks in the waste-water samples and aliphatics and aromatics in the case of coal tar. All bubble-plots are in the same scale in order to allow accurate comparisons between samples.

5.3 Results and disussion

After the execution of the TOPS1 experiment it was seen that the *ex-situ* reactor cannot produce sufficient amounts of tars (at least not enough to represent sampling periods) as most of the produced tar appears to create a lining on the reactor pipes and sample vessels making tar

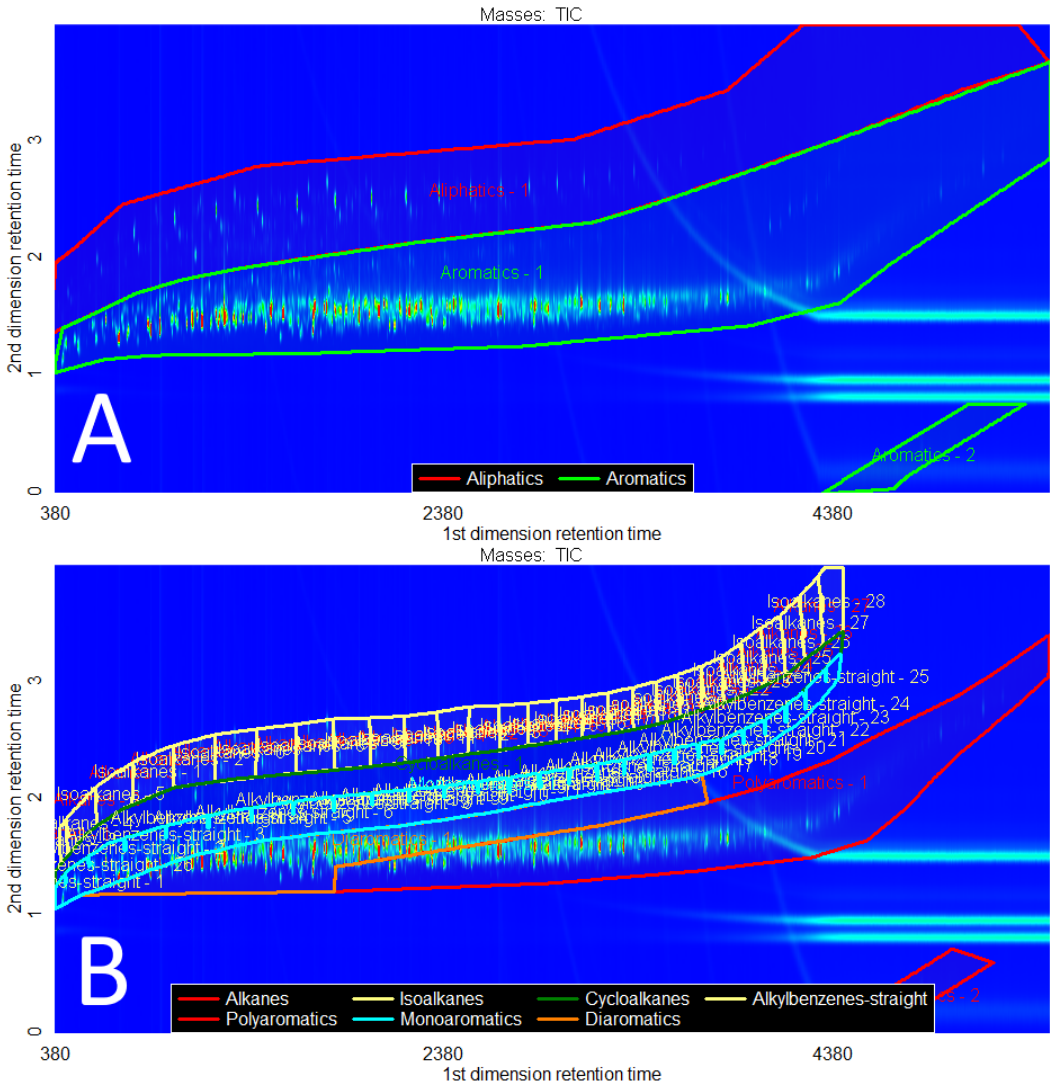

Figure 5.5: A: Two-dimensional chromatogram illustrating the mapping of the aliphatics and aromatics regions **B:** Two-dimensional chromatogram illustrating the mapping of extended classes

sampling difficult or even impossible to get samples. This was probably due to the fact that the amount of coal that was gasified was relatively small and the gas separation system was designed with a focus on operation and syngas cleaning rather than tar sampling; so, from the TOPS trials only waste-water was used. Including tar samples in the study was desirable since it has been studied more that waste-water as it is considered more representative to link with UCG related parameters such as reactor conditions, coal structure etc[42,43]; for this reason, the tar samples from Barbara II trial were included in the study.

Results and insights of the following analysis can be possibly applied to large-scale UCG trials provided that the conclusions made from *ex-situ* experiments may be considered applicable to actual field scale UCG trials. As mentioned earlier, field scale UCG trials may have some distinctive characteristics that differentiate them from lab scale UCG trials. The most

prominent differences are water ingress in the large scale reactor zone from the surrounding strata and the need to constantly monitor reactor pressure conditions and adjust it to the surrounding hydrostatic pressure in order to achieve containment of the UCG effluents within the cavity. Also, the infrastructure of the production well is different, especially regarding the proximity of gas cooling systems to the reactor. In UCG experiments that are performed on a lab reactor, the operating pressure is chosen to represent the depth of the simulated UCG trial and it is usually considered as an initial parameter during the experimental design. Additionally, in a real scale UCG experiment, heavy molecular weight SVOCs are expected to condense to a degree on the cooler parts of the production pipeline[42,46,119].

5.3.1 Recovery study

The composition of waste-water from underground coal gasification may affect the partition coefficients that take part in liquid-liquid partitioning and liquid-liquid extraction, thus, it is important to monitor the recovery of SVOCs in order to account for introduced sources of variation from the sample preparation process. This is particularly true when analysing samples from a time series since the carbon content in the waste-water of a series of samples collected from different time points may vary. The selected surrogates are given in Section 5.2.3.1. Water soluble compounds are expected to have different solubility in pure water and water that is heavily contaminated, since the affinity of the compound with the solvent (in this case waste-water) may change due to the higher organic content. Reports in the literature suggest changes in the carbon content of the effluents from a UCG trial ranging from 9000mg/L to 2300mg/L for total organic carbon (TOC) and 33000 to 1700 for chemical oxygen demand (COD)[60]. Aggregate analysis of TOPS1 waste-water samples performed at GIG also indicate large variation in TOC ranging from 1400mg/L to 65mg/L[162]. Based on the above, recovery is a parameter that must be determined since variations in recoveries may affect statistical analysis, so producing recovery values for a range of compounds may act as a safeguard when interpreting compositional variation between samples.

Surrogate recovery values for the TOPS1 study for normal extractions and back-extractions can be seen in Table 5.3. Recoveries appear to be between the 70-130% set with the minimum being 73.2% for 4-fluoro-2-methylpyridine and the highest 110.2% for 4-bromo-2.6-dimethylphenol; the average relative standard deviation for all recoveries was 1.70±0.4%. Injections where the internal standard was outside of the control chart areas were removed. This was the case for only one injection for TOPS1. Table 5.3 also provides the recoveries after the removal of acidic components and illustrates the performance of the back-extraction removal process. Specifically for the acidic surrogates, removal efficiencies are 91.7% for 4-fluorophenol and 83.7% for 4-bromo-2,6-dimethylphenol. Recovery for 4-fluoro-2-methlypyridine also appears to be affected by the back-extraction process as the recovery

is approximately 31% smaller. This is probably due to the lower salt content of the back extaction solution. However, precision is not expected to be affected by the reduction in recovery.

Table 5.3: Recoveries for the extraction of waste-water samples from the TOPS1 experiment. For the normal extraction recoveries appear to be within the 70-130% range. For the back extraction, phenolic compounds are effectively removed and the recovery of 4-fluoro-2-methylpyridine also appears to be affected. In all cases the relative standard deviation of the recoveries is below 7%. SR1: 4-fluoro-2-methylpyridine, SR2: 4-fluorophenol, SR3: 1-fluoronaphthalene, SR4: 5-fluoroindole, SR5: 4-bromo-2,6-dimethylphenol

Normal extraction							
Compound	P1	P2	P3	P4	P5	P6	%RSD
SR1	76.1	74.7	73.7	74.3	73.2	74.5	1.3
SR2	85.6	84	84.9	83.3	88.5	83.3	2.3
SR3	94.9	92.6	92.9	94.3	95.1	97.2	1.8
SR4	106.8	102.9	105.9	105.1	104.7	102.7	1.6
SR5	108.8	106	110.2	109.7	109	106.7	1.5
Back extraction							
Compound	P1	P2	P3	P4	P5	P6	%RSD
SR1	45.1	42.3	43.3	43.8	42.3	43	2.4
SR2	7	7	7.1	7.1	6.8	7.1	1.7
SR3	90.8	91.2	94.4	101.4	92.1	90.7	4.4
SR4	85.7	86.5	86.8	95.1	87.6	88.2	3.9
SR5	17.7	17.7	17.5	17.6	17.5	18.1	1.3

As mentioned above, in total, 9 samples were taken during the TOPS8 gasification trial in 9 sampling periods. Recoveries for each sample and each surrogate appear in Table 5.4. Recoveries appear to be closely within the 70-130% range with the lowest one being 68.7% for 4-fluoro-2-methylpyridine and the highest one being 110.5% for 4-bromo-2,6-dimethylphenol. Performance of the back-extraction method by means of surrogate recovery for the acidic components also appear in Table 5.4 and are close to those of TOPS1.

As mentioned above, the gasification trial that took place at Barbara mine was performed within a course of 8 days and samples were taken at the surface every 24hours. Recovery values for the surrogates are within the 70-130% range, with 1-bromo-2-naphthol showing the highest recovery at 118.2% and 4-bromo-2,6-dimethylphenol the minimum at 89.1%. The average relative standard deviation for all compounds is 1.88 ± 0.60.

5.3.2 Hannah IVB exploratory data analysis

As mentioned above, the study from Humenick and Mattox [60] includes data from both tar/oil and waste-water, however, only tar data was used. This is due to several reasons. Firstly, there is limited information on the time that the samples spend in the separating vessels which appears to be too long. This leads to the assumption that extensive partitioning of analytes between the organic phase (tar/oil) and the aqueous phase may have taken place, so

Table 5.4: Recoveries for the extraction of waste-water samples from the TOPS8 experiment. SR1: 4-fluoro-2-methylpyridine, SR2: 4-fluorophenol, SR3: 1-fluoronaphthalene, SR4: 5-fluoroindole, SR5: 4-bromo-2,6-dimethylphenol. Recovery range is: lowest 68.7% for 4-fluoro-2-methylpyridine, highest 110.5% for 4-bromo-2,6-dimethylphenol. Values are close to the 70%-130% recovery range

Normal extraction										
Compound	P1	P2	P3	P4	P5	P6	P7	P8	P9	%RSD
SR1	70.4	68.9	69.5	82.5	68.2	70.1	70	67.8	77.3	6.9
SR2	84.5	81.4	85	90.8	82.1	84.6	85.5	91.3	91.9	4.6
SR3	95.5	95.7	94.3	87.6	94	98.5	95	101.4	96.1	3.9
SR4	102.8	104.2	102.7	97.9	101.7	103.2	102.7	106.1	102.4	2.1
SR5	106.5	109.3	108	102.6	105.5	108.1	106.7	110.5	105.6	2.2
Back-extraction										
Compound	P1	P2	P3	P4	P5	P6	P7	P8	P9	%RSD
SR1	48.1	49.7	47.6	49.6	47.7	45	46.3	45.3	44.6	4.1
SR2	7.1	7.6	7.2	6.7	7.5	7	7	6.4	6.3	6.4
SR3	95.7	97.4	96.3	100.8	96.2	91.4	94	89.5	89.7	4
SR4	90.3	91.4	90.1	91.1	91.4	86.9	88.8	86.3	86	2.5
SR5	18.2	18.1	18.3	18.6	19	17.7	18.1	17.1	17.9	3

Table 5.5: Recoveries from extraction of the tar samples from the Barbara mine in-situ experiment. Values are within the 70-130% range with the minimum being 118.2% for 1-bromo-2-naphthol and the minum being 89.1% for 4-bromo-2,6-dimethylphenol. The average relative standard deviation is 1.88±0.60. SR1: 4-fluoro-2-methylpyridine, SR2: 4-fluorophenol, SR3: 1-fluorododecane, SR4: 1-fluoronaphthalene, SR5: 5-fluoroindole, SR6: 4-bromo-2,6-dimethylphenol, SR7: fluorene-d10, SR8: 1-bromo-2-naphthol, SR9: chrysene-d12

Compound	Outset	24	48	72	96	120	144	168	%RSD
SR1	108	103.9	103.1	104.4	105.5	101.4	101.4	99.4	2.6
SR2	94.9	94.8	92.8	93.2	93.1	94.5	94.5	93.2	0.9
SR3	95.9	94.1	96.8	96.3	99.4	93.4	93.4	93.6	2.2
SR4	94.3	90.6	89.3	89.8	90.8	90.6	90.6	89.4	1.7
SR5	91	89.2	90.3	89.2	92	91.6	91.6	91.9	1.3
SR6	89.8	89.1	89.6	89.1	90.6	92.5	92.5	94.6	2.2
SR7	102.5	99.4	100.3	101.1	102.4	103.8	103.8	102.1	1.5
SR8	113.2	110.6	112.1	111.7	114.5	118.2	118.2	115.6	2.5
SR9	105	99.6	101.7	101.3	105.2	103.1	103.1	100.7	2

the waste-water samples may have limited information regarding the UCG process as they may be saturated with content leached from the tar/oil phase during equilibration. Secondly, although solvent extraction was used to treat the waste-water samples, no recovery values are provided so the quality of the data from the waste-water analysis cannot be properly assessed.

The Hanna IV *in-situ* coal gasification trial was performed in Hanna, Wyoming with the oversight of the Laramie Energy Technology Center. This is one of the few UCG trials with publicly available information that includes well documented studies of secondary effluents. Data for SVOC and details regarding the test can be found in the study published by Hu-

menick and Mattox [60]. Although DNAPL samples are referred to as "oil" in the publication by the authors, it can be assumed that the samples are actually tar since they correspond to the sedimented phase separated by gravity from the waste-water. The sampling schedule for the trial can be seen in Table 5.2.

The dataset includes 178 features, each one referring to the concentration of an individual compound or a small group of isomers. Data analysis was performed as indicated in Section 5.2.4.5. Since the dataset refers to concentrations, no normalisation to an internal standard is needed and a simple glog transformation is enough to bring the distribution close to normality. It doesn't appear that samples are clustered according to their sampling time during the UCG burn (Figure 5.6B). All sorts of different evolution patterns are followed by the various SVOCs in the tar (Figure 5.6C), however the most prominent trend appears to be the one having high levels at the beginning of the trial with levels reducing towards the end of the trial. However, as it can be seen by focusing at sample 34, there are some compounds that have their levels increasing as the gasification progresses. Correlation analysis (Figure 5.6A) performed on the dataset provided some interesting results. Three compounds appear to have a very strong positive correlation (R^2>0.96) with sampling time while most of the strongest correlations with sampling time are negative. Some correlation coefficients appear being remarkably high such as the one for 9-methylphenanthrene with a correlation coefficient of R^2=0.997 and M,P-xylenes with an R^2=-0.9986. On another note, those compounds that appear to have positive correlation with time, also have a higher molecular weight while those that have negative correlation with time have a lower molecular weight like methylated benzenes (Table 5.6). This may suggest a change in the kinetics of the aromatisation reactions.

Table 5.6: Positive and negative correlation values of the top 5 features for each category. Values of the t-stat, p-value and false discovery rate (FDR) are given for each one of the top features.

Positive	correlation	t-stat	p-value	FDR
9-methylphenanthrene	0.99714	41.729	1.50E-12	1.33E-10
2-methylanthracene	0.98683	19.294	3.05E-09	4.50E-08
methyldibenzofuran.1	0.97443	13.715	8.24E-08	6.34E-07
3-methylbiphenyl	0.95785	10.544	9.76E-07	5.23E-06
4-methylbiphenyl	0.95123	9.7511	2.00E-06	1.04E-05
Negative	correlation	t-stat	p-value	FDR
M,P-xylenes	-0.9986	-59.8	4.15E-14	7.35E-12
ethylbenzene	-0.99623	-36.311	5.97E-12	3.52E-10
n-propylbenzene	-0.99557	-33.487	1.33E-11	5.90E-10
1,2,3-trimethylbenzene	-0.99526	-32.37	1.87E-11	6.60E-10
o-xylene	-0.99418	-29.179	5.21E-11	1.54E-09

Model validation showed an overall good model (R^2 = 0.9986, Q^2 = 0.9968, no over-fitting - 5.7). The scores plot from the PLS-DA model is shown in Figure 5.8A. As it appears both the first and second components explain a good portion of the variation (78.5%) with

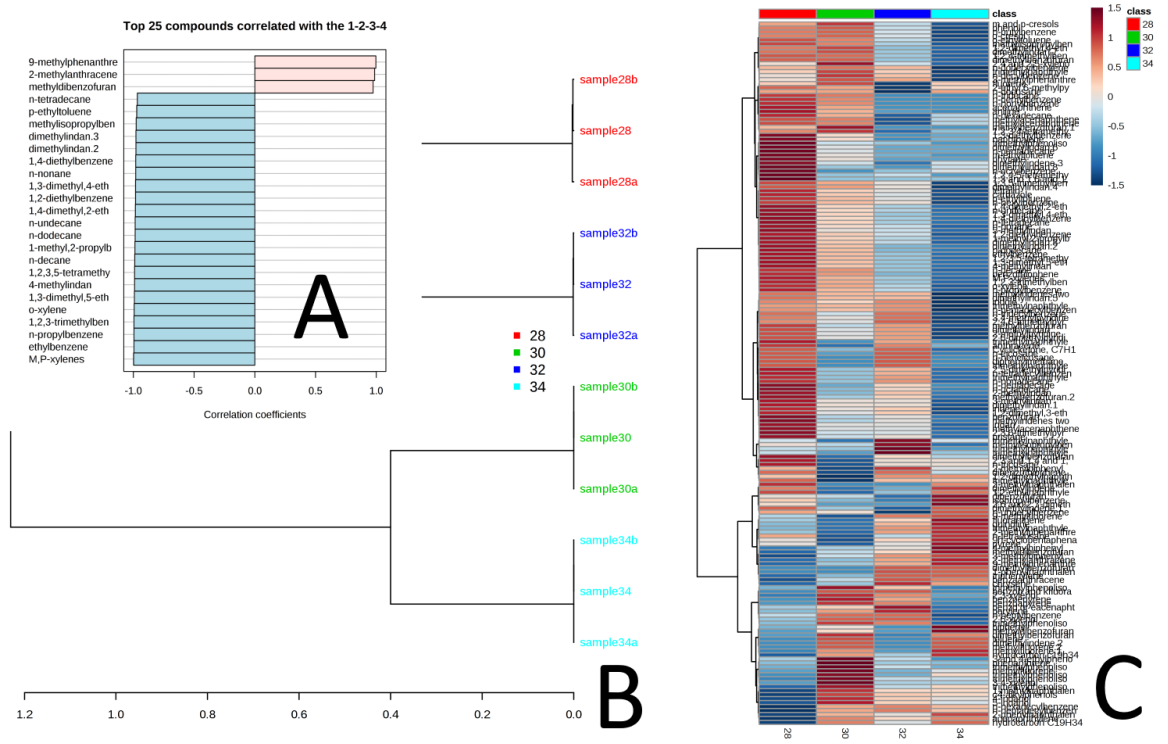

Figure 5.6: **A:** Top 25 features with the highest positive or negative correlation with gasification time **B:** Dendrogram depicting samples that are grouped according to composition **C:** Heatmap of all the compounds in the Hanna IVB dataset. Values are normalised and autoscaled and compounds are grouped according to their behaviour during the gasification. Samples are order according to gasification time. An elongated version of the heatmap is provided in Figure Appendix A.3.4

the second component needed to differentiate between samples 30 and 32. VIP scores for the first component are shown in Figure 5.8B. Top feature is toluene along with long chain methylated benzenes and other methylated compounds. Something worth mentioning is that no PAHs appear to be in the VIP list. This may indicate that their concentrations do no change dramatically during the UCG burn.

5.3.3 TOPS1 exploratory data analysis

The TOPS1 trial resulted in a total of six samples (Section 5.2), with each one representing a sampling period. Both internal standards used here appear to have almost identical relative standard deviations across samples. Running a control chart on the injections for both phenol-d6 and naphthalene-d8 (Figure Appendix A.3.1) shows that almost all integrals are within the upper and lower control limits with only one point closely outside the limits for naphthalene-d8. It is worth mentioning that the drift appears to be almost identical for the two compounds. The relative standard deviation of phenol-d6 before normalising was 11.21$\pm$3.20% and after normalising to naphthalene-d8 became 1.88% which indicates

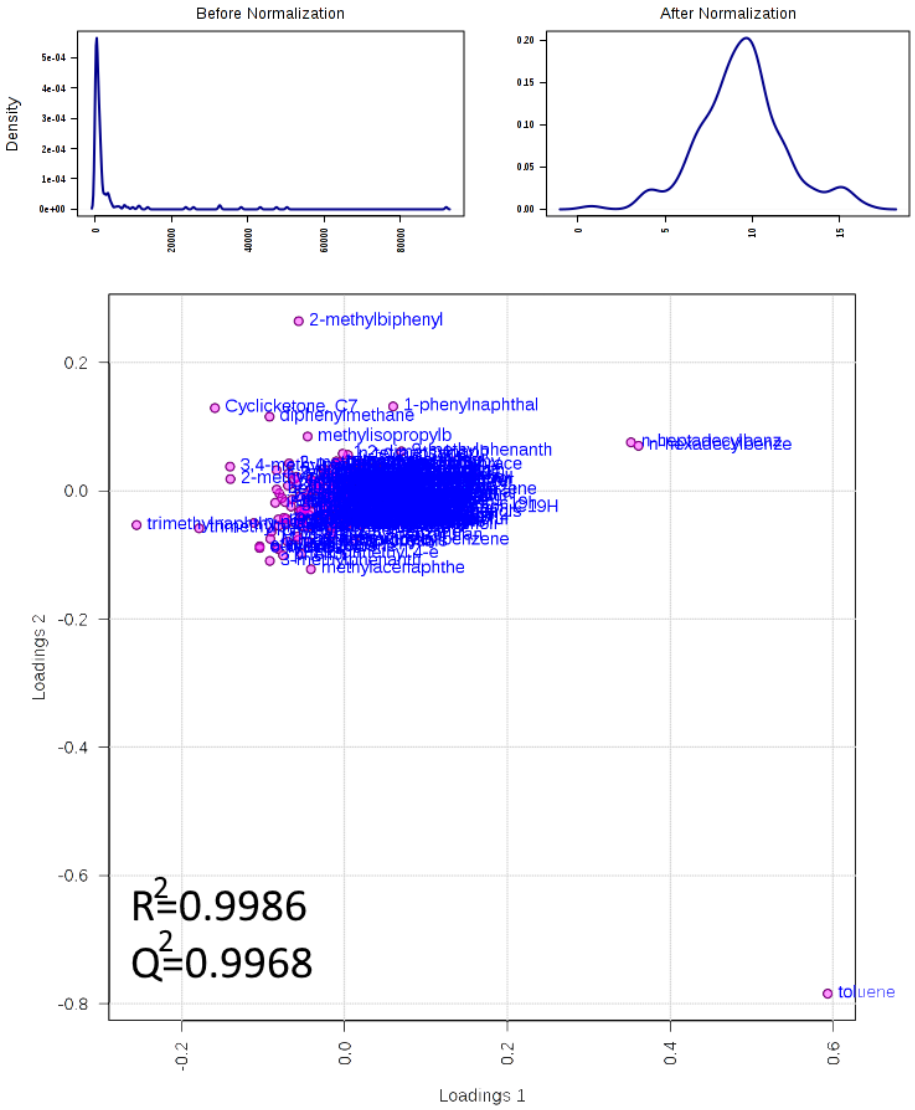

Figure 5.7: TOP data distribution before and after normalisation **Bottom** Loadings scores along with the validation values of R^2 and Q^2

the range of expected instrumental variation (GC-MS). Regarding surrogates, the average relative standard deviation was 11.08% before normalisation and 5.15±2.10% after normalisation indicating the approximate expected overall experimental variation.

Data analysis was performed as indicated in Section 5.2.4.5, p.80. Data processing resulted in a list of 146 features. Clustering of the samples does not appear to follow any trend of the sampling timeline (Figure 5.9B). Only samples from the 4th and 5th sampling periods appear to cluster together. Most of the features follows a similar pattern with the highest concentration during the 3rd sampling period (Figure 5.9C). However, there are features that appear to have their levels reduced or increased during the gasification experiment, with some of them fluctuating (Figure 5.9C).

Correlation analysis following increasing gasification time that was performed on the dataset,

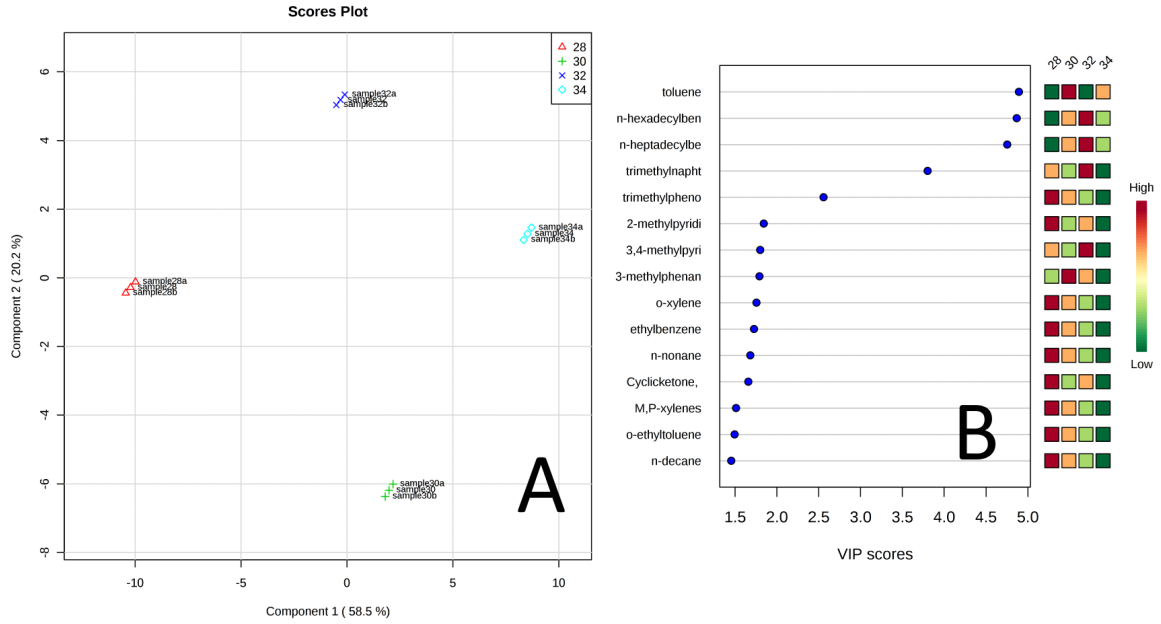

Figure 5.8: A: Scores plot from the PLS-DA model for the Hanna IVB trial. A lot of the variation in the first component may be attributed to sample 34 which is towards the end of the gasification run and significantly different than the rest of the sample. **B:** VIP scores of the 15 more important features. A VIP score of 2 is typically considered as a threshold for defining the most important features. Alkanes and low molecular weight aromatics occupy the highest positions

shows that more features appear to have a negative correlation than a positive correlation with gasification time (Figure 5.9A). As it appears, negative correlations are stronger than positive correlations indicating gradual reduction of the corresponding compound's concentration in the waste-water during gasification (Table 5.7).

Table 5.7: Top 5 features with the strongest positive and negative correlation with gasification time for the TOPS1 trial

Positive	correlation	t-stat	p-value	FDR
008B	0.85429	6.574	6.40E-06	0.00011604
128B	0.8484	6.4108	8.62E-06	0.00013888
122B	0.83799	6.1427	1.42E-05	0.00020538
134B	0.72838	4.2523	0.0006083	0.0041426
140B	0.57501	2.8113	0.012546	0.020913
Negative	correlation	t-stat	p-value	FDR
032B	-0.97344	-17.007	1.15E-11	1.66E-09
034B	-0.9427	-11.302	4.87E-09	3.45E-07
105B	-0.93983	-11.004	7.14E-09	3.45E-07
084B	-0.92708	-9.8927	3.19E-08	1.16E-06
036B	-0.91159	-8.8698	1.42E-07	4.11E-06

Regarding multivariate analysis, changes in the distribution after normalisation are seen in Figure 5.10, top; it is visible that the distribution becomes closer to normal from being heavily skewed to the left. Model validation showed an overall good model (R^2 = 0.98,

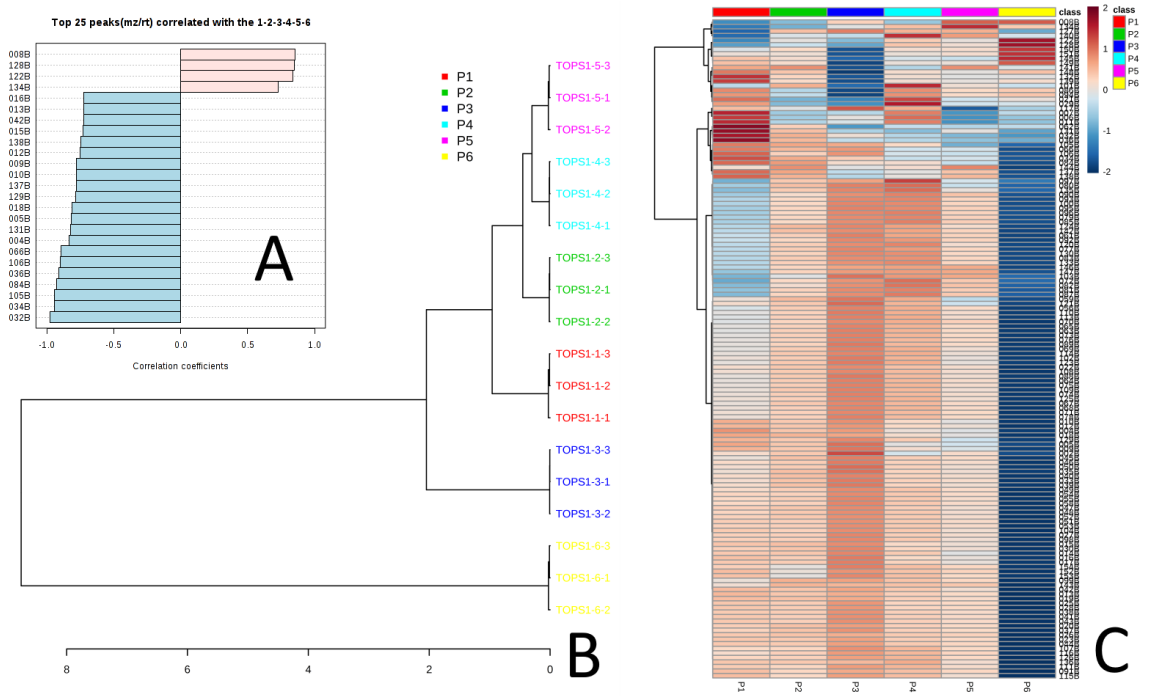

Figure 5.9: A: top 25 most strongly correlated features with gasification time **B:** Dendrogram of the samples grouped according to composition **C:** heatmap of all the features in the TOPS1 dataset. Values are normalised and autoscaled. Feature grouping is done according to evolution patterns. An elongated version of the heatmap is provided in Figure Appendix A.3.5

Q^2 = 0.96, no over-fitting - 5.10). Internal standard and the surrogates cluster in a narrow area near the 0,0 point of the loadings scatterplot (Figure 5.10).

The scores plot in Figure 5.11A shows the variation explained by each one the two components (89.7% for the first and 5.5% for the second) and it indicates that the second component is needed to explain most of the variation coming from the first 5 sampling periods while the sample from the 6th period is well separated from the rest using variation explained by the first component. By studying Figure 5.11B it can be safely assumed that most of the top ranked features have their levels quickly increasing and then decreasing during the gasification.

5.3.4 TOPS8 exploratory data analysis

Similar to the TOPS1 experiment this experiment was also performed in one replicate. The same data analysis approach was followed as above. The relative standard deviation of phenol-d6 before normalisation was 18.52%, however, this relatively high deviation was caused by an injection where the amount of phenol was so high that is affected the shape of the peak of phenol-d6 and possibly the signal of the detector for the quantifying ion (Figure Appendix A.3.2). With the repetitions for that injection removed from the calculation,

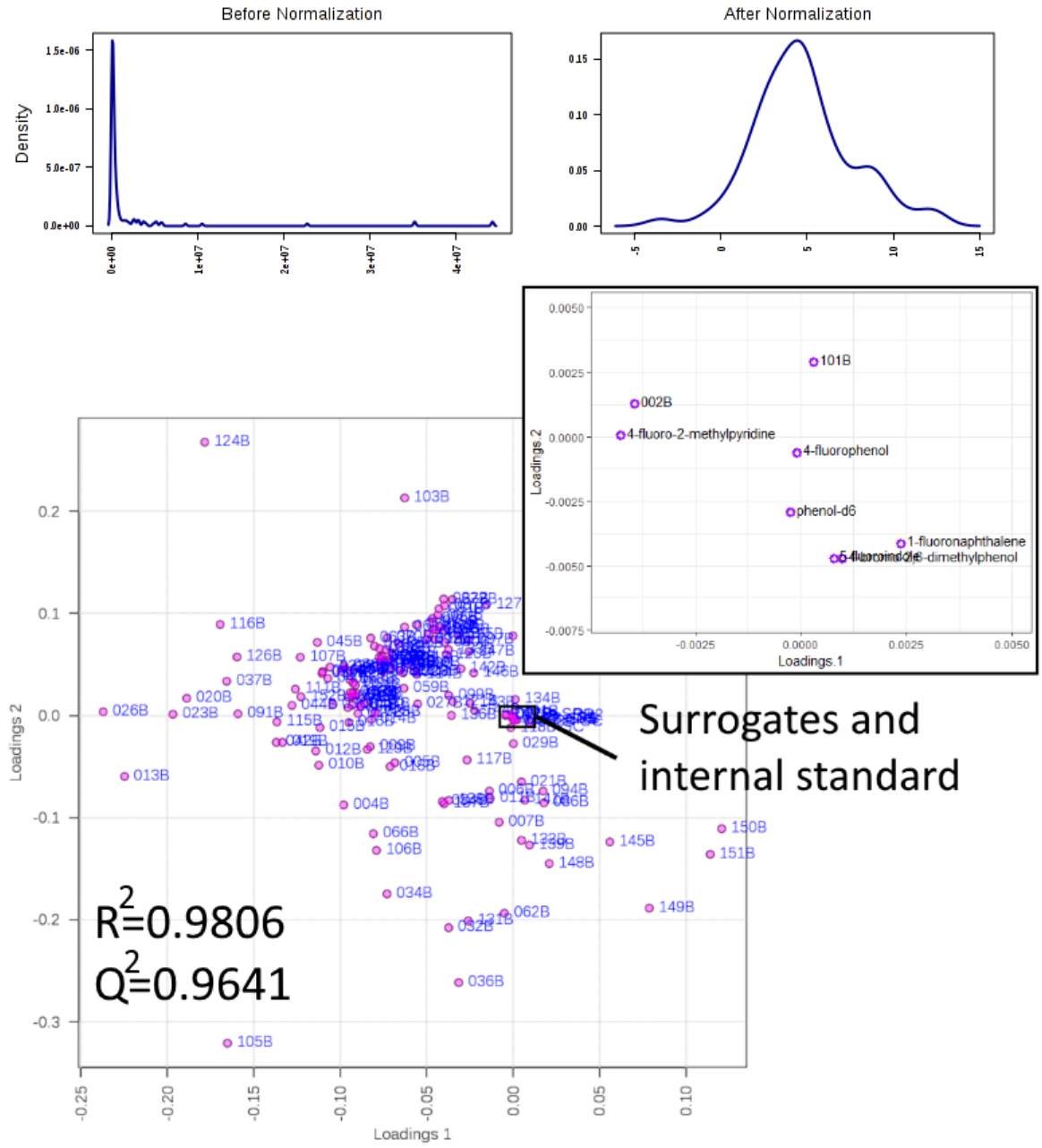

Figure 5.10: **Top** Density plot of the data from the TOPS1 trial before and after normalisation **B:** Scatterplot depicting feature loadings for the first and second components of the TOPS1 PLS-DA model. Grouping of the internal standard and surrogates is tight around the 0,0 point, indicating that the degree of experimental variation is small and that most of the variation explained by the model is due to compositional changes between the samples

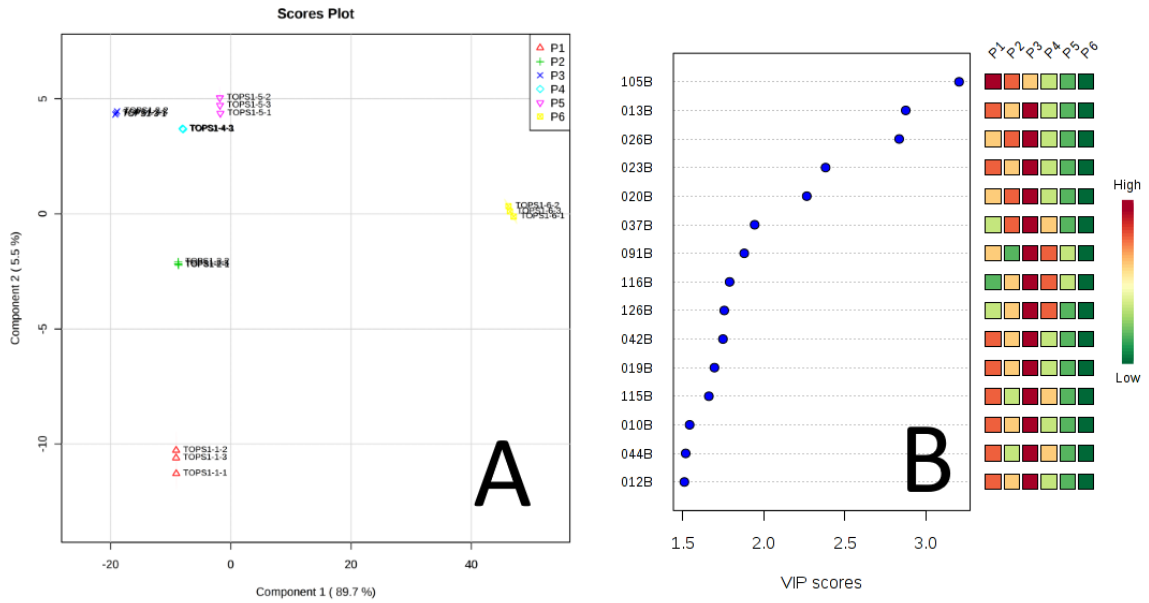

Figure 5.11: A: scatterplot of samples scores for the first and second components **B:** VIP scores for the top 15 features that mostly influence variation as ranked by the PLS-DA model for the TOPS1 trial. A VIP score of 2 is typically considered as a threshold for defining the most important features.

the RSD value falls down to 11.30%, very similar to the value of the same internal standard for the TOPS1 trial. After normalising the values with naphthalene-d8, the RSD value for phenol-d6 was 7.96% and with the affected injection removed it went down to 1.43%, similar to the amount of experimental variation that was seen in TOPS1. It must be noted that this effect was observed for phenol-d6 and the peak area values were very close to the control limit but not larger while a similar trend can be seen in naphthalene-d8 with the peak areas being much further from the control limit. This can be attributed to high concentration of phenol and naphthalene in that sample which may affect both chromatography and the detector signal since the annotated versions were almost completely co-eluting. Regarding surrogates the average RSD before normalisation was 15.19$\pm$4.19%, higher than TOPS1 and the average RSD after normalisation was 5.93$\pm$3.16% similar to approximate experimental variation seen in TOPS1.

Hierarchical clustering shows that samples from the first 3 sampling periods cluster together (Figure 5.12B). However, for the rest of the samples clustering does not appear to follow a gasification time-wise pattern. The sample from the 4th gasification period also appears not to belong in any of the clusters. Many features follow a similar pattern with their levels increasing until the 4th sampling period and then decreasing (Figure5.12C). There was a similar trend observed in the features in TOPS1. Also, some of the features appear to have their levels decreasing with increasing gasification time, while others have their levels fluctuate (Figure 5.12C).

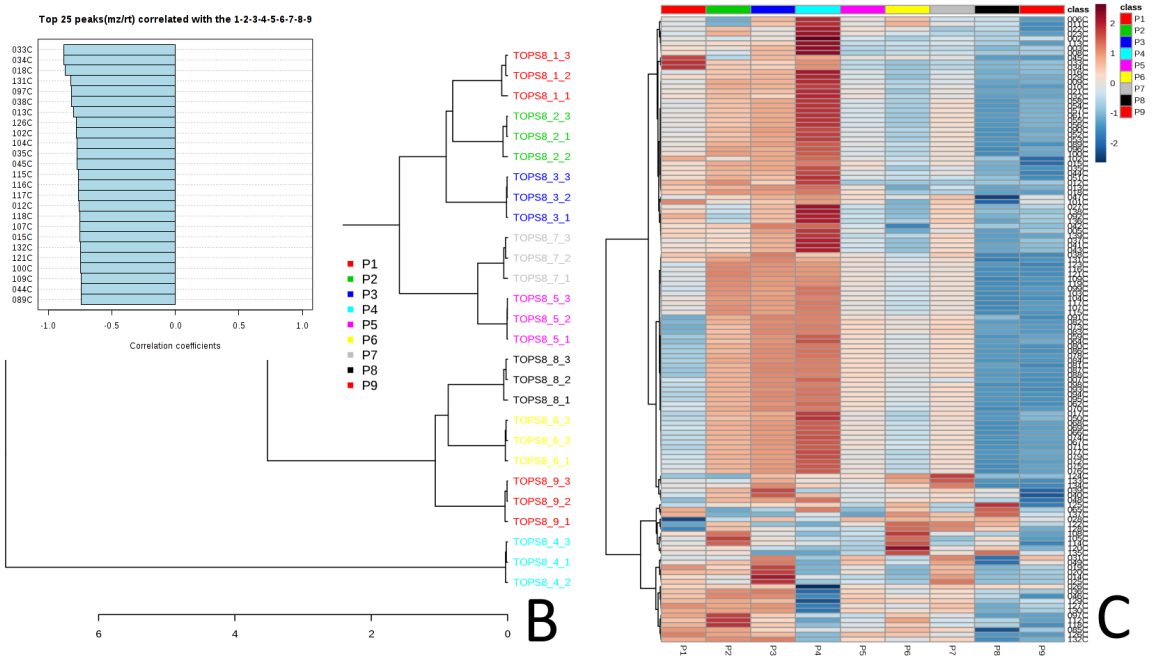

Figure 5.12: A: Top 25 features with the strongest correlation with gasification time **B:** Dendrogram attempting to group the samples according to composition **C:** heatmap depicting autoscaled features together with grouping of features according to evolution pattern similarities. Samples are order in gasification time order. An elongated version of the heatmap is provided in Figure Appendix A.3.6

In Figure 5.12A it is seen that the features that correlate negatively with increasing gasification time are more that those that appear to correlate positively. This can also be verified from Table 5.8 that includes the top 5 features from both positive and negative correlation analysis. It can be clearly seen that the negatively correlating features are much stronger than the positive ones which appear to have weak correlations. Only feature 028C shows a relatively strong positive correlation.

Table 5.8: Top 5 features with the strongest negative positive and negative correlation (Pearson's R) with gasification time

Positive	correlation	t-stat	p-value	FDR
028C	0.61496	3.8993	0.00064147	0.0013898
122C	0.3884	2.1075	0.045276	0.051631
135C	0.38528	2.0875	0.047188	0.053343
137C	0.34486	1.837	0.078125	0.086806
128C	0.24427	1.2595	0.21949	0.23011
Negative	correlation	t-stat	p-value	FDR
033C	-0.87893	-9.2139	1.63E-09	1.07E-07
034C	-0.87881	-9.2087	1.65E-09	1.07E-07
018C	-0.86536	-8.6339	5.69E-09	2.47E-07
131C	-0.82004	-7.1645	1.65E-07	4.68E-06
097C	-0.81867	-7.1281	1.80E-07	4.68E-06

Data transformation brought the distribution from heavily skewed to close to normal (Figure

5.13). Cross-validation of the model gave values of R^2=0.98 and Q^2=0.96 and the permutation test confirmed no over-fitting. Also, the grouping of the added compounds in the samples (internal standard and surrogates) can be seen in Figure 5.13, bottom; tight grouping of these features also indicates that the variation explained by the model derives mainly from compositional differences between the samples.

Both components contribute to explain the variation in the model with 64.7% of variation explained from the fist component and 16.9% for the second component (Figure 5.14A). Although the first component differentiates almost equally among the samples, the second component separates the sample that came from the 4th sampling period more than the rest of the samples. Most of these top features appear to either have their levels reduced throughout the course of the gasification experiment or heavily fluctuating (Figure 5.14B).

5.3.5 Barbara mine exploratory data analysis

The *in-situ* gasification trial performed at the Barbara mine can be seen as a case-study with the possibility of providing insight and rough conclusions that may be applicable, generally, in other similar *in-situ* UCG experiments. Regarding sample preparation, surrogate and internal standard selection was not limited from solubility as it was with waste-water since the matrix of the samples is coal tar, so a more extensive list of surrogates and internal standards can be used. The internal standard used for normalisation for this experiment was phenanthrene-d10. The relative standard deviations for phenol-d6 and naphthalene-d8 before normalisation were 5.03% and 5.01% respectively and after normalisation it was lowered to 1.73% and 1.69% which indicate the expected instrumental variation, close to the values observed for TOPS1 (1.88%) (Figure Appendix A.3.3). Regarding the surrogates, the average RSD was 5.84$\pm$0.65% before normalisation and 2.07$\pm$0.5% after normalisation which indicates the amount of expected experimental variation. It is clearly observed that the amount of experimental variation for tar extraction is significantly lower (2.07$\pm$0.50% for Barbara mine, 5.15$\pm$2.10% for TOP1 and 5.93$\pm$3.16% for TOPS8). This was expected since the tar extraction method is an assisted dilution that does not involved mass transfer through different phases such as in liquid-liquid extraction, where the matrix may affect the partition coefficients of the various compounds as well. Details about the gasification experiments at the Barbara mine can be seen in a relevant publication from GIG[143].

Data processing resulted in the extraction of a total of 245 features that correspond to individual unidentified compounds. The same data analysis approach was used as above but here before processing, the data were normalised to phenanthrene-d10. Clustering shows that the samples belong to 3 major clusters where the top cluster includes samples taken at the beginning, 24 and 48hrs, the middle cluster includes samples taken at 72 and 96hrs and the bottom cluster includes samples taken at 120, 144 and 168hrs (Figure 5.15B). Based on

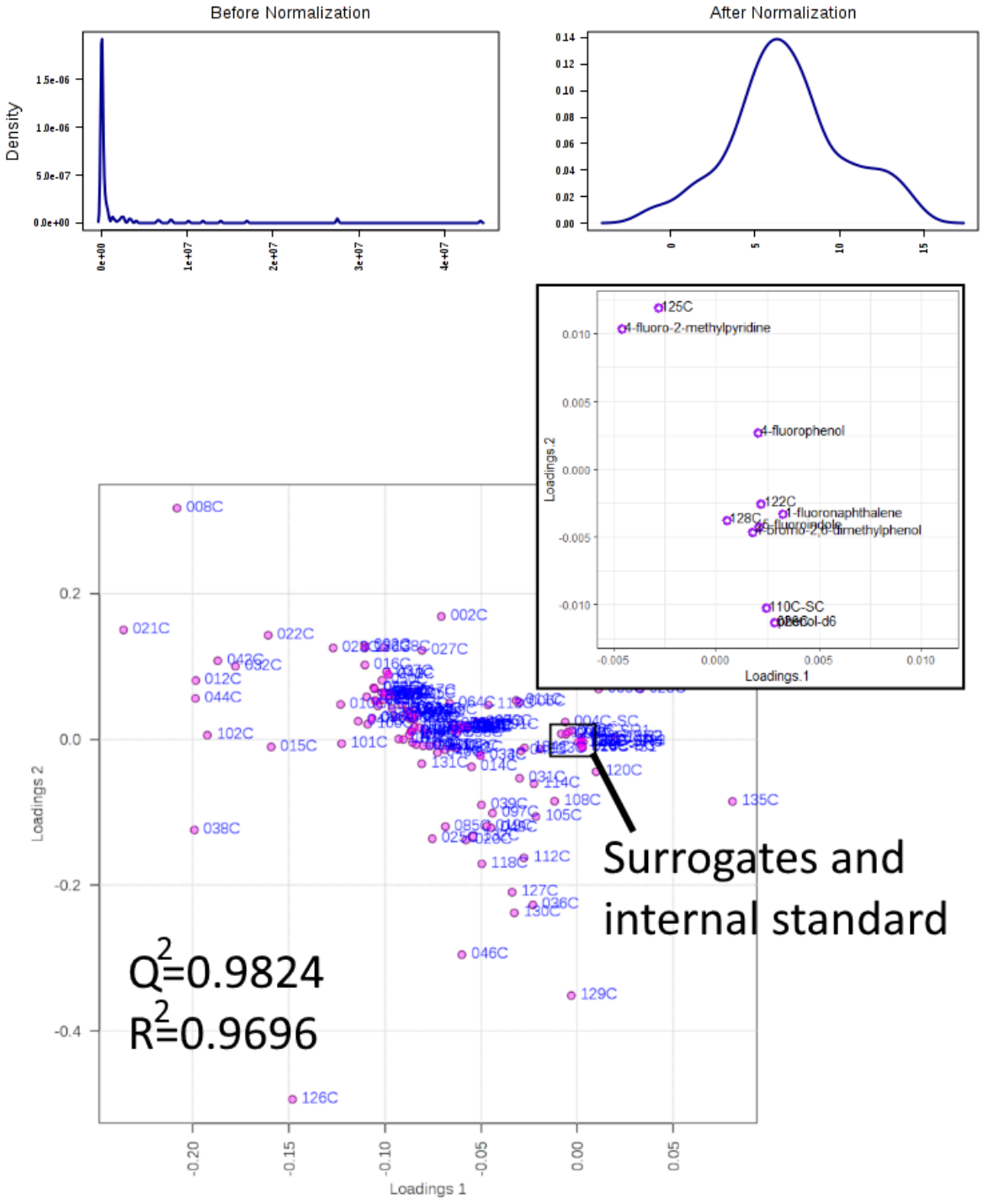

Figure 5.13: **Top** Density plot of the distribution of data from the TOPS8 trial before and after normalisation **Bottom** Scatter plot of feature loadings from the TOPS8 PLS-DA model. As seen internal standards and loading are grouped in a very small area near the 0,0 point further indicating that the degree of variation is very low and most of the variation explained by the components can be traced to variation in sample composition

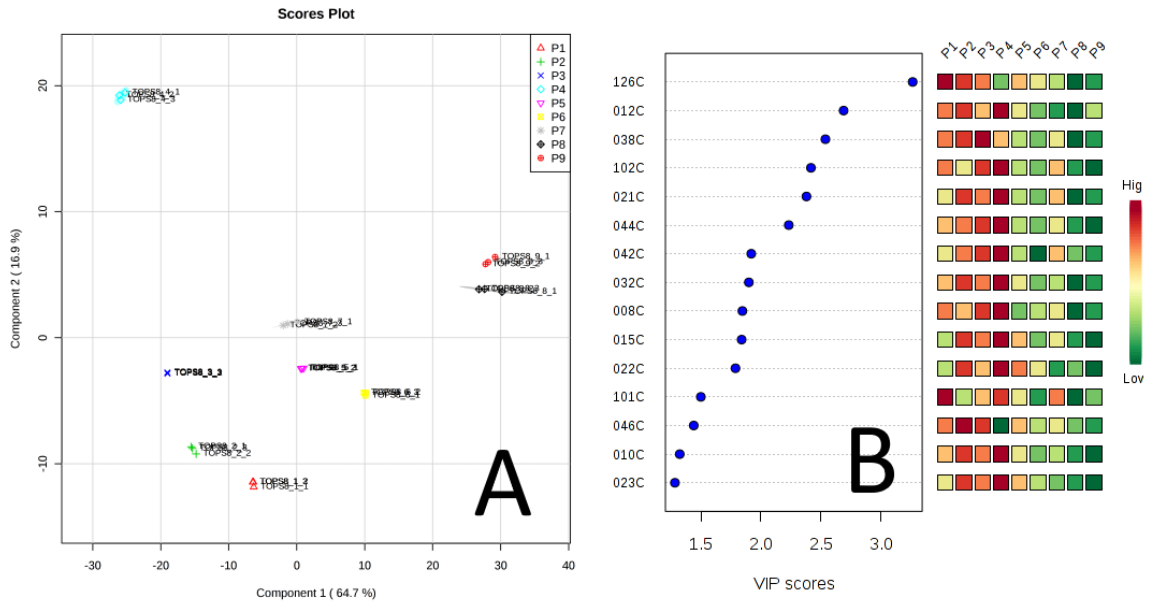

Figure 5.14: A: Scores plot of the first two components from the TOPS8 PLS-DA model. **B:** VIP scores of the top 15 features as ranked by the PLS-DA model. A VIP score of 2 is typically considered as a threshold for defining the most important features.

the clustering behaviour we can classify the samples as those that belong to the following periods: early gasification, mid-gasification and late gasification. Features can be classified in 3 major groups, those which level increases during the gasification, those with their level decreasing during the course of the gasification and those which level fluctuates during the gasification (Figure 5.15C). The sample taken at 120hrs after gasification initiation appears to have a higher SVOC content. The majority of the features appear to have their levels increase up to 120hrs after gasification initiation and then their levels either remain relatively stable or decrease. Also, a significant number of features appear to have higher levels until 120hrs where they rapidly decrease.

Results from further pattern investigation using the same normalisation parameters and applying correlation analysis for features that have a strong Pearson r correlation with increasing gasification time appear in Figure5.15A. The top features for positive and negative correlation are given in Table5.9.

Before and after images of the distribution can be seen in Figure 5.16,top; it is clear that the transformation brings the distribution close to normal. Variance explained by the PLS-DA model was 65.4% for component 1 and 28.6% for component 2. Cross validation shows good values (R^2=0.985 & Q^2=0.978) and the permutation test showed the model is not over fitted. Internal standards and surrogates appear to be grouped in a very small area in the 0,0 region of the loadings plot (Figure 5.16, bottom), providing further evidence for the validity of the model and indicating that the degree of variation that can be attributed to compositional differences between the samples is high while the variation cause by the sample preparation

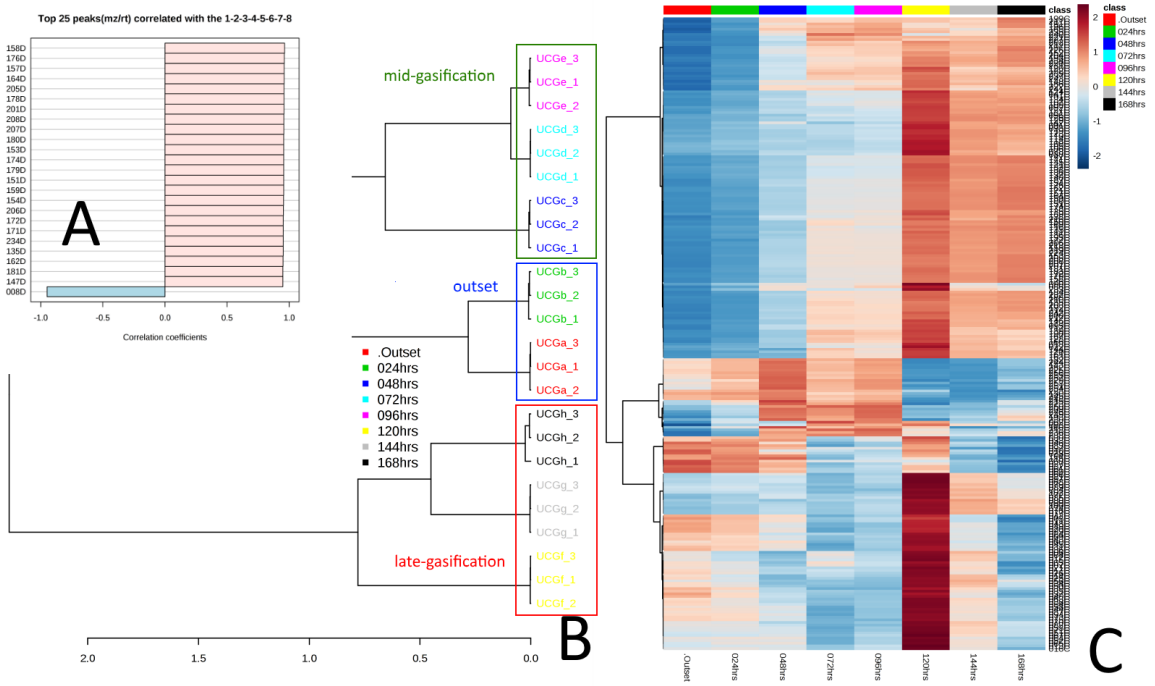

Figure 5.15: **A**:Tops 25 features with the highest correlation with gasification time **B**: Dendrogram of the barbara mine gasification experiments samples. The samples can be classified into 3 categories: early, mid- and late gasification. **C**: heat map of all the features of the experiment along with their relative peak ratios in each sample appear of the right. Samples are ordered according to time and features are group according to clustering. An elongated version of the heatmap is provided in Figure Appendix A.3.7

Table 5.9: Positive and negative correlation values of the top 5 features for each category. Values of the t-stat, p-value and FDR are given for each one of the top features.

Positive	correlation	t-stat	p-value	FDR
158D	0.96795	18.078	1.09E-14	1.66E-12
157D	0.96565	17.43	2.31E-14	1.66E-12
176D	0.96462	17.162	3.18E-14	1.66E-12
164D	0.96411	17.033	3.71E-14	1.66E-12
153D	0.96267	16.681	5.69E-14	1.66E-12
Negative	correlation	t-stat	p-value	FDR
008D	-0.95174	-14.546	9.10E-13	9.22E-12
130D	-0.89967	-9.6661	2.23E-09	7.33E-09
069D	-0.89178	-9.2445	4.94E-09	1.52E-08
228D	-0.86482	-8.0793	5.01E-08	1.30E-07
027D	-0.85325	-7.6743	1.17E-07	2.84E-07

and analysis process is very low.

A scatter plot of the fist and the second component appear in Figure 5.17A. Both components contribute to the separation between the samples, however samples corresponding to 72 and 96hrs remain grouped together. Tops 15 features as ranked by the first component can be seen in Figure 5.17. Feature 008D appears to contribute to the model significantly more than the rest of the features. All the top features apart from feature 008D and 027D appear to have

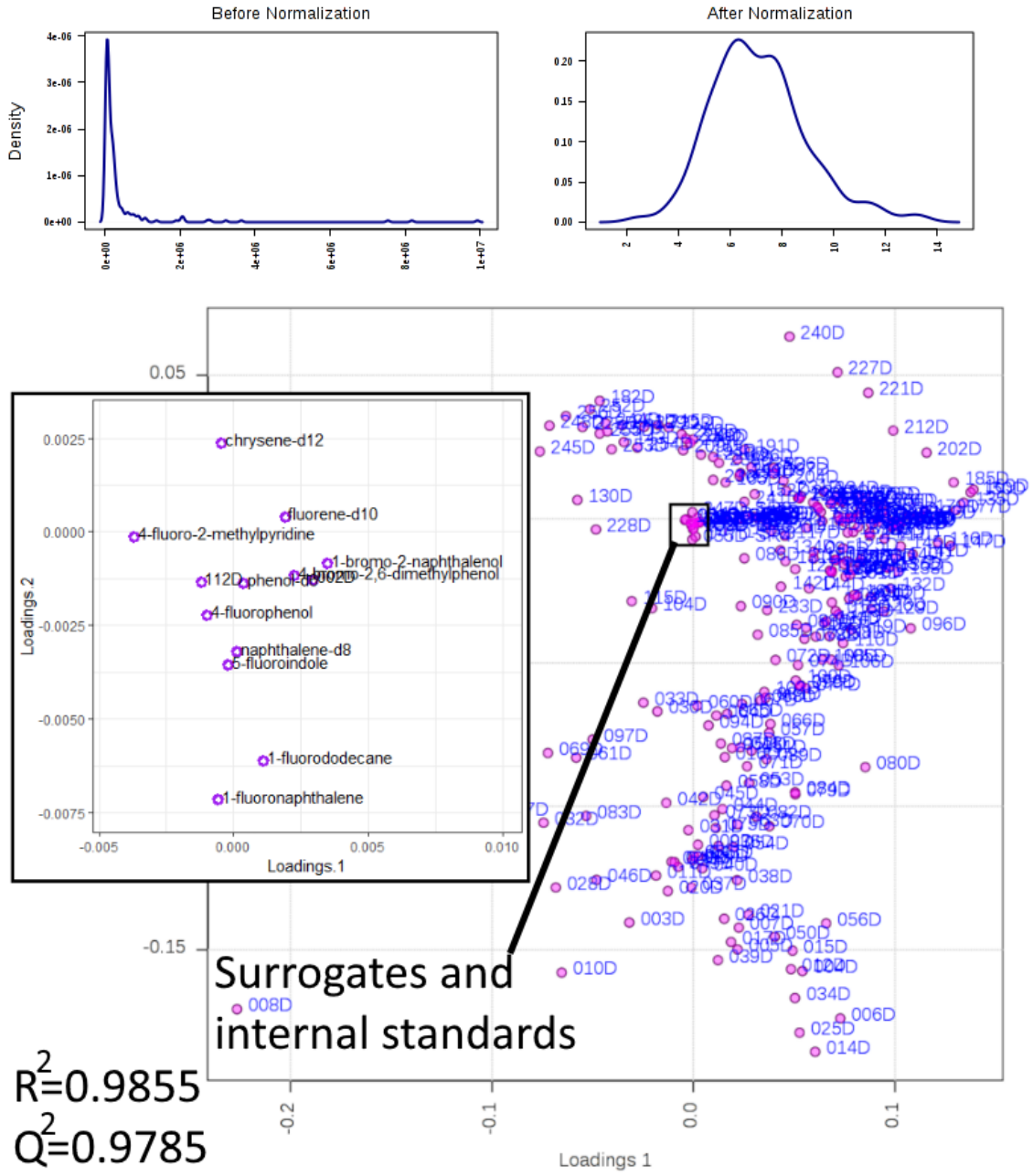

Figure 5.16: Top Density plot of the data from the Barbara II trial before and after normalisation **B:** Scatterplot depicting feature loadings for the first and second components of the TOPS1 PLS-DA model. Grouping of the internal standard and surrogates is tight around the 0,0 point, indicating that the degree of experimental variation is small and that most of the variation explained by the model is due to compositional changes between the samples

their levels increase with gasification time.

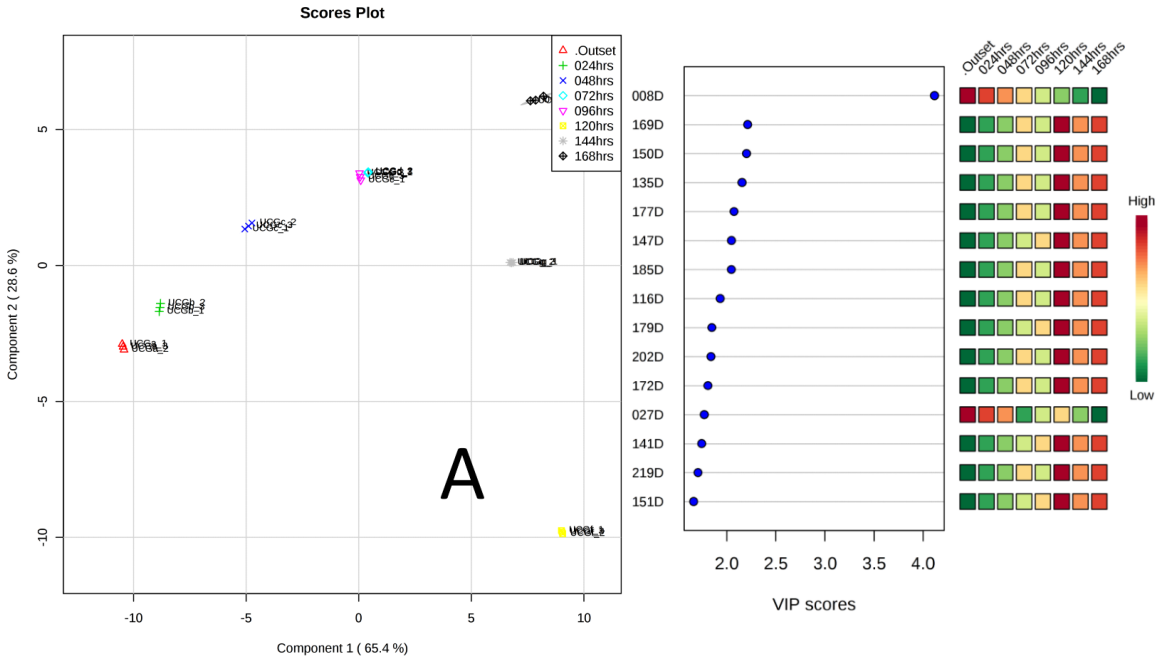

Figure 5.17: Scatterplot of the first and second components of the PLS-DA model (A). Both components contribute significantly to explain the variation between the samples. As it can be seen from the plot clear discrimination of THE sample pair 72-96hrs is impossible. On the right (B) a feature ranking graph that is calculated from contributions to the the first component of the model can be seen. Contribution from feature 008D is significantly higher the that rest of the features. A VIP score of 2 is typically considered as a threshold for defining the most important features.

5.3.6 Combined critical compound study

The analysis that was described in sections 5.3.2, 5.3.3, 5.3.4 and 5.3.5 was performed in order to study each gasification trial separately as a case study but also to identify any possible trends between UCG trials. Features that were selected as significant from all four sections are given in Table 5.10. Obviously, the feature pool from the UCG trials performed at Hanna is limited to those compounds that were quantified and reported from Humenick and Mattox [60]. However, it may provide useful information that can possibly confirm any trends identified from the analysis of tars produced during the Barbara II test.

Before interpreting any results, general issues that may arise from comparing the different samples matrices should be discussed. Generally, it can be said that the concentration of an SVOC in waste-water is limited by its water solubility. In the case of UCG waste-water, a compound's solubility may change due to the fact that UCG waste-water can be heavily burdened with dissolved organic components, thus, the affinity of an SVOC with the carbon-rich waste-water is expected to increase along with its solubility (at least without taking

Table 5.10: List of important features as derived from PLS-DA and correlation analysis

	TOPS1		TOPS8		Barbara II		Hanna IVB	
	Feature ID	Correlation	Feature ID	Correlation	Feature ID	Correlation	Feature ID	Correlation
Pos1	008B	0.85429	028C	0.61496	158D	0.96795	9-methylphenanthrene	0.99714
Pos2	128B	0.8484	122C	0.3884	157D	0.96565	2-methylanthracene	0.98683
Pos3	122B	0.83799	135C	0.38528	176D	0.96462	methyldibenzofuran.1	0.97443
Pos4	134B	0.72838	137C	0.34486	164D	0.96411	3-methylbiphenyl	0.95785
Pos5	140B	0.57501	128C	0.24427	153D	0.96267	4-methylbiphenyl	0.95123
Neg1	032B	-0.97344	033C	-0.87893	008D	-0.95174	M,P-xylenes	-0.9986
Neg2	034B	-0.9427	034C	-0.87881	130D	-0.89967	ethylbenzene	-0.99623
Neg3	105B	-0.93983	018C	-0.86536	069D	-0.89178	n-propylbenzene	-0.99557
Neg4	084B	-0.92708	131C	-0.82004	228D	-0.86482	1,2,3-trimethylbenzene	-0.99526
Neg5	036B	-0.91159	097C	-0.81867	027D	-0.85325	o-xylene	-0.99418
	Feature ID	VIP score	Feature ID	VIP score	Feature ID	VIP score	Feature ID	VIP score
VIP1	105B	3.2053	126C	3.2639	008D	4.1163	toluene	4.8934
VIP2	013B	2.8757	012C	2.6888	169D	2.2116	n-hexadecylbenzene	4.8672
VIP3	026B	2.8353	038C	2.5373	150D	2.2006	n-heptadecylbenzene	4.7534
VIP4	023B	2.3807	102C	2.417	135D	2.1554	trimethylnaphthylene isomer.5	3.8018
VIP5	020B	2.2648	021C	2.3796	177D	2.0739	trimethylphenolisomer.2	2.5569
VIP6	037B	1.9427	044C	2.2322	147D	2.0481	2-methylpyridine	1.8424
VIP7	091B	1.8786	042C	1.92	185D	2.047	3,4-methylpyridines	1.7998
VIP8	116B	1.7881	032C	1.8999	116D	1.9323	3-methylphenanthrene	1.7908
VIP9	126B	1.7551	008C	1.8462	179D	1.8473	o-xylene	1.7549
VIP10	042B	1.7473	015C	1.8397	202D	1.8386	ethylbenzene	1.7256
VIP11	019B	1.6945	022C	1.7885	172D	1.8079	n-nonane	1.6812
VIP12	115B	1.66	101C	1.5001	027D	1.7707	Cyclicketone, C7H10O	1.6577
VIP13	010B	1.5414	046C	1.4409	141D	1.7445	M,P-xylenes	1.5109
VIP14	044B	1.5169	010C	1.3243	219D	1.7066	o-ethyltoluene	1.4939
VIP15	012B	1.5089	023C	1.2843	151D	1.6616	n-decane	1.4536

into account any effects that dissolved inorganic components - such as salts - may have on the solubility on an SVOC). However, this increase cannot be expected to be indefinite and eventually an upper limit in the concentration of the SVOC in the UCG waste-water will be reached. This effect is going to be more obvious in the case of SVOCs with limited water solubility such as high molecular weight PAHs. This leads to the question whether UCG waste-water can be realistically used as a proxy for studying the production of SVOCs from a UCG process, particularly in the case of high molecular weight PAHs. Regardless, analysis of waste-water remains important in order to identify SVOCs in the waste-water with a possible economic value but also for risk assessment and environmental monitoring purposes.

On the other hand, UCG produced tar, and generally coal tar, is a super-concentrated matrix of components that derives from coal utilisation processes. Its composition may be a result of many phenomena that take place during the UCG process and it is not limited by solubility so it can be expected to carry much more information regarding the process from which it is derived from and, providing storage conditions are adequate so that no weathering takes place, it may be treated as a historical record that can be used retroactively to study various aspects of the experiment that are associated with SVOCs production.

Features that have a positive strong correlation with sampling time for the TOPS1 experiment are relatively limited, with only 4 features having an R^2 above 0.6. However, negative correlations appear to be stronger (Table 5.10 - TOPS1). Regarding TOPS8, there is a sig-

nificant lack of features that are positively correlated with sampling time since the strongest correlation is 0.61 for feature 028C which appears to be the only positive correlation with an R^2 above 0.6. Negative correlations exist, although they do not appear to be as strong as in TOPS1. On the other hand, features from tar samples that derive from the Barbara II UCG run, appear to have both strong positive and negative correlations. This also appears to be true for compounds in tar samples from the Hanna IVB experiment. Especially regarding the Hanna IVB experiment, the negative correlations appear to be very strong (9-methylphenanthrene and M,P-xylenes with an $R^2 > |0.99|$).

The VIP scores deriving from PLS-DA are specific to the four experiments since each PLS-DA model is fitted to each dataset, so comparing VIP values between experiments may not be as fair as comparing correlation coefficients between experiments. Rather than comparing VIP values, more weight is given on whether or not a specific feature or compound exists in the list of the features that were ranked higher from the PLS-DA model. Table 5.11 includes the identification attempt of those features that were either in the top 5 features that have a stronger correlation with sampling time (implying stronger correlation with gasification duration) or in the top 15 features that contribute more to sample variation as ranked by each PLS-DA model.

Each feature in Table 5.11 is included along with its retention index. Compounds are identified based on reference standards or matches to library spectra. However, isomers are not identified separately, and individual compound identifications are putative.

Table 5.11 was searched for compounds that may appear more than one time and in more than one experiment. In total, 6 compounds seem to fit the criteria mentioned: C1-cyclopentanone seems to appear in both TOPS1 and TOPS8 experiment (010C and 010B) as a significant feature in PLS-DA. The evolution pattern in both cases appear to be negatively correlated with gasification time. This means that this compound is either depleted from the coal through gradual devolatilisation downstream from the gasification front or being consumed in a secondary reaction that becomes more intense with increasing temperature. The same can be assumed when studying the evolution patterns for indole (101C and 105B) in plots C and F that correspond TOPS1 and TOPS8 respectively. C2-pyridine (023B and 021C) appears in TOPS1, TOPS8 and HannaIVB (actually the 1,3,4 isomers). Evolution patterns for all of the 3 compounds can be seen in Figure 5.18. Plots A and D correspond to C1-cyclopentanone in TOPS1 and TOPS8 respectively. Evolution pattern plots B,E,G and H correspond to C2-pyridine(s) in TOPS1, TOPS8 and Hanna IVB respectively.

Methyldibenzofuran isomers appear to be increasing during the course of the gasification in the Barbara II trial (features 158D and 164D). Methyldibenzofuran is ranked high for positive correlation in the Hanna IVB and the compound patterns are compared in Figure 5.19. All of the features appear to have an overall increasing trend. Generally, all compounds with time-

Table 5.11: Combined list of important features from PLS-DA and correlation analysis (by increasing retention index) (NA refers to compounds that were completely unidentified and question marks to identifications with low confidence)

Index no	Compound	Identification method	Experimental RI
008C	C1-pyridine	Library	1022.4
008B	3-methylbut-3-enyl 3-methylbutanoate	Library	1023.5
010C	C1-cyclopentanone	Library	1031.8
010B	C1-cyclopentanone	Library	1032.4
012C	2-furanmethanol	Library	1038.8
012B	C2-pyridine	Library	1044.0
013B	C1-pyridine	Library	1045.5
008D	Phenylethyne	Library	1049.0
015C	C2-cyclopentanone	Library	1053.0
018C	C1-benzamine	Library	1087.6
019B	C2-pyridine	Library	1098.9
020B	C3-pyridine	Library	1113.7
023B	C2-pyridine	Library	1123.3
021C	C2-pyridine	Library	1125.6
022C	C2-pyridine	Library	1128.8
023C	C3-pyridine	Library	1132.7
026B	C3-pyridine	Library	1148.1
028C	2-chlorophenol?	Library	1153.9
032B	Benzofuran	Library	1171.0
032C	C1-cyclopentenone?	Library	1193.4
033C	Benzonitrile	Standard	1193.9
034B	Benzonitrile	Standard	1195.0
034C	Benzonitrile	Standard	1195.6
027D	Benzonitrile	Standard	1199.6
036B	Indene	Library	1220.3
037B	C4-pyridine	Library	1223.6
038C	C3-cyclopentenone	Library	1244.7
042B	C2-cyclopentenone	Library	1252.1
042C	C3-benzamine	Library	1253.3
044B	Na	-	1253.7
044C	C3-benzamine	Library	1256.0
046C	Acetophenone	Library	1282.4
069D	Benzothiophene	Library	1451.9
084B	Quinoline	Library	1526.7
091B	Diol	Library	1566.7
097C	C1-quinoline	Library	1591.8
101C	Indole	Standard	1617.2
105B	Indole	Standard	1617.3
102C	C1-indole	Library	1623.3
115B	C1-diol	Library	1671.7
116B	C2-diol	Library	1679.2
122B	C1-indanol	Library	1713.9
116D	Alkane (C17)	Library	1717.1
126B	C2-diol	Library	1736.2
128B	C3-quinoline	Library	1753.6
130D	Acenaphthylene	Standard	1774.7
135D	Alkane (C18)	Library	1813.0
134B	p-Heptylacetophenone?	Library	1826.1
122C	NA	-	1826.5
141D	C3-naphthalene	Library	1848.6
126C	C3-quinoline	Library	1852.3
147D	C3-naphthalene	Library	1882.1
150D	Alkane (C19)	Library	1905.5
151D	C3-naphthalene	Library	1906.6
153D	Aromatic-oxygen	Library	1916.0
128C	Methoxybiphenyl	Library	1926.1
140B	o-phenyl-anisole?	Library	1926.3
157D	9H-xanthene	Library	1932.3
158D	C1-dibenzofuran	Library	1946.9
164D	C1-dibenzofuran	Library	1977.1
131C	C1-napthalenol	Library	1989.8
169D	Alkane (C20)	Library	2012.2
172D	C4-naphthalene	Library	2023.3
176D	C1-9H-fluorene	Library	2040.6
177D	NA	Library	2041.3
179D	C4-napthalene	Library	2054.7
185D	Alkane (C21)	Library	2114.2
135C	Benzo[f]quinoline	Library	2281.7
202D	Alkane (C23)	Library	2306.7
137C	4-Azafluorene	Library	2309.6
219D	C2-phenanthrene	Library	2498.4
228D	4-ring-PAH	Library	2637.9

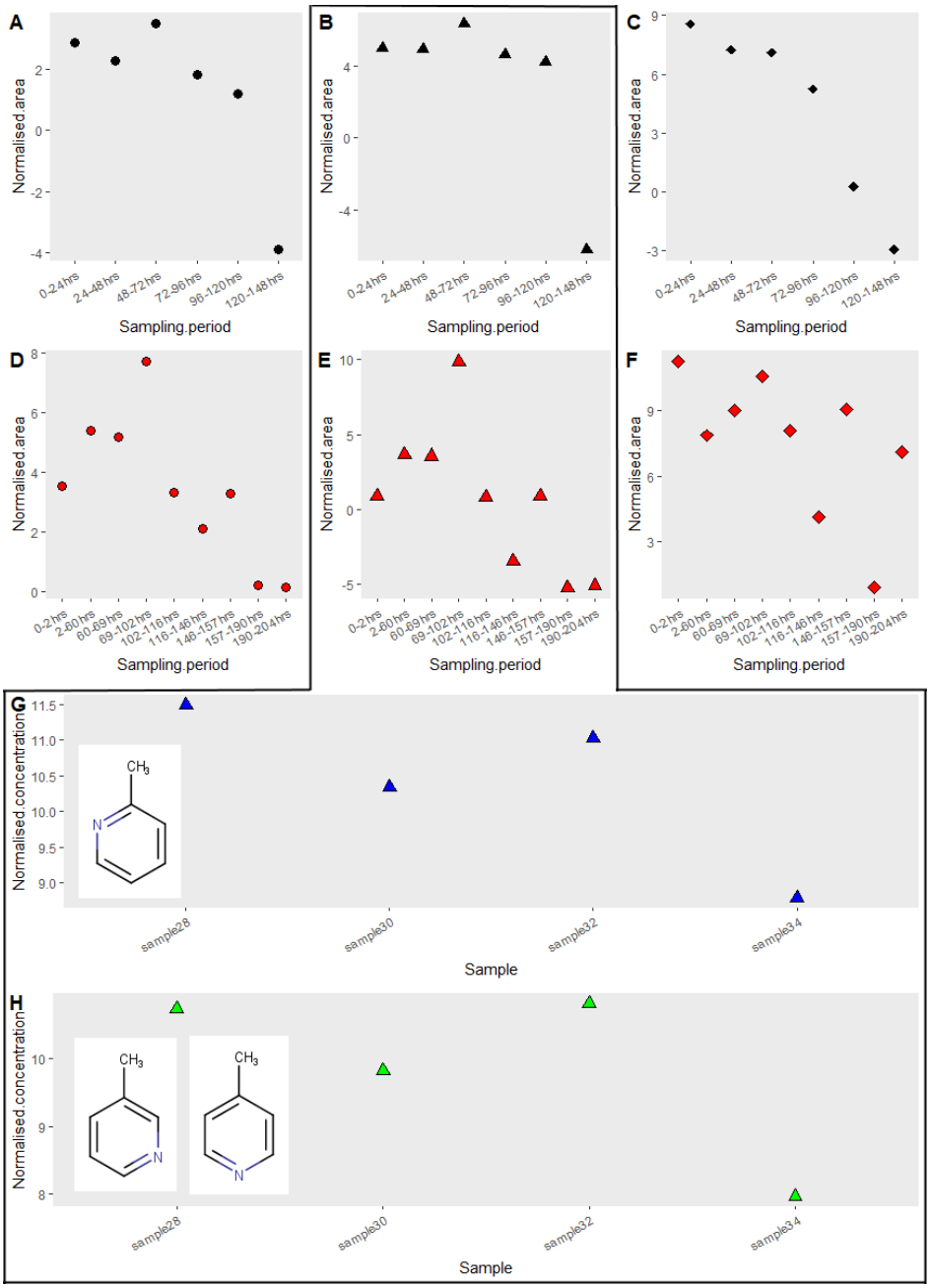

Figure 5.18: Evolution patterns for compounds that appear in multiple trials. **A&D** C1-cyclopentanone in TOPS1 and TOPS8 respectively; **B&E** C2-pyridine in TOPS1 and TOPS8 respectively with **G&H** for 1-methylpyridine and 3,4-methylpyridines for Hanna IVB; **C&F** indole in TOPS1 and TOPS8 respectively. Generally, C1-cyclopentanone, C2-pyridine and indole has similar patterns in each TOPS experiment

positive correlated patterns are of high interest since they may be produced via secondary reactions in the coal as the temperature increases with gasification progress.

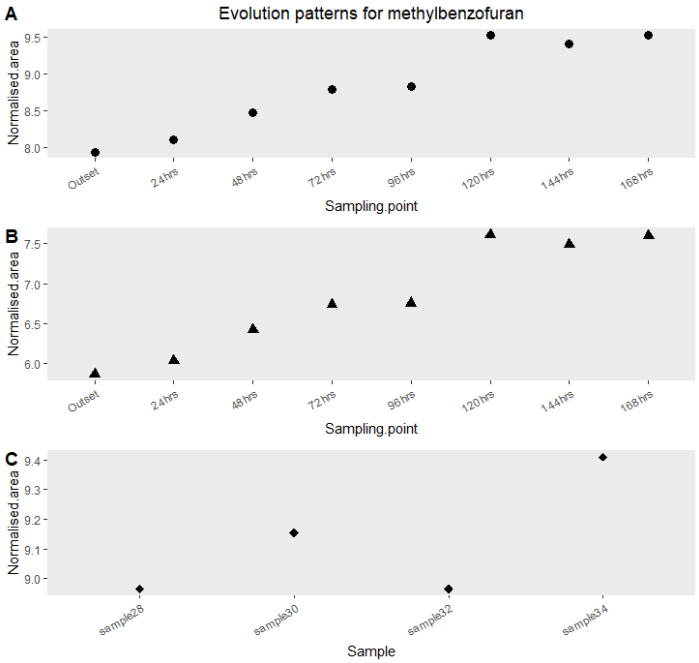

Figure 5.19: Evolution patterns for methylbenzofurans. **A&B** correspond to 158D and 164D while **C:** corresponds to methyldibenzofuran. Evolution pattern shows that the level of the compounds is increasing in the tar during the course of the gasification

Benzonitrile seems to be appearing in TOPS1 (034B), TOPS8 (033C, 034C) and Barbara II (027D) experiments as a feature with negative correlation to gasification time. The evolution patterns for benzonitrile for all three experiments can be seen in Figure 5.20.

As it appears in all three experiments and in both matrices (waste-water and tar), benzonitrile appears to be negatively correlated with gasification time. Unfortunately, the compound was not reported in the Hanna IVB dataset in order to historically confirm this trend.

The evolution pattern comparison that appears in Figure 5.21 shows the patterns of the top features for positive and negative correlation with gasification time and the top-rated feature by PLS-DA for each experiment.

Identification of the illustrated features can be found in Table 5.11 and the corresponding values for correlation and PLS-DA scores in Table 5.10. Regarding the TOPS1 experiment (5.21A), the feature 008B identified as 3-methyl-3-enyl-methylbutanoate appears to have a positive correlation with time which indicates that the levels of the compound are gradually increasing in the production stream. Feature 032B (top negatively correlated) identified as benzofuran and feature 105B (top PLS-DA feature) identified as indole are decreasing.

For TOPS8 (5.21B), feature 028C (top positively correlated feature) identified as potentially chlorophenol is increasing. Chlorinated compounds may be produced through reactions with

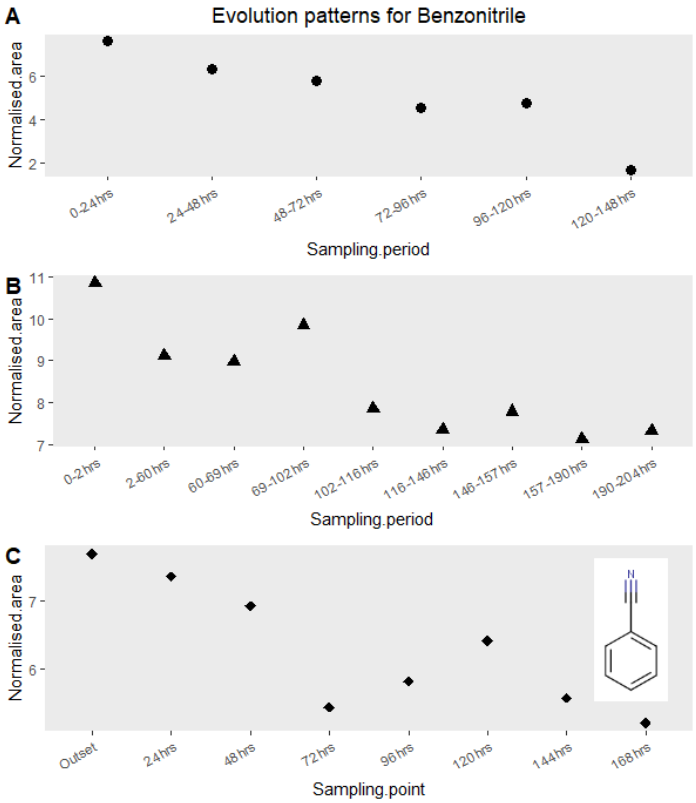

Figure 5.20: Evolution patterns of benzonitrile in all three gasification trials; **A:** TOPS1, **B:** TOPS8, **C:** Barbara II. The compound is not reported in the Hanna IVB appendix

chlorine in coal[163] as chlorine may have existed in some form inside the coal (Section 2.2.3). Feature 033C which is identified as benzonitrile is decreasing (top negatively correlated feature). Feature 126C which is identified as a C3-quinoline is seen to be fluctuating (top PLS-DA ranked feature).

Regarding the Barbara II trial (Figure 5.21C) feature 008D, which is both the top negatively correlated compound but also the top ranked PLS-DA feature is identified as phenylethyne. The positive correlated feature is 158D which is identified as C1-dibenzofuran.

Finally, for the Hanna IVB trial (Figure 5.21D), the top positively correlated compound is 9-methylphenanthrene, the top negatively correlated compound is M,P-xylenes which corresponds to both m and p isomers and the top PLS-DA ranked feature is toluene which appears to fluctuate.

The evolution patterns of three compounds o-xylene, phenol and naphthalene, that are commonly used in pyrolysis modelling studies, including phenanthrene, were also monitored in order to study similarities of their behaviour between different experiments. These are presented in Figure 5.22. Phenanthrene was not detected using GC-MS in the samples from TOPS8 so its pattern is not included in the corresponding figure.

The patterns corresponding to o-xylene shows that the compound's levels are stable through-

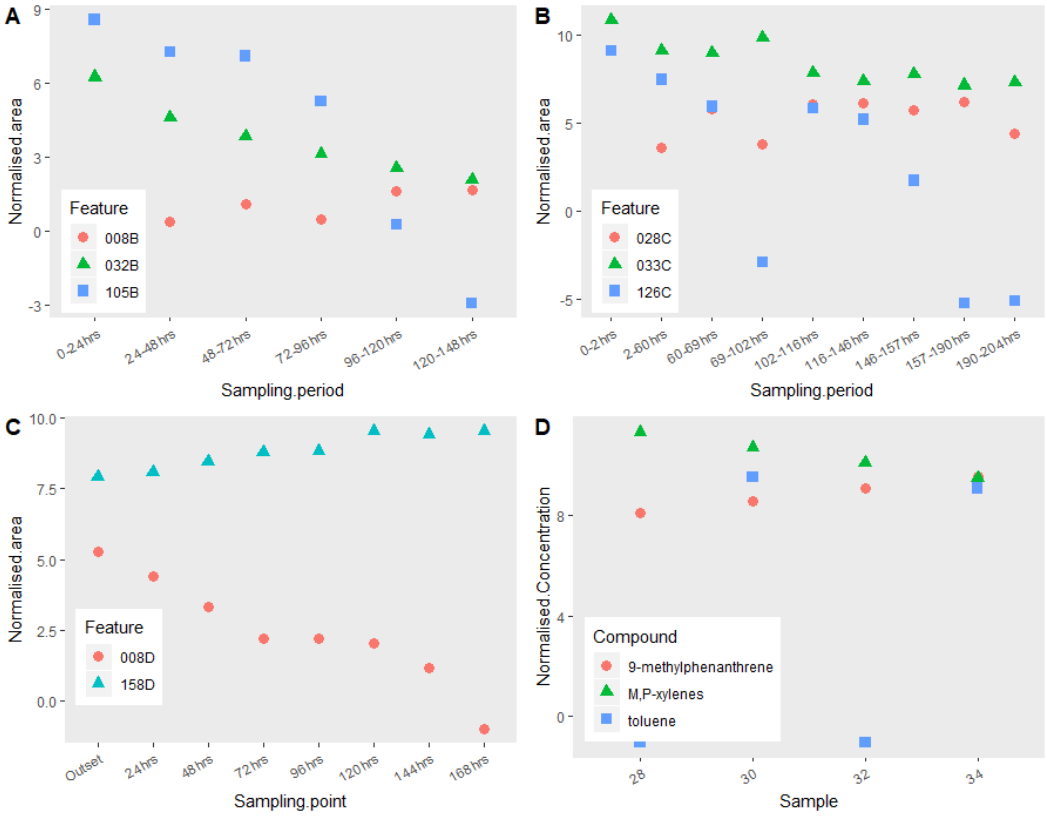

Figure 5.21: Evolution pattern plots of the top first features for positive and negative correlation with gasification time including the top first feature with the highest VIP score. **A:** TOPS1, **B:** TOPS8, **C:** Barbara II, **D:** Hanna IVB. Top positive correlations: TOPS1-008B, TOPS8-028C, Barbara II-158D, Hanna IVB-benz[a]anthracene; top negative correlations: TOPS1-032B, TOPS8-033C, Barbara II-008D, Hanna IVB-1,2,3-trimethylbenzene; top PLS-DA VIP: TOPS1-105B, TOPS8-126C, Barbara II-008D Hanna IVB-undecane

out the course of the experiments except than Hanna IVB where it is dropping. The patterns corresponding to phenol also do not have significant similarities. Interestingly, o-xylene and phenol appear having a similar behaviour in the Hanna IVB experiment (dropping). Apart from the aforementioned compounds another notable behaviour is that of naphthalene and phenanthrene in the Barbara II experiment. Naphthalene levels in the tar appear to slowly drop while phenanthrene levels increase but it does not appear that any of these compounds have a consistent time-wise behaviour. Regardless, stable levels through time may indicate a steady production which may be the case in some of the patterns e.g o-xylene. This would indicate that the compound is being constantly produced/devolatilised during gasification.

5.3.7 GCxGC-TOFMS effluent imaging

Samples from TOPS1, TOPS8 and the Barbara II experiment were also analysed using the GCxGC-TOFMS technique. The two-dimensional chromatograms were collated together in order to visualise the content of SVOCs in the samples during the experiment. Pie plots are

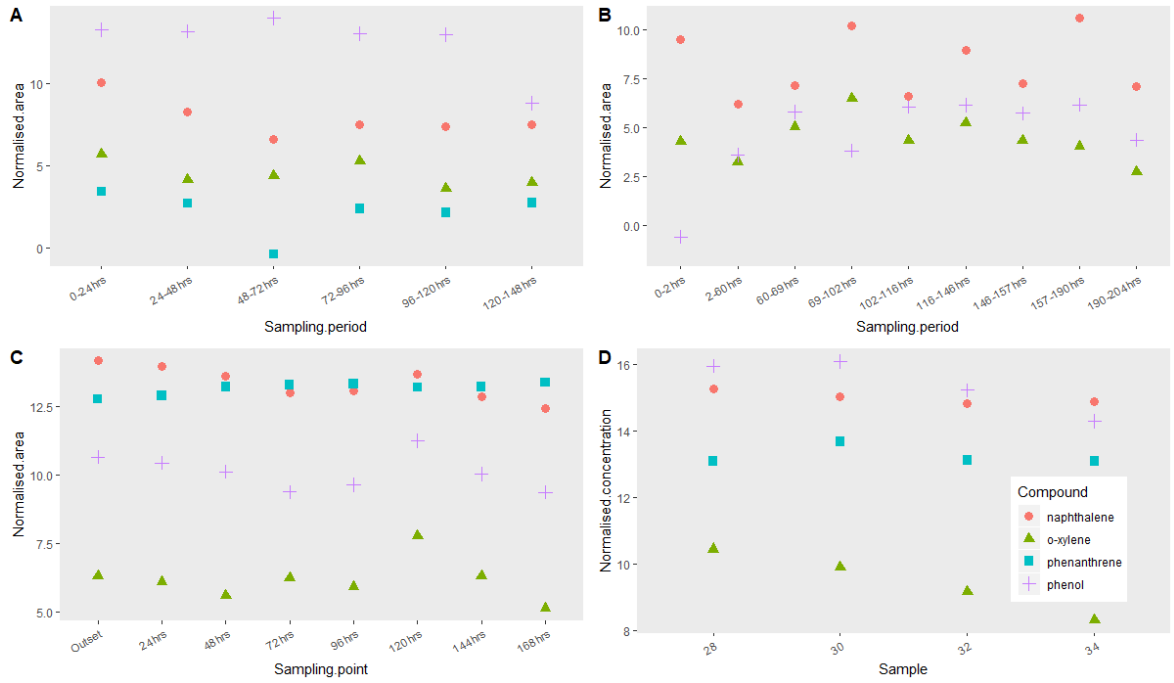

Figure 5.22: Evolution patterns of specific compounds that are usually included in pyrolysis studies. **A:** TOPS1, **B:** TOPS8, **C:** Barbara II, **D:** Hanna IVB. Phenanthrene was not detected in TOPS8 with GC-MS. The legend in **D** applies to all figures

attached to each plot that indicate the percentage of mid-high polarity compounds and low polarity compounds in the case of waste-water and aliphatics and aromatics in the case of UCG coal tar. Polarity was chosen to differentiate major groups in waste-water since this is what governs separation in the second dimension. Regarding tar, aliphatics and aromatics are two groups that are clearly defined, and this separation may also provide information regarding gasification conditions (Section 2.3.2 & 2.3.3).

Two dimensional GCxGC-TOFMS plots that provides imaging of the SVOC content for the TOPS1 experiment can be seen in Figure 5.23. For each image the total number of peaks and the total area are also given to quantitatively indicate the total SVOC load of each sample.

By studying Figure 5.23 one can see that the percentage of mid-hi and low polarity compounds is between 11-13% in most of the samples except sample 3 and sample 6 (Figure 5.233 and 6). Sample 3 corresponds to the period of the highest SVOC production as indicated by the total peak area. Sample 6 corresponds to the period near the end of the gasification experiment. It is clear, both by looking at the bubble plot and the pie chart that during this period the amount of high polarity compounds is significantly reduced. Also the amount of late eluting low polarity compounds also appears reduced. This may mark the period where most of the volatile content of the coal in the reactor is reduced and the increase in late eluters may be attributed to an increase in aromatisation reactions.

Figure 5.24 provides bubble plots and corresponding pie charts for the TOPS8 experiment.

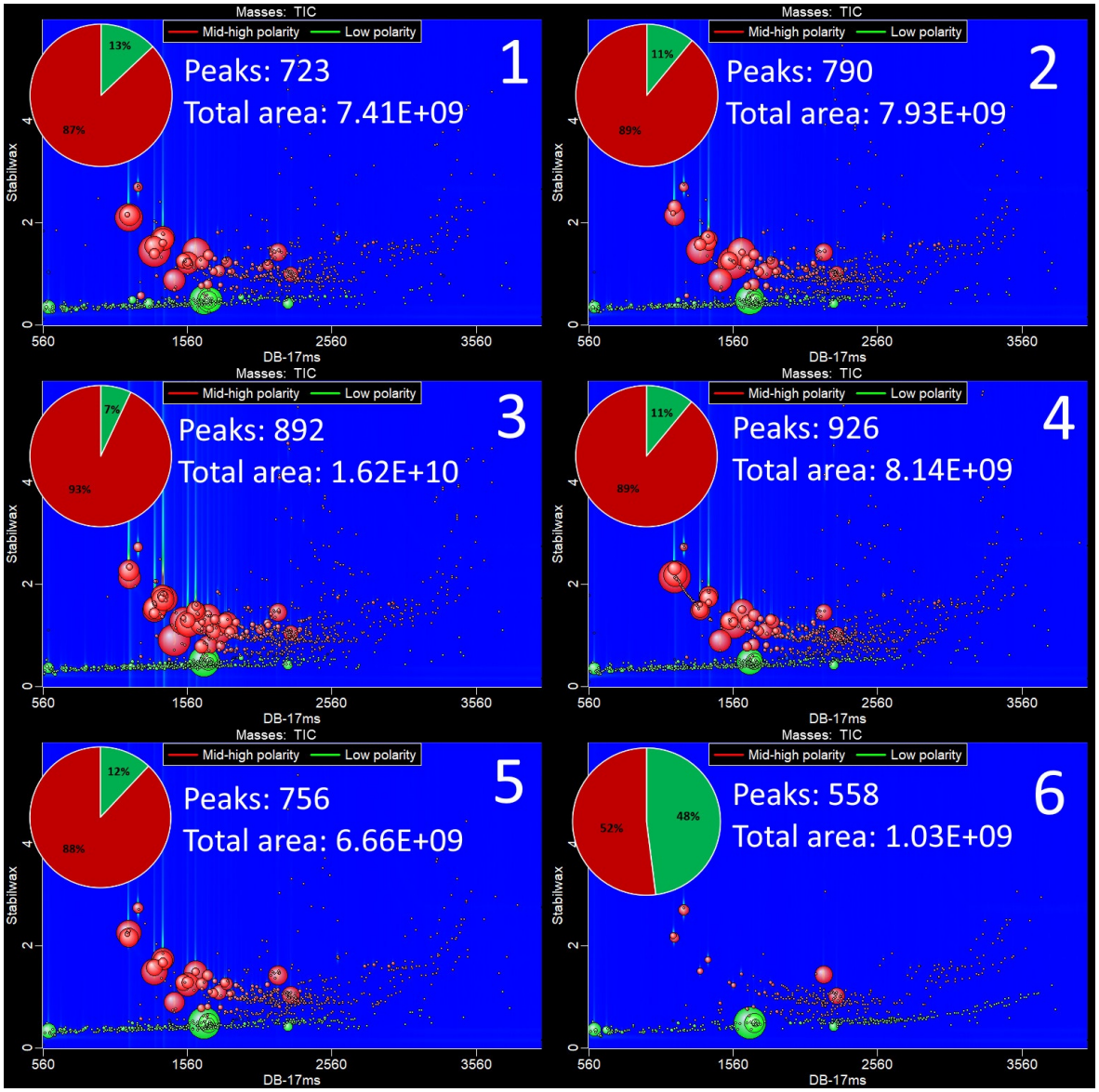

Figure 5.23: Bubble plots depicting visually the amount of high polarity compounds (red) and low polarity compounds (green) in the TOPS1 experiment. Size of the bubbles is Each plot is accompanied by a pie plot that is attached on the top left corner of each plot. The values of identified peaks and total peak area are also provided. Plots are numbered in time order according to their sampling periods during the gasification experiment. All plots are plotted in the same scale in all axes.

For the first 4 sampling periods the amount of high polarity compounds in the samples is increasing with a corresponding increase in total peak area. However, this is not the case for the last 5 samples where the corresponding amounts are fluctuating with no obvious pattern apart from the fact that the amount of high polarity compounds is lower than those during the first 4 periods.

Regarding the Barbara II experiment and tar samples, the corresponding GCxGC-TOFMS analysis can be seen in Figure 5.25. The GCxGC setup for tar analysis is different to that for

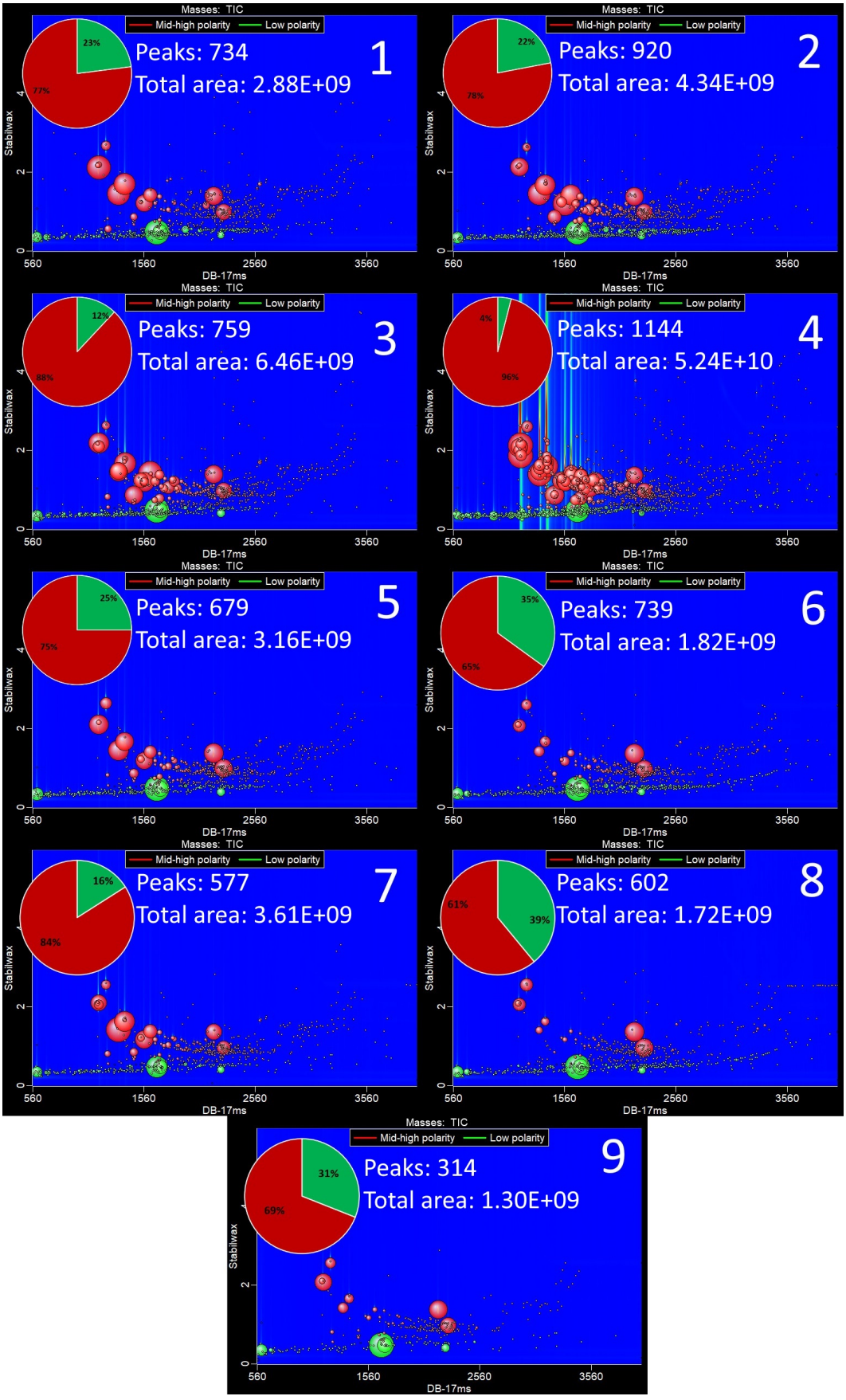

Figure 5.24: Bubble plots depicting visually the amount of high polarity compounds (red) and low polarity compounds (green) in the TOPS8 experiment. Size of the bubbles is Each plot is accompanied by a pie plot that is attached on the top left corner of each plot. Plot are numbered in time order according to their sampling periods during the gasification experiment. All plots are plotted in the same scale in all axes.

waste-water analysis; a reverse phase set-up is used for tar and a normal-polar phase setup for waste-water. Consecutively, the areas of the two dimensional chromatograms correspond to groups of different chemical properties. The two major groups that can be distinguished in the chromatogram is aliphatic (red) and aromatic compounds (green). The percentage of each on the groups is calculated by summing the areas of the peaks that correspond to each group and dividing by the total area of the chromatogram.

One can see that for the first 5 samples the percentages of aliphatics and aromatics remain relatively stable (Figure 5.251-5). However, there is a sudden increase in the percentage of aliphatics in sample 6. Although at first this change appears to be small regarding the percentage increase (which is around 1%) it is noticeable as can be seen by the bubble plot in Figure 5.25-6. This sudden change in composition is also visible in the heatmap generated from GC-MS data as seen in Figure 5.15C. During the same period there is also a noticeable increase in the total peak area.

Composition extraction from the 2D GCxGC data for coal tars is not limited only to major groups but it can also provide more specific information regarding other groups as well. Figure 5.26 shows the percentage of major groups in the tar samples which are monoaromatics, diaroamatics and polyaromatics. By studying the figure, it becomes obvious that there is a major change in the composition of the tar effluent taking place during the 6th sampling point. In this point the amount of monoaromatics increased along with the amount of diaromatics, while polyaromatics decreased. Looking at the composition of samples 1 to 5 it appears that the effluent composition is stabilising but suddenly changes with sample 6.

Figure 5.27 reveals a similar picture although the percentages of these classes in total sample composition is very small. Specifically, it appears that the percentage of all alkanes (alkanes, isoalkanes and cycloalkanes) is increased in sample 6, something which as mentioned above can also be seen by studying the bubbleplots in Figure 5.25. However, percent changes illustrated here are small and cannot be considered as significant as major group changes.

Figure 5.28 shows two radar plots that correspond to the total area of C10 to C34 n-alkanes (5.28A) and the percentage of an n-alkane in the total n-alkane area for each sample (5.28B). Both figures refer to the Barbara II trial. Regarding the comparison of alkanes by area per alkane it is clearly seen in Figure (5.28A) that more alkanes are produced after 120hrs of gasification for which the total amount is decreasing as the gasification progresses from that point to the end. However, regarding the previous samples it can be seen that the number of n-alkanes is slightly increasing with time from the beginning of the gasification. It can be seen that at the beginning of the gasification the n-alkanes are lighter with C14 having the highest percentage and the n-alkanes gradually become heavier with samples that correspond to 48,72 and 96hrs showing a decrease in the lighter n-alkanes and an increase in the heavier n-alkanes (>C23) (Figure 5.28B). Interestingly, after 120hrs the alkanes C17-C19 have the

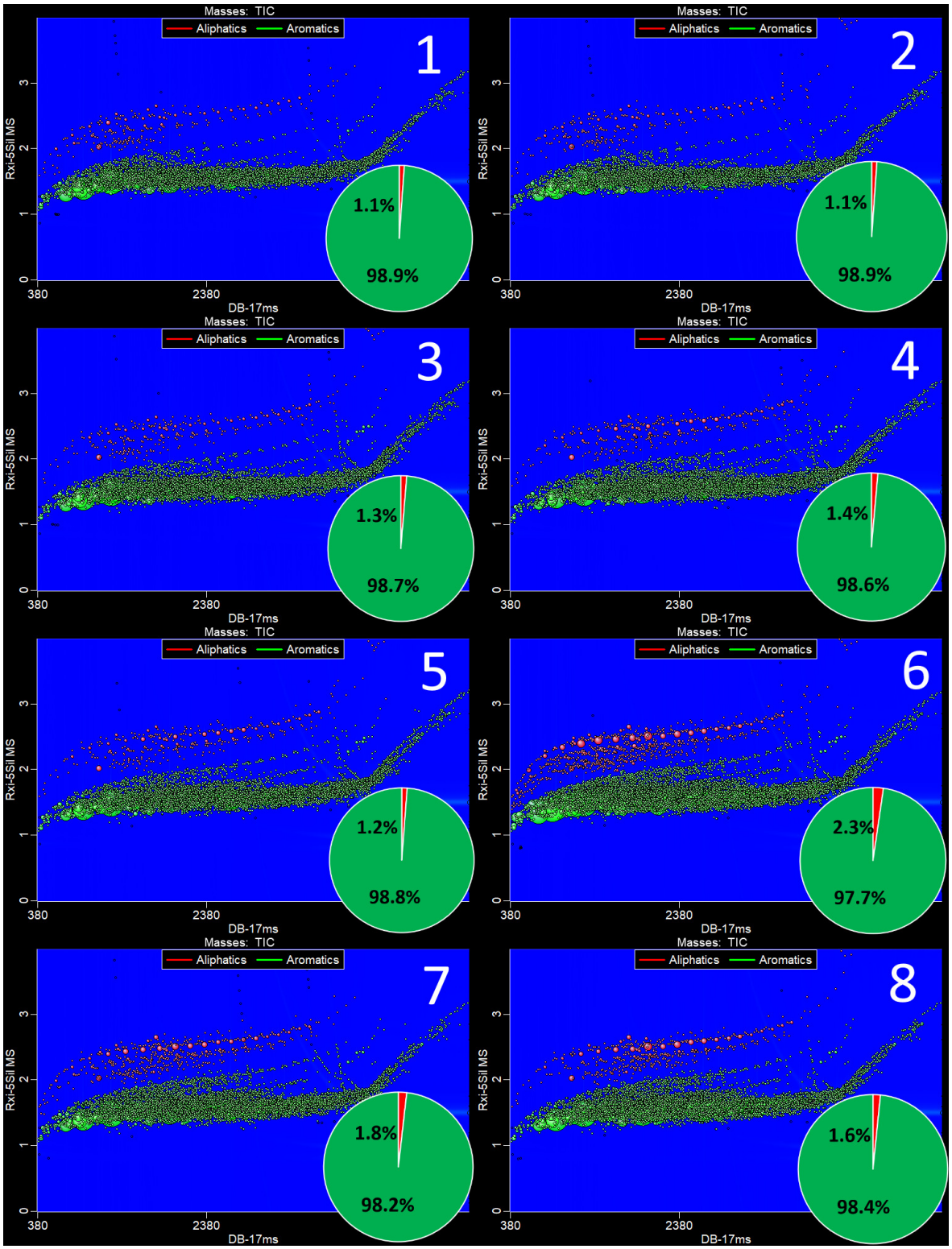

Figure 5.25: Bubble plots depicting visually the amount of aliphatics (red) and aromatics (green) in the Barbara II experiment. The size of the bubbles is proportionate to the area of each peak. Each plot is accompanied by a pie plot that is attached on the top left corner of each plot. Plot are numbered in time order according to their sampling periods during the gasification experiment. All plots are plotted in the same scale in all axes.

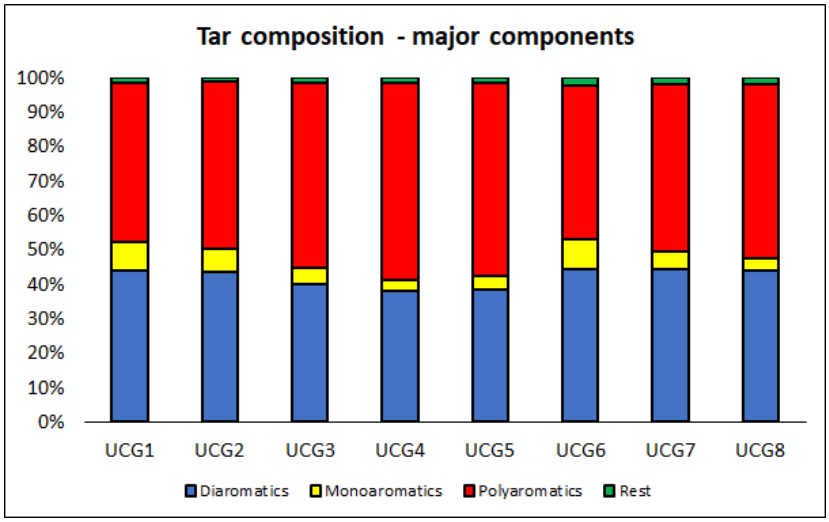

Figure 5.26: Percent stacked barplot depicting the percentage of the major groups in tar analysed with GCxGC-TOFMS. It is obvious from the graph that polyaromatics are slowly increasing and monoaromatics with diaromatics are decreasing until the 5th time point. A sudden increase in the percentage of diaromatics and monoaromatics is observed at the 6th time point.

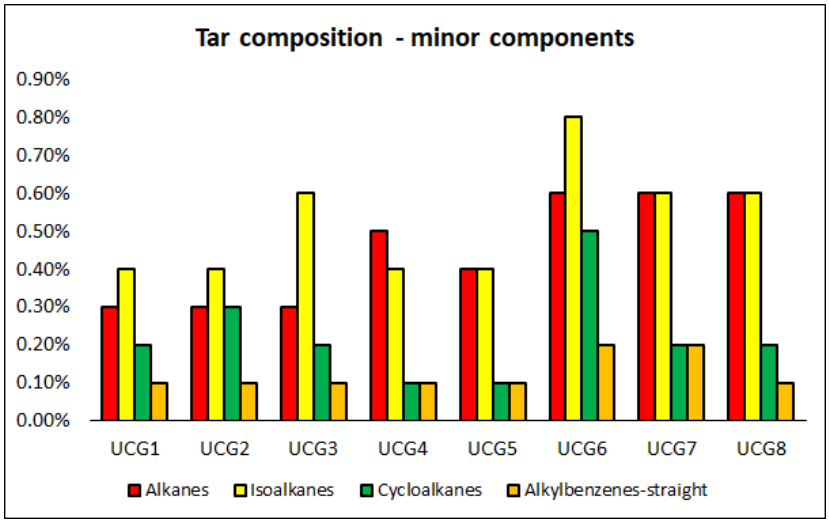

Figure 5.27: Barplot depicting the percentage of the minor components in the coal tar samples for the specific time points. As it appears alkanes, isoalkanes and cycloalkanes are relatively stable or fluctuating for the first 5 but appear to peak in the 6th time point

highest percentage in the samples with n-alkanes above C23 having a lower percentage than those seen at previous samples.

The behaviour of n-alkylbenzenes during the Barbara II trial is shown in Figure 5.29, with Figure 5.29A showing a radar plot to compare the area of n-alkylbenzenes (starting from C2 to C25) and Figure 5.29B showing the percentage differences between the n-alkylbenzenes. The area of n-alkylbenzenes is larger after 120hrs of gasification very similar to that of the n-alkanes. With C6-alkylbenzene showing the largest area for the first 5 samples and C6-

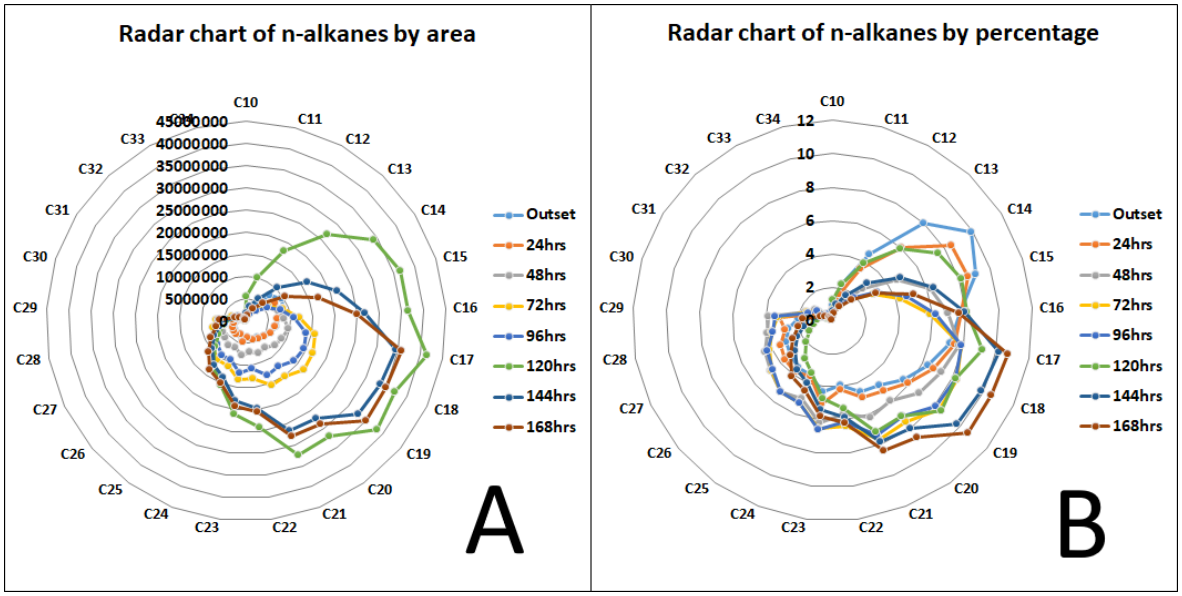

Figure 5.28: Barplot depicting the percentage of the minor components in the coal tar samples for the specific time points. As it appears alkanes, isoalkanes and cycloalkanes are relatively stable or fluctuating for the first 5 but appear to peak in the 6th time point

alkylbenzene showing the largest area for the last 3 samples. This becomes more obvious by studying the percentage differences; as can be seen in Figure 5.29B C6-alkylbenzene starts at a high percentage during the beginning of the gasification and gets lower as the gasification progresses. This is observed for the first 5 samples. After sample 6 and onwards, C8-alkylbenzene is the alkylbenzene with the highest percentage however in samples 7 and 8 the percentage of heavier n-alkylbenzenes becomes higher.

All of the above evidence indicate an event taking place close to the 6th sampling point. The changes that appear during the 6th sampling point are possibly associated with what is being described in the corresponding experiment[143] as a loss of tightness in the gasification cavity and detection of syngas in the mine galleries. This indicates that after effects of this event are seen in the signature of the coal tar. This becomes more visible by studying the GCxGC-TOFMS chromatograms as subsequent frames (Figure 5.30) where an increase in peaks and intensity in the areas associated with alkanes is visible after sample no 6.

5.4 Conclusions

Combined analysis of samples from all the available UCG trials but also from combined data from a literature source showed that there may be some global indicators that have persistent behaviour during a UCG trial. Evidence presented above suggest that this may be true for benzonitrile, C1-cyclopentanone, C1-pyridine, indole and dimethylbenzofurans. This would, of course, require further verification since all the studied UCG trials were

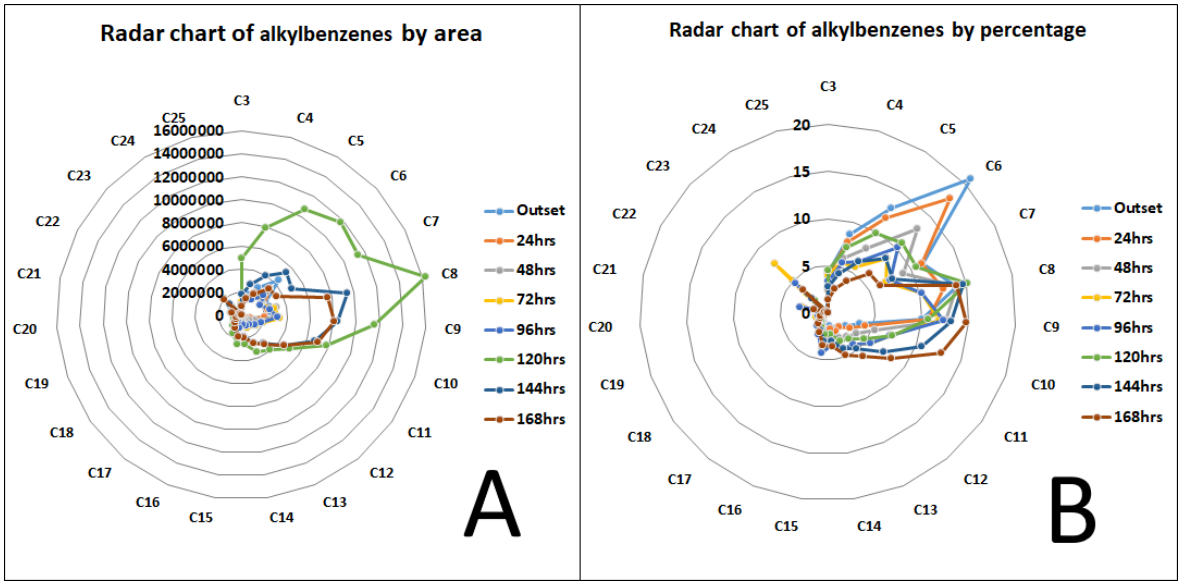

Figure 5.29: Barplot depicting the percentage of the minor components in the coal tar samples for the specific time points. As it appears alkanes, isoalkanes and cycloalkanes are relatively stable or fluctuating for the first 5 but appear to peak in the 6th time point

performed only once with no replication. However, the production trends of compounds that are usually used as representative, such as phenol and naphthalene, was found not to be consistently time-wise positive or negative correlated with time during the trials. However, a continuous steady pattern as seen in some of the experiments may indicate continuous and steady production. Overall, the compounds showed above as having a persistent behaviour throughout trials are limited to those that performed the best in a series of metrics defined by the author. This does not mean that there are no other compounds that may be more representative of a UCG process or that future trials will not contradict the present evidence. Yet, to the author's knowledge this was the first application of an untargeted exploratory statistical approach to the analysis of the SVOC content from time-series sampled secondary effluents from UCG.

By studying SVOC data from the Barbara II trial there is evidence showing that the composition of the tar changed significantly in samples corresponding to the late gasification period (samples taken at 120, 144 and 168hrs). Generally, there appears to be an increase in the overall SVOC content of the tar, with alkanes being one of the compound groups that are seen to have their percentage increase but also other groups such as the polyaromatics that were seen to decrease. Although these effects are expected to be exaggerated when normalising and autoscaling (which is the case in the heatmaps produced from GC-MS data) we can conclude that these changes may be caused by an abrupt change in the gasification process. The fact that abrupt changes in a UCG burn are reflected in the coal tar content further indicates that coal tar is a sample representative of the UCG process that if taken in frequent intervals it can be used as a historical record for each UCG burn.

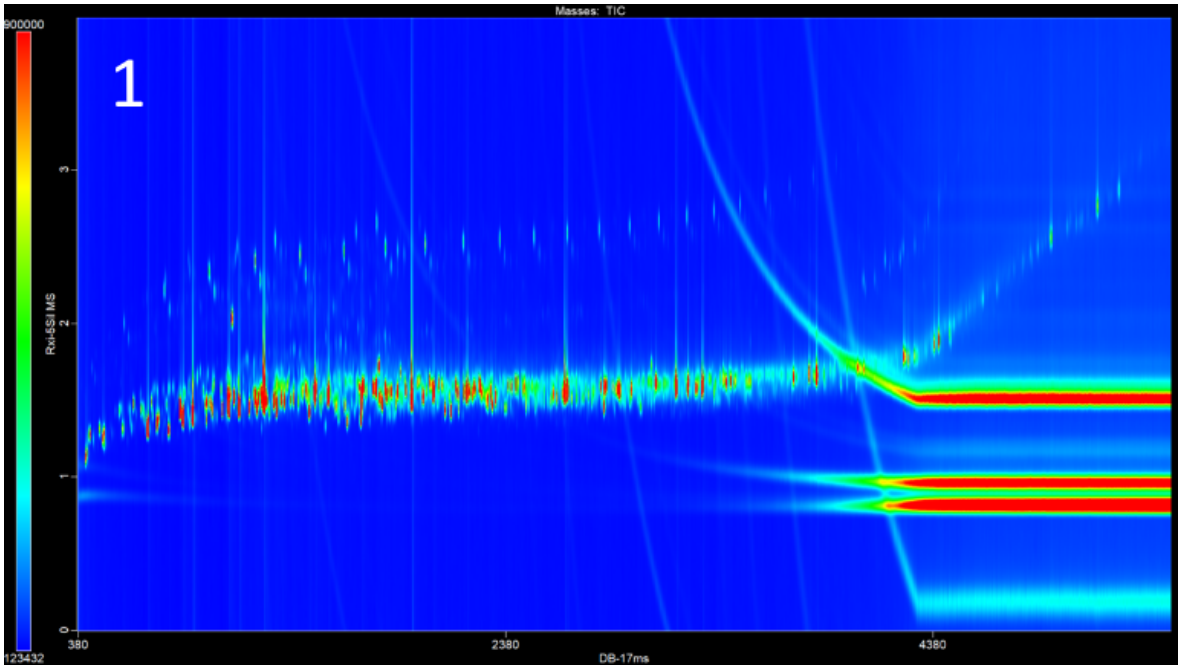

Figure 5.30: Click the image to play. This video works only on Adobe Acrobat Reader (https://get.adobe.com/uk/reader/) and the electronic version of the thesis

Cumulatively, it can be assumed from the analysis of the samples originating both from TOPS1 and TOPS8 but also from the Barbara mine that coal tar may be more representative than waste-water, and it is suggested as the primary effluent to assess SVOC production during UCG. This does not derive only from the results presented above which show that tar samples carry more information but also from the fact that, as mentioned earlier, an upper limit in the solubility of most SVOCs in waste-water is expected. Regardless, waste-water analysis is invaluable in terms of assessing its content for retrieval of components of high economic value but also for process risk assessment, treatment strategies and environmental impacts assessment. However, the sampling issues that accompany coal tar must be taken into consideration as it is challenging to combine tar sampling with fast and efficient syngas cleaning in *ex-situ* UCG experiments.

The previously developed methods for the analysis of waste-water and tar in Chapters 3 and 4 respectively, were applied in this chapter in the analysis of actual samples collected from 2 *in-situ* and one *ex-situ* UCG trials. Results show that both methods and the untargeted data analysis pipeline are efficient for this type of samples, all the way from sample preparation to data analysis and to representative compound suggestion. Overall, the suggested methodologies are fit-for-purpose in identifying both trends and compounds representative of these trends. The precision of the sample preparation methods was proven not only by using traditional chemical analysis metrics such as the RSD of surrogates between samples but also using PLS-DA loadings where the surrogates were shown to cluster within a small area of the loadings plot around the 0,0 point. As shown above, further sample analysis (using a

technique as GC-MS or GCxGC-TOFMS) is expected to provide information that is linked almost exclusively to the SVOC composition of each sample, providing a fast and effective way to analyse secondary effluents not only from an Underground Coal Gasification trial but from other coal conversion processes as well.

Chapter 6

Enhanced SVOC analysis of UCG secondary effluents by means of ultrasonication assisted derivatisation

6.1 Introduction

As detailed in previous chapters, secondary effluents from coal gasification are very complex samples that include a diverse range of SVOCs. UCG produced waste-water, as shown in Chapter 6 includes a large number of mid to high polar compounds. This is expected since SVOCs need to have at least a small degree of polarity in order to be soluble in water. Overall, the compounds that are dissolved in UCG waste-water range from low-polarity to very high polarity, for example, pyrene which can be found in UCG waste-water is relatively unpolar while dimethylhydantoins which can also be found in gasification waste-water are very polar, and as shown in Chapter 3, very difficult to extract using LLE. Some of the polar compounds that can be found in UCG secondary effluents have a labile hydrogen such as phenols, organic acids such as benzoic acid but also nitrogen and sulphur containing compounds such as indoles.

While most of the aforementioned compounds can be analysed with gas chromatography, chromatographic separation can be challenging especially with polar compounds such as phenols since the high affinity/reactivity of these compounds with GC stationary phases may create adverse chromatographic effects such as bad peak symmetry and may also affect resolution and sensitivity. Also, the relative low volatility of some of the heavier and more polar phenols further hinders chromatography, limiting the amount of phenols that can be

analysed by gas chromatography. Consecutively, these limitations also affect the amount of produced results. These issues may be resolved by transforming phenols into trimethylsilyl ethers and esters, which are more volatile, more thermally stable and less reactive than their non-silylated counterparts and, thus, have much better chromatographic properties.

To the author's knowledge there are no reports in the literature that describe methods for derivatising samples from UCG, however there are available methods that refer to the derivatisation of samples deriving from coal gasification. Gauchotte-Lindsay *et al.* [111] applied a design of experiments approach to develop a method for the derivatisation of coal tar ASE extracts from FGMP sites. The study included the application of a Circumscribed Central Composite (CCC) design with three factors: temperature, time and reagent (N,N-bis(trimethylsilyl)-trifluoroacadetamide (BSTFA) & 1% trimethylchlorosilane (TMCS)) concentration ratio to tar. Optimised conditions suggested by the method are: 60°C for 60 min after adding equal amounts of sample and BSTFA. The study resulted in the total increase of the detected phenols for the same samples when analysed with no derivatisation. Recently, Gallacher *et al.* [115] reported a similar derivatisation method using BSTFA with 1% TMCS and placing the sample in an oven at 70 °C for 60 min. This study specifically mentions that sterically hindered phenols such as 2,4,6-trimethylphenol cannot be derivatised and the same is expected to apply for both previously mentioned methods since the derivatisation conditions are practically identical.

Silylation can be used with any compound that has a labile hydrogen such as acids, alcohols, amines, and amide groups. This is done by displacement of the active proton in the -OH, -SH and -NH groups. The most common reagents for silylation is BSFTA and BSA (bis(trimethylsilyl)acetamide) whereas a general reaction would be [164,165]:

$$R_3Si-X + R'-H \longrightarrow R_3Si-R' + HX$$

Mechanistically, the reactions is considered a nucleophilic attack (or S_{N2}) where the electronegative heteroatom acts upon the silicon atom to produce a bimolecular transition state (Figure 6.1). The basicity of the leaving group (X) must be high enough and exceed that of the -Y group so that the negative charge is stabilised and the reaction is drawn to completion. For more information on the theoretical aspects of silylation the reader is referred to the work of Pierce [164].

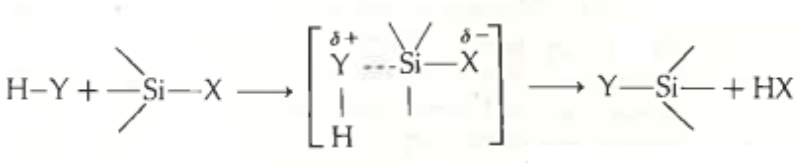

Figure 6.1: Sylilation mechanism depicting the nucleophilic attack from the -Y group to the silicon atom. Copied from Pierce [164]

An example of the compounds in UCG secondary effluents that may undergo derivatisation

is provided in Figure 6.2. The large majority of derivatisable compounds are expected to be phenolic such as phenol and catechol, but organic acids are also expected to be found along with nitrogen heterocycles and possibly thiols. Whether all of the possible compounds will be derivatised heavily depends on the derivatisation method.

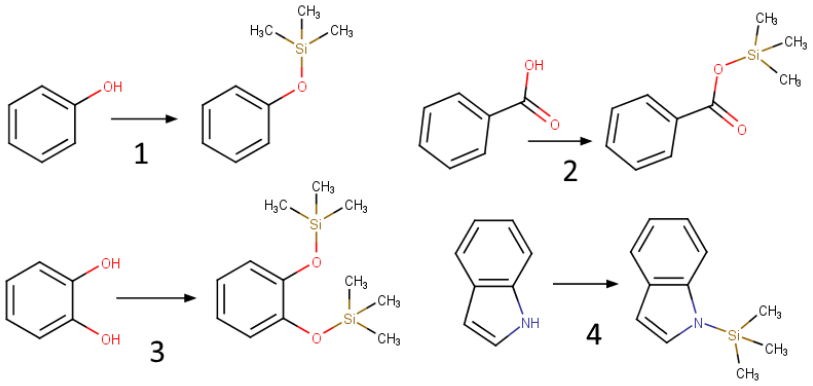

Figure 6.2: Examples of compounds with a functional group that contains a labile hydrogen and can undergo silylation. **1:** Phenol **2:** Benzoic acid **3:** Catechol **4:** Indole

The ease of silylation generally is associated with each functional group with the following order (easier to harder): alcohol > phenol > carboxylic acid > amine > amide. However, functional groups are not the only factors that can affect reactivity but also other factors such as steric hindrance also have a significant role. For example the reactivity in the case of alcohols follows the order: primary > secondary > tertiary[166]. A reported example of a sterically hindered phenol is 2,4,6-trimethylphenol, which was unable to derivatise with the previously mentioned method[115]. Similarly sterically hindered phenols would be 2,6-Di-tert-butyl-4-methylphenol or butylated hydroxytoluene (BHT - figure 6.3).

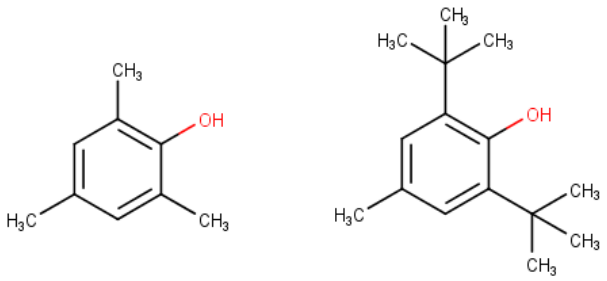

Figure 6.3: Sterically hindered phenols. **Left:** 2,4,6-trimethylphenol **Right:** butylated hydroxytoluene

As mentioned in previous chapters the use of ultrasonication in analytical chemistry has been studied extensively during the past two decades as it offers several benefits in the analytical process, especially during the sample preparation stage[71,72,167]. One of the most

interesting applications of ultrasonication is in analytical derivatisation, which can be basically considered as an application of sonochemistry[168]. A review from Delgado-Povedano and Luque de Castro[72] discusses several applications of ultrasonication to derivatisation for both discontinuous and continuous approaches. In particular, the potential of ultrasonication is demonstrated in a method reported from Orozco-Solano *et al.*[169] regarding the analysis of sterols and fatty alcohols where the process of leaching, saponification and derivatisation is reduced from 26h to 75min. Also a method reported from Sánchez Ávila *et al.*[170] on the analysis of triterpenic compounds demonstrates that the application of ultrasonication may reduce the time needed to silylate the triterpenic compounds from 3 and half hours to 5mins. Similar results are reported by Liu *et al.*[171] in the profiling of biological metabolites where the methoxymation and silylation time was reduced from a total of 20h to just 30min.

This chapter describes the development of a rapid derivatisation method for UCG related effluents. The method describes the use a novel ultrasonication system for use with very small vessels along with rapid derivatisation technique developed for the exhaustive derivatisation and analysis of even sterically hindered phenols. Further focus is given to the application of the developed derivatisation method in actual samples, including investigating the enhancements that the method can provide in the analysis of new compounds in the waste-water and tar samples. The method was applied to both waste-water and tar samples.

6.2 Materials and methods

6.2.1 Chemicals

Chemicals used in the chapter for preliminary experiments and the optimisation of ultrasonication assisted derivatisation (UAD) development are listed as follows: Cyclopentylmethylether, 4-fluorophenol and 4-bromo-2,6-dimethylphenol purchased from Alpha Aesar (Heysham, UK). BSTFA with 1% TMCS was purchased from Thermo Scientific. Pyridine, toluene, phenol, pyrocatechol, 2,4,6-trimethylphenol, naphthol, o-cresol, p-cresol and 2-methylnaphthalene purchased from Sigma Aldrich. Additional chemicals used for repeatability and in-matrix derivatisation evaluation experiments are listed as follows: phenol-4-tert-octyl, 1-acenaphthenol, 9-hydroyxyfluorene, 9-phenanthrol, 9-antracenemethanol, 1-hydoxypyrene, phenol-d6, naphthalene-d8, phenanthrene-d10, 4-fluoro-2-methylpyridine, 1-fluorododecane, 1-fluoronaphthalene, 5-fluoroindole, fluorene-d10, 1-bromo-2-naphthol, chrysene-d12, 2,4,6-trimethylphenol-d11. The real samples that were derivatised were composites of the samples of each UCG trial time series with the same volumes added from each sample when preparing the composite. Composites are used as a representative sample for the entire experiment as they contain all of the compounds per experiment.

6.2.2 Instrumental

6.2.2.1 HIVS

A UP200St ultrasonic processor with VialTweeter (S26d10x10VialT) and an attached vial press (UP200xt) (Hielscher Ultrasonics GmbH, Teltow, Germany) was used for sample sonication during UAD with the 0.3mL vials attached as show in Figure6.4 (more information can be found on the manufacturer's website[92]).

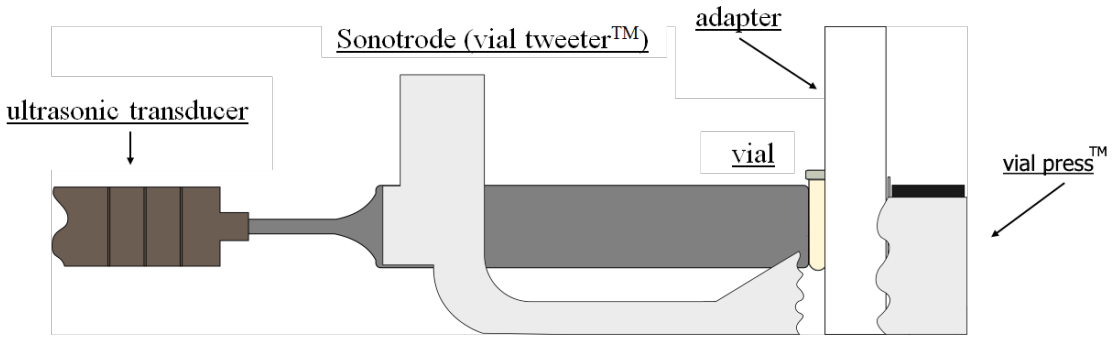

Figure 6.4: Hielscher VialTweeter™sonotrode system with the attached vial press used for sample sonication. Set-up for the sonication of micro-size sample vessels. Image ©*Ioannis Sampsonidis*

6.2.2.2 GC-FID

Gas chromatographic analysis for preliminary experiments and sonication optimisation was performed on an Agilent 7890B gas chromatograph with an flame ionisation detector (FID) equipped with a phenyl arylene polymer DB-5 30m*0.250mm*0.25um column (J&W Scientific). The following temperature program was used: 13°C/min from 80°C (which was maintained for 5min) to 125°C (which was maintained for 5min), then 40°C/min to 250°C (which was maintained for 3min). Split ratio was 1:10 except the case of actual UAD development where a ratio of 1:350 was used, inlet temperature was 250°C and injection volume was 1μL in all cases.

6.2.2.3 GC-MS and GCxGC-TOFMS

Gas chromatographic analysis for stability, repeatability and in-matrix derivatisation evaluation was performed on an Agilent 7890A gas chromatograph coupled to a 5975C mass spectrometer. The system was equipped with a 60m*0.25mm*0.25um (50%-Phenyl)-methylpolysiloxane phase DB-17MS column. For the stability and repeatability study the following conditions were used: initial temperature 70°C (hold for 0.2min) then 3.5°C/min to 320°C.

Inlet temperature was held at 250°C, transferline temperature at 260°C, MS source at 230°C and quad temperature at 150°C. Injection volume was 1uL, split ratio 1:40 and the column flow was held stable at 1.4mL/min. For the in-matrix derivatisation evaluation the intial temperature was set at 70°C (hold for 0.2min) then to 220°C at 10°C/min then to 320 °C at 60°C/min (hold for 24min). Inlet temperature was held at 250°C, transferline temperature at 260°C, MS source at 230°C and quad temperature at 150°C. Injection volume was 1uL, split ratio 1:200 and the column flow was held stable at 1.4mL/min. For the parameters of the SIM method used for the analysis and parameters for the GCxGC-TOFMS analysis the reader is referred to Section 3.2 and Section 4.2. All samples were analysed for the presence 2,4,6-trimethylphenol-d11 and 2,4,6-trimethylphenol-d11-TMS using AMDIS with no filters and the most sensitive settings.

6.2.3 Derivatisation study

Derivatisation of UCG samples aims primarily at phenols which, as reported above, are some of the most abundant compounds found in UCG secondary effluents. Since the number of different phenols in coal tar samples can be very large, derivatisation optimisation can either be performed on a real sample by using a surrogate and monitoring its recovery or by optimising the process for a single phenol which should be harder to derivatise than the other phenols in the sample, so that when it is completely derivatised, the rest of the phenols would have been derivatised as well. Here, the second approach was used. The phenol considered for 2,4,6-trimethylphenol which is sterically hindered (Figure 6.3).

6.2.3.1 Initial factor screening for UAD

The effect that catalysts have on silylation was initially reviewed by Pierce [164] and, specifically in the case of pyridine, it is reported by Orata [172] and Kumirska *et al.* [173]. The suggested mechanism of the catalytic action of pyridine is that it acts as a hydrogen scavenger by reacting with the labile hydrogen during the bimolecular transition stage (Figure 6.1), thus driving the reaction forward.

In order to verify the catalytic effect of pyridine and to perform an initial investigation of the effect of other sonication parameters in order to define a proper experimental area, a screening experiment was designed following a design of experiments approach (DOE), that is described in chapter 3, using Minitab® [174] and a Plackett-Burman design. The effect of solvent, sonication time, sonication amplitude and addition of pyridine was investigated. CPME was compared with toluene in order to test for any negative effects that CPME may have in comparison with a common extraction solvent such as toluene. The experimental design for this study can be seen in Table 6.1. All the runs were created with Minitab®

and were randomised. For this experiment two solutions were prepared: 20ppm of 2,4,6-trimethylphenol and 1-methylnaphthalene in CPME and in toluene. The ratio of 8:1:1 sample:pyridine:BSTFA was used for each run that included pyridine. For runs with no pyridine the ratio 8:1:1 sample:solvent:BSTFA was used. Samples from each run were analysed using the GC-FID immediately after each run.

Table 6.1: Design used for derivitisation factor screening

RunOrder	Time [min]	Solvent	Pyridine	Amplitude [%]
1	0.5	CPME	Yes	40
2	0.5	Toluene	Yes	40
3	0.5	Toluene	No	40
4	0.5	CPME	Yes	60
5	1.5	Toluene	No	40
6	1.5	Toluene	Yes	60
7	1.5	CPME	No	60
8	1.5	CPME	Yes	40
9	0.5	Toluene	No	60
10	1.5	Toluene	Yes	60
11	0.5	CPME	No	60
12	1.5	CPME	No	40

6.2.3.2 Illustration of the effect of steric hindrance on derivatisation

In order to better illustrate the effect of steric hindrance, a simple experiment was devised: a 20ppm mix (A1) in CPME of 2,4,6-trimethylphenol along with 5 other phenols: phenol, 4-fluorophenol, pyrocatechol, 4-bromo-2,6-dimethylphenol and naphtol with 2-methylnaphthalene as an internal standard was prepared. A fast gas chromatography method was developed for separating the 6 phenols and the internal standard. 160μL of mixture A1 were transfer in a 300μL round bottom crimp cap glass vial and 20μL of pyridine and BSTFA (ratio of sample:pyridine:BSTFA of 8:1:1) were added and the vial was vigorously mixed at 3000rpm for 10 seconds. A 1μL volume of A1 was injected into the gas chromatograph, once at the beginning of the reaction, 20 minutes after reaction initiation and approx. every 20 minutes afterwards (12 injections in total). This experiment was performed in triplicate. This experiment provides data for product yields between reaction initiation and the first and second injections after 20 and 40 minutes, and this proved not to have enough resolution (time-wise) for some compounds, in order to obtain more information on yields in smaller reaction times, the reaction was performed 7 additional times and injections were made at 2, 5, 10, 15, 20, 25 and 35 minutes.

6.2.3.3 Sonication condition optimisation for aliquots from UCG samples

Considering the results from the first DOE study described above, a new DOE study was designed with a wider selection of factor levels and more representative UCG phenol concentrations. In order to proceed with such a design several assumptions had to be made. These assumptions have to do mostly with the concentration of phenols in the UCG samples and whether the method is able to successfully derivatise to completion all phenols inside these samples. After reviewing relevant UCG literature and initial phenol analysis data for UCG waste-water samples coming from the GIG a total concentration of phenolics of 3500 mg/l in the block reactor experiment waste-water was assumed. Assuming an enrichment factor of 30 and 100% extraction efficiency during waste-water extraction, a final aliquot may have up to 105,000 mg/L of phenolics. A simulated waste-water extract was prepared with a mixture of 6 phenols: three phenols that are commonly found in UCG waste-water, phenol, o-cresol and p-cresol, 4-fluorophenol and 2-bromo-4,6-dimethylphenol to further increase the total phenolic content of the mixture and, lastly, 2,4,6-trimethylphenol as the phenol to be derivatised harder, all in a concentration of 17,500 mg/L. The reagent ratio was sample:pyridine:BSTFA 1:1:2 which is higher in pyridine and BSTFA than the ratio used in the previous experiments since this ratio was reported as the optimised reagent ratio by Kumirska *et al.* [173]. Final maximum concentration in the final derivatised sample is 4375 mg/L. The internal standard was 1-methylnaphthalene in the same concentration as the phenols although it was prepared in pyridine and added with the catalyst. For the analysis of the derivatised samples, the same GC-FID method that was used in the previous experiments was used with the reported change in the split ratio in order to accommodate such high concentration with minimizing chromatographic issues.

The investigation of the optimal derivatisation conditions was performed using a a factorial design with a 2^3 base with 8 centre points and 8 axial points involving 24 runs in total and it was performed in two blocks. The design can be seen in Table 6.2. This response optimisation process was initiated using Minitab® Minitab Inc [174] and the integrated assistant for response optimisation. The first block of experiments was performed using the base design 2^3 with 4 centre points. After obtaining information on curvature the software suggested another block of experiments by adding 8 axial and 4 centre points. The entire design was analysed afterwards in Minitab® using a response surface methodology (RSM) approach.

Additional runs were performed at 60% amplitude and 70s time and at 50% amplitude and 60s time with both solvents (two for each solvent) in order to test for repeatability.

Table 6.2: Modelling design for optimisation of the derivatisation conditions

RunOrder	CenterPt	Blocks	Amplitude [%]	Time [s]	Solvent
1	0	1	45	40	CPME
2	1	1	70	70	Toluene
3	1	1	70	70	CPME
4	1	1	20	70	Toluene
5	1	1	20	70	CPME
6	1	1	20	10	CPME
7	1	1	70	10	Toluene
8	1	1	20	10	Toluene
9	0	1	45	40	Toluene
10	1	1	70	10	CPME
11	0	1	45	40	CPME
12	0	1	45	40	Toluene
15	-1	2	45	70	Toluene
16	-1	2	70	40	CPME
17	0	2	45	40	CPME
18	-1	2	45	70	CPME
19	-1	2	45	10	CPME
20	0	2	45	40	Toluene
21	0	2	45	40	Toluene
22	-1	2	20	40	CPME
23	-1	2	45	10	Toluene
24	0	2	45	40	CPME
13	-1	2	20	40	Toluene
14	-1	2	70	40	Toluene

6.2.3.4 Derivative stability, precision and in-matrix precision

To test the stability of the trimethylsilyl derivatives, 10μL of a standard phenolic mixture were added in a 300μL round bottom vial. The mixture contained the following phenolic compounds in CPME: phenol, p-cresol, 3,5-xylenol, 1-naphthol, 2,4,6-trimethylphenol, 1-acenaphthenol, 9-phenanthrol, 9-anthracenemethanol, o-cresol, 2,4-xylenol, catechol, phenol-4-tert-octyl, 3-phenylphenol, 9-hydroxyfluorene, 1-hydroxypyrene in 100mg/L. Following mixture addition, 10 μL of a 400mg/L solution of 2,4,6-trimethylphenol-d11 in pyridine was added in the vial and vortexed briefly for a few seconds. Finally, 20μL of BSTFA with 1% TMCS were added, the vial was capped and placed on the sonication probe were it was sonicated with the previously determined optimised conditions: 50% amplitude with a 100% pulse for 60s. The vial was then removed and 2μL of a 420 mg/L internal standard solution containing phenol-d6, naphthalene-d8 and phenanthrene-d10 was added and the mixture injected for analysis. The vial was capped, placed on the autosampler at room temperature and analysed subsequently after 4, 11, 24 and 48hrs. The vial was resealed with a new septum

after each injection. An underivatised version of the mixture (swapping BSTFA for CPME) was also injected for reference. The precision of the derivatisation process was tested by repeating the above process 6 times and placing the samples at -80°C until analysis immediately after derivatisation.

The effect of derivatisation in a real sample was assessed by applying the derivatisation process in an extracted coal tar pitch. The tar pitch sample was previously spiked with a surrogate mixture and extracted with the extraction method described in Section 4.3.1, p.62. The surrogate mixture contained the following annotated compounds: 4-fluoro-2-methylpyridine, 4-fluorophenol, 1-fluorododecane, 1-fluoronaphthalene, 5-fluoroindole, 4-bromo-2,6-dimethylphenol, fluorene-d10, 1-bromo-2-naphthol and chrysene-d12. For the analysis of surrogates, a quantitative method was developed with 6 concentration levels used for all compounds: 1.125, 2.25, 4.5, 9, 22.5 and 45 mg/L. Details of the calibration curve include internal standards for each surrogate, retention times and ions used to quantify each compound are shown in Table 6.3.

Table 6.3: SIM method parameters for surrogate analysis

Compound	Internal standard	Retention time	Quantifying ion
4-fluoro-2-methylpyridine	phenol-d6	4.73	111
4-fluorophenol	phenol-d6	7.57	112
1-fluorododecane	napthalene-d8	9.72	57
1-fluoronaphthalene	napthalene-d8	10.63	146
5-fluoroindole	napthalene-d8	13.64	135
4-bromo-2,6-dimethylphenol	napthalene-d8	14.22	200
fluorene-d10	phenanthrene-d10	16.35	176
1-bromo-2-naphthol	phenanthrene-d10	16.96	222
chrysene-d12	phenanthrene-d10	22.06	240

The derivatisation process for each sample was the same as described above (Section 6.2.3.3) and each derivatised sample was analysed with the targeted SIM method as above. The coal tar pitch extract was derivatised with the same method used for derivatisation stability and precision assessment as describe above. Surrogate recovery was calculated using equation6.1, where C_2 is the concentration provided from chemstation and C_1 is the maximum concentration in the derivatisation mixture. Surrogate concentration in the coal tar extract was expected to be 100mg/L (assuming a 100% recovery), while diluting in a 1:1:2 sample:pyridine:BSTFA (1% TMCS) would result in a measured concentration of 25mg/L for a 100% recovery.

$$Recovery[\%] = \frac{C_2}{C_1} * 100 \tag{6.1}$$

6.3 Results and discussion

6.3.0.1 Initial factor screening for UAD

Factorial regression with 1st order terms with no interactions between terms and by considering all the factors regardless of their p-value, results in the plot in figure 6.5. The pareto chart sets a threshold (in this case 2.36) where any factors with higher standardised effect value are significant. The response used for the study is the relative response factor (RRF) (Equation 6.2) of 2,4,6-trimethylphenol. The addition of pyridine appears the only significant of the four studied factors on the derivitisation reaction, within the selected experimental area. Any potential significance of the other factor effects may be suppressed in this experiment due to the immense effect of pyridine and the relatively small value range of factor levels. The addition of pyridine appears to be largely beneficial in the derivatisation of phenols by providing a significant decrease in the time needed to drive the reaction forward.

$$RRF = \frac{R_T * C_{IS}}{R_{IS} * C_T} \tag{6.2}$$

where R_T is the peak area of the target compound, C_{IS} is the concentration of the internal standard, R_{IS} is the peak area of the internal standard and C_T is the concentration of the target compound)

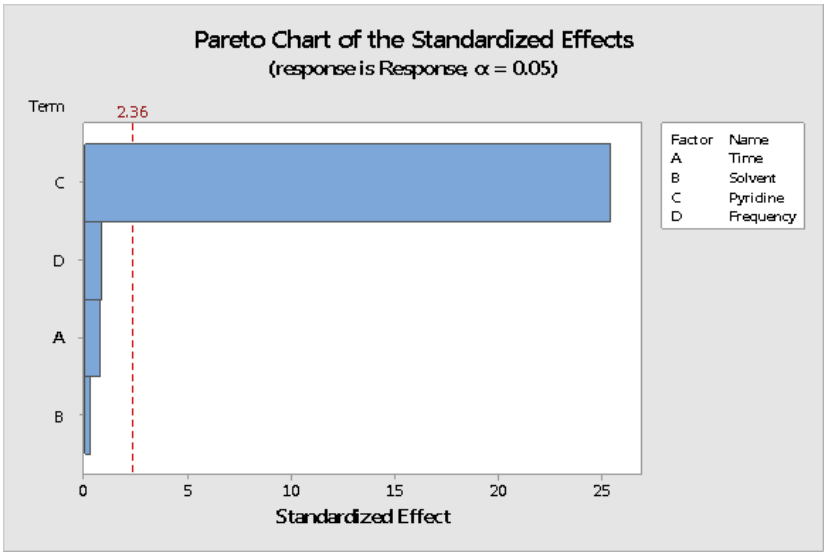

Figure 6.5: Pareto plot of standardised effects for the screening experiment. Red line indicates threshold for statistical significance (P-value=0.05). Pyridine has a significant effect on derivitisation.

6.3.0.2 Illustration of the effect of steric hindrance on derivatisation

It takes a significantly higher amount of time for the RRF of 2,4,6-trimethylphenol to maximise and stabilise than the rest of the phenols (Figure 6.6). The reaction appears to be complete approximately 70 mins after initiation hence only data for the first 127 mins is shown in the plot.

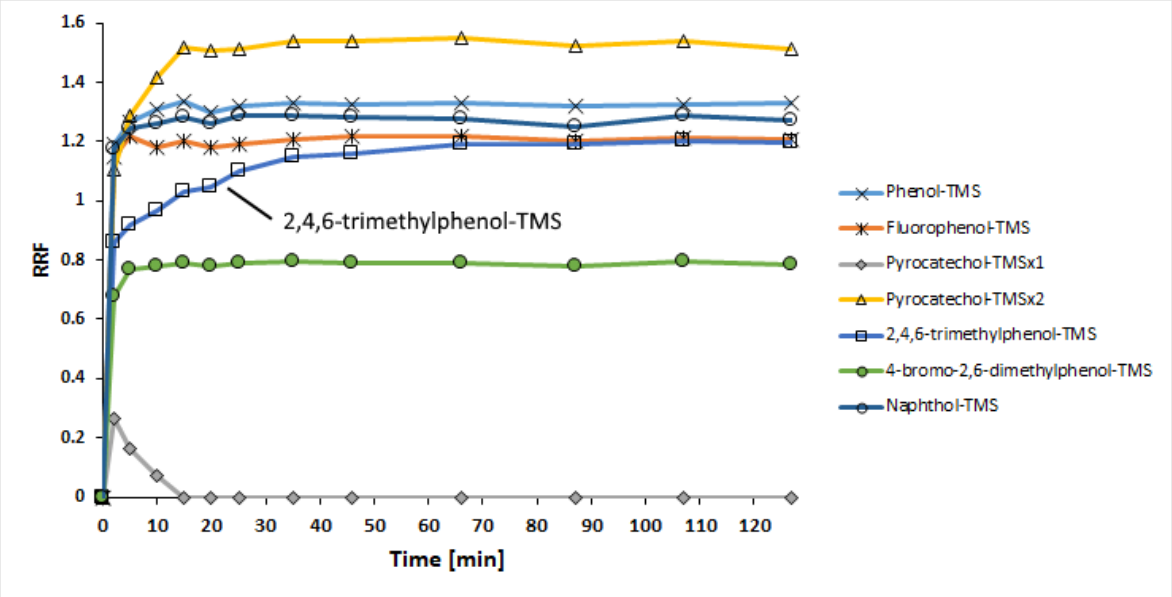

Figure 6.6: Relative response factor vs time for phenols. The plot is a composite of replicate no3 from the steric hindrance experiment and the additional runs for the extra time resolution with the axis limited to 120mins. For full graphs the reader is referred to Figures Appendix A.4.1 and Appendix A.4.2.

Pyrocatechol is derivatised fast at first to the mono-substituted TMS derivative but the bi-substituted TMS derivative takes a significantly longer amount of time to be produced. This indicates that the TMS group that attaches to the first oxygen sterically hinders the reaction towards the bi-substituted TMS derivative (Figure 6.7). However, even when this is the case catechol appears to be derivatised after 15min.

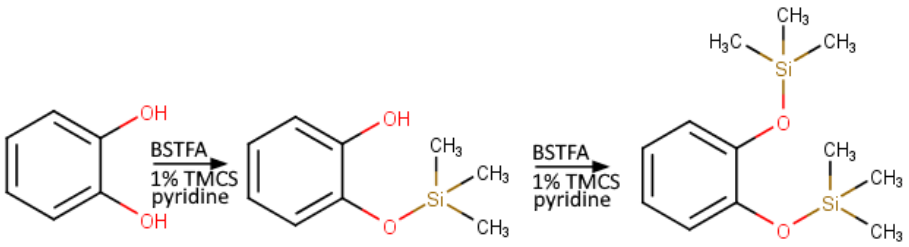

Figure 6.7: Trimethyl silylation of catechol. The trimethylsilyl group on the mono-substituted derivative at the first step of the reaction sterically hinders the silylation of the second hydroxyl group

6.3.0.3 Sonication condition optimisation for aliquots from UCG samples

The optimisation of the sonication parameters (factors: amplitude, time and solvent - Table 6.2) was performed by fitting a response surface regression model (RSM) to the data. The model was built by testing first and second order terms including all first order interactions using backwards elimination with an alpha value threshold set to α=0.05 so that only significant effects are included; the response was the of RRF of 2,4,6-trimethylphenol. The created model included sonication frequency (amplitude) and time and their first order interaction. As the frequency and time increases (Figure A.4.3) so does the RRF of 2,4,6-trimethyphenol-TMS. Also, higher frequencies and longer sonication times seem to have a cumulative effect on the response. This can be attributed to a temperature increase in vial by applying sonication for longer time. Temperature has shown to enhance the silylation reaction[111]. A contour plot that shows how sonication frequency and time affect the response can be seen in Figure 6.8. Operating the sonicator at higher frequencies did increase vial breakage incidents and although this was not tested systematically it can be said that a lower frequency and higher time would be preferred to minimise the chances of vial breakage and sample loss.

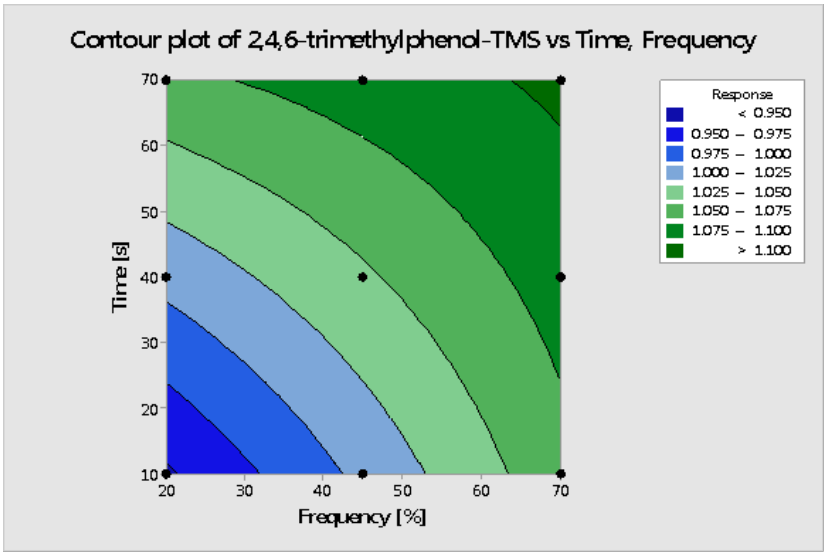

Figure 6.8: Contour plot depicting the relationship of RRF versus Time and Frequency

Since the instrument provides a reading for the amount of power delivered to the vial during the sonication, the use of this value was considered to further describe the derivatisation. The instrument software calculates the total amount of energy delivered to the vial for each sonication run by multiplying power (Watts) with time (seconds). The total delivered energy is given in Joules (Equation 6.3).

$$J = W * s \tag{6.3}$$

However, it should be noted that the amount of actual energy delivered to the vial contents

may be different than the amount calculated due to various losses in the system e.g. if the vial fits imperfectly the energy may be used up in vibrating the vial rather than sonicating its content. A model based on power and response factor can be seen in Figure 6.9. This model was constructed with data from the RSM model and additional runs performed for repeatability checks. For this specific system the RRF of 2,4,6-trimethyphenol-TMS can be represented by the fitted line. Repeatability runs provided an RSD_1=1.06% for 60% amplitude and 70s time and an RSD_2=0.45% for 50% amplitude and 60s time. It was decided to proceed with the following conditions as optimal: 50% amplitude and 60s time.

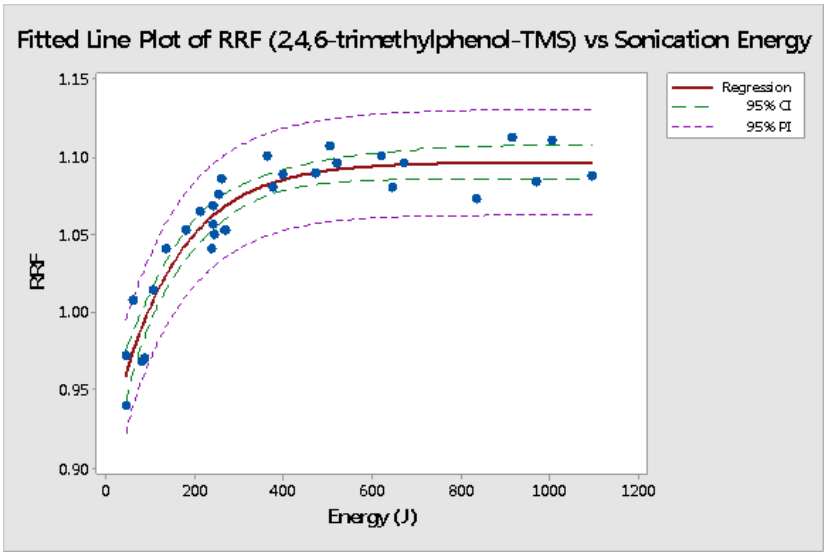

Figure 6.9: Fitted line plot depicting the relationship between RRF and sonication energy

As shown above, an effort was made to develop the derivatisation method with phenol concentration similar to that of actual samples, however, verifying the completeness of the derivatisation in actual samples is also very important as the total amount of derivatisable components in unknown. Thus, in order to monitor reaction completion in actual samples a surrogate was introduced: 2,4,6-trimethylphenol-d11. This is the deuterated version of 2,4,6-trimethylphenol which was used as the model compound for method development. The deuterated version is added as a surrogate along with pyridine in the derivatisation reaction as a way to measure the derivatisation reaction completion and precision in actual samples. Since, as mentioned above, 2,4,6-trimethylphenol is derivatised last due to steric hinderance, the same behaviour is expected from the deuterated version. No recovery values can be provided since there is no commercially available standard for the derivatised compound, however, by not detecting the underivatised compound when derivatising a sample, we can assume that derivatisation for the phenolic content of the sample is complete. Also, since the same amount is added into each sample, this compound can be used together with other surrogates to monitor the instruments precision. Since this compound does not exist in any of the accessed mass spectrum libraries, the spectra of both the non-derivatised and

derivatised version (as experimentally determined by GC-MS) are provided in Figure 6.10.

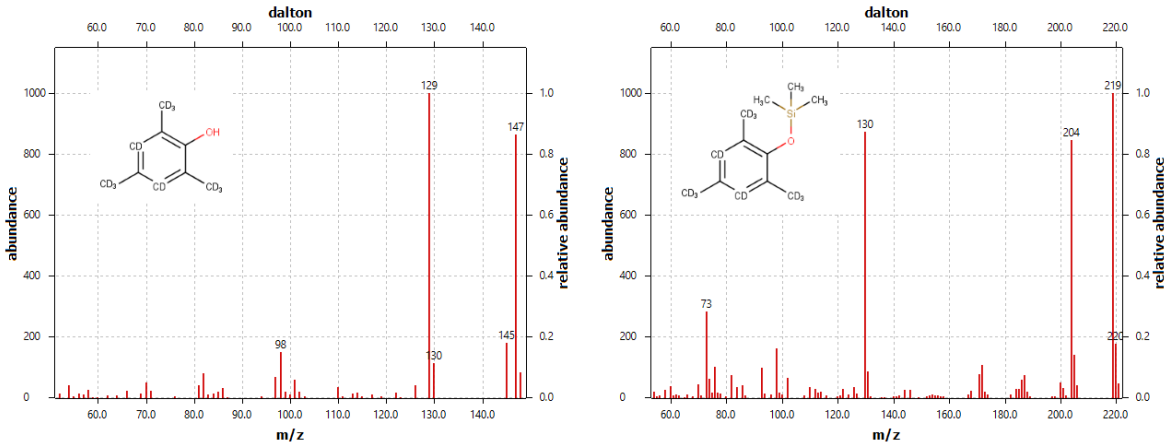

Figure 6.10: Mass spectra of 2,4,6-trimethylphenol-d11 and the derivatised counterpart as extracted by AMDIS

6.3.0.4 Derivative stability, precision and in-matrix precision

Since precision analyses were performed by storing all samples in -80°C immediately after sonication, it can be assumed that if the trimethylsilyl derivatives are stable in room temperature, then any monitored variation in the analysis of the samples stored in -80°C may be attributed directly to handling and experimental processes. Good precision values are needed especially when comparing time series samples or performing multivariate statistics.

The response factor of the trimethylsilyl derivatives appear to be stable for at least 24hrs in room temperature provided that the vial is recapped after each injection (Figure 6.11 for light compounds and Figure 6.12 for heavier compounds). Since the experiment was performed in one replicate the behaviour in time was not modelled.

As mentioned above, derivatisation precision was tested by monitoring the response factor of the studied phenols in the technical mixture in 6 derivatisation replicates. Average RSD was 3.1% with the minimum being 0.5% for phenol-d6 and the maximum 6.4% for 1-hydroxypyrene (Table 6.4). By further investigating the relative chromatograms, neither 2,4,6-trimethylphenol-d11 nor 2,4,6-trimethylphenol were detected in any of the replicates, which indicates that derivatisation is complete.

In-matrix precision was measure by derivatising an extracted coal tar pitch sample. Recovery data for surrogates can be seen in Table 6.5. The surrogate 4-fluoro-2-methylpyridine was left out as it was co-eluting with interferences (possibly originating from the pyridine reagent) yielding multiple 100% recovery values.

All phenolic surrogates are derivatised as they all have labile hydrogens (Table 6.5). Another interesting observation is that recovery for 5-fluoroindole indicates that this surrogate

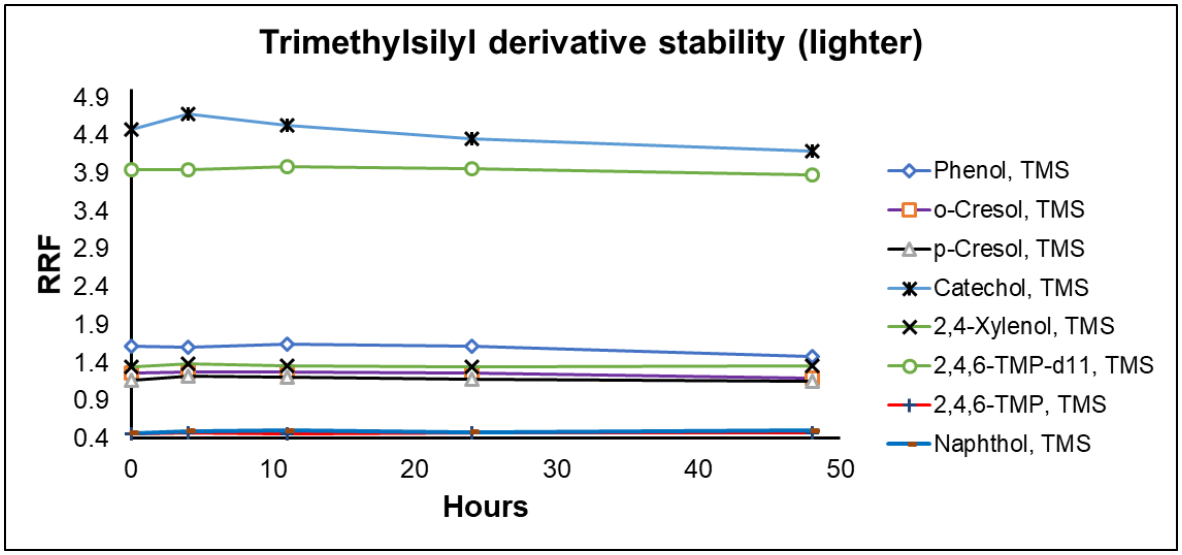

Figure 6.11: Stability of the lighter derivatised phenolic compounds in a 48-hour period. Since the experiment was not replicated not error bars are provided.

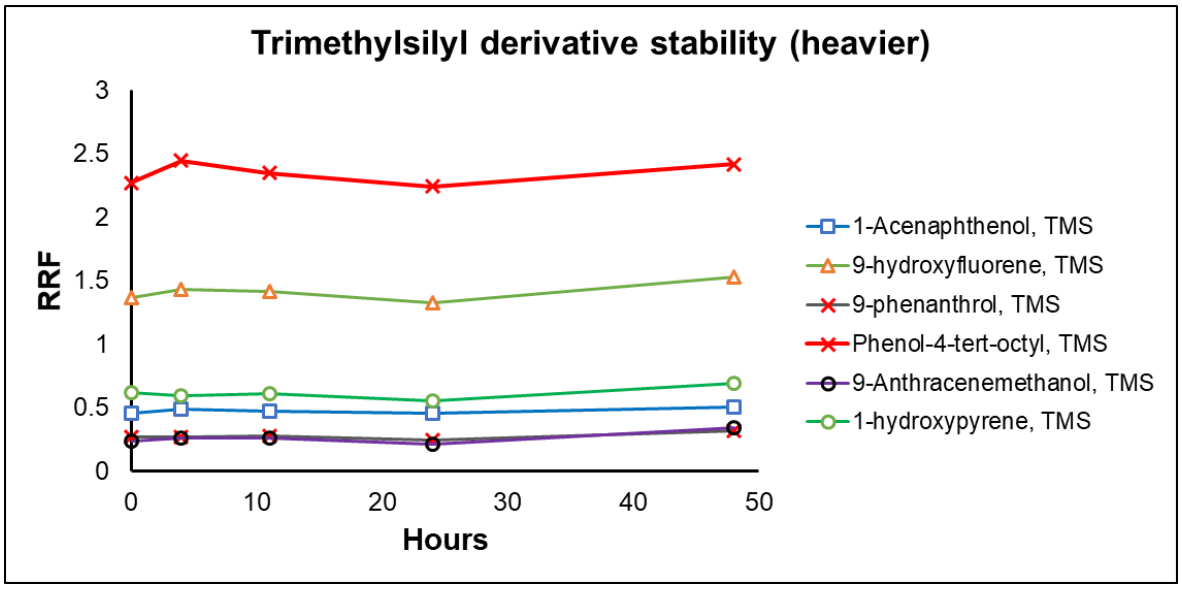

Figure 6.12: Stability of the heavier derivatised phenolic compounds in a 48-hour period. Since the experiment was not replicated no error bars are provided

is derivatised as well. The previously reported methods by Gauchotte-Lindsay *et al.* [111] that did not employ UAD or pyridine reported this compound as un-derivatised, so this result further indicates the potential use of the current method in the derivatisation of nitrogen heterocyclic compounds with labile hydrogens. Since the derivatised version of this compound is not listed in mass spectrum libraries, the extracted spectra from AMDIS is provided in Figure 6.13. Regarding the surrogates that do not have labile hydrogens, all of the recoveries are well within the 70-130% accepted recovery range as stated in U.S. EPA SW-846 Method 8000D.

Table 6.4: Precision data for the trimethylsilyl derivatives. Values given are the average, the standard deviation and the relative standard deviation (where n=6)

Compound name	Average	Stdev	%RSD
Phenol-D6, TMS	1.59	0.01	0.5
Phenol, TMS	1.21	0.03	2.1
o-cresol, TMS	0.94	0.02	2.3
p-cresol, TMS	0.88	0.03	3.0
Catechol, TMS	3.28	0.08	2.5
2,4,6-trimethylphenol-d11, TMS	2.91	0.08	2.8
2,4,6-trimethylphenol, TMS	0.34	0.01	2.4
Phenol-4-tert-octyl-TMS	1.71	0.06	3.6
Naphthol, TMS	0.35	0.01	3.4
3-phenylphenol, TMS	0.6	0.02	3.6
1-Acenaphthenol, TMS	0.35	0.01	3.0
9-hydroxyfluorene, TMS	1.01	0.03	2.9
9-phenanthrol, TMS	0.18	0.01	4.1
9-Anthracenemethanol, TMS	0.17	0.01	6.4
1-hydroxypyrene, TMS	0.41	0.02	4.5

Table 6.5: Precision data for the surrogate recovery. Values given are the average, the standard deviation and the relative standard deviation (where n=6). Recoveries for the surrogates that undergone silylation are well below 10%

Surrogate	Average recovery [%]	Stdev	RSD[%]
4-fluorophenol	3.80	0.19	5.0
1-fluorododecane	102.83	2.63	2.6
1-fluoronaphthalene	101.37	2.24	2.2
5-fluoroindole	1.77	0.05	2.8
4-bromo-2,6-dimethylph...	7.69	0.51	6.6
fluorene-d10	101.10	2.23	2.2
1-bromo-2-naphthol	3.17	0.23	7.3
chrysene-d12	83.47	1.94	2.3

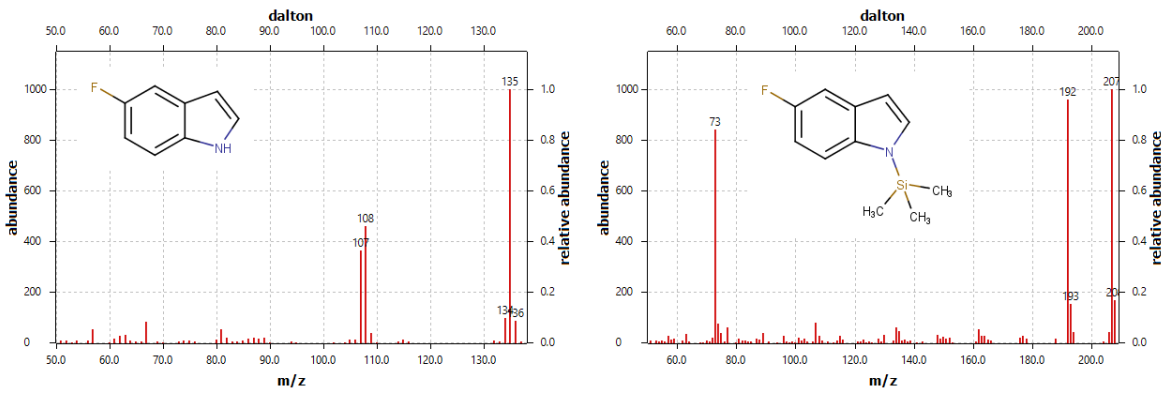

Figure 6.13: Mass spectra of 5-fluoroindole along with the derivatised version as extracted from AMDIS

6.3.1 Untargeted analysis of the derivatised effluent extracts

6.3.1.1 Overview

Figure 6.14 shows the GC-MS (top) and GCxGC-TOFMS (bottom) chromatograms of the derivatised composite sample from the TOPS1 experiment. Just by visual inspection of the graph more peaks appear to be detected using GCxGC-TOFMS especially in the middle and close to the end of the chromatogram. The non-derivatised surrogate was not identified in any of the samples suggesting complete derivatisation for phenolic compounds.

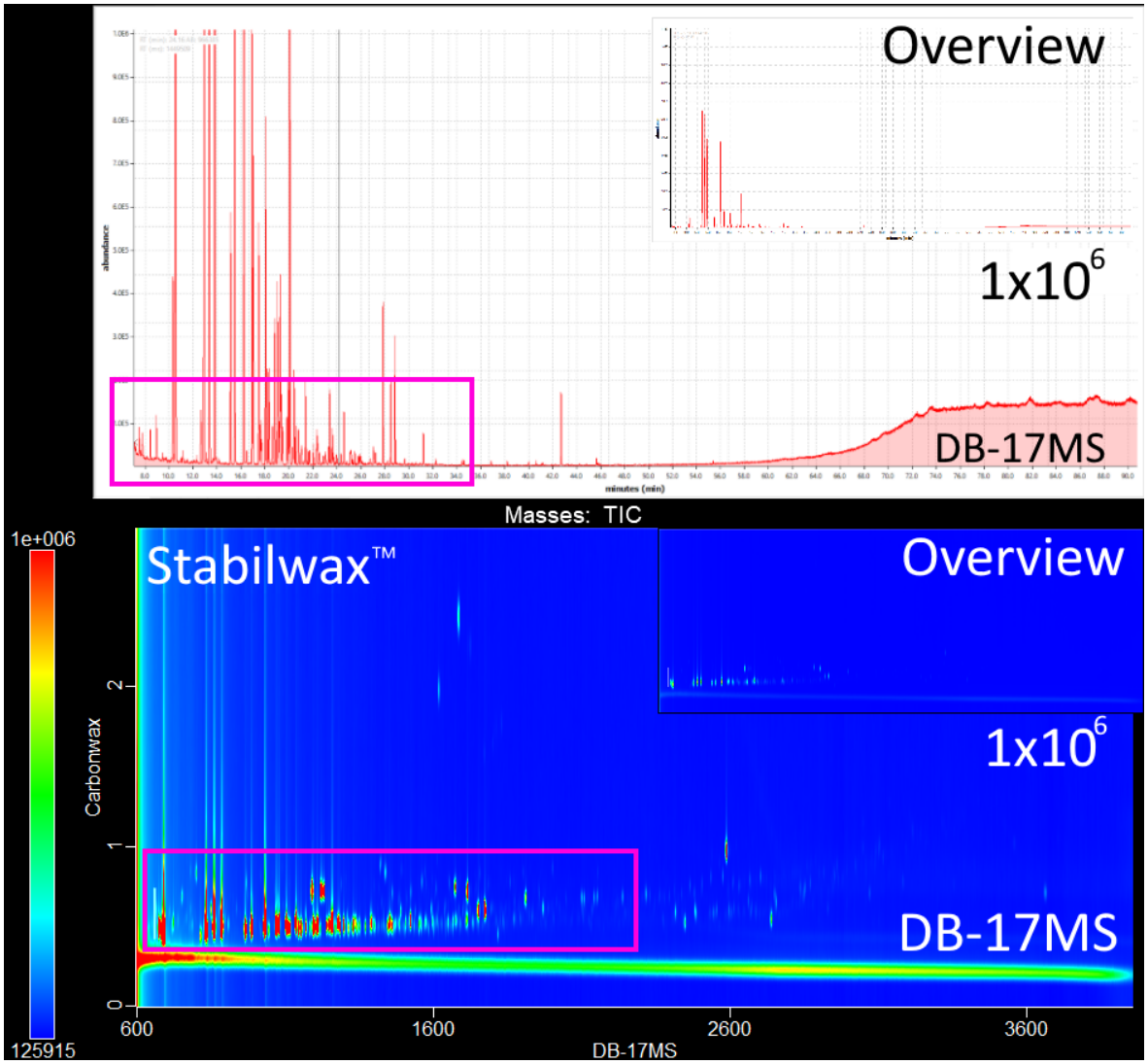

Figure 6.14: Top: GC-MS Chromatogram of the derivatised composite sample from TOPS1 **bottom:** GCxGC-TOFMS chromatogram of the derivatised composite sample from TOPS1. Areas where the bulk of the peaks are eluted are indicated with a purple rectangle

Analysis of the derivatised composite sample from the Barbara II trial using both GC-MS and GCxGC-TOFMS appear in Figure 6.15. Both chromatograms are shown to be rich in peaks, however, the comprehensive separation that appears in the chromatogram of GCxGC-

TOFMS is expected to provide more information since elution bands of compounds with similar properties clearly appear in the chromatogram.

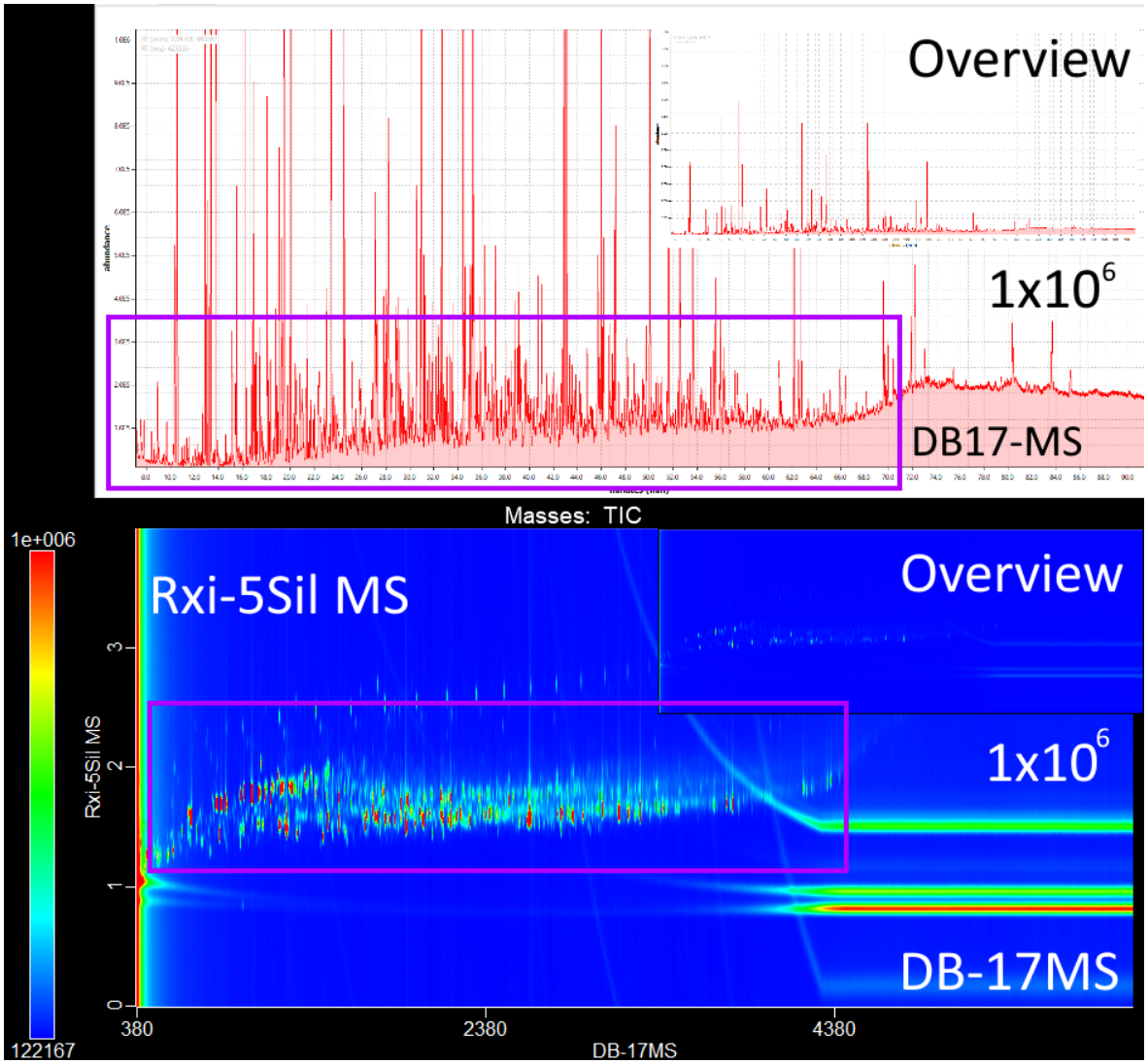

Figure 6.15: Top: GC-MS Chromatogram of the derivatised composite sample from the Barbara II trial **bottom:** GCxGC-TOFMS chromatogram of the derivatised composite sample from the Barbara II trial. Areas where the bulk of the peaks are eluted are indicated with a purple rectangle

Figure 6.16 shows the GCxGC-TOFMS chromatogram corresponding to mass 73 of the most concentrated sample from the TOPS1 series time series (sample 3) and the same chromatogram for the composite. As can be seen the high retention of phenols in the second dimension is reduced in the derivatised sample since the trimethylsilyl derivatives are not polar enough to interact with the Stabilwax column in the same degree as the underivatised phenols. However, the number of peaks that appear in the chromatogram is clearly higher in all parts of the chromatogram. This suggests that phenolic compounds which would otherwise be not easily detectable due to volatility and polarity issues are now detected as a result of the derivatisation process. However, the GCxGC setup that was shown to be superior

for the comprehensive separation of the underivatised waste-water samples somewhat loses its separation power due to the reduced amount of interactions with the secondary column although some underivatised polar compounds still show significant retention.

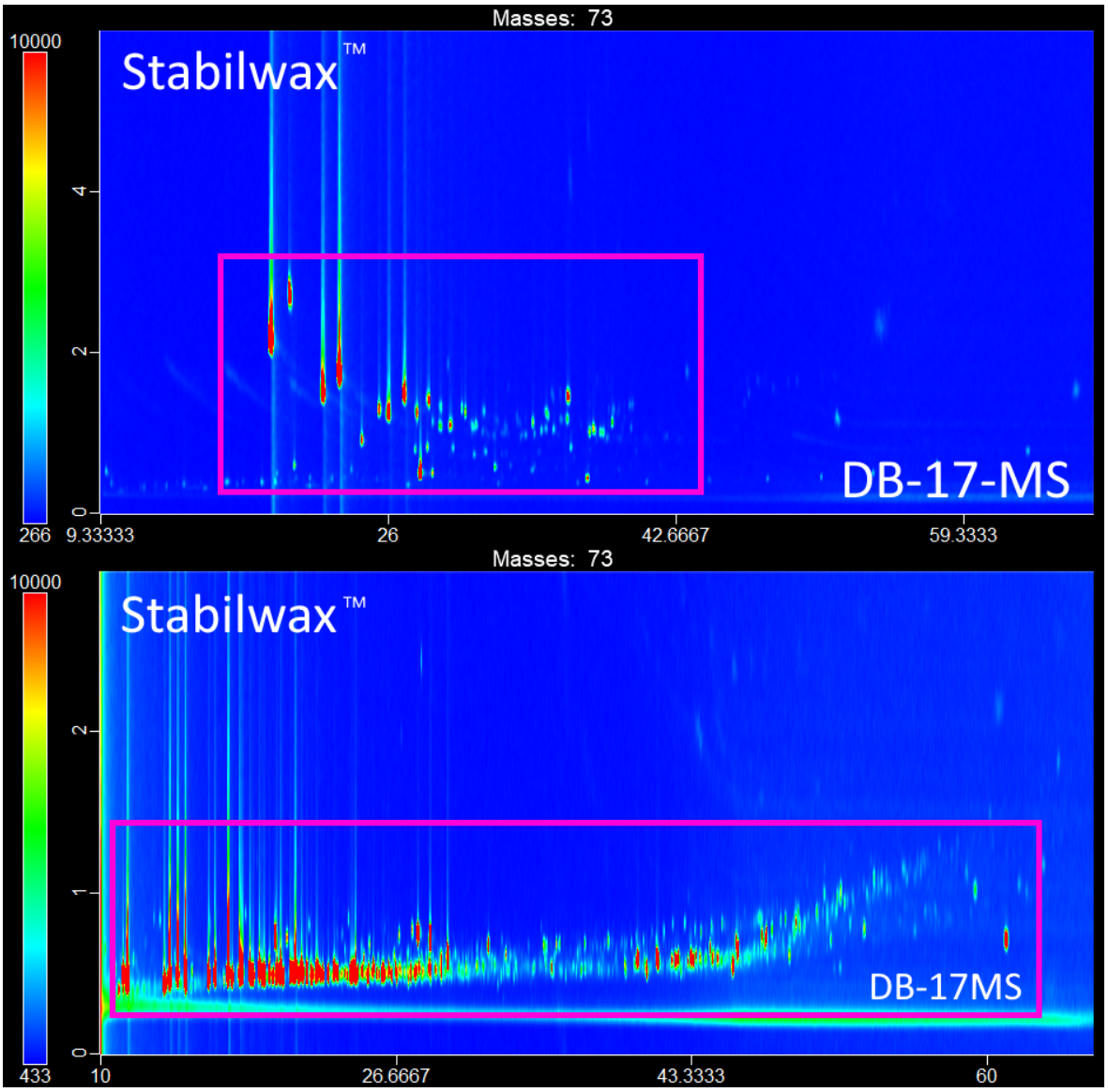

Figure 6.16: Top: GCxGC-TOFMS chromatogram of the TOPS1-3 samples **bottom:** GCxGC-TOFMS chromatogram of the derivatised composite sample from TOPS1. Areas where the bulk of the peaks are eluted are indicated with a purple rectangle

The same chromatogram as above for the derivatised composite from Barbara II trial and the chromatogram from sample 6 for the analysis of tars appears in Figure 6.17. The number of peaks that are detected at the derivatised sample is much greater that those detected in underivatised sample and this can be confirmed just by visual comparison the chromatogram. This indicates the high number of compounds with a labile hydrogen in the tar from UCG. Generally, it can be observed that the derivatised compounds are eluted between the elution area of aromatics and aliphatics which is less populated, providing more effective usage of

chromatogram space.

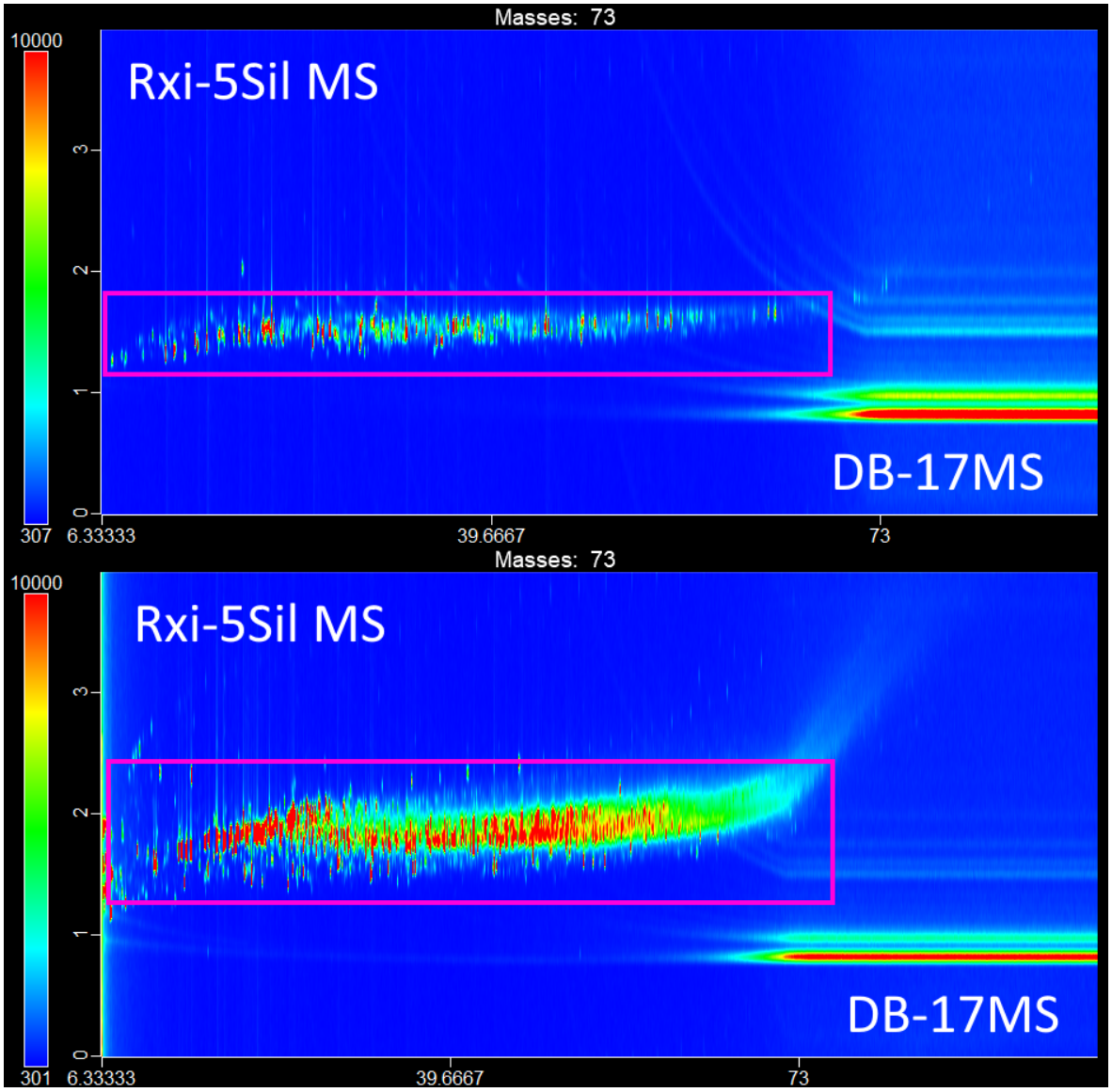

Figure 6.17: Top: GCxGC-TOFMS chromatogram of sample 6 from the Barbara II trial series **bottom:** GCxGC-TOFMS chromatogram of the derivatised composite sample from the Barbara II trial. Areas where the bulk of the peaks are eluted are indicated with a purple rectangle

6.3.1.2 Phenolic compounds

One significant difference between the derivatised and non-derivatised samples is the behaviour of phenols in the waste-water sample in the polar normal phase setup. The non-derivatised sample (TOPS1-P3) (Figure 6.18, left) phenol, 4-fluorophenol and the cresol isomers are better retained and separated in the second dimension however, in the derivatised sample (composite), the polarity differences between the compounds are practically reduced as expected and so does their affinity with the Stabilwax column. As expected, their 1st

dimension retention is significantly reduced, and they are hardly retained in the 2nd dimension as they elute in, practically, the same secondary retention time. However, they are all clearly separated in the first dimension, including the m and p isomers that were co-eluting. Chromatography also appears superior as peak shape is much better.

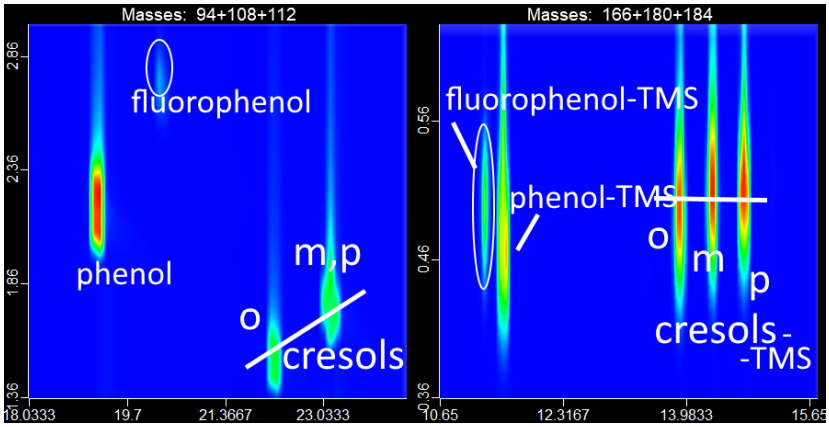

Figure 6.18: left separation of phenol, 4-fluorophenol and cresol isomers in the polar normal phase setup for the non-derivatised sample (TOPS1-P3) and (**right**) in the derivatised sample (composite). Although retention in the first and second dimension is limited in the derivatised sample all the compounds are clearly separated

Similar behaviour can be seen in the non-derivatised and derivatised samples from the Barbara II trial. Since the column setup here is different, the reduction in polarity from derivatisation actually increases the retention in the second dimension while it decreases it in the first dimension. Regardless, derivatisation also results in better separation and peak shapes as above (Figure 6.19). One interesting observation is the behaviour of 4-fluorophenol. In both polar normal phase setup and reverse phase setup 4-fluorophenol behaves as more polar than phenol in the underivatised samples and less polar than phenol in the derivatised samples. It is possible that the reverse-phase set-up may work slightly better for the analysis of the derivatised wastewater samples.

The derivatised composite Barbara II sample appeared to be very high in phenolics. Classes of phenolics can be clearly separated with the use of specific masses as per Gauchotte-Lindsay *et al.*[111]. Here the added advantage is the derivatisation of diols and sterically hindered phenols. Various classes of phenolics along with an overall view of general elution areas can be seen in Figure 6.20. Phenolics elute clearly above other non-oxygenated hydrocarbons. Phenols with 6 carbons atoms and higher are also detected along with other hydroxylated compounds such as hydroxy PAHs. Large hydroxylated compounds are identified such as hydroxypyrene A large number of heavier molecular weight derivatised compounds are detected, a many of which cannot be identified by available libraries.

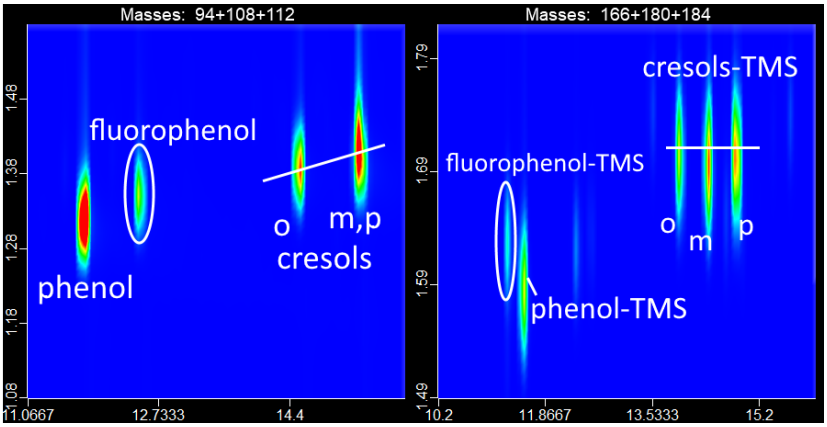

Figure 6.19: left separation of phenol, 4-fluorophenol and cresol isomers in the reverse phase set-up non-derivatised sample (Barbara II - 7) and (**right**) in the derivatised sample (composite). Retention is reduced in both dimensions after derivatisation and all the compounds are clearly separated

6.3.1.3 Nitrogen and sulphur aromatic compounds

Most of the nitrogen compounds that are reported in coal tar studies are heterocyclic such as pyridines, indoles and mixed heterocyclic compounds with those that have a pyrrole ring being usually those that have a labile hydrogen and can be derivatised. As indicated above with 5-fluoroindole, the method is capable of derivatising, at least to some degree, nitrogen containing compounds that are amongst the harder to silylate.

5-fluoroindole, indole and carbazole along with their trimethylsilyl derivatives were all found in the derivatised tar composite sample from Barbara II and identified using standards (un-derivatised counterparts). The peak area ratio of un-derivatised to derivatised was in the case of 5-fluoroindole approximately 3%, in the case of indole approx. 2% and in the case of carbazole approx. 41%. Ratios could be possibly improved with additional method development. Location of the compounds along with their trimethylsilyl derivatives in the chromatogram appear in Figure 6.21. Mass spectra for derivatised labile nitrogen containing heterocycles were limited in the available library but structurally similar compounds are expected to be derivatised at least to some degree.

Sulphur containing compounds that can be silylated are only thiols since sulphur heterocycles do not have a labile hydrogen. Although thiols are not generally reported in coal tar related literature, benzenethiol was identified with reservation (using library matching) in the tar composite from Barbara II along with the derivatised compound. The area ratio of non-derivatised to derivatised was approximately 36%. Location of the two compounds in the chromatogram are shown in Figure6.22.

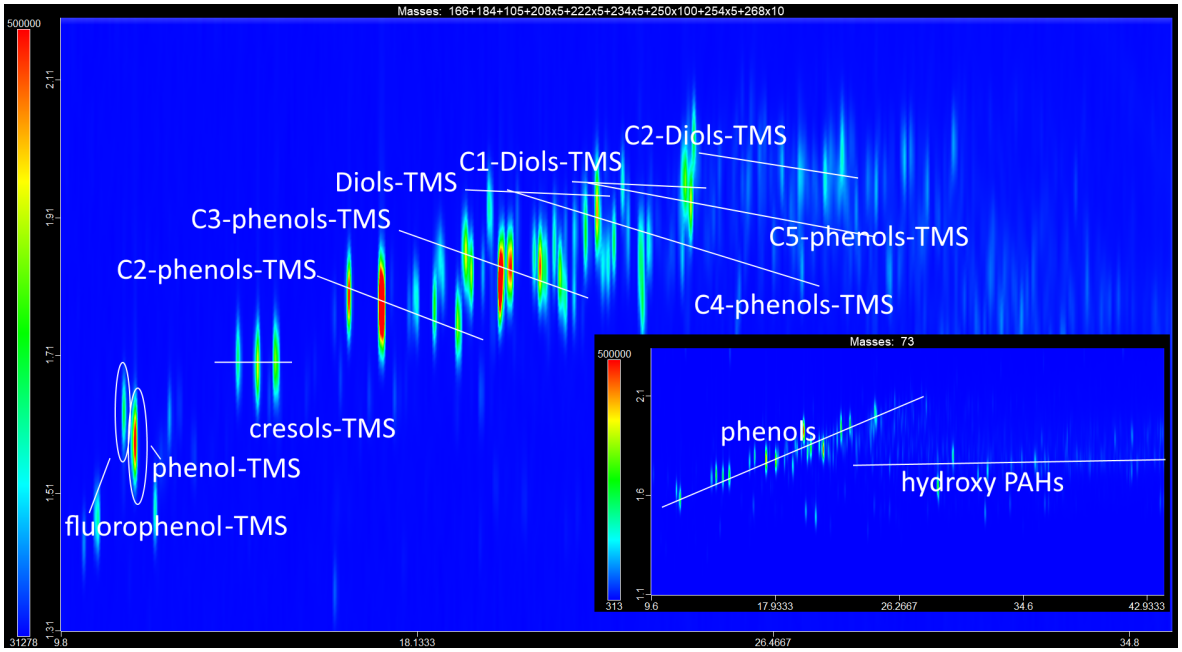

Figure 6.20: Elution areas of derivatised phenols. Methylated phenols up to 5 carbon atoms can be separated easily along with the derivatised diols and methylated diols. Methylated phenols with more than 5 carbon atoms elute in the area along with hydroxylated PAHs and other compounds

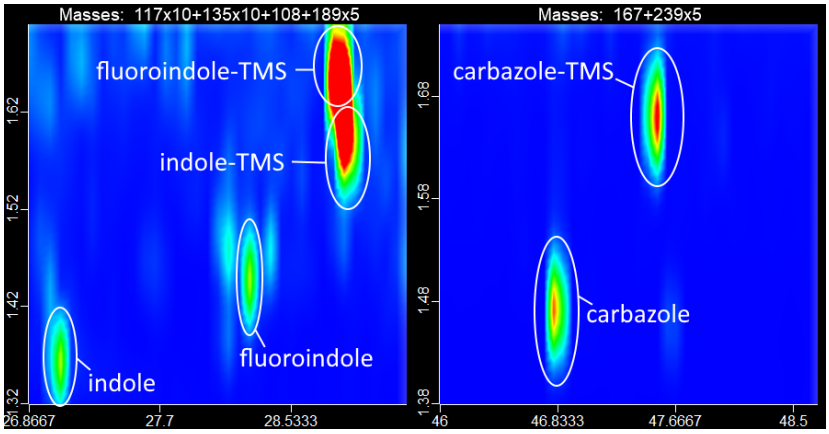

Figure 6.21: Location of 5-fluoroindole, indole and carbazole in the two-dimensional chromatogram along with their derivatised counterparts. In the case of indole the differences in retention time between derivatised and non-derivatised are larger than those of carbazole

6.3.1.4 Organic acids

Organic acids like benzoic acid have been previously reported in studies of coal gasification effluents. Only the derivatised benzoic acid was found in the composite from Barbara II indicating complete derivatisation. Another interesting observation is that in the derivatised sample saturated fatty acids become detectable and their elution pattern is clearly defined the same way as n-alkanes and n-alkylbenzenes. This can be seen by looking at the elution pattern in Figure 6.23 where they appear to elute between n-alkanes and n-alkylbenzenes. This

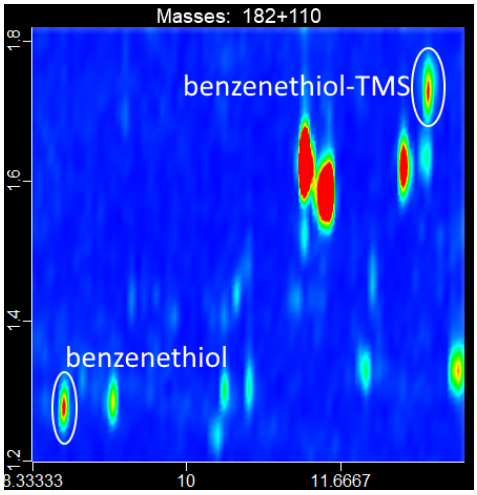

Figure 6.22: Benzene thiol and the derivatise counterpart as they appear in the two-dimensional chromatogram of the derivatised composite sample from Barbara II

clear elution pattern allows their identification through their logical order of elution. As they are unlikely to endure moderately high temperatures[175], let alone gasification temperatures the source of the fatty acids can be attributed to contamination from lubricants/plasticizers or even post-collection microbial growth in the sample. If they did exist in the coal structure, they would most probably be devolatilised downstream in the UCG cavity while temperatures were relatively low. In any case, their clear detection further adds to the value of the derivatisation method.

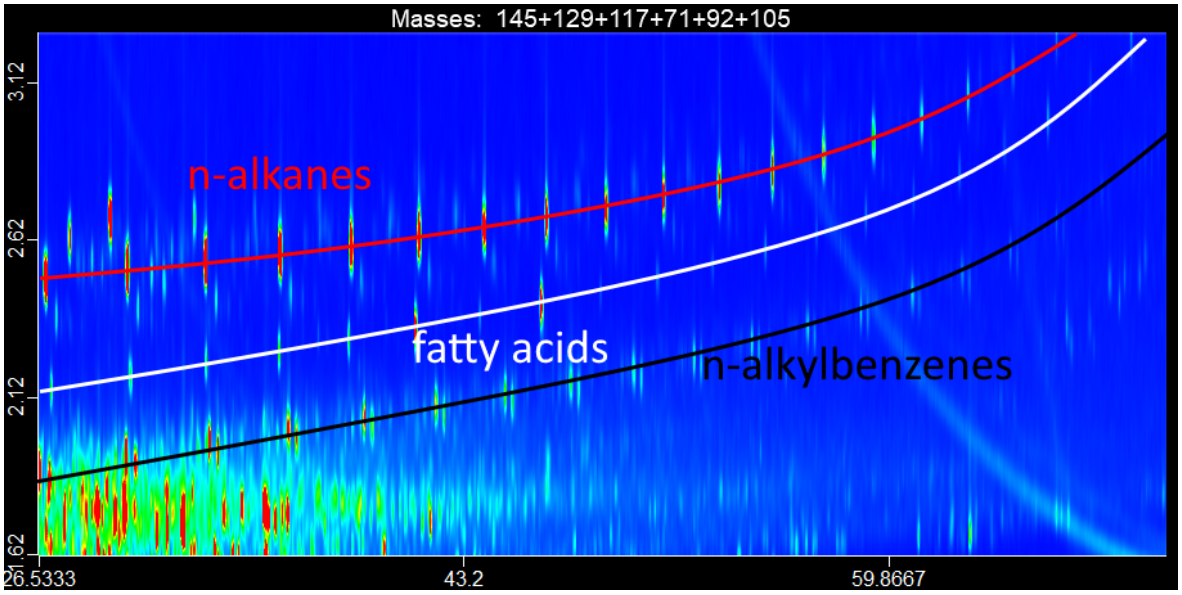

Figure 6.23: Elution of saturated fatty acids in the reverse phase GCxGC-TOFMS setup. The acids that were previously undetectable are not clearly detected. They elute between n-alkanes and n-alkylbenzenes. The elution pattern allows their identification using the logical order of elution.

The lighter saturated fatty acid in the Barbara II derivatised composite sample appears to be

pentanoic acid and the heavier lacceroic acid (dotriacontanoic acid) which appear with their position indicated in the two-dimensional chromatogram in Figure 6.24.

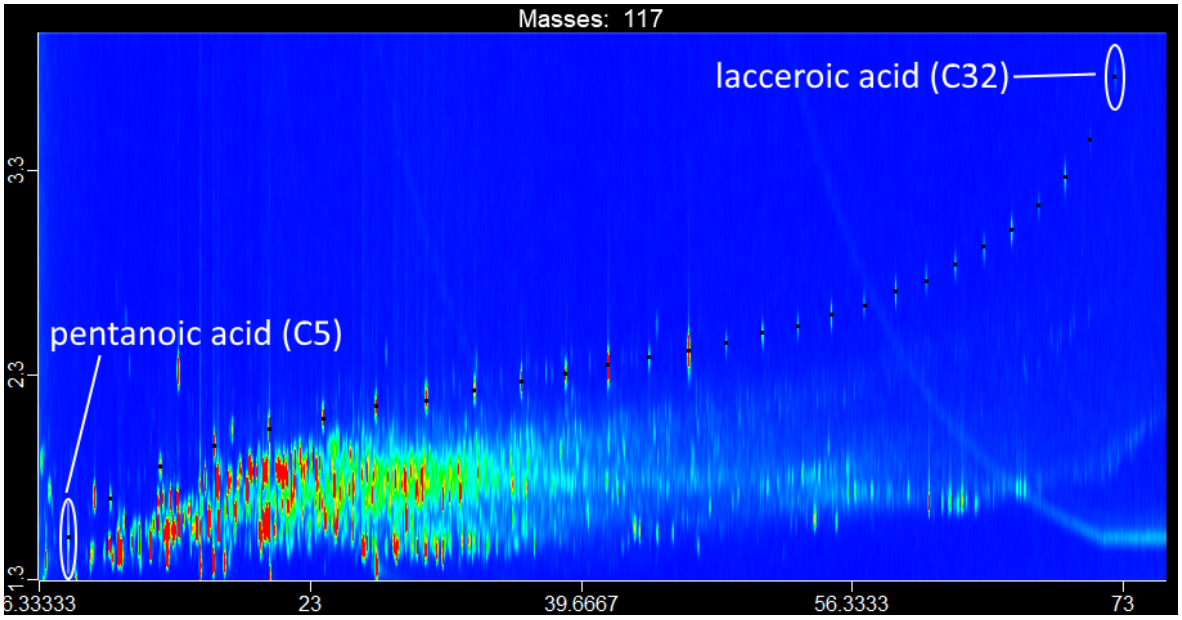

Figure 6.24: Two-dimensional chromatogram of the derivatised Barbara II coal tar composite sample indicating the peaks corresponding to the saturated fatty acids along with the lighter detected fatty acid (pentanoic acid) and the heaviest detected fatty acid (lacceroic acid)

The mass spectra of pentanoic trimethylsilyl ester and lacceroic acid trimethylsilyl ester are provided in Figure 6.25. Chromatof® successfully identified the spectra of up to eicosanoic acid trimethylsilyl ester and the rest are identified using the logical order of elution. Lacceroic acid was not positively identified using the NIST library since the molecular weight of the trimethylsily ester is 523 and the cut-off mass of the detection method was 500u.

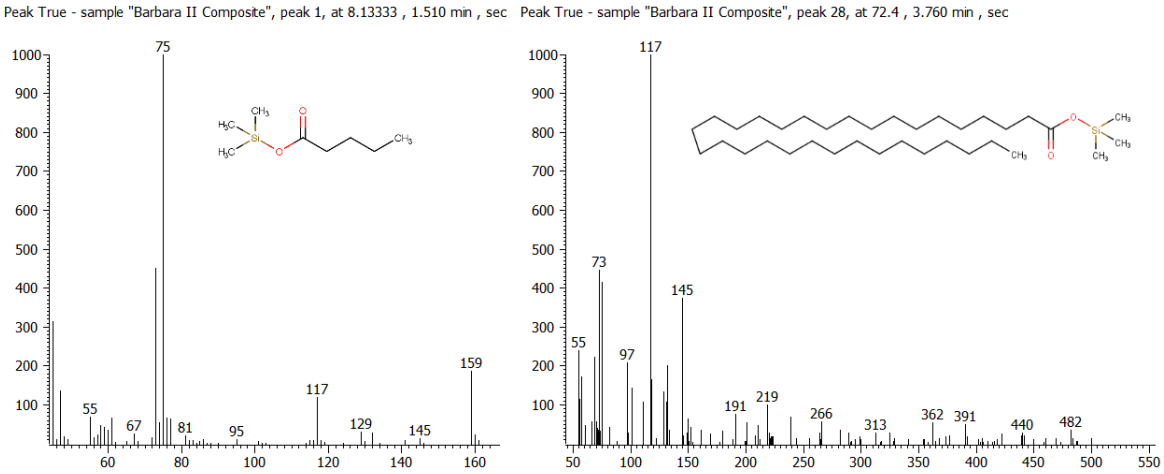

Figure 6.25: Mass spectra of the trimethylsilyl esters of pentanoic acid lacceroic acid as produced during the analysis of the Barbara II composite sample

The retention times for the first and second dimension for the trimethyl silyl esters of the 28 fatty acids are plotted with the number of carbon atoms similarly to alkanes and alkylbenzenes in Chapter 4. Scatterplots are fitted with a second order polynomial in the case of the first dimension retention time and a third order polynomial equation in the case of the second dimension retention time. Fit of the data to the equations in both cases as indicated by the Pearson r correlation coefficients was above 0.99 as can be seen in Figure 6.26

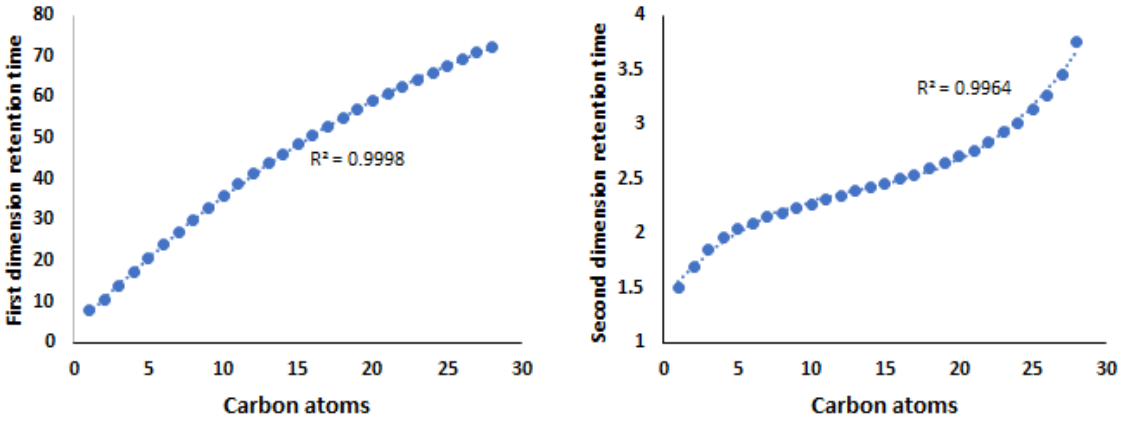

Figure 6.26: Scatterplots plotting the first dimension (**left**) and second dimension (**right**) retention time of the fatty acid trimethylsilyl esters with the carbon atom number of the corresponding saturated fatty acids. The first dimension retention time-carbon number plot can be described by a second order polynomial equation while the second dimension retention time-carbon number plot can be described by a third order polynomial equation

An analysis of the percentage of each fatty acid in the total fatty acids is given in Figure 6.27. The total ion current was used for height/area calculations. As can be seen, the most abundant fatty acids appeared to be caprilic (C8 - 8.3%), pelargonic (C9 - 8.4%), capric (C10 - 9.75%), palmitic (C16 - 14.4%) and stearic (C18 - 13.7%).

6.4 Conclusions

The derivatisation method described above provides a robust and precise approach to the trimethylsilylation of phenolic compounds. The method includes the addition of pyridine which acts as a catalyst for the trimethylsilylation reaction and the use of the HIVS to provide additional energy to the reactions for a rapid complete derivatisation in approx. 1 minute of even sterically hindered phenols. The method is both faster and capable to derivatise more compounds that the methods reported in previous studies. Apart from phenolic compounds the method also appears to be applicable for the derivatisation of nitrogen and sulfur compounds that have a labile hydrogen which are harder to derivatise than phenols, indicating that the field of application can be expanded further. Although it is utilised here in an un-

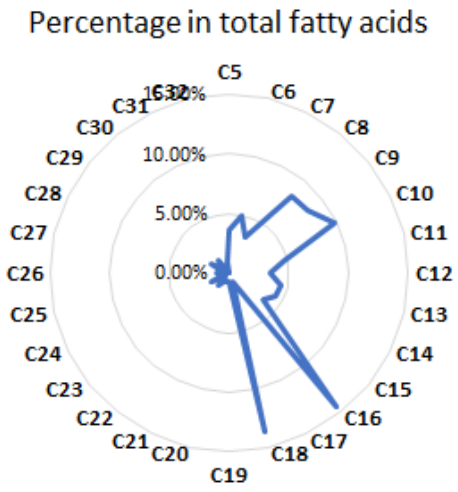

Figure 6.27: Percentage of the area of each fatty acid to the total fatty acid area. The fatty acids with the highest percentage are - by order of increasing carbon atoms: caprilic (C8 - 8.3%), pelargonic (C9 - 8.4%), capric (C10 - 9.75%), palmitic (C16 - 14.4%) and stearic (C18 - 13.7%)

targeted analysis capacity it may be used quantitatively with minimal method development provided standards become accessible. An illustration of the finalised UAD method is provided in Figure 6.28.

The chemistry of the first dimension column in both GC-MS and GCxGC-TOFMS was kept the same as in the literature but with double the length. However, the "polar" normal phase setup that included a Stabilwax column on the second dimension and was used in previous chapters to successfully separate the wastewater extract shows, in the case of the derivatised samples, reduced resolution. The use of a reverse phase setup with a low polarity secondary phase may show higher resolution although the evidence suggests that this is increase may not be significantly higher; however, this may prove to be sample dependant as only one waste-water sample was studied in this chapter.

All of the evidence suggest that the phenolic content of the Barbara II composite sample was completely derivatised; the reverse phase setup that was employed here proved more than adequate to separate this complex mixture. This demonstrates that the developed method is fit-for-purpose for the analysis of derivatised coal tar samples. Derivatised compounds appear to elute between the main elution areas of aliphatics and aromatics, thus, the chromatogram area is utilised much more efficiently. Results also indicated that tars from UCG have a very large amount of derivatisable components that are primarily hydroxylated, something which may aid in future tar comparison studies, such as those for source appointment. Although unexpected, the derivatisation of other compound classes such as saturated fatty acids, nitrogen containing heterocycles and thiols further shows the potential of the developed method which may very well have applications in the analysis of extracts from samples

of completely different background.

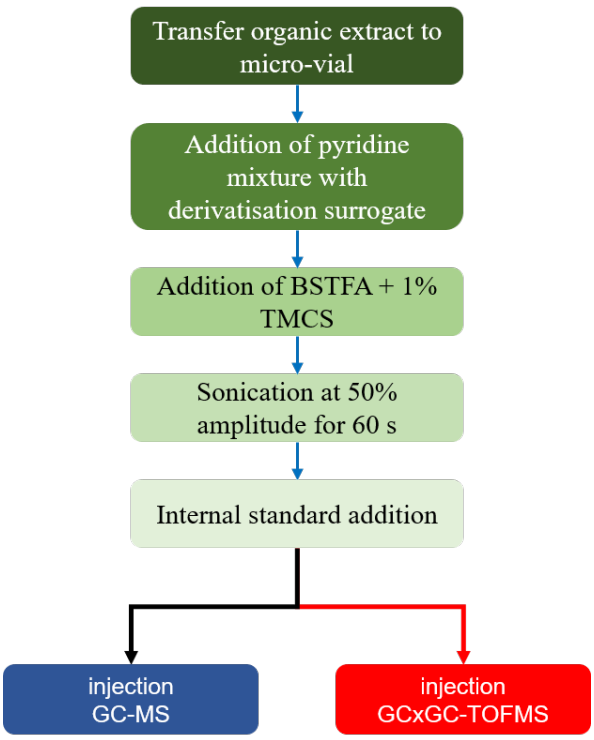

Figure 6.28: Illustration of the finalised UAD method

Chapter 7

Water-tar leaching studies of UCG produced tars

7.1 Introduction

Materials such as char and ash that is left inside the cavity after a UCG burn, may pose a risk for groundwater contamination mainly through leaching of chemical species from the cavity material (char/tars) to the groundwater. Therefore, it is desirable to establish a body of knowledge that deals with the leaching behaviour of the chemical species of concern so that appropriate planning/risk assessment can be performed before a UCG operation.

Literature specifically focused on the study of the leaching of SVOC from coal tar is relatively limited. Lee *et al.* [89] leached PAHs in water from eight tars using a batch equilibration technique that include end-over-end rotation for 12-18hrs several hours and equilibration in the dark for a 3-7 days. The study showed that there was no difference in the concentration in the leachate after equilibration for 3 days. It was further shown that the release of PAHs from the tar phase was solubility driven. Regarding solid materials, Maharaj *et al.* [176] performed water leaching experiments on lignite coal from the Balkan region using various temperatures (room temperature, hot bath, soxhlet extraction) and identifying in the extracts PAHs, phenols, benzene and degradation products of lignin. There are other studies that are focused on the leaching of inorganic species from coal derived material however they are further from the scope of the present thesis.

Apart from the studies that focus on SVOCs, there are several studies that deal with the leaching of bulk organics, or targeted species from materials derived from underground coal gasification. Xu *et al.* [177] performed leaching experiments of grounded gasified coal and analysed the leachates for inorganics and total organic carbon (TOC) under various pressure regimes. Specifically regarding TOC, the study concluded that leaching values were close to

background, however increasing pressure increases the TOC leached up to a constant value. Oliver and Spackman[178] performed 30-day batch leaching tests from coal that had been thermally treated to different temperatures and measured inorganics and TOC. All measured changes were reported being close to analytical accuracies. Humenick *et al.*[179] performed a study that included both leaching of organics from char, activated char & ash and adsorption of organics (TOC and phenols) from these materials. The study concluded that only the non-activated char leached measurable amounts of TOC and the activated char was the most effective adsorbent.

This chapter describes two leaching experiments: one that was performed within the context of the TOPS project to obtain knowledge regarding the leaching/solubility of organic matter from UCG tar in waters of different salinity (implying here increased UCG depth) and a second leaching experiment that was performed with different tars types in order to obtain knowledge regarding the type of SVOCs that will leach from different tars of increasing weathering/processing. To the author's knowledge this is the first study that looks on the leaching of bulk SVOCs from tars of very different backgrounds but also of organics from tar in water of increasing salinity.

7.2 Materials and methods

7.2.1 Chemicals

Cyclopentylmethylether (CPME - stabilised with 50ppm BHT) and 4-fluorophenol were obtained from ACROS Organics. Cyclohexane, 1-fluoronaphthalene, 5-fluoroindole, 1-fluorododecane, fluorene-d10, chrysene-d12 and 1-bromo-2-naphthol were obtained from Sigma Aldrich. Reagents 4-fluoro-2-methylpyridine and 4-bromo-2,6-dimethylpyridine were obtained from Alfa Aesar. Phenol-d6 and naphthalene-d8 were obtained from Supelco and lastly, dichloromethane, sea salts, $AgSO_4$, Na_2SO_4, H_2SO_4, $HgSO_4$ and CaCl were obtained from Fisher. Phenanthrene-d10 was obtained from Isotec. All of the reagents were of analytical grade or better.

Coal tar pitch was provided by Koppers Carbon Materials & Chemicals Pty Ltd, weathered tar was provided from the University of Strathclyde (sample no.8; see McGregor *et al.*[109]) and underground coal gasification tar was provided from an in-situ UCG experiment performed from the Polish Central Mining Institute located in Katowice, Poland (sample 2 from Barbara II trial - see Chapter 5).

For SVOC leaching a 0.01N $CaCl_2$ solution was prepared by dissolving 0.555g of $CaCl_2$ in 1000mL H_2O. For the salinity based UCG tar-water leaching experiment three types of water were prepared for leaching: pure water (milli-Q), water with 5g/kg salinity (0.5% - water A),

which was prepared by dissolving 5g of sea salts (Sigma Aldrich) in 1L of pure water, and water with 35g/kg salinity (3.5% - water B), prepared by dissolving 35g of sea salts in 1L of pure water.

Reagents for COD analysis for salinity-based leaching samples were prepared following guidelines suggested by Freire and Sant'Anna [180] for determining COD in samples with high salinity. The acid reagent was prepared by adding 2.43g $AgSO_4$ to 250mL H_2SO_4 (solution D1) and the digestion solution (solution D2) values was prepared by adding 2.55g of $K_2Cr_2O_7$ and 16.66g $HgSO_4$ in a conical flask adding water and slowly adding 28mL of sulfuric acid and then topping up with water to 200mL. The calibration curve for COD analysis was prepared by adding 2.1254g of KPH in 1000mL of milli-Q H_2O preparing a 2500 mg/L COD stock solution and diluting accordingly to resulting concentrations of 750, 500, 250, 150mg/L and a blank for 0mg/L COD.

7.2.2 Salinity-based leaching from UCG tars

UCG tar salinity-based leaching experiments were performed following Lee *et al.* [89]: approximately 0.3g of tar were weighted (with a 0.001g accuracy) into 9 40mL glass vials (3 replicates for each type of water). The vials were topped-up (all air was removed) with three types of water as per Table 7.1 (3 vials for each type). They were sealed with PTFE lined septa caps, covered with aluminium foil and transferred to a rotary shaker (roto-shake genie - Scientific Industries Inc, NY). Three blanks were included, one for each type of water. The vials were subsequently agitated, end-over-end for 19h at 10rpm and then left to equilibrate in the dark for 3 days.

7.2.3 SVOC leaching from different tar types

Water-tar partitioning experiments for SVOCs were performed with 3 types of tar (Table 7.1). Here, the tars may be considered as tars of different weathering/processing. The tars from UCG are freshly produced tars, the weathered tars from former manufactured gas plants have undergone a significant weathering process of several decades [88] while the coal tar pitch has been distilled in order to be enriched in the heavier components and obtain desirable properties [181]. SVOC leaching was performed adapting the guidelines from Lee *et al.* [89]. Approximately 0.4g of tar were weighted in a 100mL borosilicate glass with a 0.001g accuracy. Each bottle was topped up with 0.01N $CaCl_2$ so that no air remained inside. Samples were placed in an orbital shaker and were subsequently shaken at 200rpm for 18h and then placed in the dark for equilibration for approximately 3 days. Following equilibration, the samples were stored at 4°C until analysis. Each experiment was performed in duplicate and a blank was added as control.

Table 7.1: Types of tar used for the SVOC leaching experiment along with their origin

Tar type	Origin	Water used
Underground Coal Gasification	UCG pilot trial, GIG	milli-Q
Weathered FMGP	FMGP site, England	Water A
Coal tar Pitch	Commercial	Water B

7.2.4 Analysis for aggregate organic constituents (COD & TOC)

Before analysis the leachates from the SVOC leaching process were removed from the fridge and approximately 40mL of each sample were filtered through a 25mm CF/F glass filter mounted on a 15mL glass microanalysis filter holder with a fritted glass filter support (Merck-Millipore, Merck KGaA, Darmstadt, Germany). For the salinity-based leaching process, the leachates were transferred to a 50mL centrifuge tube and then centrifuged at 5000 rpm for 15min. 30mL of the supernatant was transferred to a clean 50mL centrifuge tube and then centrifuged at 5000rpm for an additional 15min. For total organic carbon (TOC) analysis all of the samples were diluted with a 1:5 ratio and analysing using a Shimadzu TOC-L total carbon analyser. Dilution was especially important for high salinity samples to reduce the amount of chlorine in the samples and prevent overloading of the halogen scrubber of the instrument. Each sample was analysed 2 or 3 times depending on injection similarity as measured by the instrument. Total TOC values were calculated by removing the value of the blank. Particularly for the salinity-based leachates, since they were exhibiting colour, brief analysis on the visible spectrum was performed by loading 0.8mL of each sample into the well of a Corning Costar 3548 Polystyrene plate and scanning from 390 to 800nm using a Tecan infinite 200Pro plate reader.

Chemical oxygen demand (COD) analysis, samples from the SVOC leaching study were analysed using the LCI400 Hach cuvette test according to ISO 15705. High salinity values (thus high chlorine concentrations) can negatively impact COD analysis, as Freire and Sant'Anna [180] suggest when using the closed acid reflux colorimetric method; this was expected for the samples from the salinity-based leaching process. This issue was dealt with by adding a larger quantity of $HgSO_4$, thus promoting the formation of HgCl. For each analysis 1.25mL of each sample was transferred to COD digestion tubes. High salinity value samples were diluted 1:3 with milli-Q water to further reduce the effect of high chlorine. Afterwards, 0.75mL of solution D2 and 1.75mL of solution D1 were added to the digestion tube. The tubes were shaken and then put in a block digestion tube for 2hours. After digestion the tubes were shaken and allowed to cool down to room temperature before analysis and any particles were allowed to settle. Each tube was then placed on HACH DR2800 spectrophotometer and the absorbance was measured at 600nm. Each sample was digested twice, with each replicate running in the same reaction batch, including standards. Sample concentrations were

calculated with the batch's calibration curve and the mean of the two replicates was used for results. Total COD values were calculated by removing the value of the blank.

7.2.5 SVOC extraction from leachates

Water leachates were analysed with the waste-water extraction method that was developed and reported in Chapter 3. Following filtration, 9mL of each sample were transferred to a 15mL glass centrifuge tube, spiked with 10uL of the surrogate solution and 0.225g of Na_2SO_4 were added into each tube and then vortexed until all the salt was diluted. Then the pH of each solution was adjusted to <2 using HCl and 9uL of the 2.2mmol CTAB solution were added to a resulting CTAB concentration of 0.0022mmol. Following brief vortexing 170uL of CPME were added into the solution, the tube was mounted on the vialtweeter sonotrode and then sonicated for 28s at 40W with a 50%pulse. Phase separation was performed by centrifuging at 2500rpm for 7min. The aqueous phase was transferred to a new 15mL tube and 1.125g of Na_2SO_4 were added and vial was vortexed until all the salt was dissolved. Following salt dissolution, the pH was adjusted to >12 using KOH and 60uL of CPME were added into the solution and the tube was mounted on the sonotrode and sonicated for 28s at 40W with a 50%pulse. The tube was then centrifuged at 2500rpm for 7min, the aqueous phase was discarded, and the organic phases combined in a 1.5mL autosampler vial and stored at -24°C. Each extraction was performed in duplicates.

7.2.6 Gas chromatography analysis

The leachate extracts from the SVOC leaching process were analysed using targeted GC-MS for recovery determination, un-targeted GC-MS for total SVOC analysis and GCxGC-TOFMS for both un-targeted and polarity percentage analysis. The extracts were also derivatised in order to provide a graphical comparison for derivatisable components. The methods used for each analysis are the same those described in Section 6.2.

7.2.7 Data analysis

Details for the data processing flow for statistical analysis are given in Chapter 5. All peaks areas were normalised to the actual weight of the added tar (surrogates and standards excluded). Instrumental variation and sample stability were monitored with the use of relative standard deviations and quality control charts for the internal standards (Figure A.5.2). Effectiveness of internal standard normalisation was assessed using a control chart for the response factor of the second internal standard. The internal standard used for normalisation for the untargeted analysis was naphthalene-d8. Components were firstly matched in

AMDIS with an in-house built compound database that includes 53 individual compounds. Features that are identified with a standard are indicated with a star next to their name. Consecutively additional identifications are made for the unidentified components by comparing component spectra with spectra from the NIST11 spectral database using an 80% spectra match. Features identified with a match below 80% and unlikely identifications are given a question mark.

7.3 Results and discussion

7.3.1 Salinity-based leaching from UCG tars

Visual observation of the leachates from the salinity experiment shows a yellow tint with an increasing intensity as the salinity increases (Figure 7.1, **top**). Also, after the removal of the leachates, the tar's consistency appears slightly different (Figure 7.1, **bottom**) with the tar that came into contact with the high salinity water appearing less aggregated.

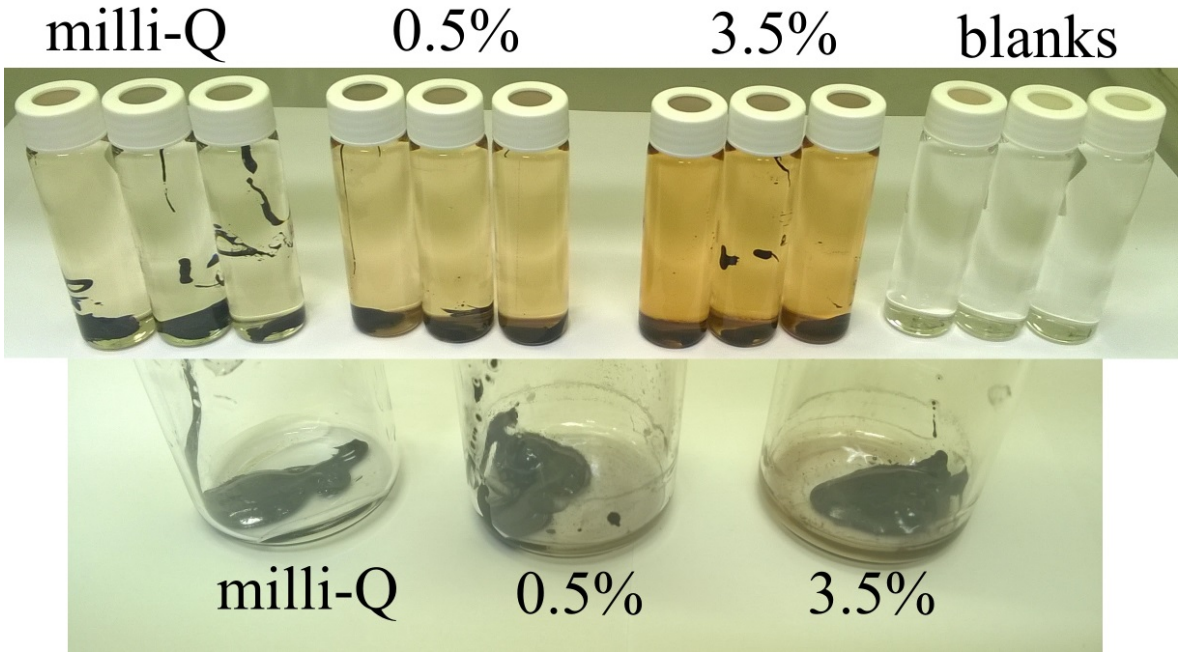

Figure 7.1: UCG tar leachates. On top are leachates before removal for the sample container. At the bottom are UCG tars after the removal of the leachate. Indication 0.5% and 3.5% refers to salinity in the leachates

Analysis of aggregate organic constituents in leachates can be seen in Figure 7.2. The calibration curve for the COD analysis can be seen in Figure A.5.1. Values for TOC (Figure 7.2, A) and COD appear to be decreasing as salinity increases. A one-way ANOVA analysis

shows that difference between each of the three means is statistically significant. This reduction in organic constituents could be attributed to the increased salinity of the water in which organic compounds are expected to have reduced solubility[98]. However, as mentioned above, increasing salinity shows an increase in the colour of the leachate. Further analysis of the samples on the visible spectrum gave the absorption spectra given in Figure 7.3 where a significant absorption can be seen close to 490nm in both 0.5% and 3.5% salinity leachates. Since aggregate organic constituents in the leachates are reduced as the solubility increases, further research is needed to determine which components are responsible for the absorption increase in the visible spectrum. A similar colour can be seen in the leachate from UCG as it appears in Figure 7.4 so it can be assumed that this is a phenomenon related to UCG tar (or possibly tars deriving from similar processes).

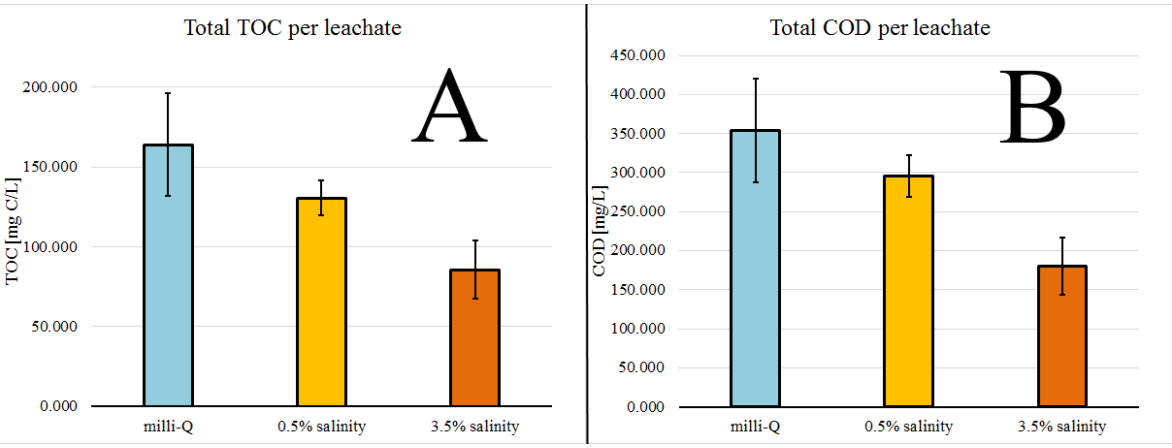

Figure 7.2: Aggregate organic constituents in UCG tar leachates, TOC (A) and COD (B)

Regarding SVOCs in the salinity-based leachates, the method developed in chapter 3 cannot be applied directly in the case of these leachate as the salinity is significantly different with possible effects on the performance of the extraction method. This must be studied further, possibly leading into further development/modification of the method. However, as shown above, TOC and COD values have a strong linear correlation with the bulk of the SVOCs in all tar leachates so the same is expected to apply in the salinity-based leachates since the effect of the salinity is accounted for by removing the corresponding values of the blanks. Thus, it is expected that an increase in the salinity of the water may bring a reduction in the amount of SVOCs that will leach into the water from the tar phase.

7.3.2 SVOC leaching from different tar types

Visual observation of the leachates from UCG tar show a slight yellowish tint while the rest of the leachates appear colourless (Figure 7.4). This can be attributed to the existence of sub-humic acids (see Section 2.3.1) in the UCG tar. Recovery values for surrogates are given

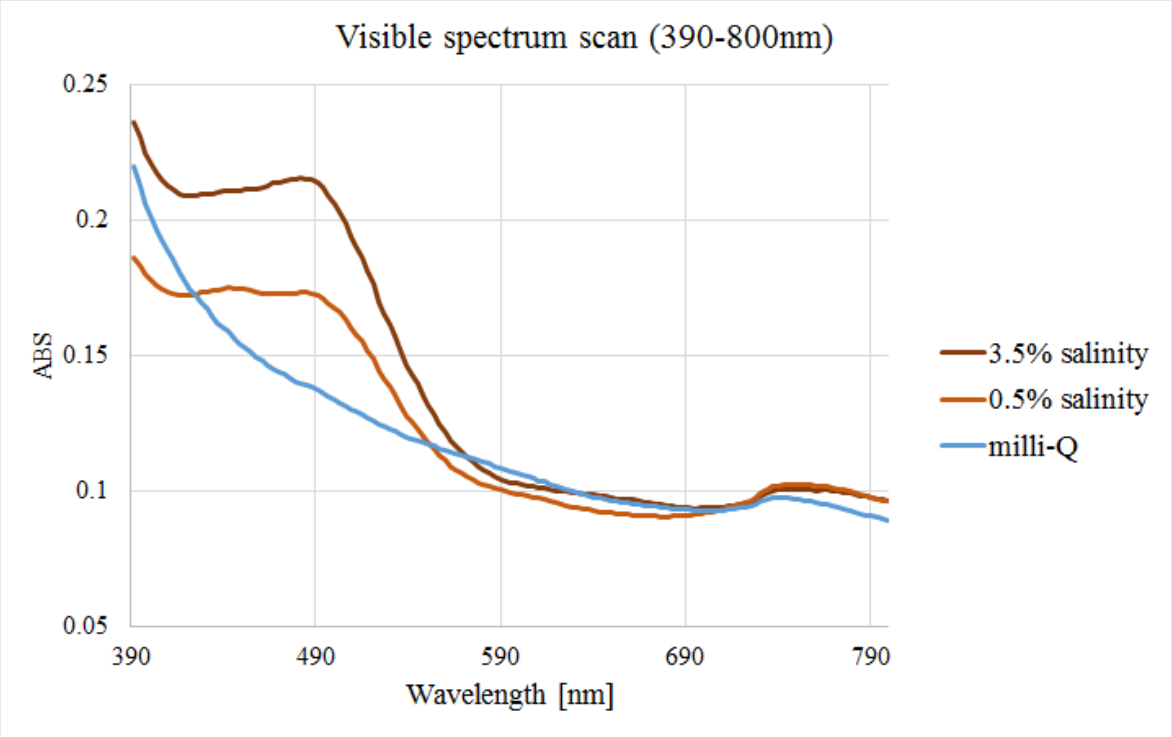

Figure 7.3: Leachate absorption spectra in the visible range

in Figure 7.5. Recovery values for all leachates are in line with the expected recovery values as they were established during method development for low solvent level.

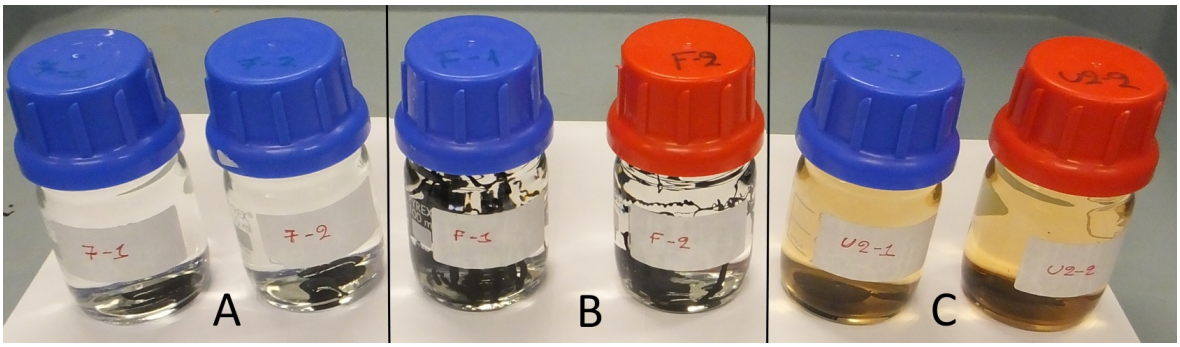

Figure 7.4: Leachates from **A:** weathered former manufactured gas plant tar **B:** pitch **C:** UCG tar. The leachates from WFMGP tar and pitch are colourless while UCG tar leachate has a slight yellowish tint

Instrumental variation and sample stability during untargeted analysis was assessed with the two internal standards phenol-d6 and naphthalene-d8. Assessment of the peak areas show the relative standard deviations in all extracts for the internal standards are 17.80% for phenol-d6 and 15.66% for naphthalene-d8. After subtraction of the peak area of naphthalene-d8 the relative standard deviation for the peak area ratio for phenol-d6 is reduced to 1.76%. Corresponding control charts for both peak areas and peak area ratios appear in Figure A.5.2. At this point it can be safely assumed that normalisation using naphthalene-d8 will significantly

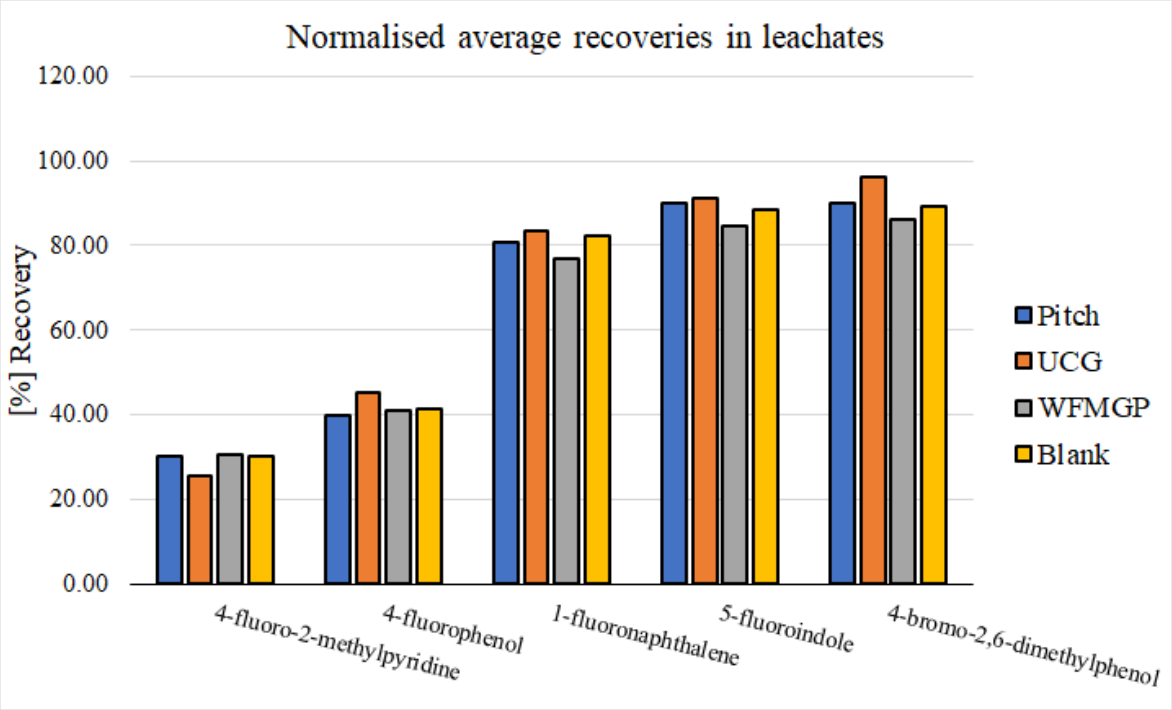

Figure 7.5: Recoveries of the surrogates from the extraction of SVOCs from leachates into CPME. All recoveries are within the expected recovery range as established during method development

reduce instrumental variation in the samples. This is shown in Table 7.2 where the reduction in RSD from peak area to peak ratio ranges from 6.89% for 4-fluoro-2-methylpyridine (17.98% to 11.09%), to 16.04% for phenol-d6 (17.8% to 1.76%).

Table 7.2: Peak areas and peak ratios of surrogates and internal standards before and after normalisation with naphthalene-d8. Where: 4-f-2-mp is 4-fluoro-2-methylpyridine, ph-d6 is phenol-d6, nap-d8 is naphthalene-d8, 5-f-ind is 5-fluoroindole and 4-br-2,6-dmp is 4-bromo-2,6-dimethylphenol

Peak areas

	4-f-2-mp	ph-d6	f-nap	nap-d8	5-f-ind	4-br-2,6-dmp
Average	4674951	2069582	37274144	5194887	25337156	3137014
Stdev	840650	368286	5838893	896563	3894194	483206
RSD[%]	17.98	17.80	15.66	17.26	15.37	15.40

Peak ratios

	4-f-2-mp	ph-d6	f-nap	5-f-ind	4-br-2,6-dmp
Average	0.902	0.398	7.199	4.899	0.607
Stdev	0.1	0.007	0.37	0.309	0.043
RSD[%]	11.09	1.76	5.14	6.31	7.08

The component selection process resulted in a combined list of 234 individual components, including internal standards, surrogates and solvent components. Initially, data analysis was performed by fitting a PCA model to the data so that a first assessment can be made on how

well classes are separated. The first and second component explain 96.9% of the variation. Pitch and UCG tar leachates group together very well (Figure 7.6), however leachates from WFMGP tar are not grouped together at the same degree. However, surrogates and internal standard group very well on a tight area around the 0,0 point of the loadings plot (Figure 7.7, **top right**), indicating that the degree of variation introduced by the extraction and analysis process is minimal and that most of the variation explained by the model is due to the chemical composition of the leachates.

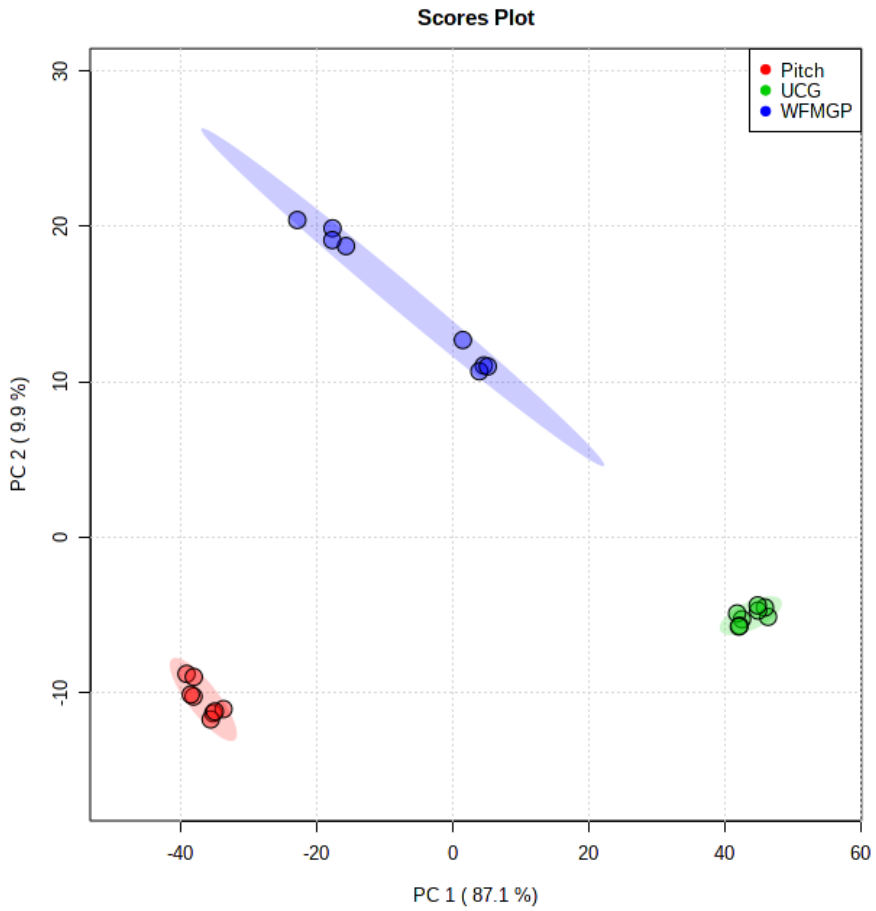

Figure 7.6: Scores plot from the PCA model that was fitted to the leachate data. Coloured regions around samples correspond to the 95% confidence interval regions for the PCA model. By studying the plot one can see that the groupings for pitch and UCG tar leachates is much better that those from WFMGP leachates.

Suboptimal grouping of the WFMGP leachates can be explained by the leaching process not being as reproducible as leaching from pitch and UCG tar. This becomes clearer in the heatmap in Figure 7.8; there are obvious differences in the levels of some features between the two WFMGP tar leaching replicates (W1 and W2) as indicated by the colour of the corresponding features. Any differences between the two leaching replicates from pitch and UCG tar are far less visible. This may be attributed to the fact that the WFMGP tar is much more viscous and appears drier, so a lesser degree of homogeneity is expected in comparison

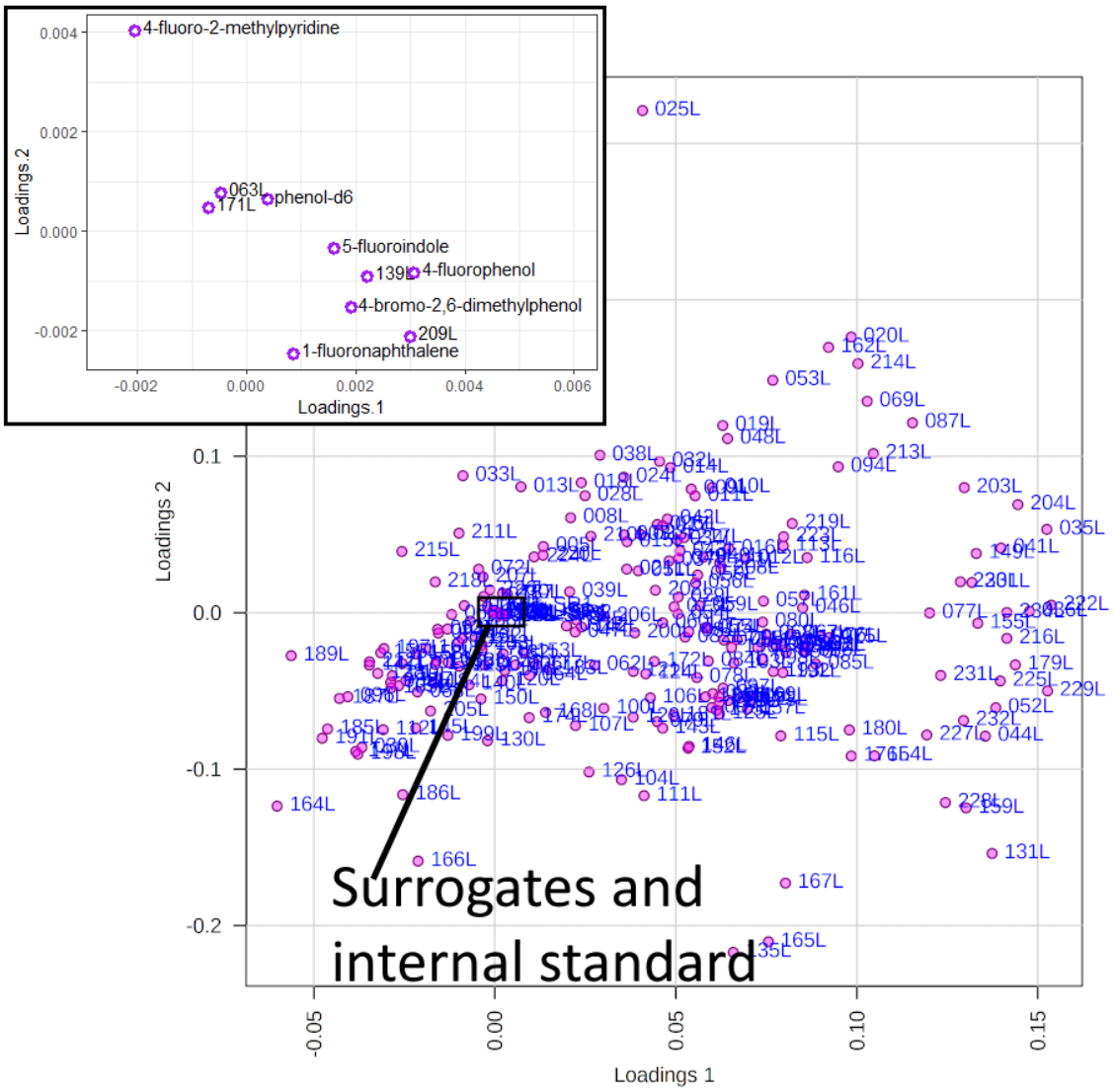

Figure 7.7: Loadings plot from the PCA model that was fitted to the leachate data. The zoom in region on the top left corner shows that the surrogates and the internal standard are grouped on a small area around the 0,0 point of the graph

to the other two tars which are much less viscous.

Fitting a PLS-DA model on the dataset yields a very similar scores plot (Appendix Figure A.5.4). Although PLS-DA considers class information to fit the model, class separation remains very close to those from the PCA model. The top 25 components ranked by the model are given in Figure 7.9. Feature 025L appears to be at the top of the list and it also appears to be the one contributing more to class separation in the PCA model as can be seen by the PCA biplot (Appendix Figure A.5.5). However, feature 025L maybe also be contributing to explain variation between the two leachate replicates from WFMGP tar since the orientation of the corresponding vector in the bi-plot is directed towards the WFMGP class.

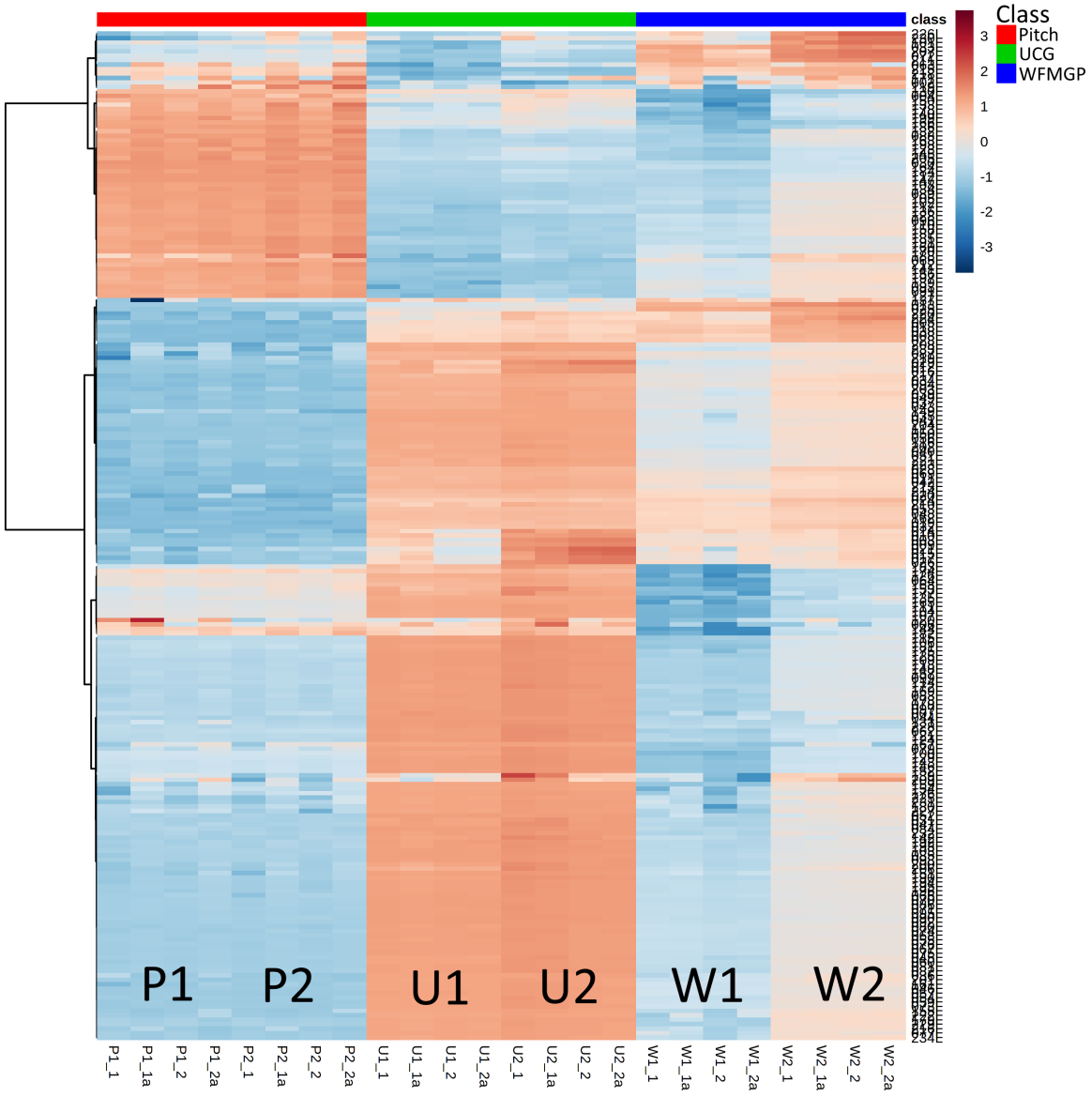

Figure 7.8: Heatmap of all of the studied features in the leachates from WFMGP tar, UCG tar and pitch. There is a obvious difference in the levels of the two leachate replicates from WFMGP tar. An elongated version of the heatmap is provided in Appendix Figure A.5.3

As the PLS-DA model does not produce a significantly different class separation than PCA, a sparse PLS-DA (sPLS-DA) model was fitted by taking into account the first two components and using the top 10 variables. As can be seen by the scores plot, that sPLS-DA model produced a much clearer class separation. Furthermore, it appears that the first component explains the variation in a way that can be attributed to the degree of tar weathering/processing since UCG is freshly produced tar from gasification, WFMGP tar is expected to lose a lot of the volatile content due to weathering and pitch is actually a distilled tar where most of the volatiles have been removed during distillation. Interestingly, the second component explains variation between WFMGP tar and pitch-UCG tar together. It is therefore interesting to produce loading scores for both components (Figure 7.9, B & C).

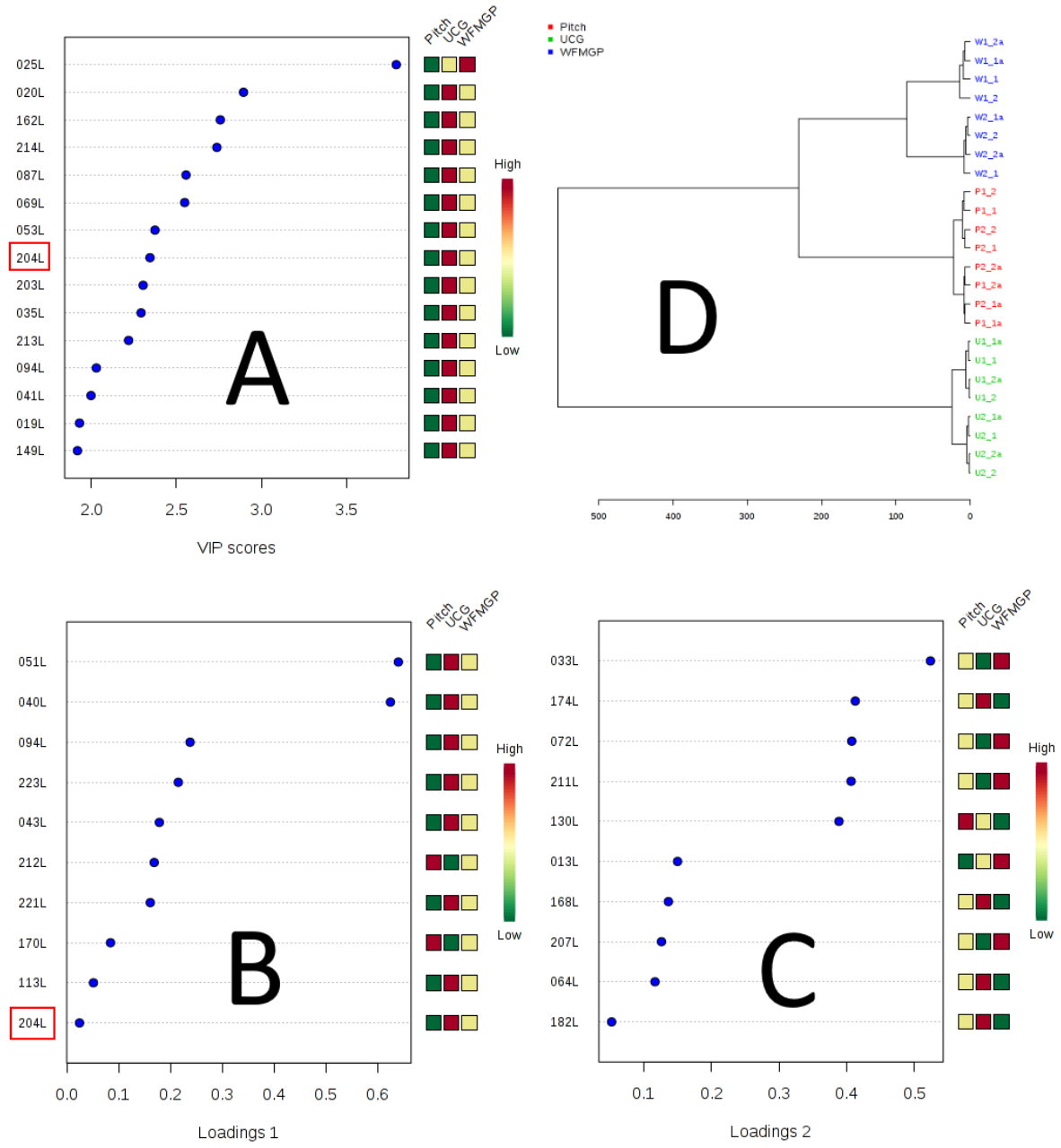

Figure 7.9: **A:** VIP scores from the top 15 features as ranked by the PLS-DA model (with embedded heatmap) **B:** top 10 features with the highest loadings for the 1st component as ranked by the sPLS-DA model (with embedded heatmap) **C:** top 10 features with the highest loadings for the 2nd component as ranked by the sPLS-DA model (with embedded heatmap) **D:** hierarchical clustering of the leachates from all three tar classes using Pearson's r as the distance measure - Features that appear in more than one ranking plot are indicated with a red square

Table 7.3: Top ranked features by the PLS-DA and the sPLS-DA models provided along with the corresponding VIP and loading scores from each model. For the PLS-DA model the top 15 features are given for the first component and for the sPLS-DA model 10 features are given for each one of the two components. The table includes also information regarding the level of each compound in a leachate class where **L** stands for low level, **M** for medium level and **H** for high level

#	Index	Comp. 1 (PLS-DA)	Comp. 1 (sPLS-DA)	Comp. 2 (sPLS-DA)	Compound	Pitch	UCG	WFMGP
1	025L	3.7921	-	-	Octanol	L	M	H
2	020L	2.8948	-	-	C2-benzene	L	H	M
3	162L	2.7587	-	-	Acenapthylene	L	H	M
4	214L	2.7384	-	-	Dibenzofuranol	L	H	M
5	087L	2.5574	-	-	C4-phenol	L	H	M
6	069L	2.5493	-	-	Benzofuran	L	H	M
7	053L	2.375	-	-	C4-benzene	L	H	M
8	204L	2.3457	0.024382	-	C2-naphthol	L	H	M
9	203L	2.3052	-	-	C2-naphthol	L	H	M
10	035L	2.2934	-	-	C3-cyclopentenone	L	H	M
11	213L	2.22	-	-	Dibenzofuranol	L	H	M
12	094L	2.0306	0.23798	-	C3-phenol	L	H	M
13	041L	1.9994	-	-	C3-cyclopentenone	L	H	M
14	019L	1.9319	-	-	C3-benzene	L	H	M
15	149L	1.9197	-	-	C5-benzene	L	H	M
16	051L	-	0.64024	-	C4-benzene	L	H	M
17	040L	-	0.62493	-	Acetophenone	L	H	M
18	223L	-	0.21518	-	Hydroxyfluorene	L	H	M
19	043L	-	0.17865	-	C2-phenol	L	H	M
20	221L	-	0.16103	-	Hydroxyfluorene	L	H	M
21	113L	-	0.051289	-	Indenol	L	H	M
22	212L	-	-0.16864	-	Acridine	H	L	M
23	170L	-	-0.084309	-	Dibenzofuran	H	L	M
24	174L	-	-	0.41264	Hydroxybiphenyl	M	H	L
25	130L	-	-	0.38847	C2-naphthalene	H	M	L
26	168L	-	-	0.13637	C2-indole	M	H	L
27	064L	-	-	0.11655	C1-benzonitrile	M	H	L
28	182L	-	-	0.052372	Naphthonitrile	M	H	L
29	033L	-	-	-0.52377	C3-pyridine	M	L	H
30	072L	-	-	-0.40741	Benzothiophene	M	L	H
31	211L	-	-	-0.40646	Benzoquinoline	M	L	H
32	013L	-	-	-0.14986	C3-benzene	L	M	H
33	207L	-	-	-0.12613	Phenanthrene	M	L	H

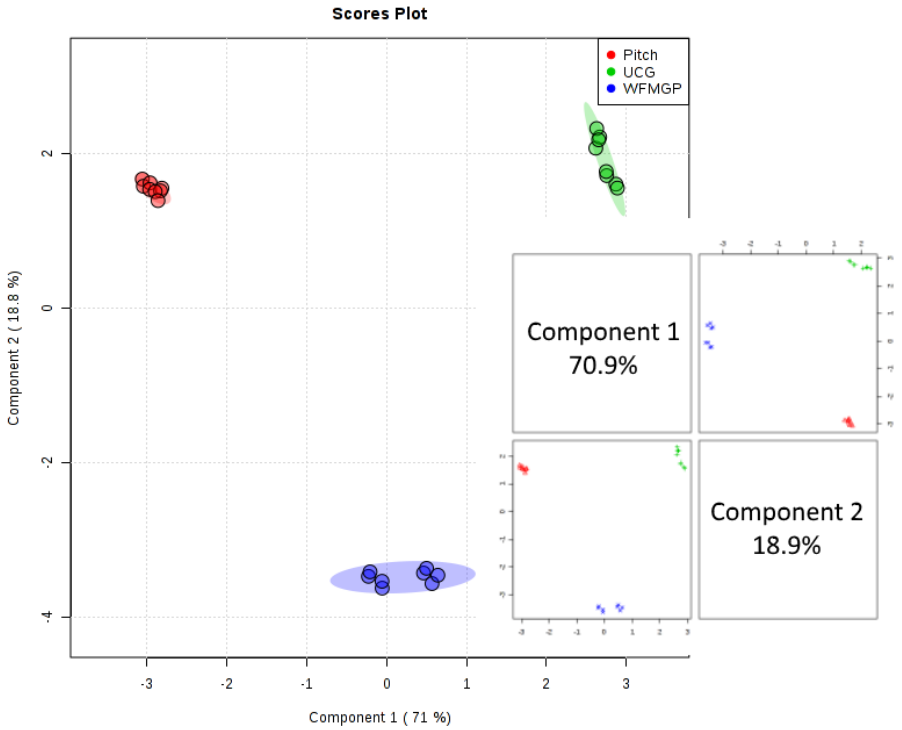

Figure 7.10: Scores plot produced from the sPLS-DA model along with percentages of variation explained by each component

Most of the compounds that are ranked high in the PLS-DA model are oxygen containing compounds (10 out of 15 - Figure 7.9, Table 7.3) and all of them follow the same pattern, high levels in UCG tar, medium levels in WFGMP tar and low levels in pitch. One exception is octanol that has high levels in WFMGP tar. Since this compound in the UCG tar and pitch leachates is almost non-existent, its origin would be of interest as, to the author's knowledge, it has not previously been reported in gasification literature. The other hydrocarbons follow the same pattern as in the oxygen containing compounds. This further adds to the assumption that the first component of the PCA describes the degree of weathering/processing as oxygen containing compounds are known to reduce with weathering. The same trend appears in the case of the first components of the sPLS-DA model however here acridine and dibenzofuran follow the oposite trend with high levels in pitch and low levels in UCG tar. The second component of the sPLS-DA model tells a different story where some features appear low in WFMGP tar and high in UCG tar (nitriles and hydrocarbons) and the opposite (benzothiophene and benzoquinoline). No observation on weathering can be made here but it could be these differences are traceable in the structure of the coal of origin.

A component driven, pair-wise comparison would help to delve more deeply in the variation between classes. According to the first component of the sPLS-DA model, there is more variation between UCG tar and pitch. This is further confirmed by looking at the hierarchical clustering of the three classes (Figure 7.9D) where pitch clusters with WFMGP tar leaving

UCG tar the most dissimilar of the two.

An appropriate multivariate technique to perform a statistical comparison between UCG tar and pitch is orthoPLS-DA (oPLS-DA). An oPLS-DA model was fitted to the data originating from these two classes and the scores plot from the fitted model is provided in Figure 7.11. The t-score (horizontal axis) corresponds to the between-classes variation and the orthogonal score to within-classes variation. Cross validation of the model shows good values for all three metrics (R^2X, R^2Y, Q^2) which continue to be significant even after a 2000 permutations test (Figure Appendix A.5.6) so the model appears to be valid.

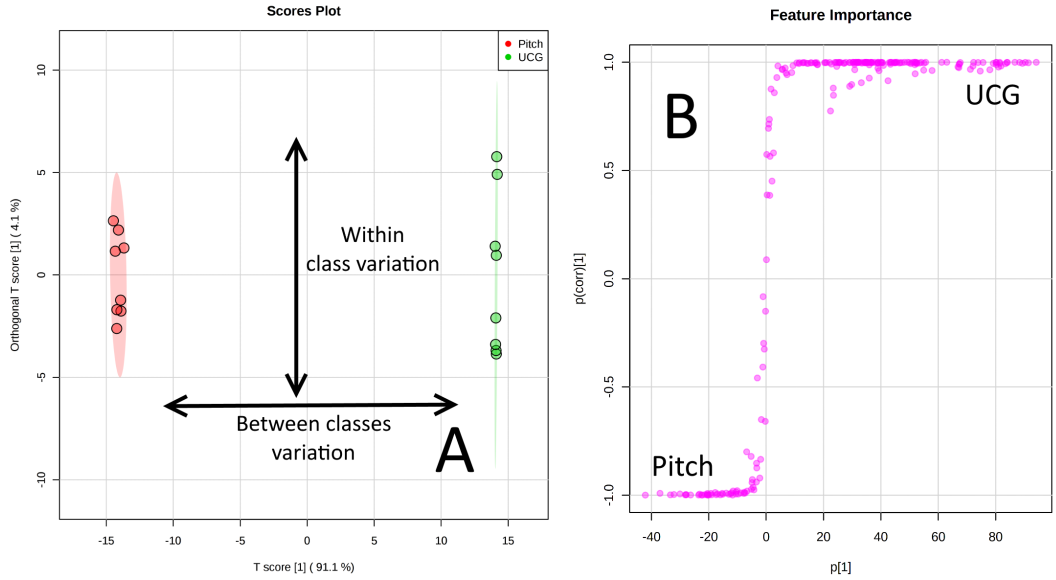

Figure 7.11: A: Scores plot from the oPLS-DA model depicting variation within a class and between classes **B:** S-plot generated from the oPLS-DA model

The s-plot that appears in Figure 7.11 combines covariance and correlation from the orthoPLS-DA model. The horizontal axis describes the magnitude of a variable and the vertical axis the correlation of each variable. Features with high magnitude contribute more to class variation and a high absolute correlation values represents higher reliability. Consecutively, ideal markers exhibit high reliability and high magnitude. By studying the plot one can see that the majority of the features are reliable and a significant number of features have a high magnitude as well. As it appears, UCG tar includes more features with a high magnitude than pitch (171 features with positive correlation and 62 features with negative correlation). Table 7.4 includes the top 20 features with the highest magnitude for both UCG tar and Pitch.

Two additional oPLS-DA models were prepared for performing comparisons for the rest of the pairs: WFMGP-UCG and Pitch-WFMGP (Figure A.5.7). Features correlated with UCG tar have an, overall, higher reliability (Table 7.5). Probably the most important finding from the table is that features that have a high correlation with WFMGP tar are mainly nitrogen containing heterocycles. This is similar with results provided in Table 7.4, where nitrogen

Table 7.4: Top ranked features from the first oPLS-DA model. **Left** of the table are the features that have positive correlation and higher magnitude in UCG tar leachate and on the **right** side of the table are those features that have a negative correlation and higher magnitude in pitch leachates. Compounds marked with * are identified with standards while compounds marked with ? are tentatively identified. The rest of the compounds are library matches.

	Top ranked UCG tar features				Top ranked pitch features			
#	Index	p[1]	p(corr)	Compound	Index	p[1]	p(corr)	Compound
1	035L	94.158	0.9995	C3-cyclopentenone	164L	-42.084	-0.9995	Acenapthene
2	222L	91.416	0.9973	N/A	189L	-36.973	-0.9913	Napthaleneamine
3	204L	90.339	0.9992	C2-Naphthol	191L	-33.355	-0.9984	Phenlylpyridine
4	036L	89.339	0.9949	C2-cyclopentenone	185L	-32.117	-0.9969	Phenlylpyridine
5	229L	88.348	0.9990	N/A (oxygen inc)	187L	-30.020	-0.9943	Napthaleneamine
6	041L	86.699	0.9994	C3-cyclopentenone	096L	-28.171	-0.9985	Quinoline
7	234L	84.096	0.9990	N/A (quinone)	198L	-27.887	-0.9970	1-Acenapthenol
8	179L	83.932	0.9992	Naphthalenecarbonitrile	147L	-27.861	-0.9980	C1-indole
9	216L	83.459	0.9934	Biphenyldiol	030L	-26.300	-0.9991	Indane
10	149L	81.884	0.9825	C5-benzene	141L	-23.500	-0.9992	C2-quinoline
11	203L	81.468	0.9946	C2-Naphthol	212L	-23.220	-0.9949	Acridine
12	052L	81.408	0.9994	Hydrocarbon	112L	-22.506	-0.9989	Indole
13	225L	81.006	0.9777	Biphenol	128L	-22.246	-0.9995	C1-quonoline
14	201L	80.302	0.9991	C2-naphthol	156L	-21.309	-0.9973	C2-quinoline
15	131L	80.210	0.9892	C1-diol	197L	-20.634	-0.9971	Nitrosocarbazole
16	044L	80.108	0.9994	N/A (oxygen inc)	186L	-20.446	-0.9920	Diphenylmethane
17	155L	79.168	0.9945	Indanone	105L	-20.416	-0.9989	C1-quinoline
18	233L	77.978	0.9651	N/A (oxygen inc)	089L	-20.277	-0.9995	N/A (nitrogen inc)
19	232L	75.609	0.9988	Biphenol	110L	-19.866	-0.9982	C1-quinoline
20	087L	74.630	0.9591	N/A (phenol inc)	166L	-19.229	-0.9918	C3-naphthalene

containing heterocycles are also features that have higher correlation with pitch. On the other hand, features that are correlated with UCG tar appear to be be oxygen containing compounds and some hydrocarbons. This may suggest that the coal that pitch and WFMGP tars originate from had a higher nitrogen content, where the coal that the UCG tar originate from had a higher oxygen content. However, one has to take into account that oxygen containing compounds are more susceptible to heat and the weathering process. Regardless, the most substantial observation from the provided evidence is that there is clear differentiation between leachates from different tars that have undergone different process.

Since the comparison of UCG tar with both pitch and WFMGP tar yielded somewhat similar results the next step is to compare pitch and WFMGP tar leachates in order to identify which features can differentiate between these two. Table 7.6 provides the top 20 features from the oPLS-DA model that correlate with WFMGP tar (positive) and pitch (negative) leachates. The most obvious difference is that WFMGP tar appears to contain higher levels of oxygen containing compounds, something which adds to the hypothesis that the first component of the PLS-DA model describes increasing weathering/processing. On the other hand, features with high importance for pitch are mostly PAHs and nitrogen containing compounds. Since

Table 7.5: Top ranked features from the second oPLS-DA model. **Left** of the table are the features that have positive correlation and higher magnitude in WFMGP tar leachate and on the **right** side of the table are those features that have a negative correlation and higher magnitude in UCG tar leachates. Compounds marked with * are identified with standards while compounds marked with ? are tentatively identified. The rest of the compounds are library matches.

Top ranked WFMGP tar features					Top ranked UCG tar features			
#	Index	p[1]	p(corr)	Compound	Index	p[1]	p(corr)	Compound
1	025L	33.391	0.9888	Octanol	131L	-74.172	-0.9939	C1-diol
2	189L	18.465	0.9523	Napthaleneamine	228L	-65.656	-0.9979	Methylenediphenol?
3	033L	17.102	0.9542	C3-pyridine	044L	-59.957	-0.9682	Aliphatic ketone
4	215L	16.546	0.9852	Benzoquinoline	159L	-58.181	-0.8770	C5-benzene?
5	211L	12.078	0.9835	Benzoquinoline	229L	-56.494	-0.8736	N/A (oxygen inc)
6	013L	10.274	0.9544	C3-benzene	052L	-56.431	-0.9454	Hydrocarbon
7	187L	10.116	0.8021	Napthaleneamine	165L	-54.647	-0.9375	C3-naphthalenetetrahydro?
8	218L	9.9261	0.9683	Carbazole*	232L	-54.519	-0.9489	Methylenediphenol?
9	197L	9.3244	0.9250	Azafluorene	167L	-52.768	-0.9560	C4-azulene?
10	156L	9.2824	0.9114	C2-quinoline	135L	-52.691	-0.9369	C2-naphthalene?
11	212L	9.2565	0.9552	Acridine	225L	-51.73	-0.8954	Biphenol
12	141L	9.2259	0.9222	C2-quinoline	179L	-51.527	-0.8772	Naphthalenecarbonitrile
13	096L	8.8661	0.8494	Quinoline (or iso-)	036L	-50.854	-0.9380	C2-cyclopentenone
14	128L	7.5789	0.8828	C1-quinoline	222L	-49.622	-0.8612	Hydroxyfluorene
15	185L	7.4944	0.8732	Phenlylpyridine?	227L	-49.133	-0.8796	Biphenyldiol
16	191L	7.3517	0.8466	Phenlylpyridine	216L	-48.808	-0.8923	Biphenyldiol
17	072L	6.3767	0.9612	Benzothiophene	231L	-46.987	-0.9190	N/A
18	110L	5.947	0.7988	C1-quinoline	234L	-46.603	-0.8837	Phenylbenzoic acid?
19	089L	5.4893	0.7666	Quinoline (or iso-)	154L	-45.918	-0.8721	C4-Benzoic acid?
20	207L	5.2728	0.9286	Phenanthrene*	176L	-45.217	-0.9176	C1-hydroxyacetophenone

WFMGP tar has undergone weathering and pitch has undergone heat treatment, the existence of the nitrogen containing compounds in both leachates from these tars suggests these compounds are persistent to both weathering and heat treatment. Something worth mentioning is that acenapthene is at the top of the list for both Table 7.6 and Table 7.4 however it was missing from Table 7.3. This suggest the pair-wise comparisons using oPLS-DA models may provide additional information when comparing different classes which is beneficial when performing more detailed investigations between the composition of various leachates.

The amount of high polarity SVOCs in the UCG leachate (Figure 7.12) appears much higher that those in pitch and weathered FMGP tar. Judging by the fact the SVOCs that elute in the mid-high polarity area are mostly oxygen or nitrogen containing compounds, and taking into account the abundance of phenols in the UCG samples, the increase may be attributed primarily to phenolic content.

One leachate extract per tar type was also derivatised and analysed using GCxGC-TOFMS in order to have an overall picture of the derivatisable components within each leachate. This is similar to the low-polarity and mid-high polarity percentage analysis described above but

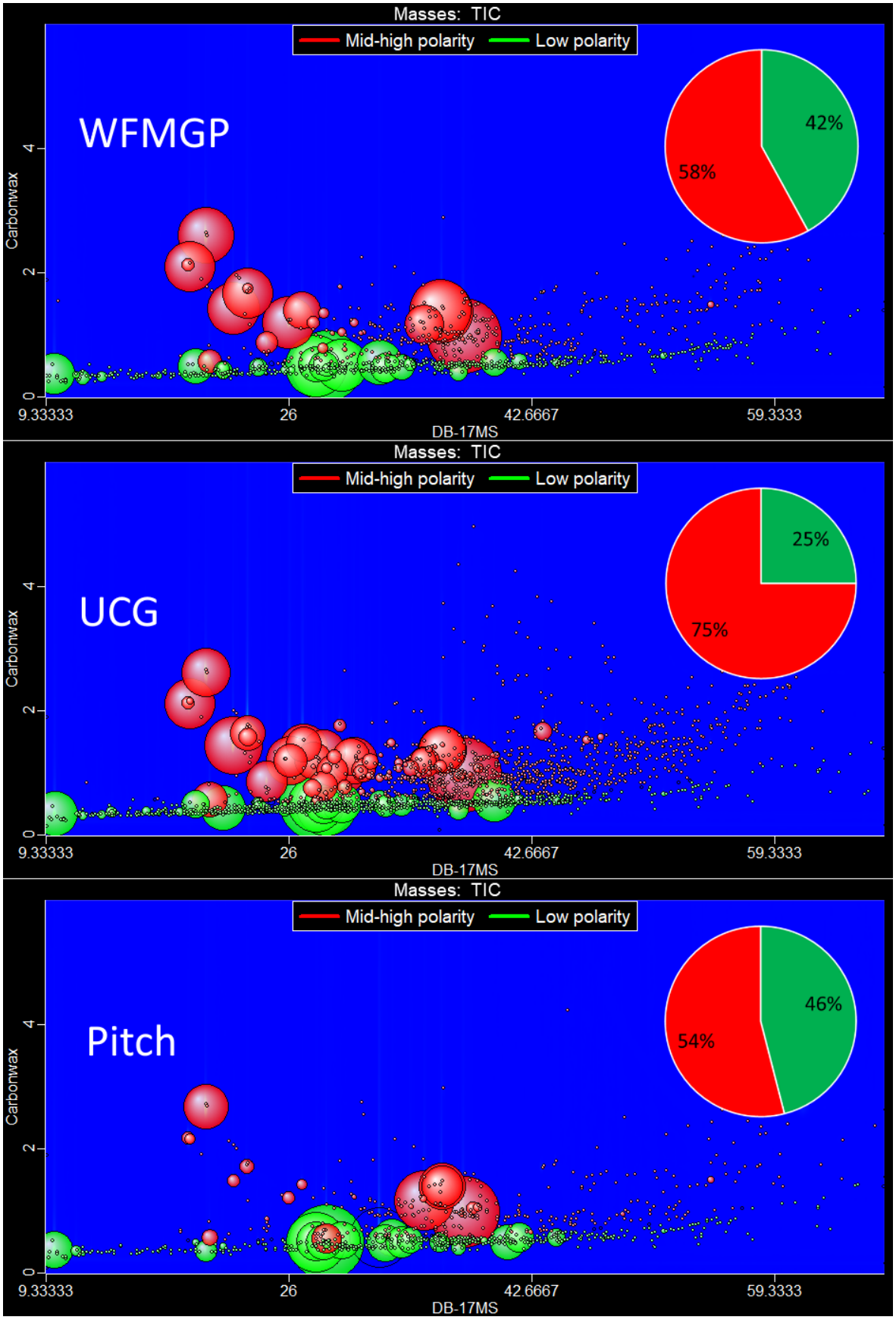

Figure 7.12: Indicative GCxGC-TOFMS chromatograms of the leachate extracts from three tar types: weathered former manufacturer gas plant tar, underground coal gasification tar and pitch. The applied processing method classifies each peak according to polarity and the total area percentages for polarity groups are shown in each chromatogram as a pie chart

Table 7.6: Top ranked features from the third oPLS-DA model. **Left** of the table are the features that have positive correlation and higher magnitude in pitch leachate and on the **right** side of the table are those features that have a negative correlation and higher magnitude in WFMGP tar leachates. Compounds marked with * are identified with standards while compounds marked with ? are tentatively identified. The rest of the compounds are library matches.

Top ranked WFMGP tar leachate features					Top ranked pitch leachate features			
#	Index	p[1]	p(corr)	Compound	Index	p[1]	p(corr)	Compound
1	025L	61.555	0.9990	Octanol	164L	-31.097	-0.9985	Acenapthene*
2	020L	47.025	0.9680	C2-benzene	166L	-30.168	-0.9927	C3-naphthalene
3	162L	44.774	0.9991	Acenapthylene*	186L	-23.738	-0.9878	Diphenylmethane
4	214L	44.475	0.9844	Dibenzofuranol	135L	-23.135	-0.7685	C2-naphthalene?
5	087L	41.457	0.9060	C4-phenol	191L	-21.18	-0.9783	Phenlylpyridine
6	069L	41.373	0.9880	Benzofuran	147L	-21.072	-0.9795	C1-indole
7	053L	38.56	0.9917	C4-benzene	198L	-20.939	-0.9580	Acenapthenol
8	204L	38.11	0.9487	C2-Naphthol	030L	-20.613	-0.9933	C3-benzene
9	203L	37.447	0.9400	C2-Naphthol	165L	-20.136	-0.7215	C3-tetrahydronaphthalene
10	035L	37.263	0.8996	C3-cyclopentenone	185L	-20.012	-0.9798	Phenlylpyridine?
11	213L	36.067	0.9553	Dibenzofuranol	112L	-17.496	-0.9786	Indole*
12	094L	32.957	0.9814	C3-phenol	187L	-15.781	-0.9190	Napthaleneamine
13	041L	32.479	0.9354	C3-cyclopentenone	145L	-15.764	-0.9729	C1-indole?
14	019L	31.368	0.9959	C3-benzene	096L	-15.4	-0.9507	Quinoline (or iso-)
15	149L	31.212	0.8617	C5-benzene	199L	-15.009	-0.9671	Acetylacenaphthene
16	222L	30.698	0.7359	Hydroxyfluorene	130L	-13.926	-0.9838	C2-naphthalene
17	048L	30.186	0.9965	C4-benzene	189L	-13.865	-0.9603	Napthaleneamine
18	201L	27.917	0.8746	C2-naphthol	167L	-13.708	-0.5309	C4-azulene?
19	233L	27.815	0.7756	C5-Azulenol?	205L	-13.246	-0.9655	Hydroxyfluorene?
20	036L	27.792	0.8165	C2-cyclopentenone	105L	-12.476	-0.9414	C1-quinoline

it is focused on the derivatisable components that are mostly phenols and some indoles. This can be used to further validate the hypothesis that the first component of the sPLS-DA model explains variation describing the reduction in the oxygen containing species. The amount of derivatised components is much higher in UCG leachate extracts and this can be seen throughout the chromatogram (Figure 7.13). It is also confirmed by the number of detected peaks for mass 73 and the sum of their areas. Extracts from leachates of WFMGP tar also seem to have more derivatisable material that those from pitch as it can be seen both by studying the figure in the red and yellow areas but also by the number of peaks and total peak area.

The leachates were analysed for aggregate organic constituents such as COD and TOC in an effort to correlate these parameters with SVOCs. As it appears, there is an obvious correlation between the chromatographic parameters and the aggregate organic constituents properties (Table 7.7). In order to formalise this correlation, linear models are fitted between the total peak areas and both COD and TOC. In all cases, correlation coefficients are higher than 0.95 indicating very strong correlations and suggesting that SVOCs as determined by chromatography are directly related to aggregate organic constituents.

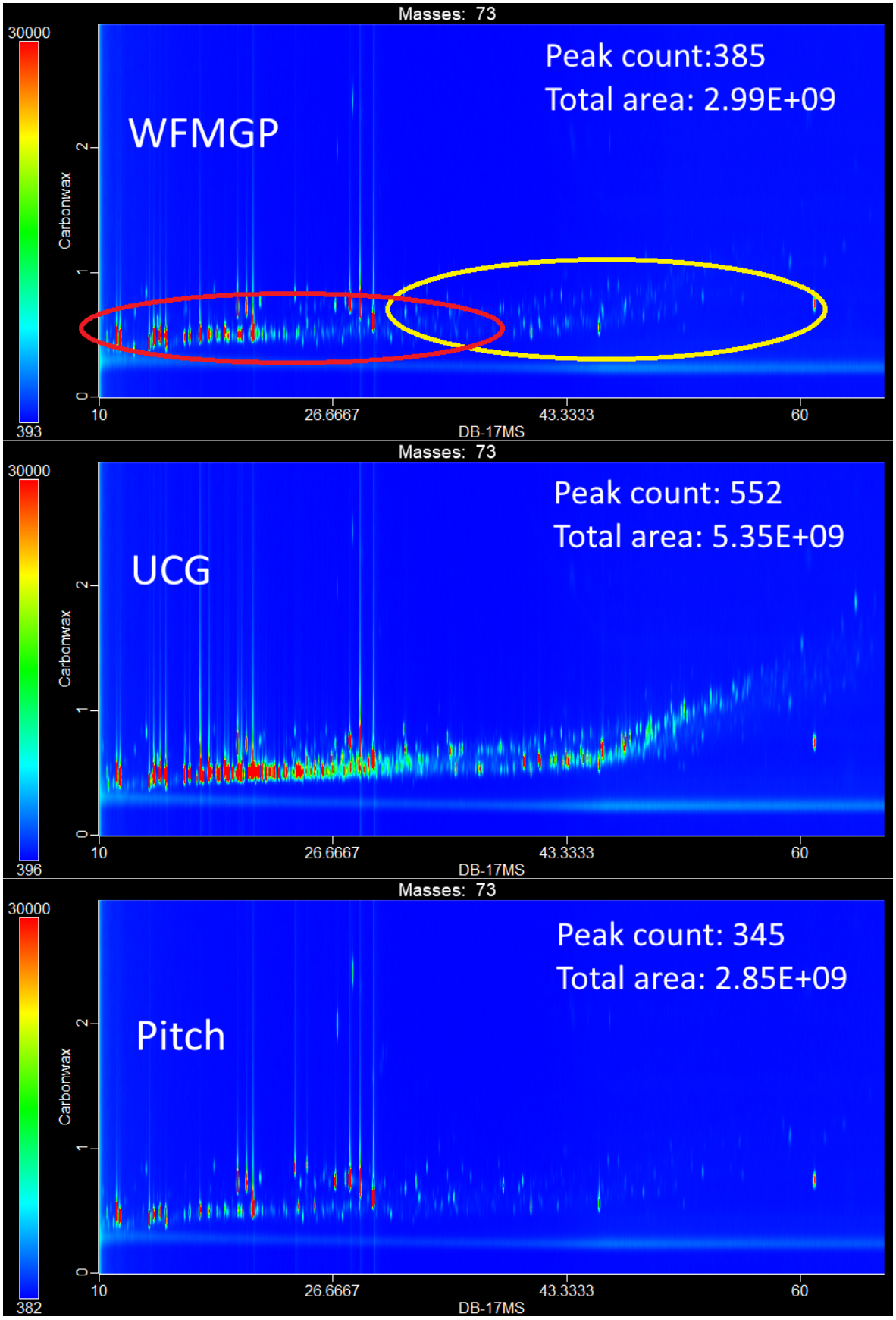

Figure 7.13: GCxGC-TOFMS chromatograms of the derivatised leachate extracts from the SVOC leaching process. It can be seen that the richest sample in derivatisable components is the leachate from UCG, both by studying the image but also from the peak count and the total area. Leachates from pitch and WFMGP tar do not exhibit very large visible differences but the latter appears to have more peaks and larger total area

Table 7.7: text

Sample	Totak area (GC-MS)	Total area (GCxGC-TOFMS)	COD mg/L	TOC mg/L
W1	581020865.4	5776286210	119	37
W2	1281465168	8383064486	211	67
U1	2493478095	13995160401	539	169
U2	2827388075	13997516201	526	166
F1	1031942475	7161188219	140	48
F2	1155026054	7999313512	168	54
Corr.-TOC	0.9647	0.9869	-	-
Corr.-COD	0.9586	0.9838	-	-

7.4 Conclusions

The clear grouping of the leachates that originate from different tar types further confirms that the developed method can be used for the classification of leachates from different origins. As indicated from the statistical analysis performed above, leachates from different types of tar can be statistically differentiated from their SVOCs signature. This leads to the conclusion that the leachates carry the chemical information of the tar that they originated from. Since leachates are expected to be a more concentrated form of contaminated groundwater, the evidence suggests that ground-water can be potentially used, along with tar, for source appointment.

A decrease in the solubility of organic matter with increasing salinity was observed with the effect possibly extending for SVOCs. The yellow tint that was observed in leachates of UCG tars may be attributed to sub-humic acids, however the increase in the intensity of the leachate colour with increased salinity is worth further investigation.

The statistical methods that were applied in Chapter 5 to identify compound markers and compound group trends were used here to provide insight into the chemical variation between the different types of samples, allowing for the elucidation of their chemical complexities.

The application is not limited in the analysis of leachates but may be further expanded in other samples, for example: groundwater that originates from contaminated sites, wastewater from different coal conversion processes, aqueous liquor from digestate pyrolysis for biomass production and partitioning water from tar/contaminated soil biog-degradation studies.

Chapter 8

Conclusions and future work

8.1 Research objectives

The research objectives that were identified during the introduction are as follows:

- Develop a fast and precise method, based on ultrasound-assisted liquid-liquid extraction, for the analysis of UCG produced waste-water without the need of fractionation; optimise gas chromatography (GC) set-ups for the analysis of these samples using GC-MS and GCxGC-TOFMS.
- Develop a method for the fast and precise analysis of UCG produced tars, based on ultrasound-assisted extraction, without the need of fractionation and the use of multiple techniques; optimise GC set-ups for the analysis of these samples using GC-MS and GCxGC-TOFMS.
- Develop a miniaturised method, based on ultrasonication, for the derivatisation of the sample extracts from the previously developed methods in order to further enhance their GC-MS and GCxGC-TOFMS analysis
- Apply data analysis approaches that can unravel the complex chemical data produced from the methods, determine chemical differences between samples and suggest SVOCs as markers/global indicators during UCG
- Test the behaviour of UCG produced tars when in contact with water with a series of leaching experiments

8.2 Conclusions

Several novelties were introduced with this thesis in the field of analytical chemistry. First is the use of CPME for analytical LLE, which, to the author's knowledge has not been used in the past in this capacity. CPME proved to be a superior solvent in the extraction of polar compounds from water when compared to traditional low-density solvents; this may help broaden the use of LLE into the extraction of compounds from water that would otherwise require the use of a different technique for extraction, e.g. solid phase extraction. The thesis introduces the high-intensity indirect vessel-wall sonication (HIVS) technique into the field of analytical chemistry. HIVS has the advantage, over traditional sonication techniques, of delivering ultrasonic irradiation directly into the contents of a vessel without the need to insert a probe into the vessel and without the energy losses that are associated with ultrasonication baths. The technique was adapted for use with three sample preparation techniques: liquid-liquid extraction, assisted solvent extraction and derivatisation; it was shown to enhance the extraction process in all cases. Another novelty is the use of a semi-polar to very polar GCxGC set-up. This set-up was shown to separate mixtures of polar compounds that would otherwise have limited separation with conventional normal phase or reverse phase set-ups.

The development of three ultrasound assisted sample preparation methods is described in the thesis that aid in the analysis of effluents from underground coal gasification. An untargeted ultrasound-assisted surfactant-enhanced salting-out emulsification micro-extraction (UASESOEME) method was developed for the close-to-exhaustive analysis of SVOCs in coal gasification waste-water. The method was shown to be fast and precise and able to provide results in less than two hours without the need for fractionation by using a polar normal phase GCxGC set-up. Coal tar was extracted by utilising ultrasound-assisted extraction (UAE), in a very fast, precise and representative way and was further analysed by applying a conventional reverse phase GCxGC set-up. This approach does not required lengthy and time consuming fractionations. The method can provide results in approximately an hour. Although DCM was used, the potential of CPME as an extraction solvent was also demonstrated. Lastly, gas chromatographic analysis in both of the above methods was enhanced by an ultra-fast ($<$1 minute) and precise miniaturised ultrasound-assisted derivatisation (UAD) method that significantly expanded the applicable SVOC range for the methods. All the developed methods were proven successful in the analysis of both waste-water and tar samples that derived from UCG trials and from coal tar leaching experiments. The suggested analysis suite provides fast SVOC characterisation in the production stream of a UCG of similar gasification trial.

A data processing methodology was developed and applied for the processing of data deriving from time-series UCG trials and leaching experiments from three tars (UCG tar, weath-

ered FMGP tar & pitch) that were extracted and analysed using the methods developed in the thesis. The data was subjected to exploratory data analysis using methodologies that are commonly used in other fields in order to search for features/compounds in the data that are either strongly associated with the gasification process or describe the chemical variation between sample classes. Regarding the time-series samples several compounds were identified and listed as possible global indicators, none of which was amongst those that are commonly used for modelling pyrolysis or relevant processes. On the other hand, analysis of tar leachates showed that these can be differentiated statistically as they carry chemical information of the tars that they originated from; however, the evidence shows that tar is a more representative matrix for UCG. Results also suggest that tars that have been weathered or heavily processed (like weathered FMGP tar and pitch) continue to leach SVOCs in the water and that the solubility of the SVOC species in the tars depends on the salinity of the water.

Overall, the applied methods, from sample preparation to data analysis, give insight in the chemical complexities of tars, waste-water and leachates, thus, providing the means to differentiate samples based on their SVOC content.

8.3 Recommended future work

Data analysis showed that there are a number of possible global indicators that may relate to the physico-chemical processes that take place during a UCG trial. Confirming these indicators with data from future UCG trials would help to establish them, so that targeted methods can be developed in order to provide operators with faster and more accurate results. Data produced from the thesis could be analysed further for potential links to process conditions; this would of course require the provision of additional data from the trial operators.

The data processing methodology for GC-MS data that was presented in Chapter 5 appears to work well for the samples. However, since GCxGC-TOFMS was shown to produce a more detailed picture of the SVOC content of the samples, the development of a GCxGC-TOFMS data processing methodology is recommended, in a similar fashion to the methodology described in the thesis. Alignment tools for GCxGC-TOFMS data were recently developed that may aid in such a task[182,183]. However, regarding pick peaking, researchers must rely on the manufacturer software for the time being; some manufacturers have already implemented the option to extract GCxGC-TOFMS data file in *.CDF form so open source peak picking software are expected to be developed in the near future.

The classification of peaks for the GCxGC-TOFMS data was performed by manually defining elution areas. Chromatof® provides the possibility (with a software upgrade) to perform this classification automatically with scripts. Since there is available literature on relevant

classification scripts[184,185], using the GCxGC-TOFMS data produced from the thesis may provide additional information on the gasification process and sample composition.

Another recommendation is to expand the application of HIVS to the analysis of solid samples, which may prove to be an alternative to other extraction techniques such as pressurised solvent extraction. Initially a sample matrix such as heavily contaminated soil an FMGP plant is recommended, for an initial assessment of the extraction capabilities of the HIVS technique. The application can be possibly expanded to less contaminated solid matrices such as sludge.

Finally, further development of the HIVS platform is recommended, particularly in miniaturising the extraction methods e.g. it might be able to perform UAD of tar in a smaller vial with much less sample, provided an appropriate adapter is made available of manufactured. Also, testing the HIVS system for multiple extraction at a time is highly recommended as this will drastically increase sample throughput.

Appendix A

A.1 Appendix for Chapter 3

A.1.1 Effluent samples from gasification trials

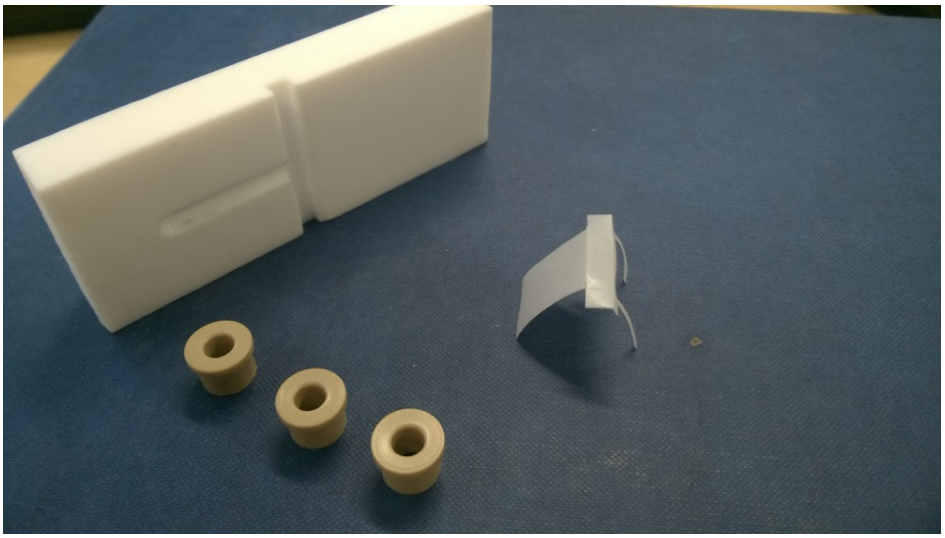

Figure A.1.1: Adapter range for the HIVS system. Image ©*Ioannis Sampsonidis*

In total there are 15 waste-water samples and 8 UCG coal tar samples provided to the University of Glasgow by the GIG (sampling schedule as in Table A.1). Six samples from the TOPS1 *ex-situ* gasification experiment performed at the GIG & nine samples from the TOPS8 *ex-situ* gasification experiment performed at the GIG (collected as in Figure A.1.2). Eight UCG tar samples from the Barbara II *in-situ* gasification experiment performed at the GIG (collected as in Figure A.1.3).

Table A.1: Sampling schedule and time points for the gasification trials performed at GIG. For TOPS1 and TOPS8 samples correspond to sampling periods of accumulating effluents within the condensation tank while for Barbara II samples correspond to a specific time point

TOPS1		TOPS8		Barbara II	
Period [hrs]	Duration [hrs]	Period [hrs]	Duration [hrs]	Sample	Time [hrs]
0-24	24	0-2	2	1	Outset
24-48	24	2-60	58	2	24
48-72	24	60-69	33	3	48
72-96	24	69-102	33	4	72
96-120	24	102-116	14	5	96
120-148	28	116-146	30	6	120
		146-157	11	7	144
		157-190	33	8	168
		190-204	14		

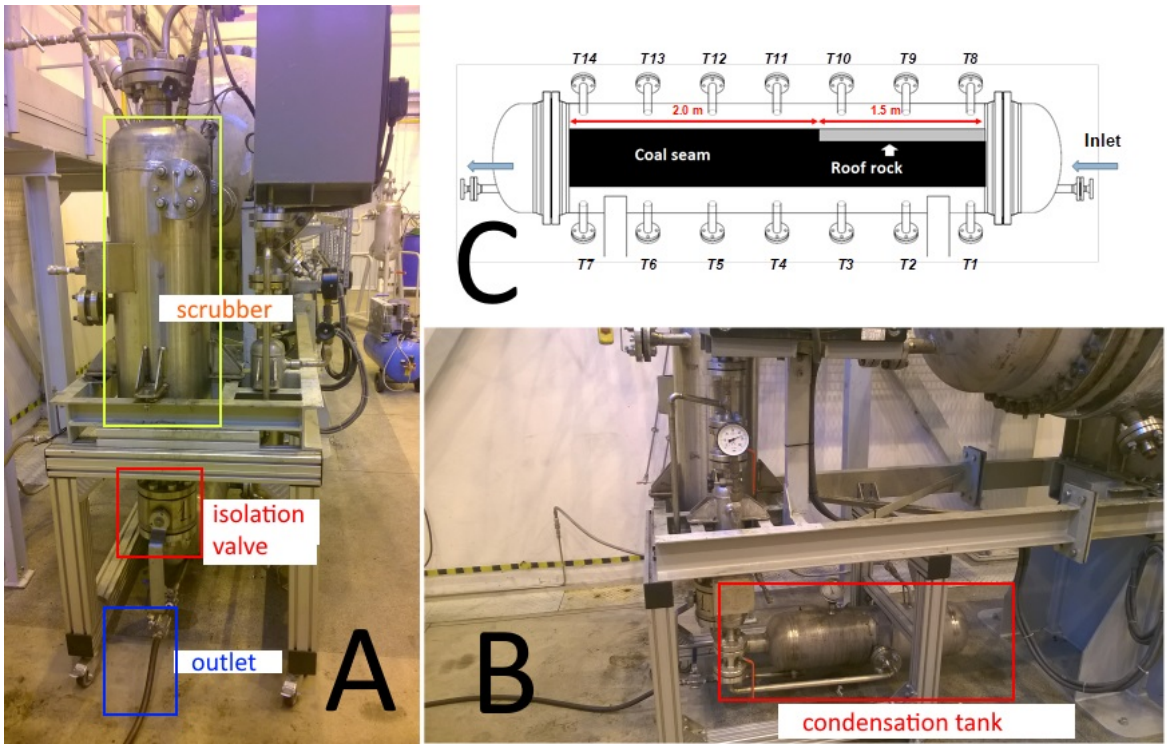

Figure A.1.2: **A:** Outlet side of the reactor illustrating the position of the gas scrubber, the condensation tank isolation valve and the condensation tank outlet; **B:** Position and orientation of the condensation tank; **C:** Overview of the reactor and the methodology used to pack the reactor with coal

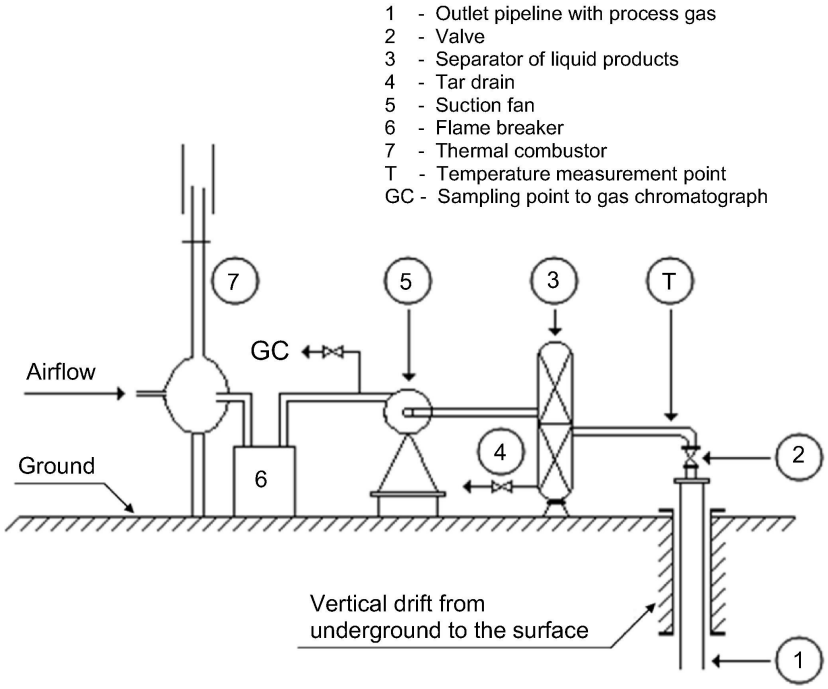

Figure A.1.3: The gaseous product collection system located at the surface that was used for the Barbara II trial. Tar samples were collected at the tar drain (4) located at the bottom of the separator of liquid products (3). Reproduced from[143] with permission.

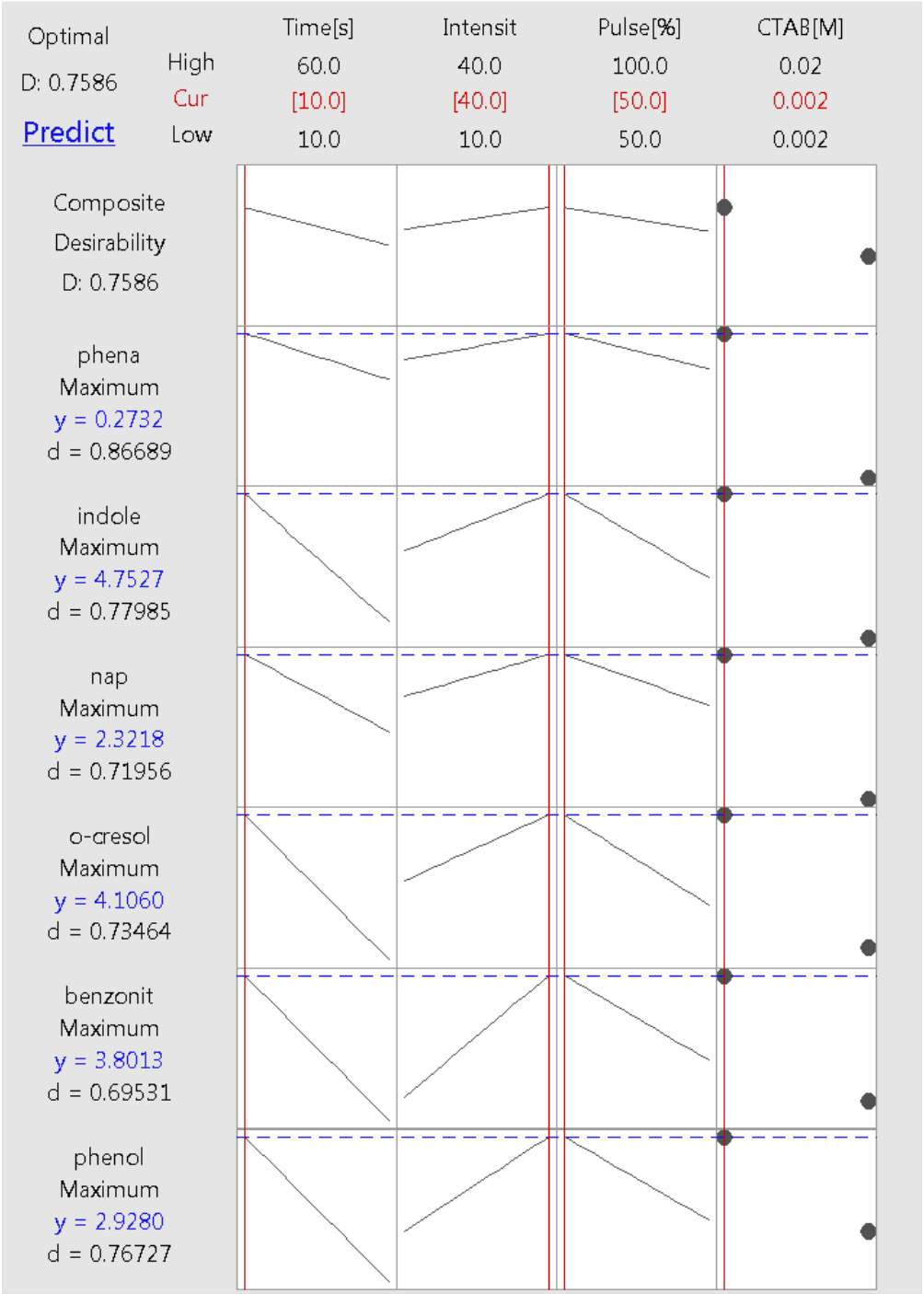

Figure A.1.4: Optimisation plot for the screening study along with the optimal values produced from Matlab's response optimiser function

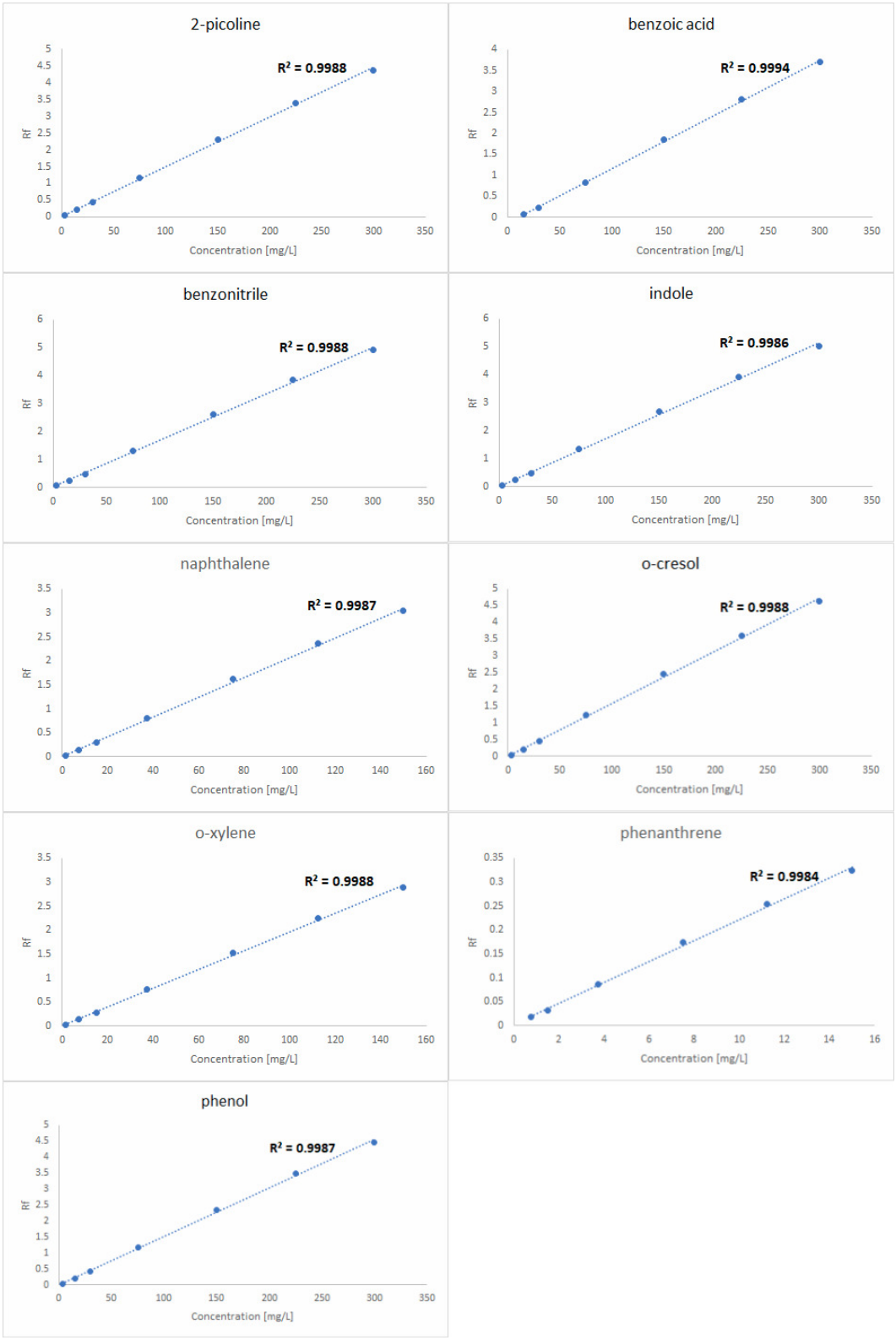

Figure A.1.5: GC-FID calibration curves for the model compounds for method optimisation/validation

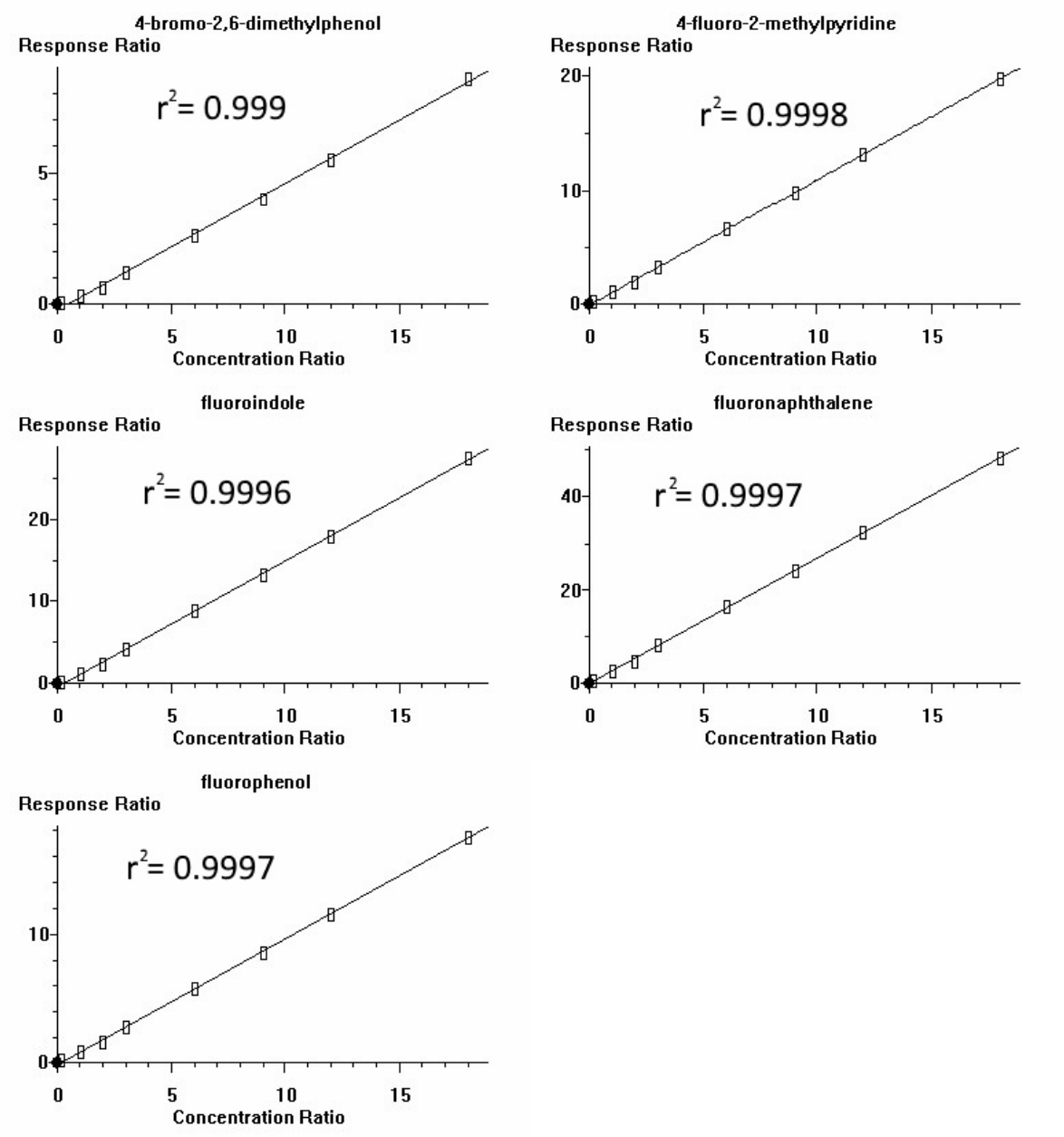

Figure A.1.6: GC-MS calibration curves for surrogates for method validation

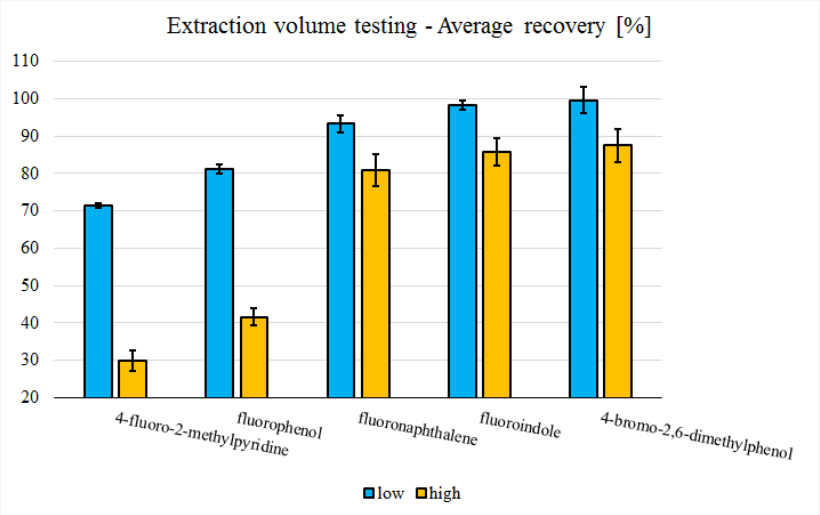

Figure A.1.7: Effect of the matrix on the recovery of the 5 selected surrogates

A.2 Appendix for Chapter 4

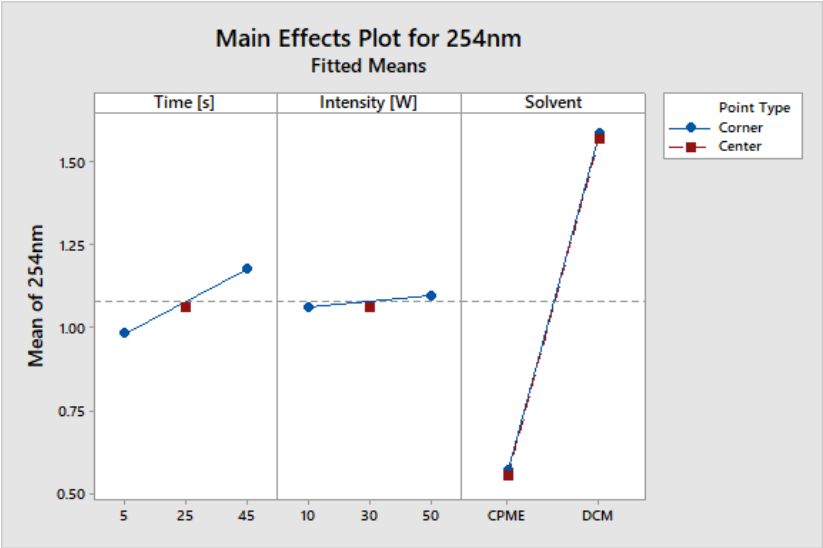

Figure A.2.1: Main effects plot for the A_{254nm} factorial regression model. The main effects shows how the response changes when altering the corresponding factor. Corner points are the maximum and minimum factor levels of the model while center points are values that lie in the middle of the two corner points

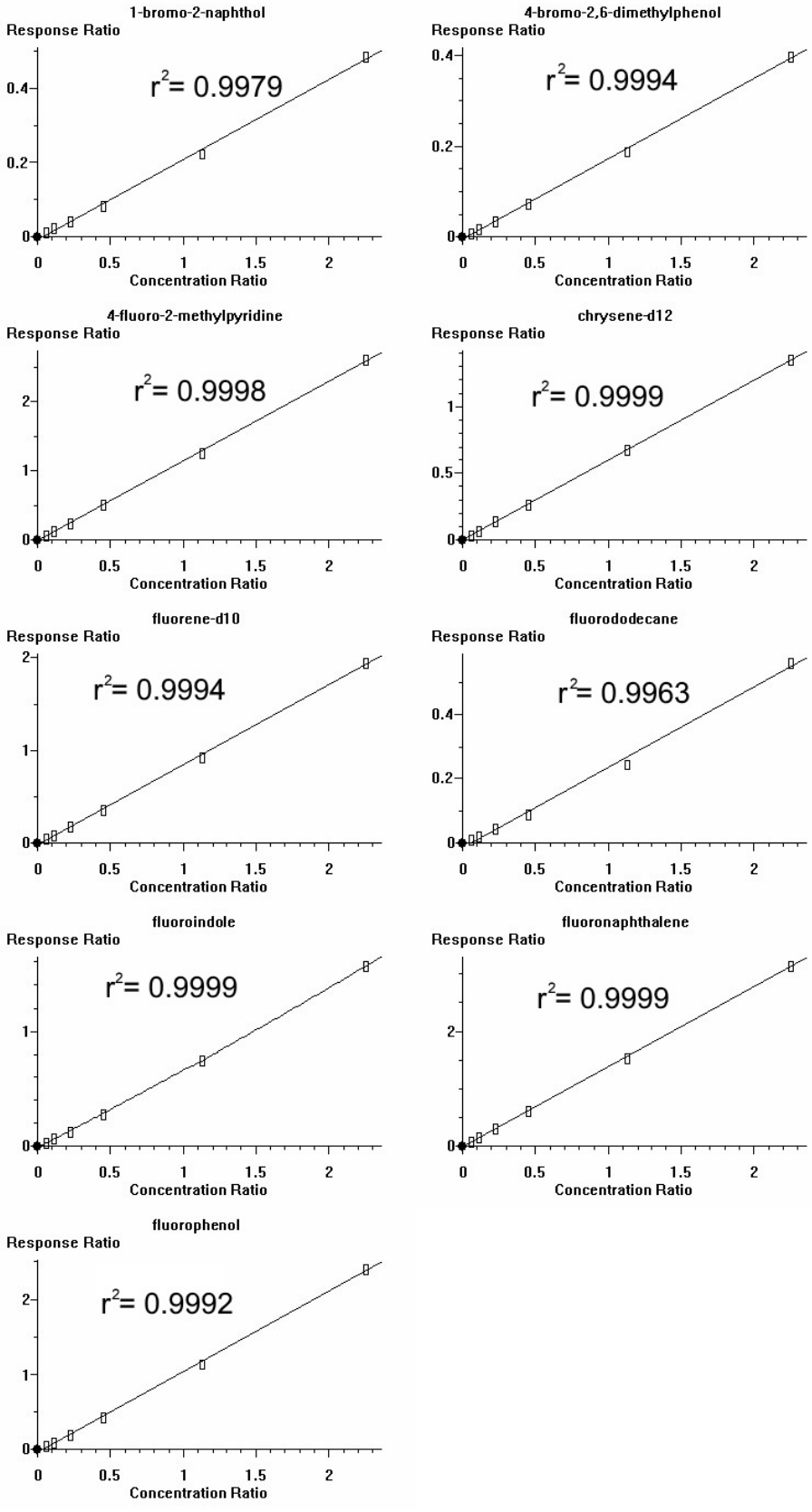

Figure A.2.2: Surrogate calibration curves for tar from the SIM GC-MS method

A.3 Appendix for Chapter 5

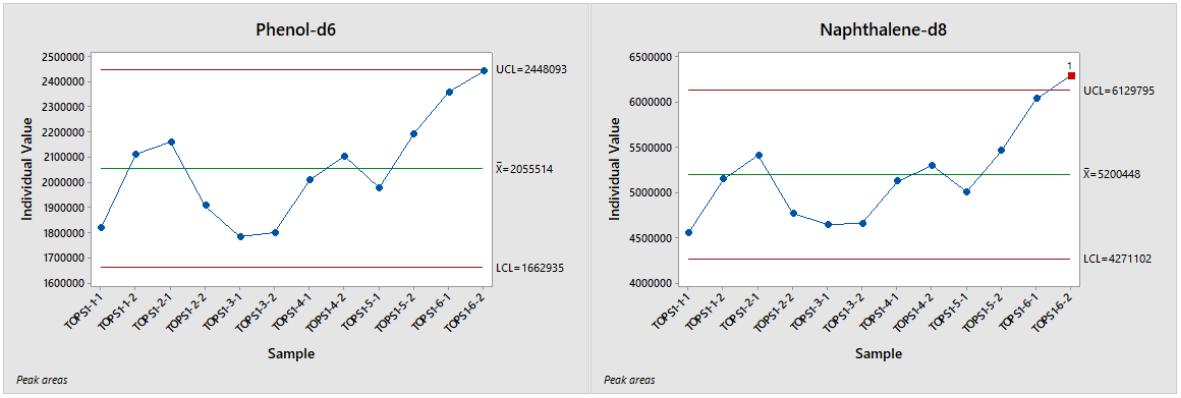

Figure A.3.1: Control charts for phenol-d6 and naphthlane-d8 for the TOPS1 experiment. Data are from peak areas

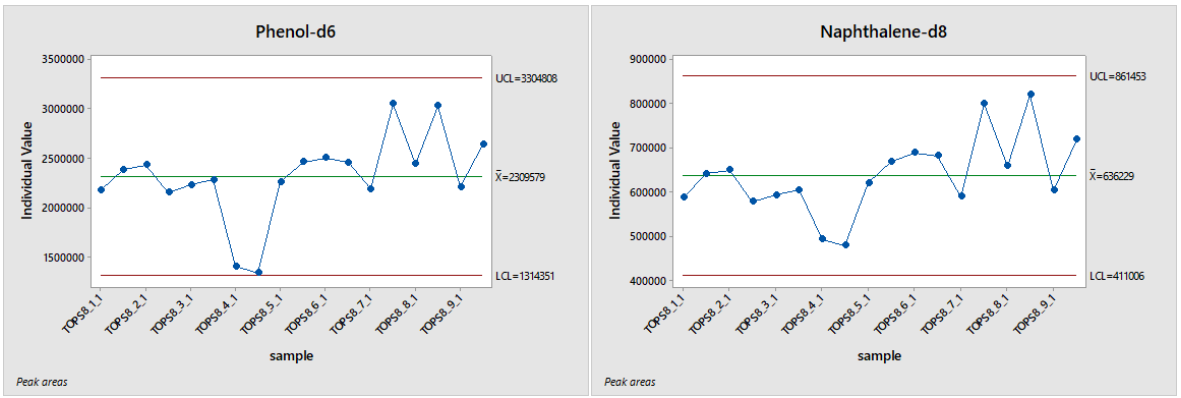

Figure A.3.2: Control charts for phenol-d6 and naphthlane-d8 for the TOPS* experiment. Data are from peak areas

Figure A.3.3: Control charts for phenol-d6 and naphthlane-d8 for the TOPS* experiment. Data are from peak areas

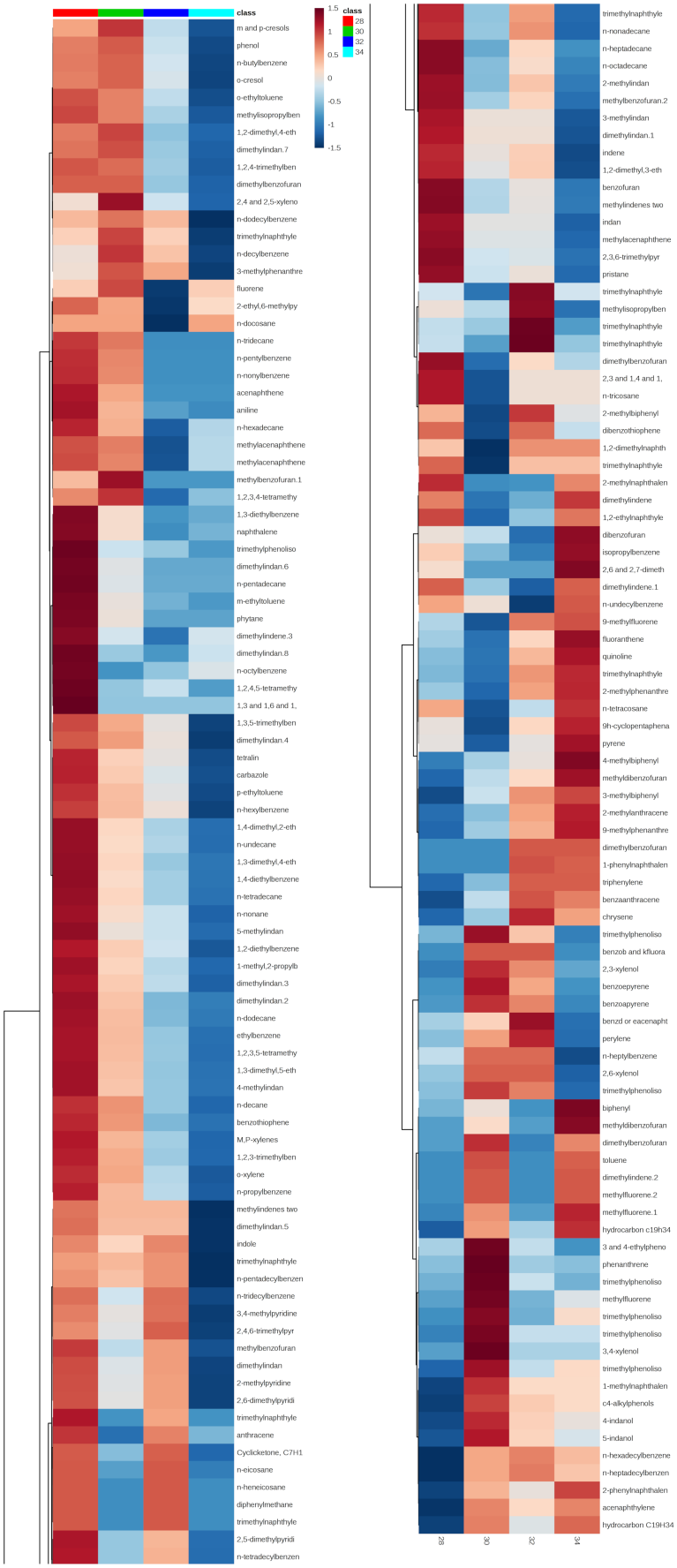

Figure A.3.4: Elongated version of the heatmap in Figure 5.6. Readers are referred to the electronic version of the thesis for increased clarity

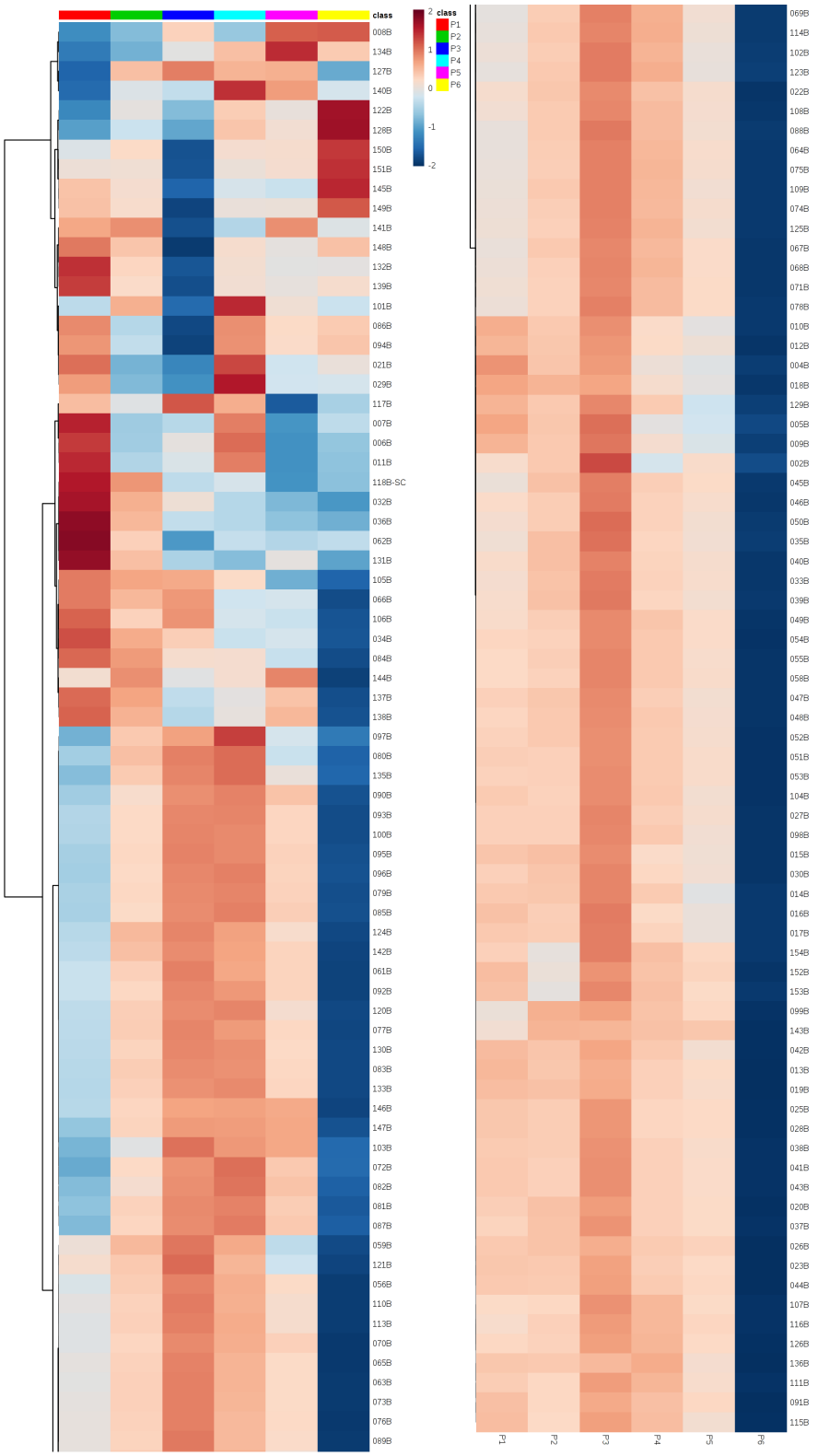

Figure A.3.5: Elongated version of the heatmap in Figure 5.9. Readers are referred to the electronic version of the thesis for increased clarity

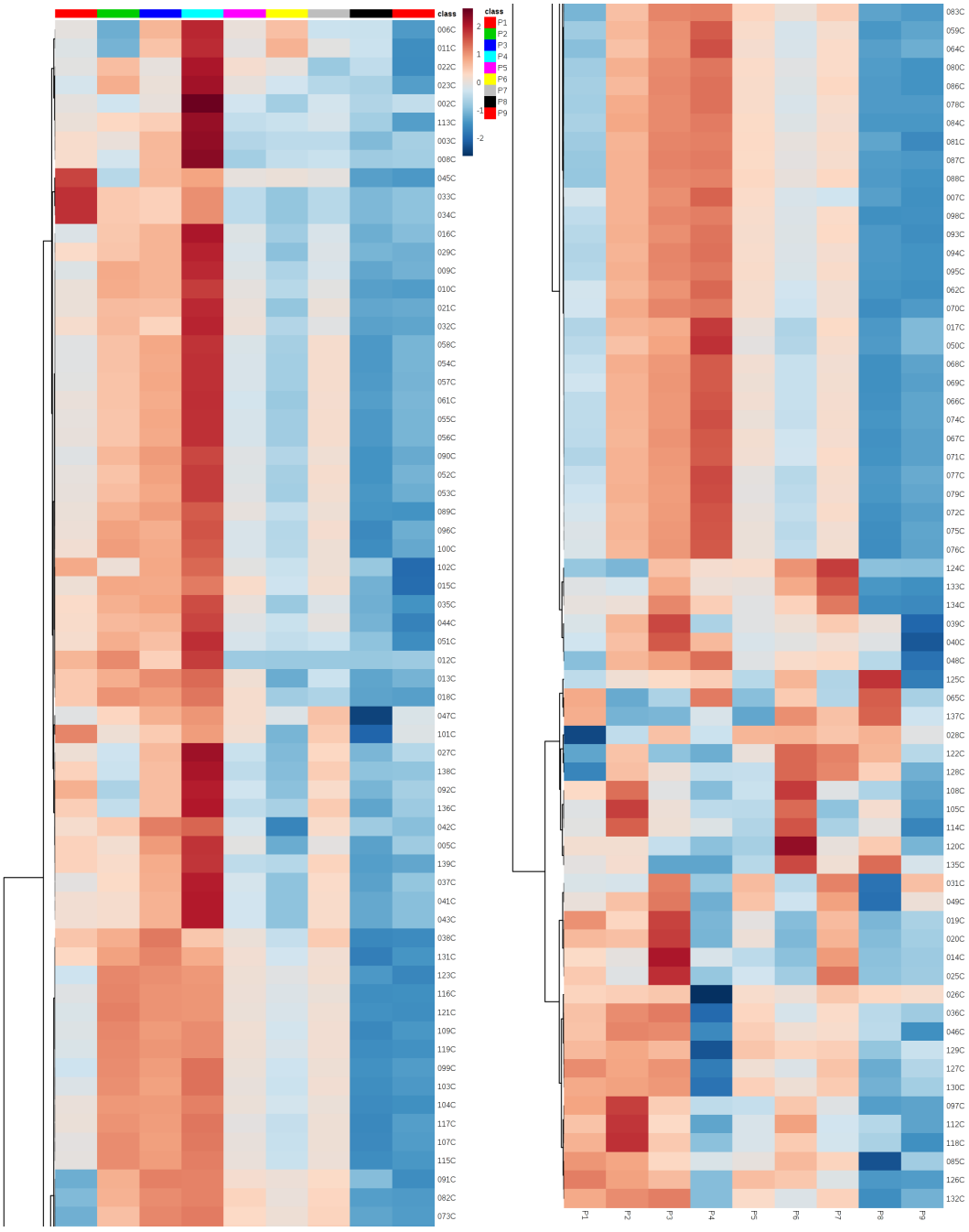

Figure A.3.6: Elongated version of the heatmap in Figure 5.12. Readers are referred to the electronic version of the thesis for increased clarity

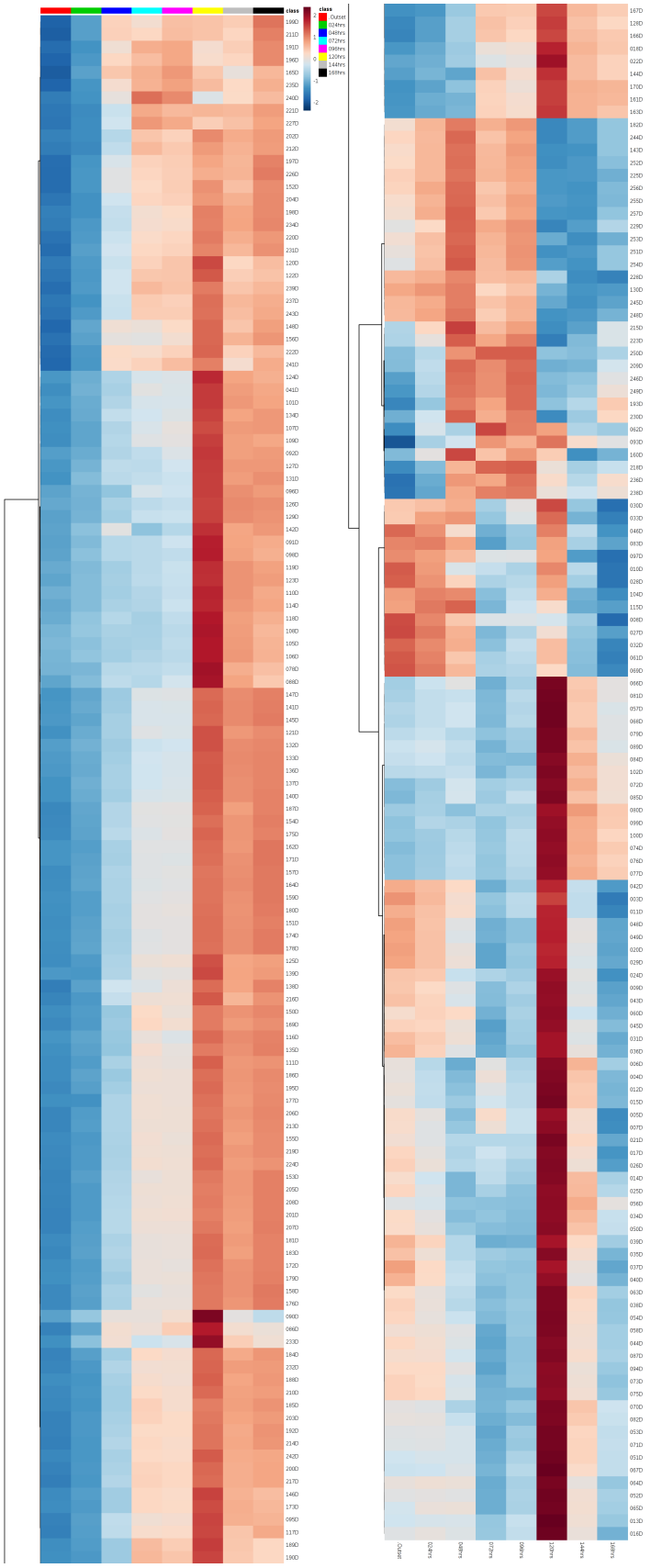

Figure A.3.7: Elongated version of the heatmap in Figure 5.15. Readers are referred to the electronic version of the thesis for increased clarity

A.4 Appendix for Chapter 6

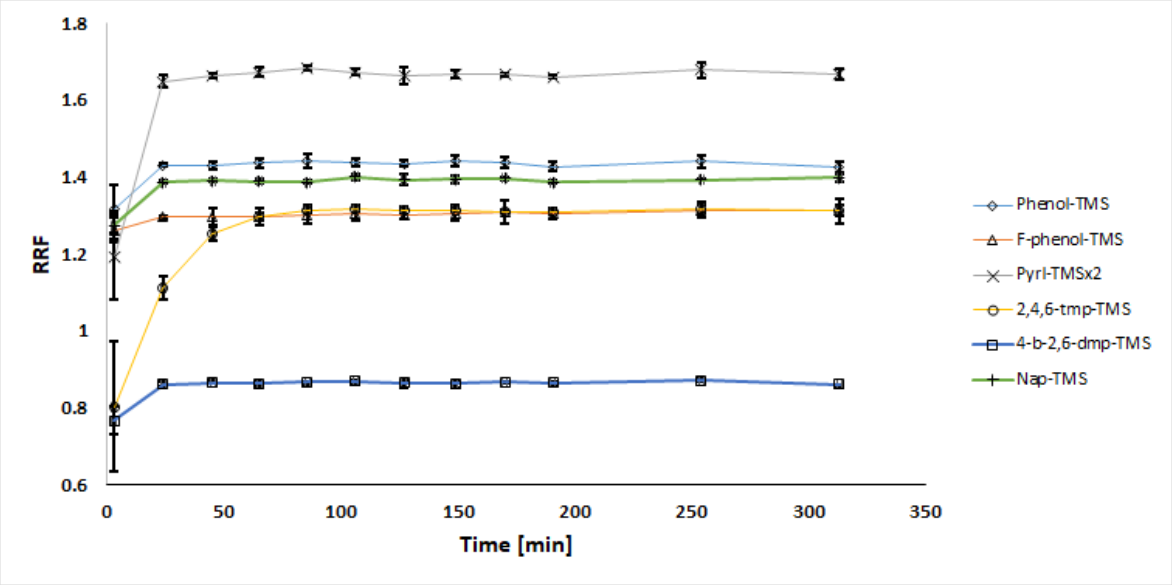

Figure A.4.1: Relative response factor vs time for phenols for all three replicates of the sterical hindrance effect

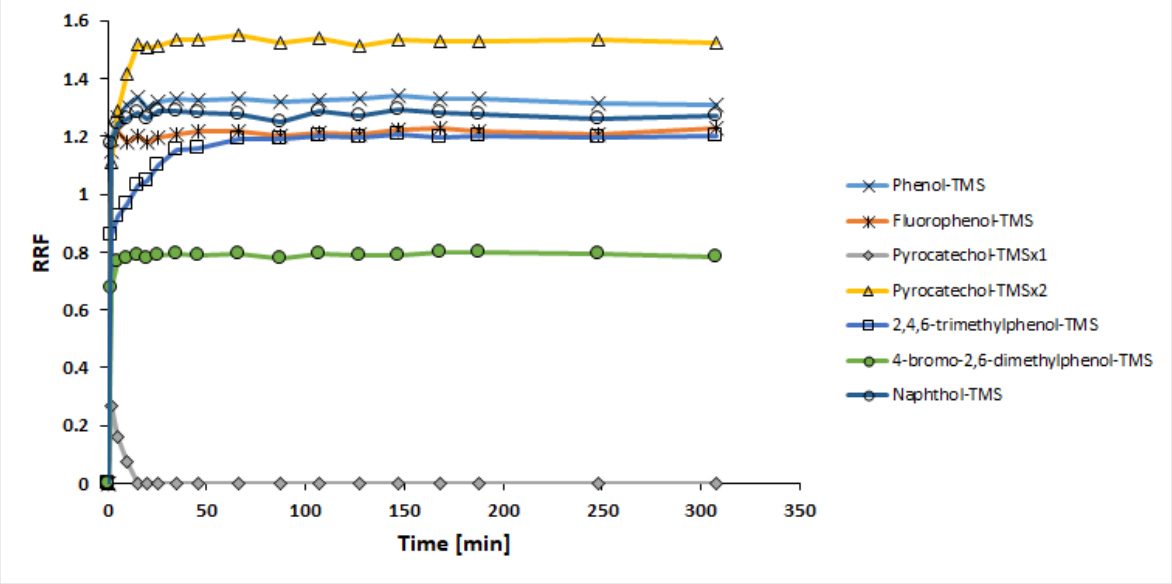

Figure A.4.2: Relative response factor vs time for phenols for replicate no 3 with the additional runs included. The

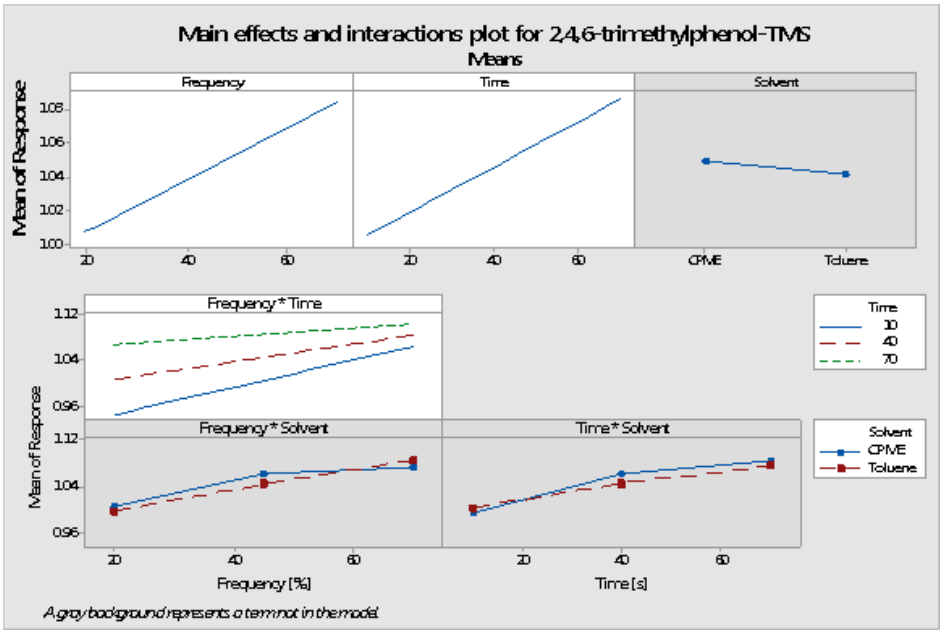

Figure A.4.3: Main effects and interactions plot for the USDe regression model. Both frequency and time have a significant effect on the derivatisation of 2,4,6-trimethylphenol. The second order interaction of frequency and time is also positive. Lower time appears to be compensated by high frequency and vice versa

A.5 Appendix for Chapter 7

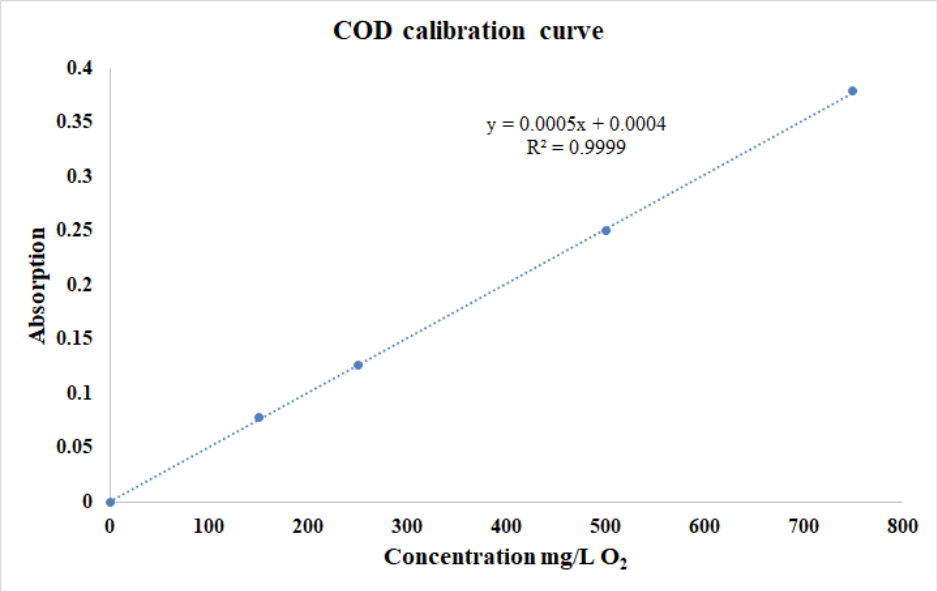

Figure A.5.1: Calibration curve for the calculation of COD in high salinity leachates

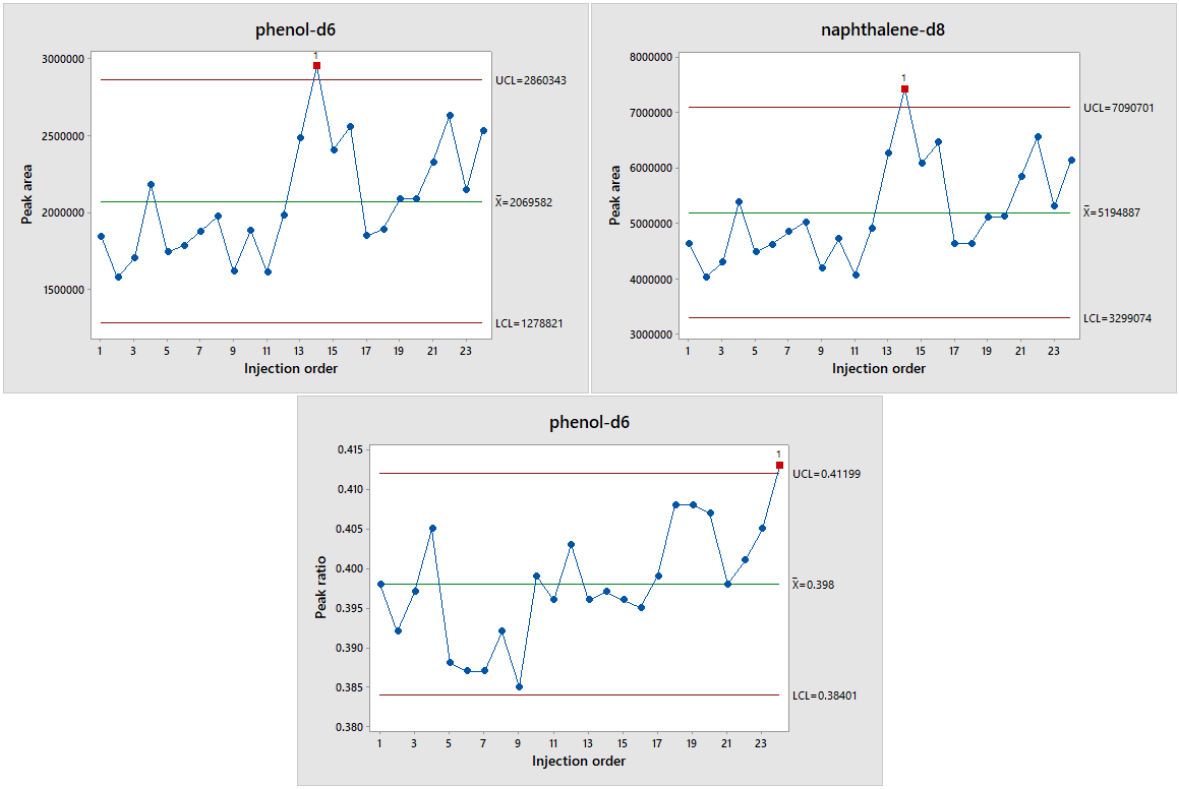

Figure A.5.2: Control charts for the internal standards in all leachates by injection order. **Top:** control charts for the peak areas for both internal standards. **Bottom:** Control charts for the peak ratio of phenol-d6 after normalisation with the peak area of naphthalene-d8

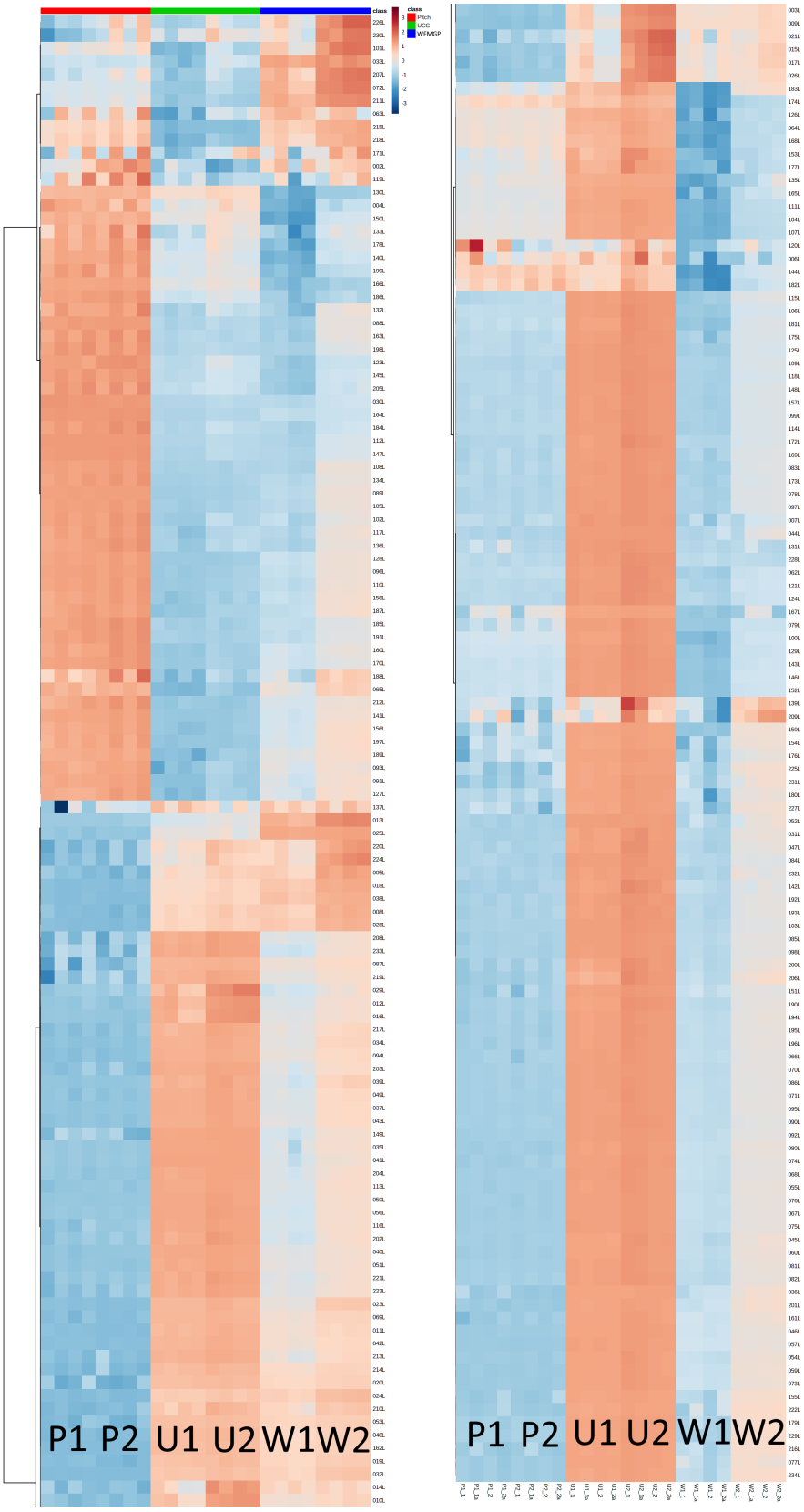

Figure A.5.3: Elongated version of the heatmap in Figure 7.8. Readers are referred to the electronic version of the thesis for increased clarity

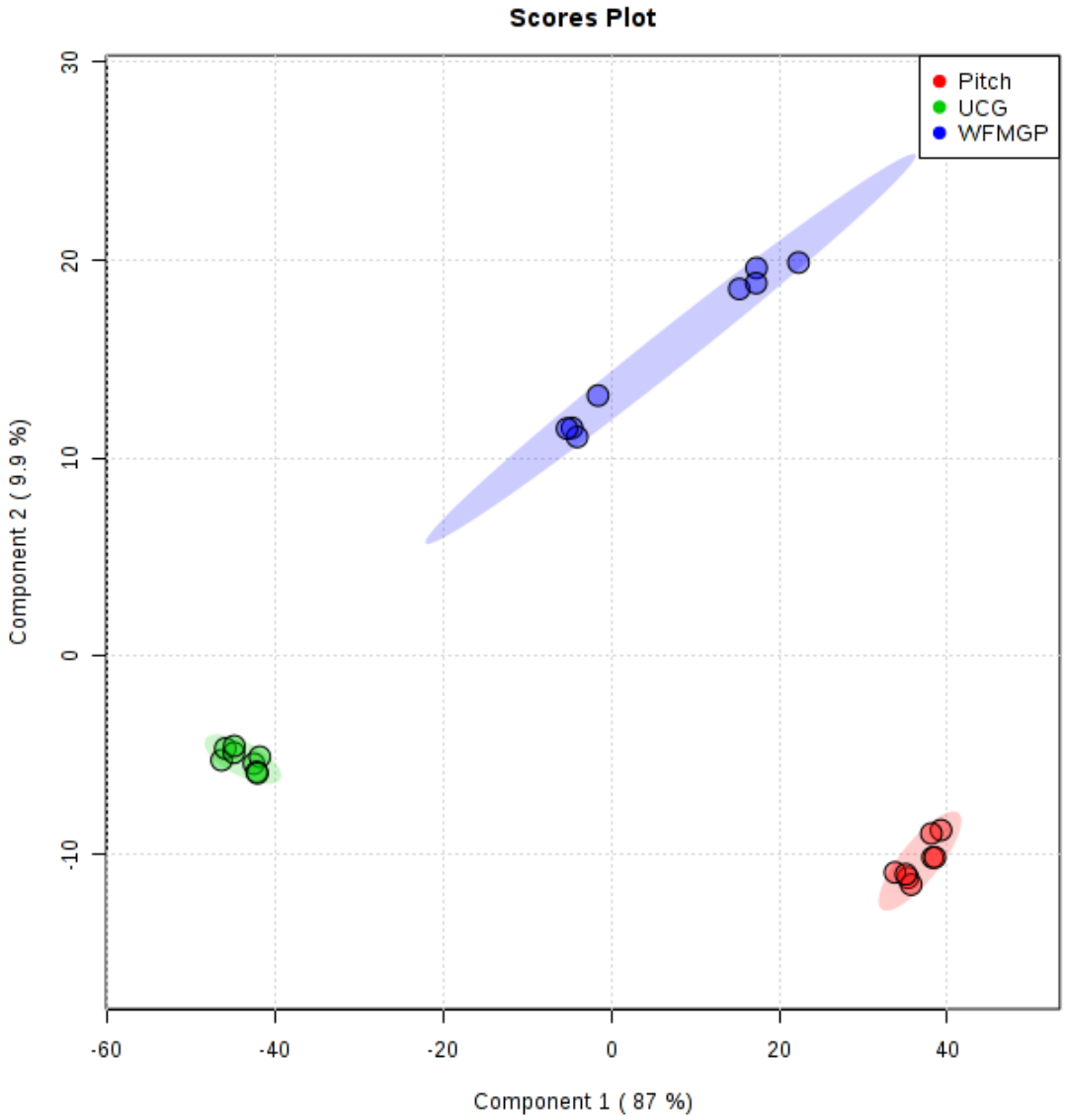

Figure A.5.4: Scores plot of the PLS-DA model for the tar leachates

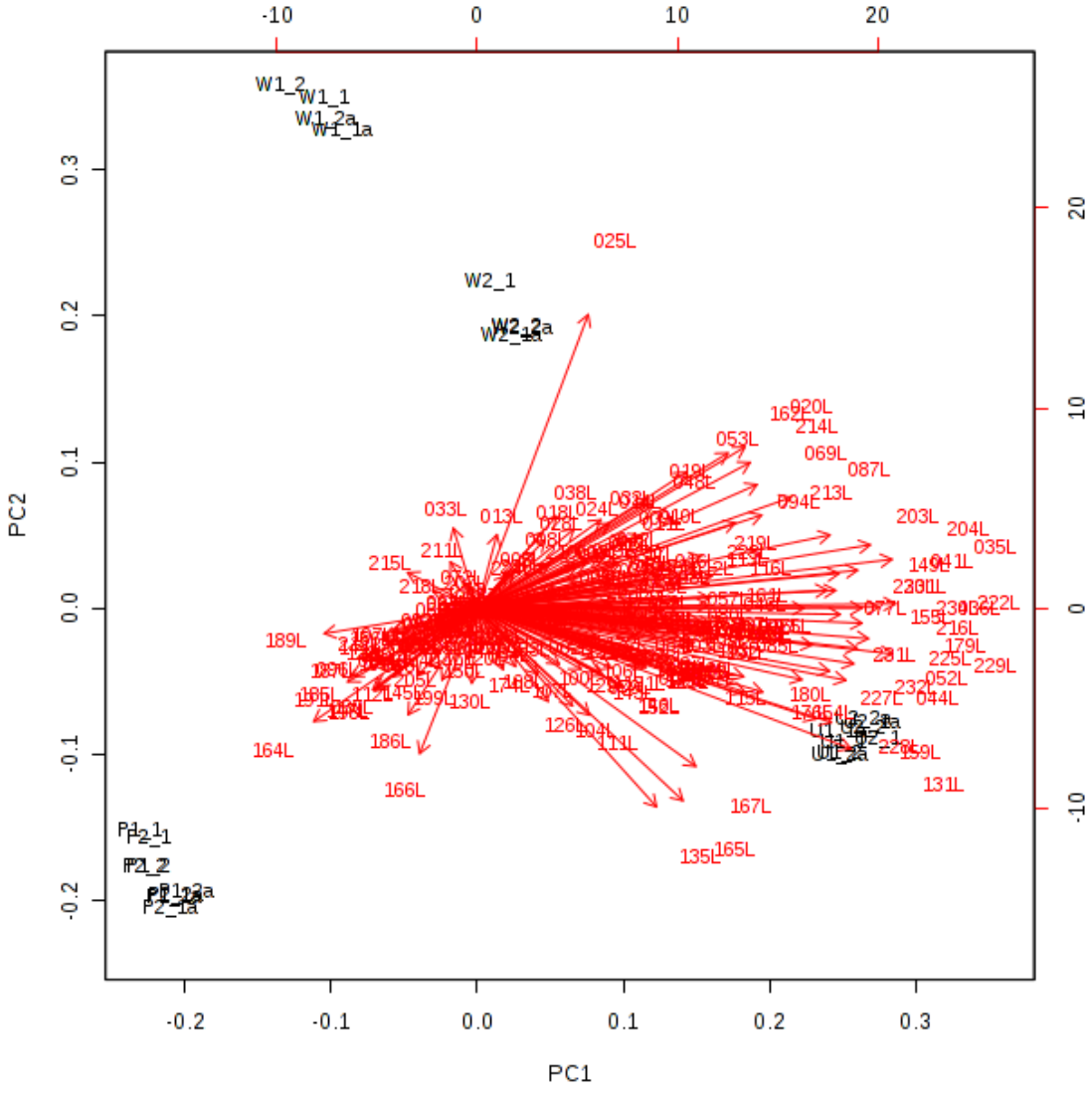

Figure A.5.5: PCA biplot of the scores plot for leachates (black text). Loadings are represented with red arrows with the arrow length and direction indicating the weight of each loading

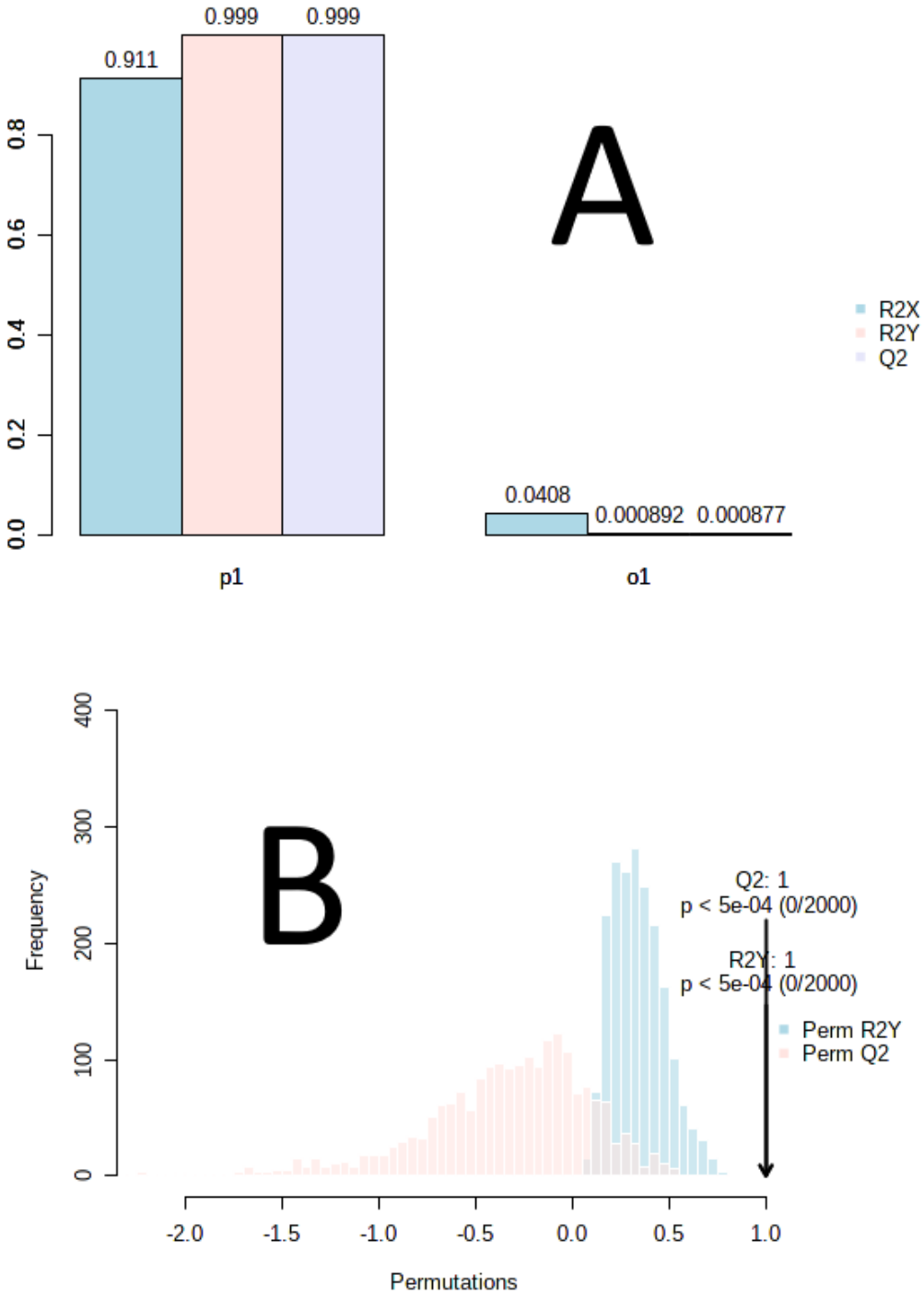

Figure A.5.6: **A:** Model overview and **B:** permutations test for the Pitch-UCG oPLS-DA model

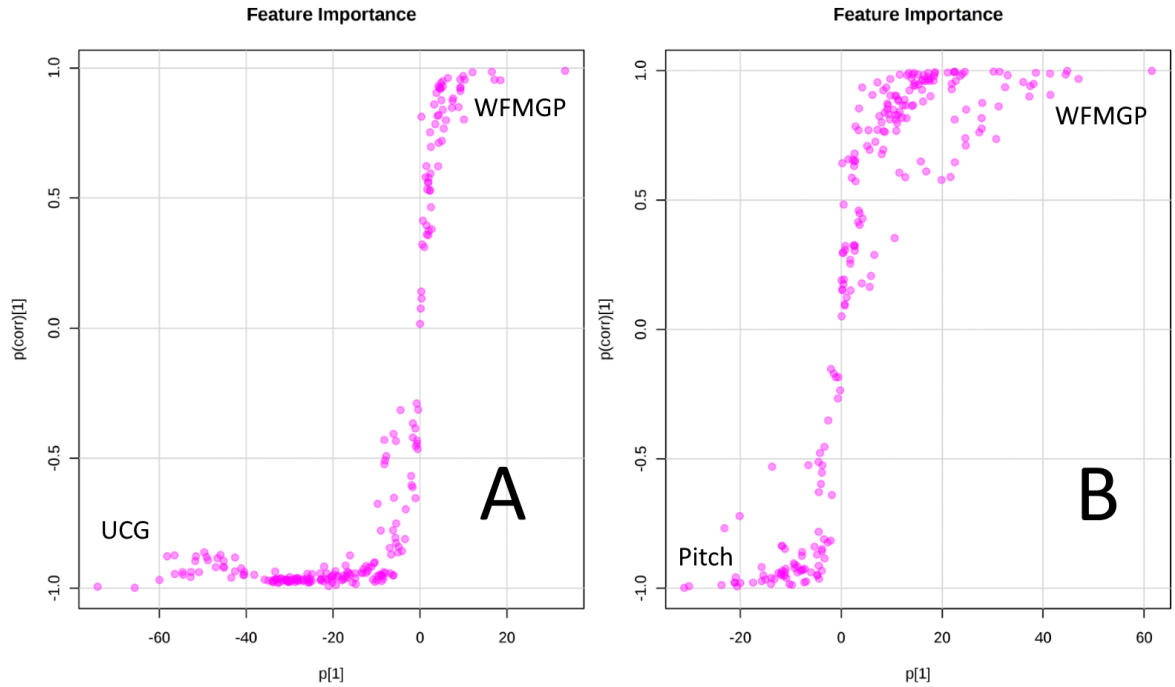

Figure A.5.7: S-plots for the oPLS-DA models. **A:** S-plot corresponding to the comparison of UCG tar and weathered FMGP tar **B:** S-plot of the oPLS-DA model that corresponds to the comparison between pitch and weathered FMGP tar

Bibliography

[1] Roddy, D. J.; Younger, P. L. Underground coal gasification with CCS: a pathway to decarbonising industry. *Energy & Environmental Science* **2010**, *3*, 400–407.

[2] Durucan, S. *et al.* TOPS: Technology Options for Coupled Underground Coal Gasification and CO2 Capture and Storage. *Energy Procedia* **2014**, *63*, 5827–5835.

[3] Berkowitz, N. *The chemistry of coal*; Elsevier: Amsterdam, New York, 1985.

[4] Elliott, M. A., Ed. *Chemistry of coal utilization. Second Supplementary Volume*; John Wiley and Sons: New York, 1981.

[5] Lowry, H. H., Ed. *Chemistry of coal utilization. Supplementary volume*; John Wiley and Sons, Inc: New York - London, 1963.

[6] Mathews, J. P.; Miller, B. G.; Song, C.; Schobert, H. H.; Botha, F.; Finkleman, R. B. The EBB and flow of US coal research 1970–2010 with a focus on academic institutions. *Fuel* **2013**, *105*, 1–12.

[7] Neavel, R. C. In *Chemistry of coal utilization. Second supplementary volume*; Elliott, M. A., Ed.; John Wiley and Sons: New York, 1981.

[8] Centucky Geological Survey, Coal type/Lithotype. `https://web.archive.org/web/20190423104247/https://www.uky.edu/KGS/coal/coal-type.php`.

[9] Greb, S.; Kentucky Geological Survey, How Coal Forms and Coal Rank Diagrams. `https://web.archive.org/web/20190423104412/https://www.uky.edu/KGS/coal/coal-diagram-download.php`.

[10] O'Keefe, J. M. K.; Bechtel, A.; Christanis, K.; Dai, S.; DiMichele, W. A.; Eble, C. F.; Esterle, J. S.; Mastalerz, M.; Raymond, A. L.; Valentim, B. V.; Wagner, N. J.; Ward, C. R.; Hower, J. C. On the fundamental difference between coal rank and coal type. *International Journal of Coal Geology* **2013**, *118*, 58–87.

[11] Elliott, M. A.; Yohe, R. G. In *Chemistry of coal utilization. Second supplementary volume*; Elliott, M. A., Ed.; John Wiley and Sons: New York, 1981.

[12] Schweinfurth, S. P. In *The National Coal Resource Assessment Overview*; Pierce, B. S., Dennen, K. O., Eds.; U.S. Geological Survey, 2009.

[13] Krevelen, D. W. V. *Coal: typology, chemistry, physics, constitution*; Elsevier Scientific: Amsterdam, 1961.

[14] Wender, I.; Heredy, L. A.; Neuworth, M. B.; Dryden, I. G. C. In *Chemistry of coal utilization. Second supplementary volume*; Elliott, M. A., Ed.; John Wiley and Sons: New York, 1981.

[15] Blom, L. ANALYTICAL METHODS IN COAL CHEMISTRY. Ph.D. thesis, TU Delft, 1960.

[16] Jensen, E. J.; Melnyk, N.; Wood, J. C.; Berkowitz, N. In *Coal Science*; Given, P. H., Ed.; AMERICAN CHEMICAL SOCIETY: WASHINGTON, D.C., 1966; Vol. 55; pp 621–642.

[17] Montgomery, R. S.; Holly, E. D. Decarboxylation studies of the structures of the acids obtained by oxidation of bituminous coal. *Fuel* **1957**, *36*, 63.

[18] Kristiansen, A. *Understanding coal gasification*; IEACR 86; IEA Coal Research: London, 1996.

[19] Howard, H. C. In *Chemistry of coal utilization. Supplementary volume.*; Lowry, H. H., Ed.; John Wiley and Sons, Inc, New York - London, 1963.

[20] Howard, J. B. In *Chemistry of coal utilization. Second supplementary volume*; Elliott, M. A., Ed.; John Wiley and Sons: New York, 1981.

[21] Veras, C. A. G.; Carvalho Jr., J. A.; Ferreira, M. A. The Chemical Percolation Devolatilization Model Applied to the Devolatilization of Coal in High Intensity Acoustic Fields. *Journal of the Brazilian Chemical Society* **2002**, *13*, 358–367.

[22] Bruinsma, O. S. L.; Moulijn, J. A. The pyrolytic formation of polycyclic aromatic hydrocarbons from benzene, toluene, ethylbenze,e, styrene, phenylacetylene and n-decane in relation to fossil fuels utilization. *Fuel Processing Technology* **1988**, *18*, 213–236.

[23] Vreugdenhil, B. J.; Zwart, R. W. R. *Tar formation in pyrolysis and gasification*; Technical Report ECN-E–08-087, 2009.

[24] Johnson, J. L. In *Chemistry of coal utilization. Second supplementary volume*; Elliott, M. A., Ed.; John Wiley and Sons: New York, 1981.

[25] Bell, D. A.; Towler, B. F.; Fan, M. *Coal Gasification and Its Applications*; Elsevier, 2011; pp 101–111.

[26] Jönsson, O. In *Fundamentals of Thermochemical Biomass Conversion*; Overend, R. P., Milne, T. A., Mudge, L. K., Eds.; Springer Netherlands: Dordrecht, 1985; pp 733–746.

[27] Jess, A. Mechanisms and kinetics of thermal reactions of aromatic hydrocarbons from pyrolysis of solid fuels. *Fuel* **1996**, *75*, 1441–1448.

[28] Couch, G. R. *Underground coal gasification*; IEA Clean Coal Centre: London, 2009.

[29] Younger, P. L.; Gluyas, J.; Cox, M.; Roddy, D. J. UNDERGROUND COAL GASIFICATION. *Ingenia* **2010**, 42–46.

[30] Younger, P. L. Hydrogeological and Geomechanical Aspects of Underground Coal Gasification and its Direct Coupling to Carbon Capture and Storage. *Mine Water and the Environment* **2011**, *30*, 127–140.

[31] Sarhosis, V.; Lavis, S.; Mostade, M.; Thomas, H. R. Towards commercialising underground coal gasification in the EU. *Environmental Geotechnics* **2016**, 1–11.

[32] Gunn, R. D.; Krantz, W. B. *Underground coal gasification: development of theory, laboratory experimentation, interpretation, & correlation with the hanna field tests*; Technical Report UCID-21853, 1988.

[33] Thorsness, C. B.; Britten, J. A. *Lawrence Livermore National Laboratory underground coal gasification project: final report*; Technical Report UCID-21853, 1989; p 27.

[34] Gibb, Sir A.; Partners, *The Underground Gasification of Coal: Report on the Work Done in Great Britain*; Sir Isaac Pitman & Sons, 1964.

[35] Khan, M.; Mmbaga, J.; Shirazi, A.; Trivedi, J.; Liu, Q.; Gupta, R. Modelling Underground Coal Gasification—A Review. *Energies* **2015**, *8*, 12603–12668.

[36] Camp, D.; White, J. Prevention of Groundwater Contamination from Underground Coal Gasification. 3rd Underground Coal Gasification Network Workshop. Brisbane, Australia, 2013.

[37] Glaser, R.; Owen, T. Generation, Control, And Recovery Of Organic Pyrolysis Products In Underground Coal Gasification. *Petroleum Science and Technology* **1987**, *5*, 275–289.

[38] Perkins, G.; Sahajwalla, V. A Mathematical Model for the Chemical Reaction of a Semi-infinite Block of Coal in Underground Coal Gasification. *Energy & Fuels* **2005**, *19*, 1679–1692.

[39] Perkins, G.; Sahajwalla, V. A Numerical Study of the Effects of Operating Conditions and Coal Properties on Cavity Growth in Underground Coal Gasification. *Energy & Fuels* **2006**, *20*, 596–608.

[40] Camp, D. W.; White, J. A. *Underground coal gasification: An overview of groundwater contamination hazards and mitigation strategies*; Technical Report LLNL-TR-668633, 2015.

[41] Bockhorn, H. In *Underground Coal Gasification and Combustion*; Blinderman, M. S., Klimenko, A. Y., Eds.; Elsevier, 2018; pp 213–252.

[42] King, S. B.; Brandenburg, C. F.; Lanum, W. J. Characterization of Nitrogen Compounds in Tar Produced from Underground Coal Gasification. *Energy Sources* **1978**, *3*, 263–275.

[43] Barbour, F. A.; Cummings, R. E. *Comparison of coal tars generated by pyrolysis of Hanna coal and UCG (underground coal gasification) Hanna IVB coal tars*; Technical Report DOE/FE/60177-2427, 1986.

[44] Barbour, F. A.; Campbell, S. L.; Covell, J. R. *Analysis of coal tars collected from Rocky Mountain 1 ELW and CRIP modules*; Technical Report DOE/MC/11076–2655, 1988.

[45] Bencini, J. E.; Davis, B. E. Gas cleanup designs for underground coal gasification. Proceedings of the eighth underground coal conversion symposium. Keystone, Colorado, United States, 1982; pp 81–92.

[46] Wiatowski, M.; Kapusta, K.; Stanczyk, K. Analysis and characteristics of tars collected during a pilot-scale underground coal gasification (UCG) trial. *Fuel* **2017**, *208*, 595–601.

[47] Kapusta, K.; Stanczyk, K. Pollution of water during underground coal gasification of hard coal and lignite. *Fuel* **2011**, *90*, 1927–1934.

[48] Stuermer, D. H.; Ng, D. J.; Morris, C. J. Organic contaminants in groundwater near an underground coal gasification site in northeastern Wyoming. *Environmental Science & Technology* **1982**, *16*, 582–587.

[49] Koolen, H. H. F.; Swarthout, R. F.; Nelson, R. K.; Chen, H.; Krajewski, L. C.; Aeppli, C.; McKenna, A. M.; Rodgers, R. P.; Reddy, C. M. Unprecedented Insights into the Chemical Complexity of Coal Tar from Comprehensive Two-Dimensional Gas Chromatography Mass Spectrometry and Direct Infusion Fourier Transform Ion Cyclotron Resonance Mass Spectrometry. *Energy & Fuels* **2015**, *29*, 641–648.

[50] Pellizzari, E. D.; Castillo, N. P.; Willis, S.; Smith, D.; Bursey, J. T. IDENTIFICATION OF ORGANIC CONSTITUENTS IN AQUEOUS EFFLUENTS FROM ENERGY-RELATED PROCESSES. *Preprints of Papers American Chemical Society Division of Fuel Chemistry* **1978**, *23*, 144.

[51] Kapusta, K.; Stanczyk, K.; Wiatowski, M.; Checko, J. Environmental aspects of a field-scale underground coal gasification trial in a shallow coal seam at the Experimental Mine Barbara in Poland. *Fuel* **2013**, *113*, 196–208.

[52] Schmidt, C. E.; Sharkey, A. G. J.; Friedel, R. A. *Mass spectrometric analysis of product water from coal gasification. Technical progress report.*; Technical Report BM-TPR-86, 1974.

[53] Blinderman, M. S., Klimenko, A. Y., Eds. *Underground Coal Gasification and Combustion*; Elsevier, 2018.

[54] Kapusta, K.; Stanczyk, K. Chemical and toxicological evaluation of underground coal gasification (UCG) effluents. The coal rank effect. *Ecotoxicology and Environmental Safety* **2015**, *112*, 105–113.

[55] Ahmed, Z. M.; Lyne, S.; Shahrabani, R. Removal and Recovery of Phenol From Phenolic Wastewater Via Ion Exchange and Polymeric Resins. *Environmental Engineering Science* **2000**, *17*, 245–255.

[56] Stamoudis, V. C. CHEMICAL AND BIOLOGICAL EVALUATION OF OILS AND TARS PRODUCED UNDER VARYING COAL DEVOLATILIZATION CONDITIONS. *Preprints of Papers American Chemical Society Division of Fuel Chemistry* **1985**, *30*, 281–287.

[57] Wang, J.; Zhao, L. Analysis of organic compounds in coal gasification wastewater. *Journal of Environmental Sciences (China)* **1992**, *4*, 84–96.

[58] Giabbai, M. F.; Cross, W. H.; Chian, E. S. K.; Dewalle, F. B. Characterization of Major and Minor Organic Pollutants in Wastewaters from Coal Gasification Processes. *International Journal of Environmental Analytical Chemistry* **1985**, *20*, 113–129.

[59] Mohr, D. H.; King, C. J. Identification of polar organic compounds in coal-gasification condensate water by gas chromatography-mass spectrometry analysis of high-performance liquid chromatography fractions. *Environmental Science & Technology* **1985**, *19*, 929–935.

[60] Humenick, M. J.; Mattox, C. F. Characterization of condensates produced during underground coal gasification. *In Situ; (United States)* **1982**, *6:1*, 1–27.

[61] Pellizzari, E.; Castillo, N.; Willis, S.; Smith, D.; Bursey, J. In *Measurement of Organic Pollutants in Water and Wastewater*; Van, H., Ed.; ASTM International: West Conshohocken, PA, 1979; pp 256–274.

[62] Pellizzari, E. D. *Identification of components of energy-related wastes and effluents*; Technical Report EPA/600/7-78/004, 1978.

[63] Scottish Environmental Protection Agency, Chlorofluorocarbons (CFCs). `https://web.archive.org/web/20190423103543/http://apps.sepa.org.uk/spripa/pages/substanceinformation.aspx?pid=114`.

[64] Tobben, P. J.; Manahan, S. E.; Sheesley, D. C. SIMPLE SOLVENT EXTRACTION SCHEME EMPLOYING DISSOLVED ORGANIC CARBON ANALYSIS FOR THE CHARACTERIZATION OF ORGANIC BY-PRODUCTS FROM SIMULATED IN SITU COAL GASIFICATION. *In Situ* **1982**, *6*, 29–46.

[65] Rezaee, M.; Assadi, Y.; Milani Hosseini, M.-R.; Aghaee, E.; Ahmadi, F.; Berijani, S. Determination of organic compounds in water using dispersive liquid–liquid microextraction. *Journal of Chromatography A* **2006**, *1116*, 1–9.

[66] Bernardo, M.; Gonçalves, M.; Lapa, N.; Mendes, B. Determination of alkylphenols in eluates from pyrolysis solid residues using dispersive liquid–liquid microextraction. *Chemosphere* **2010**, *79*, 1026–1032.

[67] Zgola-Grzeskowiak, A. Dispersive liquid–liquid microextraction applied to isolation and concentration of alkylphenols and their short-chained ethoxylates in water samples. *Journal of Chromatography A* **2010**, *1217*, 1761–1766.

[68] Suslick, K. S. Sonochemistry. *Science* **1990**, *247*, 1439–1445.

[69] Rayleigh, L. VIII. On the pressure developed in a liquid during the collapse of a spherical cavity. *The London, Edinburgh, and Dublin Philosophical Magazine and Journal of Science* **1917**, *34*, 94–98.

[70] Torres-Palma, R. A.; Serna-Galvis, E. A. *Advanced Oxidation Processes for Waste Water Treatment*; Elsevier, 2018; pp 177–213.

[71] Luquedecastro, M.; Priegocapote, F. Ultrasound-assisted preparation of liquid samples. *Talanta* **2007**, *72*, 321–334.

[72] Delgado-Povedano, M. M.; Luque de Castro, M. D. Ultrasound-assisted extraction and in situ derivatization. *Journal of Chromatography A* **2013**, *1296*, 226–234.

[73] Kotowska, U.; Kapelewska, J.; Sturgulewska, J. Determination of phenols and pharmaceuticals in municipal wastewaters from Polish treatment plants by ultrasound-assisted emulsification–microextraction followed by GC–MS. *Environmental Science and Pollution Research* **2014**, *21*, 660–673.

[74] Canals, A.; Hernández, M. d. R. Ultrasound-assisted method for determination of chemical oxygen demand. *Analytical and Bioanalytical Chemistry* **2002**, *374*, 1132–1140.

[75] Wain, A. J.; Lawrence, N. S.; Davis, J.; Compton, R. G. Ultrasonic extraction of iron from non-aqueous liquids. *The Analyst* **2002**, *127*, 8–10.

[76] Bondy, C.; Söllner, K. On the mechanism of emulsification by ultrasonic waves. *Trans. Faraday Soc.* **1935**, *31*, 835–843.

[77] Abismail, B.; Canselier, J. P.; Wilhelm, A. M.; Delmas, H.; Gourdon, C. Emulsification by ultrasound: drop size distribution and stability. *Ultrasonics Sonochemistry* **1999**, *6*, 75–83.

[78] Regueiro, J.; Llompart, M.; Garcia-Jares, C.; Garcia-Monteagudo, J. C.; Cela, R. Ultrasound-assisted emulsification–microextraction of emergent contaminants and pesticides in environmental waters. *Journal of Chromatography A* **2008**, *1190*, 27–38.

[79] Chanamai, R.; Herrmann, N.; McClements, D. J. The influence of flocculation on the ultrasonic properties of emulsions: experiment. *Journal of Physics D: Applied Physics* **1998**, *31*, 2956–2963.

[80] Young, F. R. *Cavitation*; McGraw-Hill: London; New York, 1989.

[81] Pérez-Serradilla, J. A.; Priego-Capote, F.; Luque de Castro, M. D. Simultaneous Ultrasound-Assisted Emulsification−Extraction of Polar and Nonpolar Compounds from Solid Plant Samples. *Analytical Chemistry* **2007**, *79*, 6767–6774.

[82] Saleh, A.; Yamini, Y.; Faraji, M.; Rezaee, M.; Ghambarian, M. Ultrasound-assisted emulsification microextraction method based on applying low density organic solvents followed by gas chromatography analysis for the determination of polycyclic aromatic hydrocarbons in water samples. *Journal of Chromatography A* **2009**, *1216*, 6673–6679.

[83] Ozcan, S.; Tor, A.; Aydin, M. E. Determination of polycyclic aromatic hydrocarbons in waters by ultrasound-assisted emulsification-microextraction and gas chromatography–mass spectrometry. *Analytica Chimica Acta* **2010**, *665*, 193–199.

[84] Cheng, J.; Matsadiq, G.; Liu, L.; Zhou, Y.-W.; Chen, G. Development of a novel ultrasound-assisted surfactant-enhanced emulsification microextraction method and its application to the analysis of eleven polycyclic aromatic hydrocarbons at trace levels in water. *Journal of Chromatography A* **2011**, *1218*, 2476–2482.

[85] Wu, Q.; Chang, Q.; Wu, C.; Rao, H.; Zeng, X.; Wang, C.; Wang, Z. Ultrasound-assisted surfactant-enhanced emulsification microextraction for the determination of carbamate pesticides in water samples by high performance liquid chromatography. *Journal of Chromatography A* **2010**, *1217*, 1773–1778.

[86] Pizarro, C.; Sáenz-González, C.; Pérez-del Notario, N.; González-Sáiz, J. M. Optimisation of a sensitive method based on ultrasound-assisted emulsification–microextraction for the simultaneous determination of haloanisoles and volatile phenols in wine. *Journal of Chromatography A* **2012**, *1244*, 37–45.

[87] Reboredo-Rodríguez, P.; Rey-Salgueiro, L.; Regueiro, J.; González-Barreiro, C.; Cancho-Grande, B.; Simal-Gándara, J. Ultrasound-assisted emulsification–microextraction for the determination of phenolic compounds in olive oils. *Food Chemistry* **2014**, *150*, 128–136.

[88] McGregor, L. A. Environmental Forensic Investigation of Coal Tars from Former Manufactured Gas Plants. Ph.D. thesis, University of Strathclyde, 2012.

[89] Lee, L. S.; Rao, P. S. C.; Okuda, I. Equilibrium partitioning of polycyclic aromatic hydrocarbons from coal tar into water. *Environmental Science & Technology* **1992**, *26*, 2110–2115.

[90] Mattox, C. F.; Humenick, M. J. Organic groundwater contaminants from UCG. Proceedings of the 5th Underground Coal Conversion Symposium. Alexandria, Virginia, 1979; pp 281–294.

[91] National Institute of Standards and Technology (NIST), *AMDIS (Automated Mass Spectral Deconvolution and Identification System)*; software Version 2.73. Build 2017/04/25, 2017.

[92] Hielscher Ultrasonics Gmbh, UP200St with VialTweeter for Simultaneous Sample Preparation. `http://web.archive.org/web/20190423103727/https://www.hielscher.com/up200st-with-vialtweeter-for-simultaneous-sample-preparation.htm`.

[93] Watanabe, K. Contribution of Cyclopentyl Methyl Ether (CPME) to Green Chemistry. *Chimica Oggi - Chemistry Today* **2013**, *31*, 24–27.

[94] Watanabe, K.; Yamagiwa, N.; Torisawa, Y. Cyclopentyl Methyl Ether as a New and Alternative Process Solvent. *Organic Process Research & Development* **2007**, *11*, 251–258.

[95] Farajzadeh, M. A.; Seyedi, S. E.; Shalamzari, M. S.; Bamorowat, M. Dispersive liquid-liquid microextraction using extraction solvent lighter than water. *Journal of Separation Science* **2009**, *32*, 3191–3200.

[96] Chen, P.; Sun, M.; Zhu, Z.; Zhang, J.; Shen, G. Optimization of ultrasonic-assisted extraction for determination of polycyclic aromatic hydrocarbons in biochar-based fertilizer by gas chromatography–mass spectrometry. *Analytical and Bioanalytical Chemistry* **2015**, *407*, 6149–6157.

[97] Minitab, LLC., What is response optimization? 2017; `http://web.archive.org/web/20190423103847/https://support.minitab.com/en-us/minitab/18/help-and-how-to/modeling-statistics/using-fitted-models/supporting-topics/response-optimization/what-is-response-optimization/`.

[98] Xie, W.-H.; Shiu, W.-Y.; Mackay, D. A review of the effect of salts on the solubility of organic compounds in seawater. *Marine Environmental Research* **1997**, *44*, 429–444.

[99] Nikolic, G.; Perovic, J.; Nikolic, R.; Cakic, M. Salting-out extraction of catechol and hydroquinone from aqueous solutions and urine samples. *Facta universitatis - series: Physics, Chemistry and Technology* **2003**, *2*, 293–299.

[100] Peng, J.; Wan, A. Effect of ionic strength on Henry's constants of volatile organic compound. *Chemosphere* **1998**, *36*, 2731–2740.

[101] Moradi, M.; Yamini, Y.; Esrafili, A.; Seidi, S. Application of surfactant assisted dispersive liquid–liquid microextraction for sample preparation of chlorophenols in water samples. *Talanta* **2010**, *82*, 1864–1869.

[102] Fillo, J. P.; Stamoudis, V. C.; Stetter, J. R.; Vance, S. W. *Influence of coal devolatilization conditions on the yield, chemistry, and toxicology of by-product oils and tars*; 1983.

[103] Kivelevitch, D.; Frieder, J.; Watson, I.; Paek, S. Y.; Menter, M. A. Pharmacotherapeutic approaches for treating psoriasis in difficult-to-treat areas. *Expert Opinion on Pharmacotherapy* **2018**, *19*, 561–575.

[104] International Agency for Research on Cancer (IARC), *Agents Classified By The Iarc Monographs, Volumes 1–114*; 2015.

[105] Weiler, J. F. In *Chemistry of coal utilization. Supplementary volume.*; Lowry, H. H., Ed.; John Wiley and Sons, Inc: New York - London, 1963.

[106] Karr, C. J. In *Chemistry of coal utilization. Supplementary volume.*; Lowry, H. H., Ed.; John Wiley and Sons, Inc: New York - London, 1963.

[107] Franck, H.-G. THE CHALLENGE IN COAL TAR CHEMICALS. *Industrial & Engineering Chemistry* **1963**, *55*, 38–44.

[108] Brown, D. G.; Gupta, L.; Kim, T.-H.; Keith Moo-Young, H.; Coleman, A. J. Comparative assessment of coal tars obtained from 10 former manufactured gas plant sites in the Eastern United States. *Chemosphere* **2006**, *65*, 1562–1569.

[109] McGregor, L. A.; Gauchotte-Lindsay, C.; Daéid, N. N.; Thomas, R.; Daly, P.; Kalin, R. M. Ultra resolution chemical fingerprinting of dense non-aqueous phase liquids from manufactured gas plants by reversed phase comprehensive two-dimensional gas chromatography. *Journal of Chromatography A* **2011**, *1218*, 4755–4763.

[110] McGregor, L. A.; Gauchotte-Lindsay, C.; Nic Daéid, N.; Thomas, R.; Kalin, R. M. Multivariate Statistical Methods for the Environmental Forensic Classification of Coal Tars from Former Manufactured Gas Plants. *Environmental Science & Technology* **2012**, *46*, 3744–3752.

[111] Gauchotte-Lindsay, C.; Richards, P.; McGregor, L. A.; Thomas, R.; Kalin, R. M. A one-step method for priority compounds of concern in tar from former industrial sites:

Trimethylsilyl derivatisation with comprehensive two-dimensional gas chromatography. *Journal of Chromatography A* **2012**, *1253*, 154–163.

[112] Gallacher, C.; Thomas, R.; Taylor, C.; Lord, R.; Kalin, R. M. Comprehensive composition of Creosote using comprehensive two-dimensional gas chromatography time-of-flight mass spectrometry (GCxGC-TOFMS). *Chemosphere* **2017**, *178*, 34–41.

[113] Gallacher, C.; Thomas, R.; Lord, R.; Kalin, R. M.; Taylor, C. Comprehensive database of Manufactured Gas Plant tars. Part B. Aliphatic and aromatic compounds. *Rapid Communications in Mass Spectrometry* **2017**, *31*, 1239–1249.

[114] Gallacher, C.; Thomas, R.; Lord, R.; Kalin, R. M.; Taylor, C. Comprehensive database of Manufactured Gas Plant tars. Part C. Heterocyclic and hydroxylated polycyclic aromatic hydrocarbons. *Rapid Communications in Mass Spectrometry* **2017**, *31*, 1250–1260.

[115] Gallacher, C.; Thomas, R.; Lord, R.; Kalin, R. M.; Taylor, C. Comprehensive database of Manufactured Gas Plant tars. Part A. Database. *Rapid Communications in Mass Spectrometry* **2017**, *31*, 1231–1238.

[116] King, S. B. Composition Of Selected Fractions From Coal Tars Produced From An Underground Coal Gasification Test. *Preprints of Papers American Chemical Society Division of Fuel Chemistry* **1977**, *22*, 169–184.

[117] King, S. B.; Guffey, F. D.; Gardner, G. W. An Investigation Of Aromatic Fractions From Coal Tar Produced By An Underground Coal Gasification Test. *Preprints of Papers American Chemical Society Division of Fuel Chemistry* **1977**, *22*, 113–117.

[118] Stephens, D. R.; Thorsness, C. B. Partial Seam CRIP test tar results. Proceedings of the 11th Annual Underground Coal Gasification Symposium. Denver, Colorado, United States, 1985.

[119] Wiatowski, M.; Kapusta, K.; Muzyka, R. Study of properties of tar obtained from underground coal gasification trials. *Fuel* **2018**, *228*, 206–214.

[120] U. S. Environmental Protection Agency, *Method 3580A Waste Dilution*; 1992.

[121] Hinshaw, J. V. The flame ionization detector. *LC GC EUROPE* **2006**, *19*, 1262–1272.

[122] Thomas, O., Burgess, C., Eds. *UV-visible spectrophotometry of water and wastewater*, second edition ed.; Elsevier: Amsterdam, Netherlands, 2017.

[123] Eaton, A. D., Ed. *Standard methods for the examination of water and wastewater*, 21st ed.; American Public Health Association: Washington, DC, 2005.

[124] Campbell, J. H.; Pellizzari, E.; Santor, S. *Results Of A Groundwater Quality Study Near An Underground Coal Gasification Experiment (Hoe Creek I)*; Techical Report UCRL-52405, 1978; pp 1–117.

[125] U. S. Environmental Protection Agency, *Method 8000D Determinative Chromatographic Separations*; 2014.

[126] Covell, J. R.; Dennis, D. S.; Barone, S. P. Preliminary results of the environmental program and permitting at the rocky mountain 1 underground coal gasification project. Proceedings of Fourteenth Underground Coal Gasification Symposium. Chicago, Illinois, 1988.

[127] Barbour, F. A.; Covelli, J. R. *Trace Gas, Product Water, and Particulate Characterization for Rocky Mountain 1 UCG Project. Underground Coal Gasification Test, Hanna, Wyoming*; Technical Report GRI-90/0032, 1990.

[128] Moody, C. G.; Donovan, R. C.; Mason, J. M. Groundwater chemistry changes in the Hanna no 1 coal seam during the rocky mountain 1 underground coal gasification test, Hanna, Wyoming. Proceedings of Fourteenth Underground Coal Gasification Symposium. Chicago, Illinois, 1988.

[129] Cena, R. J.; Britten, J. A.; Thorsness, C. B. Resource recovery and cavitiy growth during the rocky mountain 1 field test. Proceedings of Fourteenth Underground Coal Gasification Symposium, Schaumburg, IL. Chicago, Illinois, 1988.

[130] Meloun, M., Militký, M., Forina, M., Eds. *Chemometrics for analytical chemistry*; Ellis Horwood series in analytical chemistry; Ellis Horwood: New York, 1992.

[131] Miller, J. N.; Miller, J. C. *Statistics and chemometrics for analytical chemistry*, 6th ed.; Prentice Hall: Harlow, 2010.

[132] Kumar, N.; Bansal, A.; Sarma, G. S.; Rawal, R. K. Chemometrics tools used in analytical chemistry: An overview. *Talanta* **2014**, *123*, 186–199.

[133] Goodacre, R.; Vaidyanathan, S.; Dunn, W. B.; Harrigan, G. G.; Kell, D. B. Metabolomics by numbers: acquiring and understanding global metabolite data. *Trends in Biotechnology* **2004**, *22*, 245–252.

[134] Bijlsma, S.; Bobeldijk, I.; Verheij, E. R.; Ramaker, R.; Kochhar, S.; Macdonald, I. A.; van Ommen, B.; Smilde, A. K. Large-Scale Human Metabolomics Studies: A Strategy for Data (Pre-) Processing and Validation. *Analytical Chemistry* **2006**, *78*, 567–574.

[135] Bartel, J.; Krumsiek, J.; Theis, F. J. STATISTICAL METHODS FOR THE ANALYSIS OF HIGH-THROUGHPUT METABOLOMICS DATA. *Computational and Structural Biotechnology Journal* **2013**, *4*, 1–9.

[136] Vogt, C. R.; Kapila, S.; Manahan, S. E. Chromatographic characterisation of organic by-products of simulated in situ coal gasification. *In Situ* **1981**, *5*, 25–42.

[137] Westmoreland, P. R.; Forrester III, R. C. PYROLYSIS OF LARGE COAL BLOCKS: IMPLICATIONS OF HEAT AND MASS TRANSPORT EFFECTS FOR IN SITU GASIFICATION. *Preprints of Papers American Chemical Society Division of Fuel Chemistry* **1977**, *22*, 93–101.

[138] Westmoreland, P. R. Pyrolysis of bituminous coal blocks. Proceedings Of The 4th Annual Underground Coal Conversion Symposium. Colorado, 1978.

[139] Thorsness, C. B.; Hill, R. W. *Coal-block-gasification experiments: laboratory results and field plans*; 1981.

[140] Glaser, R. R.; Johnson, L. A. *Physical Simulation Of Underground Coal Gasification In An Eastern Bituminous Coal*; Technical Report DE87004290, 1986.

[141] Daggupati, S.; Mandapati, R. N.; Mahajani, S. M.; Ganesh, A.; Mathur, D. K.; Sharma, R. K.; Aghalayam, P. Laboratory studies on combustion cavity growth in lignite coal blocks in the context of underground coal gasification. *Energy* **2010**, *35*, 2374–2386.

[142] Boke, E.; Okutan, H.; Gur, M.; Yildiz, A. DESIGN OF A LARGE-SCALE LABORATORY EXPERIMENTAL SET-UP FOR UNDERGROUND COAL GASIFICATION OF TURKISH LIGNITES. Proceedings Of The International Energy Raw Metarials And Energy Summit. 2015.

[143] Wiatowski, M.; Kapusta, K.; Swiadrowski, J.; Cybulski, K.; Ludwik-Pardala, M.; Grabowski, J.; Stanczyk, K. Technological aspects of underground coal gasification in the Experimental "Barbara" Mine. *Fuel* **2015**, *159*, 454–462.

[144] Smith, C. A.; Want, E. J.; O'Maille, G.; Abagyan, R.; Siuzdak, G. XCMS: Processing Mass Spectrometry Data for Metabolite Profiling Using Nonlinear Peak Alignment, Matching, and Identification. *Analytical Chemistry* **2006**, *78*, 779–787.

[145] Styczynski, M. P.; Moxley, J. F.; Tong, L. V.; Walther, J. L.; Jensen, K. L.; Stephanopoulos, G. N. Systematic Identification of Conserved Metabolites in GC/MS Data for Metabolomics and Biomarker Discovery. *Analytical Chemistry* **2007**, *79*, 966–973.

[146] Tautenhahn, R.; Patti, G. J.; Rinehart, D.; Siuzdak, G. XCMS Online: A Web-Based Platform to Process Untargeted Metabolomic Data. *Analytical Chemistry* **2012**, *84*, 5035–5039.

[147] Smits, M. M.; Carleer, R.; Colpaert, J. V. PYQUAN: A rapid workflow around the AMDIS deconvolution software for high throughput analysis of pyrolysis GC/MS data. *Journal of Analytical and Applied Pyrolysis* **2016**, *118*, 335–342.

[148] Domingo-Almenara, X.; Brezmes, J.; Vinaixa, M.; Samino, S.; Ramirez, N.; Ramon-Krauel, M.; Lerin, C.; Díaz, M.; Ibáñez, L.; Correig, X.; Perera-Lluna, A.; Yanes, O. eRah: A Computational Tool Integrating Spectral Deconvolution and Alignment with Quantification and Identification of Metabolites in GC/MS-Based Metabolomics. *Analytical Chemistry* **2016**, *88*, 9821–9829.

[149] Liggi, S.; Hinz, C.; Hall, Z.; Santoru, M. L.; Poddighe, S.; Fjeldsted, J.; Atzori, L.; Griffin, J. L. KniMet: a pipeline for the processing of chromatography–mass spectrometry metabolomics data. *Metabolomics* **2018**, *14*, 52.

[150] R Core Team, R: A Language and Environment for Statistical Computing. R Foundation for Statistical Computing: Vienna, Austria, 2013.

[151] *OpenChrom Community Edition*; software Version 1.2.0 (Alder), 2017.

[152] Nezami Ranjbar, M. R.; Poto, C. D.; Wang, Y.; Ressom, H. W. SIMAT: GC-SIM-MS data analysis tool. *BMC Bioinformatics* **2015**, *16*, 259.

[153] Behrends, V.; Tredwell, G. D.; Bundy, J. G. A software complement to AMDIS for processing GC-MS metabolomic data. *Analytical Biochemistry* **2011**, *415*, 206–208.

[154] Chong, J.; Soufan, O.; Li, C.; Caraus, I.; Li, S.; Bourque, G.; Wishart, D. S.; Xia, J. MetaboAnalyst 4.0: towards more transparent and integrative metabolomics analysis. *Nucleic Acids Research* **2018**, *46*, 486–494.

[155] Xia, J.; Wishart, D. S. Metabolomic Data Processing, Analysis, and Interpretation Using MetaboAnalyst. *Current Protocols in Bioinformatics* **2011**, *34*, 1–48.

[156] Xia, J.; Psychogios, N.; Young, N.; Wishart, D. S. MetaboAnalyst: a web server for metabolomic data analysis and interpretation. *Nucleic Acids Research* **2009**, *37*, 652–660.

[157] MetaboAnalyst - user statisics. 2017; `http://web.archive.org/web/20190423103958/https://www.metaboanalyst.ca/faces/docs/UserStats.xhtml`.

[158] van den Berg, R. A.; Hoefsloot, H. C.; Westerhuis, J. A.; Smilde, A. K.; van der Werf, M. J. Centering, scaling, and transformations: improving the biological information content of metabolomics data. *BMC genomics* **2006**, *7*, 142.

[159] Xia Lab, McGill Univeristy, What is generalized logarithm transformation (glog)? `https://web.archive.org/web/20190429112630/https://www.metaboanalyst.ca/faces/docs/Faqs.xhtml`.

[160] Brereton, R. G.; Lloyd, G. R. Partial least squares discriminant analysis: taking the magic away. *Journal of Chemometrics* **2014**, *28*, 213–225.

[161] SIMCA –P and Multivariate Analysis. `http://web.archive.org/web/20190423104040/https://umetrics.com/sites/default/files/kb/multivariate_faq.pdf`.

[162] Kapusta, K. Personal email correspondence. 2016.

[163] Fynes, G.; Herod, A. A.; Hodges, N. J.; Stokes, B. J.; Ladner, W. R. The thermal emission of chlorine-containing compounds from coal following brine and chlorine gas treatments. *Fuel* **1988**, *67*, 822–830.

[164] Pierce, E. A. *Silylation of organic compounds a technique for gas-phase analysis*; Rockford, Ill., Pierce Chemical Co., 1968.

[165] Blau, K., Halket, J. M., Eds. *Handbook of derivatives for chromatography*, 2nd ed.; Wiley: Chichester ; New York, 1993.

[166] Danielson, N. D.; Gallacher, P. A.; Bao, J. J. In *Encyclopedia of Analytical Chemistry*; Meyers, R. A., Ed.; John Wiley & Sons, Ltd, 2006.

[167] Seidi, S.; Yamini, Y. Analytical sonochemistry; developments, applications, and hyphenations of ultrasound in sample preparation and analytical techniques. *Open Chemistry* **2012**, *10*, 938–976.

[168] Mason, T. J. Ultrasound in synthetic organic chemistry. *Chemical Society Reviews* **1997**, *26*, 443–451.

[169] Orozco-Solano, M.; Ruiz-Jiménez, J.; Luque de Castro, M. D. Ultrasound-assisted extraction and derivatization of sterols and fatty alcohols from olive leaves and drupes prior to determination by gas chromatography–tandem mass spectrometry. *Journal of Chromatography A* **2010**, *1217*, 1227–1235.

[170] Sánchez Ávila, N.; Priego Capote, F.; Luque de Castro, M. D. Ultrasound-assisted extraction and silylation prior to gas chromatography–mass spectrometry for the characterization of the triterpenic fraction in olive leaves. *Journal of Chromatography A* **2007**, *1165*, 158–165.

[171] Liu, Y.; Chen, T.; Qiu, Y.; Cheng, Y.; Cao, Y.; Zhao, A.; Jia, W. An ultrasonication-assisted extraction and derivatization protocol for GC/TOFMS-based metabolite profiling. *Analytical and Bioanalytical Chemistry* **2011**, *400*, 1405–1417.

[172] Orata, F. In *Advanced Gas Chromatography - Progress in Agricultural, Biomedical and Industrial Applications*; Ali Mohd, M., Ed.; InTech, 2012.

[173] Kumirska, J.; Plenis, A.; Lukaszewicz, P.; Caban, M.; Migowska, N.; Bialk-Bielinska, A.; Czerwicka, M.; Stepnowski, P. Chemometric optimization of derivatization reactions prior to gas chromatography–mass spectrometry analysis. *Journal of Chromatography A* **2013**, *1296*, 164–178.

[174] Minitab Inc, *Minitab 18 Statistical Software*; software Version 18, 2017.

[175] Charuwat, P.; Boardman, G.; Bott, C.; Novak, J. T. Thermal Degradation of Long Chain Fatty Acids. *Water Environment Research* **2018**, *90*, 278–287.

[176] Maharaj, S. V. M.; Orem, W. H.; Tatu, C. A.; Lerch, H. E.; Szilagyi, D. N. Organic compounds in water extracts of coal: links to Balkan endemic nephropathy. *Environmental Geochemistry and Health* **2014**, *36*, 1–17.

[177] Xu, B.; Chen, L.; Xing, B.; Li, L.; Zhang, L.; Wang, X.; Chen, H.; Yi, G.; Huang, G. The environmental effect of underground coal gasification semi-coke on confined groundwater. *Environmental Progress & Sustainable Energy* **2016**, 1584–1589.

[178] Oliver, R. L.; Spackman, L. K. *Results of leaching experiments conducted on samples from the Tono I UCG cavity*; Technical Report DE87014458, 1987.

[179] Humenick, M. J.; Morgan, J. R.; Nolan, B. T. Adsorption of UCG organics by coal, char, activated char and ash. *In Situ* **1987**, *11*, 327–347.

[180] Freire, D. D. C.; Sant'Anna, G. L. A Proposed Method Modification for the Determination of COD in Saline Waters. *Environmental Technology* **1998**, *19*, 1243–1247.

[181] Stadelhofer, J. W.; Marrett, R.; Gemmeke, W. The manufacture of high-value carbon from coal-tar pitch. *Fuel* **1981**, *60*, 877–882.

[182] Wei, X.; Shi, X.; Koo, I.; Kim, S.; Schmidt, R. H.; Arteel, G. E.; Watson, W. H.; McClain, C.; Zhang, X. MetPP: a computational platform for comprehensive two-dimensional gas chromatography time-of-flight mass spectrometry-based metabolomics. *Bioinformatics* **2013**, *29*, 1786–1792.

[183] Ramaker, R. C.; Gordon, E. R.; Cooper, S. J. R2DGC: threshold-free peak alignment and identification for 2D gas chromatography-mass spectrometry in R. *Bioinformatics* **2017**, *34*, 1789–1791.

[184] Weggler, B. A.; Gröger, T.; Zimmermann, R. Advanced scripting for the automated profiling of two-dimensional gas chromatography-time-of-flight mass spectrometry data from combustion aerosol. *Journal of Chromatography A* **2014**, *1364*, 241–248.

[185] Jennerwein, M. K.; Eschner, M.; Gröger, T.; Wilharm, T.; Zimmermann, R. Complete Group-Type Quantification of Petroleum Middle Distillates Based on Comprehensive Two-Dimensional Gas Chromatography Time-of-Flight Mass Spectrometry (GC×GC-TOFMS) and Visual Basic Scripting. *Energy & Fuels* **2014**, *28*, 5670–5681.